UNIVERSIDAD COMPLUTENSE DE MADRID
FACULTAD DE CIENCIAS QUÍMICAS

TESIS DOCTORAL

Eliminación de contaminantes orgánicos en sedimentos y suelos mediante oxidación química

(Removal of organic pollutants in sediments and soils by chemical oxidation)

MEMORIA PARA OPTAR AL GRADO DE DOCTOR

PRESENTADA POR

Cristina Alicia Checa Fernández

Directoras

Aurora Santos López
Carmen María Domínguez Torre

Madrid

UNIVERSIDAD COMPLUTENSE DE MADRID

FACULTAD DE CIENCIAS QUÍMICAS

TESIS DOCTORAL

Eliminación de contaminantes orgánicos en sedimentos y suelos mediante oxidación química (Removal of organic pollutants in sediments and soils by chemical oxidation)

MEMORIA PARA OPTAR AL GRADO DE DOCTOR

PRESENTADA POR

CRISTINA ALICIA CHECA FERNÁNDEZ

DIRECTORAS

Aurora Santos López y Carmen María Domínguez Torre

UNIVERSIDAD COMPLUTENSE DE MADRID

FACULTAD DE CIENCIAS QUÍMICAS

PROGRAMA DE DOCTORADO EN INGENIERÍA QUÍMICA

TESIS DOCTORAL

Eliminación de contaminantes orgánicos en sedimentos y suelos mediante oxidación química (Removal of organic pollutants in sediments and soils by chemical oxidation)

MEMORIA PARA OPTAR AL GRADO DE DOCTOR

PRESENTADA POR

CRISTINA ALICIA CHECA FERNÁNDEZ

DIRECTORAS

Aurora Santos López y Carmen María Domínguez Torre

Esta Tesis Doctoral ha sido realizada gracias al contrato como personal investigador (PAI) asociado al proyecto CARESOIL (S2018/EMT-4317) concedido por la Comunidad de Madrid. Esta Tesis Doctoral agradece el uso de equipamiento e infraestructuras al grupo de investigación Intensificación de Procesos Químicos y Medioambientales (INPROQUIMA), dirigido por la profesora Aurora Santos López, de la Facultad de Ciencias Químicas de la Universidad Complutense de Madrid y financiado con proyectos nacionales y europeos (PID2019-105934RB-I00, LIFE7/ENV/ES/000260). Esta Tesis Doctoral también agradece al programa de Doctorado en Ingeniería Química de la Facultad de Ciencias Químicas, al coordinador y responsable del programa Carlos Negro Álvarez y a los miembros de la Comisión Académica del Programa de Doctorado. Finalmente, agradece a las empresas SARGA y EMGRISA, y al Gobierno de Aragón, por el suministro de muestras, los datos facilitados y el apoyo mostrado durante la ejecución de la investigación.

En esta Tesis se ha realizado una estancia breve financiada por la Comunidad de Madrid, a través del proyecto CARESOIL (S2018/EMT-4317), con una duración de tres meses (septiembre – noviembre 2022) en el Laboratorio di Ingegneria Ambientale, Dipartimento di Ingegnería Civile, Università di Roma Tor Vergata, bajo la supervisión del profesor Renato Baciocchi.

A mis padres, hermana y amigos

INDEX

LIST OF TABLES v

LIST OF FIGURES vii

LIST OF ACRONYMS, ABBREVIATIONS, AND SYMBOLS xv

CHAPTER 1. STRUCTURE OF THE DOCTORAL THESIS 1

CHAPTER 2. SUMMARY/RESUMEN 5

2.1. Summary 7

2.2. Resumen 13

CHAPTER 3. ARTICLES COMPOUNDING THE DOCTORAL THESIS 21

ARTICLE 1 23

ARTICLE 2 27

ARTICLE 3 31

ARTICLE 4 35

ARTICLE 5 39

ARTICLE 6 43

ARTICLE 7 47

CHAPTER 4. INTRODUCTION 53

4.1. Soil pollution 55

4.1.1. Types of soil pollution attending the contamination source 58

4.1.2. Main soil pollutants 59

4.2. Remediation of soils polluted by organic compounds 61

4.3. Lindane wastes pollution: a case study 68

CHAPTER 5. SCOPES AND AIMS 73

CHAPTER 6. MATERIALS AND METHODS 77

6.1. Materials 79

6.1.1. Reagents 79

6.1.2. Soil samples 81

6.1.3. Soil contaminants (HCH particulate matter and DNAPL) 83

6.2. Experimental procedures for soil remediation 84

6.2.1. Topsoil (TS) oxidation treatments 84

6.2.2. Subsoil (SS) oxidation treatments 88

6.3. Analytical methods 91

6.3.1. Soil phase 91

6.3.1.1. Chlorinated Organic Compounds (COCs) 91

6.3.1.2. Metals 93
6.3.1.3. pH 94
6.3.1.4. Total organic carbon 94
6.3.1.5. Scanning electron microscopy (SEM) and elemental energy dispersive analysis 95
6.3.1.6. Acute toxicity 95
6.3.2. Aqueous phase 102
6.3.2.1. Chlorinated Organic Compounds (COCs) 102
6.3.2.2. Oxidants 102
6.3.2.3. Iron 103
6.3.2.4. Chlorides 104
6.3.2.5. pH 104
6.3.2.6. Surfactants 105
6.3.2.7. Acute toxicity 105

CHAPTER 7. RESULTS AND DISCUSSION 109

7.1. Soils characterization 111
7.1.1. Physico-chemical composition and pollutant concentration 111
7.1.2. Acute toxicity 118
7.1.2.1. Acute toxicity of soils 118
7.1.2.2. Acute toxicity of soil elutriates 121
7.1.2.3. Acute toxicity of soil organic extracts 124

7.2. Topsoil (TS) oxidation treatments 127
7.2.1. Oxidant evaluation: HP and PS 129
7.2.1.1. Hydrogen peroxide (HP/Fe, Fenton process) 129
7.2.1.2. Persulfate (PS) 132
7.2.2. PS activation evaluation: NaOH and T 133
7.2.3. Intensification of PS/NaOH 152
7.2.3.1. PS/NaOH/T 153
7.2.3.2. PS/NaOH/US 170
7.2.3.3. S/PS/NaOH/T 184

7.3. Acute toxicity of treated soils 198
7.3.1. Remediated Topsoil 198
7.3.2. Remediated Subsoil 207

CHAPTER 8. CONCLUSIONS 215

Characterization of polluted samples 217

Topsoil (TS) oxidation treatments 220
Acute toxicity of treated soils 226
CHAPTER 9. ONGOING AND FUTURE WORK 229
9.1. Bioremediation 231
9.2. Additional evaluation of toxicity and biodegradability 233
9.2.1. Rapid biodegradability test 233
9.2.2. *Artemia salina* 234
9.2.3. *Daphnia magna* 235
9.3. Field-scale application 236
9.4. Remediation of aqueous phases contaminated with other organic pollutants 236
9.4.1. Remediation experiments 237
9.4.2. Results 238
CHAPTER 10. REFERENCES 241
CHAPTER 11. APPENDICES 263
APPENDIX I. Others publications 265
APPENDIX II. Contributions to congresses 275

LIST OF TABLES

CHAPTER 4. INTRODUCTION **53**

Table 4.1. Summary of advantages and disadvantages of ex situ, on-site, and in situ technologies (Adapted from (UNEP 2021)). **62**

CHAPTER 6. MATERIALS AND METHODS **77**

Table 6.1. Reagents employed in this Doctoral Thesis. **79**

Table 6.2. Soil samples used in oxidation treatments and toxicity evaluation **83**

Table 6.3. Summary of the oxidation treatments studied for on-site TS (TS L2, Table 6.2) remediation**.** **85**

Table 6.4. Experimental conditions in column runs. The flow rate used in all Pv injections was 0.3 mL min^{-1}. Soil sample: SS-C L2 (Table 6.2) (Santos, García-Cervilla et al. 2022, ART. 7). **89**

CHAPTER 7. RESULTS AND DISCUSSION **109**

Table 7.1. Topsoil (TS) and subsoil (SS) inorganic characterization (mean ± standard deviation). **112**

Table 7.2. COCs concentration, TOC measured, and the percentage ratio between $TOC_{COCs,\ soil}$ /$TOC_{\ measured,soil}$ in soils and COCs in soils elutriates (V_L/W_S = 2). **113**

Table 7.3. Acute toxicity measured by Microtox® modified Basic Solid-Phase Test (a), Basic Test (b) and adapted Organic Solvent Sample Solubilization Test (c) for soils, soils elutriates, and soils organic extracts, respectively (Domínguez, Ventura et al. 2023, ART. 1). **119**

Table 7.4. Concentration and EC_{50} of HCH PM, DNAPL and pure commercial contaminants in saturated aqueous solutions (Microtox® BT) and organic (MeOH) phases (Microtox® aOSSST) (Domínguez, Ventura et al. 2023, ART. 1). **122**

Table 7.5. Pearson and Spearman correlation coefficients obtained between EC_{50} and COCs concentration (Domínguez, Ventura et al. 2023, ART. 1). **126**

Table 7.6. Operational conditions of the remediation experiments for the oxidant evaluation (Soil sample: $C_{HCHs,0}$ = 155 mg kg^{-1} (TS L2), W_S = 10 g, V_L/W_S = 2, T = 20 ºC). **129**

Table 7.7. Operational conditions of the oxidation runs for the activator evaluation (TS L2, W_S = 10 g, V_L/W_S = 2, molar NaOH:PS = 2 where applicable). **133**

Table 7.8. Operating conditions of the blank experiments. TS L2 = polluted soil ($C_{HCHs,0}$ = 358 mg kg^{-1}), TS L0 = unpolluted soil (Dominguez, Checa-Fernandez et al. 2021, ART. 3). **134**

Table 7.9. Operating conditions of the PS/NaOH/T remediation experiments ($C_{HCHs,0}$ = 373 mg kg^{-1} (TS L2), W_S = 15 g, V_L/W_S = 2, molar NaOH:PS = 2) (Checa-Fernández, Santos et al. 2021, ART. 4). **153**

Table 7.10. Experimental conditions of desorption experiments ($C_{HCHs,0}$ = 404 mg kg^{-1} (TS L2), W_S = 15 g, V_L/W_S = 2) (Checa-Fernández, Santos et al. 2022, ART. 5). **171**

Table 7.11. Operating conditions of PS/NaOH/US experiments ($C_{HCHs,0}$ = 404 mg kg^{-1} (TS L2), W_S = 15 g, V_L/W_S = 2, molar NaOH:PS = 2) (Checa-Fernández, Santos et al. 2022, ART. 5). **174**

Table 7.12. Operational conditions of solubilization experiments ($C_{HCHs,0}$ = 373 mg kg^{-1} (TS L2), W_S = 15 g, V_L/W_S = 2) (Checa-Fernández, Santos et al. 2023, ART. 6). **186**

Table 7.13. Operational conditions of polluted emulsion (PE) oxidation experiments (molar NaOH:PS > 2 (when it applies), C_{PS} = 40 g L^{-1} (when it applies), T = 40 ºC) (Checa-Fernández, Santos et al. 2023, ART. 6). **194**

Table 7.14. COC concentration in the soil phases ($C_{COC,soil}$), in the reaction supernatants ($C_{COC, aq, supernantant}$) and the elutriates ($C_{COC, aq}$ elutriate) of PS/T and PS/NaOH/T treatments. **200**

Table 7.15. PS concentration (Mm) measured at each Pv in ISCO and S-ISCO experiments of SS-C L2 (Santos, García-Cervilla et al. 2022, ART. 7). **208**

LIST OF FIGURES

CHAPTER 4. INTRODUCTION 53

Figure 4.1. Number of identified remediated, potentially contaminated, and contaminated sites reported in Europe (Panagos, Van Liedekerke et al. 2013). **55**

Figure 4.2. Annual number of publications in Web of Science on soil pollution from 2002 to 2022. **56**

Figure 4.3. Number of national policies that explicitly (directly) or indirectly address soil contamination (Rodríguez and Payá Pérez 2017). **57**

Figure 4.4. Distribution of soil-related LIFE projects (Camarsa, Sliva et al. 2014). **57**

Figure 4.5. Types of soil pollution and their transport pathway in the environment. Adapted from (Rodríguez and Payá Pérez 2017). **58**

Figure 4.6. Distribution of contaminants affecting soil in European countries (Panagos, Van Liedekerke et al. 2013). **59**

Figure 4.7. Conceptualization of NAPLs migration in the subsurface, (a) LNAPL, and (b) DNAPL. Adapted from (Jackson 2004). **60**

Figure 4.8. Categorization of methods for the remediation of soils and sediments contaminated with organic pollutants. **63**

Figure 4.9. Treatment train typically carried out for subsoil remediation. Adapted from (Domínguez, Checa-Fernández et al. 2023). **67**

Figure 4.10. Scheme of lindane production process and types of wastes produced. **68**

Figure 4.11. Location and quantities of stored/dumped HCH wastes around the world. Adapted from (Vijgen, Abhilash et al. 2011). **69**

Figure 4.12. Schematization disposal of lindane wastes by INQUINOSA and the further dispersion of contaminants in the topsoil and subsoil (Domínguez, Ventura et al. 2023, ART. 1). **70**

CHAPTER 6. MATERIALS AND METHODS 77

Figure 6.1. Location of sampling sites of TS and SS samples, in Bailín and Sardas landfills, respectively. **81**

Figure 6.2. Photograph of soil samples and their respective sources of pollution: (a) topsoil and HCH particulate matter, (b) subsoil core obtained from a borehole and DNAPL. **84**

Figure 6.3. Schematic diagram of the experimental procedures carried out for "O", "A", "T", and "U" runs. Equipment employed in reaction systems: (a) rotatory agitator (LBX), (b) constant-temperature orbital bath (Unitronic), (c) US bath (Power sonic 505), (d) US probe (Branson Digital Sonifier SFX 550). **86**

Figure 6.4. Schematic diagram of the US probe experimental setup (20 kHz, total volume = 2.68 L) (Checa-Fernández, Santos et al. 2022, ART. 5). **87**

Figure 6.5. Schematic diagram of the experimental procedure carried out for runs "S", including the surfactant-enhanced solubilization step and the subsequent treatment of the polluted emulsion. **88**

Figure 6.6. Scheme of the different stages followed in the remediation experiments. Experimental conditions are summarized in Table 6.4 (Santos, García-Cervilla et al. 2022, ART. 7). **90**

Figure 6.7. Gas chromatograph (GC). **92**

Figure 6.8. GC-FID and GC-ECD (inset) chromatograms of the sources of soil pollution: (a) HCH particulate matter and (b) DNAPL. **93**

Figure 6.9. Microwave plasma atomic emission spectrometer (MP-AES). **94**

Figure 6.10. TOC-V CSH analyser (left) and SSM 5000 solid sampler (right). **94**

Figure 6.11. Microtox® M500 Analyzer (Microbics Corporation, USA) (left) and *Vibrio fischeri* bacteria (right). **96**

Figure 6.12. Soil phase toxicity determination: modified Basic Solid-Phase Test (mBSPT) (Domínguez, Ventura et al. 2023, ART. 1) **98**

Figure 6.13. Percentage of inhibition of the luminescence of the bacterium Vibrio fischeri vs. concentration of methanol (in volume) after 30 minutes of exposure (Domínguez, Ventura et al. 2023, ART. 1). **100**

Figure 6.14. Soil extracts: adapted Organic Solvent Sample Solubilization Test (Domínguez, Ventura et al. 2023, ART. 1). **101**

Figure 6.15. Spectrophotometer (BOECO S-20 UV-VIS). **103**

Figure 6.16. Calibration curves for quantifying (a) HP at 410 nm and (b) PS at 352 nm. **103**

Figure 6.17. Calibration curve for the quantification of Fe at 510 nm. **104**

Figure 6.18. Ion chromatograp (Metrohm 761 Compact IC). **104**

Figure 6.19. Elutriates (aqueous phase): Basic Test (Domínguez, Ventura et al. 2023, ART. 1) **107**

CHAPTER 7. RESULTS AND DISCUSSION 109

Figure 7.1. Photograph of contaminated TS. **113**

Figure 7.2. COCs distribution in TS samples (total COCs concentration is included in the legend) (Domínguez, Ventura et al. 2023, ART. 1). **114**

Figure 7.3. COCs distribution in SS-C (a) and SS-F (b) samples (COCs concentration is included in the legend) (Domínguez, Ventura et al. 2023, ART. 1). **115**

Figure 7.4. COCs concentration in the elutriates (V_L/W_S=2) *vs*. soils (Domínguez, Ventura et al. 2023, ART. 1). **116**

Figure 7.5. COCs distribution in (a) HCH particulate matter and (b) DNAPL (Domínguez, Ventura et al. 2023, ART. 1). **117**

Figure 7.6. (a) Soil toxicity ($1/EC_{50,\ soil}$, Microtox® mBSPT), (b) Elutriate toxicity ($1/EC_{50,\ elutriate}$, Microtox® BT), and (c) Soil organic extract toxicity ($1/EC_{50,\ organic}$, Microtox® aOSSST)

vs. COCs concentration. The unfilled markers denote the reference soil samples (L0) (Domínguez, Ventura et al. 2023, ART. 1). **120**

Figure 7.7. Inhibition (%) of *Vibrio fischeri* bioluminescence *vs.* the concentration of HCH PM and DNAPL (a) in the Basic Test and b) in the adapted Organic Solvent Sample Solubilization Test (b). The absolute concentration of the contaminant is included in the legend (Domínguez, Ventura et al. 2023, ART. 1). **123**

Figure 7.8. Soil organic extract toxicity ($1/EC_{50,\ organic}$, Microtox® adapted Organic Solvent Sample Solubilization Test) *vs.* soil toxicity ($1/EC_{50,\ soil}$, Microtox® mBSPT) (Domínguez, Ventura et al. 2023, ART. 1). **126**

Figure 7.9. Hydrogen peroxide conversion and remaining iron in solution with reaction time in Fenton experiments (O1 and O2, Table 7.6). Experimental conditions: V_L/W_S = 2, 20 ºC, $C_{HCHs,0}$ = 155 mg kg^{-1} (TS L2), pH ≈ 7, C_{Fe} = 0.5 g L^{-1} (Dominguez, Romero et al. 2021, ART. 2). **129**

Figure 7.10. COCs conversion in the soil phase at different reaction times in Fenton experiments (O1 and O2, Table 7.6). Experimental conditions: V_L/W_S = 2, 20 ºC, $C_{HCHs,0}$ = 155 mg kg^{-1} (TS L2), pH ≈ 7, C_{Fe} = 0.5 g L^{-1} (Dominguez, Romero et al. 2021, ART. 2). **130**

Figure 7.11. Conversion of HCHs in the soil phase and PS in the aqueous phase with reaction time in run O3 (Table 7.6). Experimental conditions: V_L/W_S = 2, $C_{HCHs,0}$ = 155 mg kg^{-1} (TS L2), C_{PS} = 40 g L^{-1}, 20 ºC, circumneutral pH (Dominguez, Romero et al. 2021, ART. 2). **132**

Figure 7.12. Distribution of TCB isomers in the hydrolysis of α-HCH and β-HCH at pH ≥ 12 (Dominguez, Romero et al. 2021, ART. 2). **135**

Figure 7.13. Conversion of α-HCH, β-HCH and COCs and fraction of $C'_{TCBs}/C_{HCHs,0}$ in the soil phase with reaction time in runs A1 and A2 (Table 7.7). Experimental conditions: V_L/W_S = 2, C_{HCHs} = 155 mg kg^{-1} (TS L2), C_{PS} = 40 g L^{-1} (Dominguez, Romero et al. 2021, ART. 2). **137**

Figure 7.14. Conversion of PS in the aqueous phase with reaction time in runs O3 (PS without activator) A1 (PS/NaOH) and A2 (PS/T) (Table 7.6 and Table 7.7). Experimental conditions: V_L/W_S = 2, $C_{HCHs,0}$ = 155 mg kg^{-1} (TS L2), C_{PS} = 40 g L^{-1} (Dominguez, Romero et al. 2021, ART. 2). **139**

Figure 7.15. Conversion profiles of α-HCH and β-HCH with reaction time at the three temperatures tested. Operating conditions: $C_{HCHs,0}$ = 358 mg kg^{-1} (TS L2), C_{PS} = 40 g L^{-1}, V_L/W_S = 2, 100 rpm, pH_0 = 7 (A3-A5) (Dominguez, Checa-Fernandez et al. 2021, ART. 3). **140**

Figure 7.16. Conversion profiles of γ-HCH, δ-HCH, and ε-HCH with reaction time at the three temperatures tested. Operating conditions: $C_{HCHs,0}$ = 358 mg kg^{-1} (TS L2), C_{PS} = 40 g L^{-1}, V_L/W_S = 2, 100 rpm, pH_0 = 7 (A3-A5) (Dominguez, Checa-Fernandez et al. 2021, ART. 3). **141**

Figure 7.17. Conversion profiles of HCHs, dechlorination degree, and chlorine balance with reaction time at (a) 35 ºC, (b) 45 ºC, and (c) 55 ºC. Operating conditions: $C_{HCHs,0}$ = 358 mg kg^{-1} (TS L2), C_{PS} = 40 g L^{-1}, V_L/W_S = 2, 100 rpm, pH_0 = 7 (A3-A5) (Dominguez, Checa-Fernandez et al. 2021, ART. 3). **143**

Figure 7.18. Normalized concentration profiles of HCHs and chlorinated intermediate compounds in the soil phase at (a) 35 ºC, (b) 45 ºC, (c) 55 ºC. Operating conditions:

$C_{HCHs,0}$ = 358 mg kg^{-1} (TS L2), C_{PS} = 40 g L^{-1}, V_L/W_S = 2, 100 rpm, pH_0 = 7 (A3-A5) (Dominguez, Checa-Fernandez et al. 2021, ART. 3). **145**

Figure 7.19. Reaction pathway for the oxidation of HCHs-polluted soil by thermal activation of PS (Dominguez, Checa-Fernandez et al. 2021, ART. 3). **146**

Figure 7.20. Concentration of PS with reaction time in the absence of soil (B4-B6) and in the presence of unpolluted (TS-L0, B7-B9) and polluted (TS-L2, A3-A5) soil at (a) 35 ºC, (b) 45 ºC, (c) 55 ºC. Operating conditions: C_{PS} = 40 g L^{-1}, 100 rpm, pH_0 = 7 (all the experiments), $C_{HCHs,0}$ = 358 mg kg^{-1} (TS L2), V_L/W_S = 2 (when applicable) (Dominguez, Checa-Fernandez et al. 2021, ART. 3). **147**

Figure 7.21. Evolution of the efficiency in the consumption of PS at the three temperatures tested. Operating conditions: $C_{HCHs,0}$ = 358 mg kg^{-1} (TS L2), C_{PS} = 40 g L^{-1}, V_L/W_S = 2, 100 rpm, pH_0 = 7 (A3-A5) (Dominguez, Checa-Fernandez et al. 2021, ART. 3). **149**

Figure 7.22. Conversion of HCHs, dechlorination degree and chlorine balance at (a) 3 days and (b) 9 days when working with different initial concentrations of PS. Operating conditions: $C_{HCHs,0}$ = 358 mg kg^{-1} (TS L2), 55 ºC, V_L/W_S = 2, 100 rpm, pH_0 = 7 (A5-A9) (Dominguez, Checa-Fernandez et al. 2021, ART. 3). **150**

Figure 7.23. Conversion of PS and solution pH evolution with reaction time reaction when working with different initial concentrations of PS. Operating conditions: $C_{HCHs,0}$ = 358 mg kg^{-1} (TS L2), 55 ºC, V_L/W_S = 2, 100 rpm, pH_0 =7 (A5-A9) (Dominguez, Checa-Fernandez et al. 2021, ART. 3). **151**

Figure 7.24. Efficiency in the PS consumption (Eq. (7.7)) at 3 and 9 days of reaction time when working with different initial concentrations of PS. Operating conditions: $C_{HCHs,0}$ = 358 mg kg^{-1} (TS L2), 55 ºC, V_L/W_S = 2, 100 rpm, pH_0 = 7 (A5-A9) (Dominguez, Checa-Fernandez et al. 2021, ART. 3). **152**

Figure 7.25. Conversion of α-HCH, β-HCH, COCs, and PS, dechlorination degree (Cl^-/Cl_0), and pH after 3 days of treatment. Experimental conditions: $C_{HCHs,0}$ = 373 mg kg^{-1} (TS L2), T = 40 ºC, 100 rpm, V_L/W_S = 2, C_{PS} = 40 g L^{-1}, pH_0 = 7 (T3) and pH_0 = 13 (C_{NaOH} = 13.5 g L^{-1}) (T4 and T5) (Checa-Fernández, Santos et al. 2021, ART. 4). **155**

Figure 7.26. Scheme for the degradation of HCH isomers by alkali-activated PS (pH > 12). Soil and aqueous phases were represented in brown and blue, respectively (Checa-Fernández, Santos et al. 2021, ART. 4). **156**

Figure 7.27. Conversion of β-HCH (a) and COCs (b) and dechlorination degree (c), with reaction time at different temperatures (40 ºC (T4), 50 ºC (T5) and 60 ºC (T6)). Experimental conditions: $C_{HCHs,0}$ = 373 mg kg^{-1} (TS L2), 100 rpm, V_L/W_S = 2, C_{PS} = 40 g L^{-1}, C_{NaOH} = 13.5 g L^{-1} (Checa-Fernández, Santos et al. 2021, ART. 4). **157**

Figure 7.28. pH (a) and PS conversion (b) with reaction time at different temperatures (40 ºC (T4), 50 ºC (T5), and 60 ºC (T6)). Experimental conditions: $C_{HCHs,0}$ = 373 mg kg^{-1} (TS L2), 100 rpm, V_L/W_S = 2, C_{PS} = 40 g L^{-1}, C_{NaOH} = 13.5 g L^{-1} (Checa-Fernández, Santos et al. 2021, ART. 4). **159**

Figure 7.29. Remaining concentration of TCBs generated ($TCBs'/HCH_0$) with reaction time according to the different variables studied: Temperature (a), V_L/W_S ratio (b), PS concentration at 40 ºC (c), and 50 ºC (d). Operational conditions: Table 7.9 (Checa-Fernández, Santos et al. 2021, ART. 4). **160**

Figure 7.30. Evolution of $PS_{efficiency}$ with reaction time according to the different variables studied: Temperature (a), V_L/W_S ratio (b), PS concentration at 40 ºC (c), and 50 ºC (d). Operational conditions: Table 7.9 (Checa-Fernández, Santos et al. 2021, ART. 4). **161**

Figure 7.31. Concentration of CB generated in the soil phase as an intermediate oxidation compound with reaction time at 40, 50 and 60 ºC (T4, T6, and T7). Experimental conditions: $C_{HCHs,0}$ = 373 mg kg^{-1} (TS L2), 100 rpm, V_L/W_S = 2, C_{PS} = 40 g L^{-1}, C_{NaOH} = 13.5 g L^{-1} (Checa-Fernández, Santos et al. 2021, ART. 4). **162**

Figure 7.32. Conversion of β-HCH (a) and COCs (b), and dechlorination degree (c) with reaction time at V_L/W_S ratios of 1 (T6) and 2 (T8). Experimental conditions: $C_{HCHs,0}$ = 373 mg kg^{-1} (TS L2), T = 50 ºC, 100 rpm, C_{PS} = 40 g L^{-1}, C_{NaOH} = 13.5 g L^{-1} (Checa-Fernández, Santos et al. 2021, ART. 4). **163**

Figure 7.33. pH (a) and PS conversion (b) with reaction time at V_L/W_S ratios of 1 (T6) and 2 (T8). Experimental conditions: $C_{HCHs,0}$ = 373 mg kg^{-1} (TS L2), T = 50 ºC, 100 rpm, C_{PS} = 40 g L^{-1}, C_{NaOH} = 13.5 g L^{-1} (Checa-Fernández, Santos et al. 2021, ART. 4). **164**

Figure 7.34. Conversion of β-HCH (a, d) and COCs (b, e) in the soil phase and dechlorination degree (c, f) with reaction time using different initial PS concentrations at 40 ºC and 50 ºC, respectively (Table 7.9). Experimental conditions: $C_{HCHs,0}$ = 373 mg kg^{-1} (TS L2), 100 rpm, V_L/W_S = 2, NaOH/PS = 2 (Checa-Fernández, Santos et al. 2021, ART. 4). **165**

Figure 7.35. Evolution of pH (a, c) and PS conversion (b, d) with reaction time using different initial PS concentrations at 40 ºC, and 50 ºC, respectively (Table 7.9). Experimental conditions: $C_{HCHs,0}$ = 373 mg kg^{-1} (TS L2), 100 rpm, V_L/W_S = 2, NaOH/PS = 2 (Checa-Fernández, Santos et al. 2021, ART. 4). **167**

Figure 7.36. Separation of phases by gravitational sedimentation as a function of time in the presence of water (T1) and in the PS/NaOH/T system (T4) (Table 7.9) (Checa-Fernández, Santos et al. 2021, ART. 4). **168**

Figure 7.37. Conversion of β-HCH, COCs and PS, TCBs'/$HCH_{0,}$ and pH at different stirring rate (10, 50, and 100 rpm) after 7 days (T13, T14, and T4). Experimental conditions: $C_{HCHs,0}$ = 373 mg kg^{-1} (TS L2), T = 40 ºC, V_L/W_S = 2, C_{PS} = 40 g L^{-1}, C_{NaOH} = 13.5 g L^{-1} (Checa-Fernández, Santos et al. 2021, ART. 4). **170**

Figure 7.38. Effect of the US application on the desorption of COCs (a) and Cl^- (b) to the aqueous phase. The blue line represents the experimental value obtained at equilibrium conditions (D_{eq}, pH > 12, t ≥ 24 h). Operational conditions summarized in Table 7.10 (Checa-Fernández, Santos et al. 2021, ART. 4). **172**

Figure 7.39. SEM images of the soil (TS L2) before treatment (a-b), after the US application at alkaline conditions (desorption experiment, D2) (c-d) and after the remediation treatment PS/NaOH/US ($U10^b$) (e-f) (Checa-Fernández, Santos et al. 2022, ART. 5). **173**

Figure 7.40. Effect of US application at isothermal conditions. Operational conditions: $C_{HCHs,0}$ = 404 mg kg^{-1} (TS L2), W_S = 15 g, V_L/W_S = 2, molar NaOH:PS = 2, C_{PS} = 40 g L^{-1}, US power = 350 W (when applicable, U2), T = 22ºC (Table 7.11) (Checa-Fernández, Santos et al. 2022, ART. 5). **175**

Figure 7.41. Temperature increase as a function of US power (0-245 W, corresponding to 0-91 W L^{-1}) (US probe, 20 kHz, 2.5 L) (Checa-Fernández, Santos et al. 2022, ART. 5). **177**

Figure 7.42. Effect of US application on (a) PS conversion (in the presence of polluted and unpolluted soil) and (b) β-HCH and total COCs conversion (in the presence of polluted soil) at different US power. T_{3h} = temperature reached at final reaction time. Operational conditions: $C_{HCHs,0}$ = 404 mg kg^{-1} (TS L2), W_S = 15 g, V_L/W_S = 2, molar NaOH:PS = 2, C_{PS} = 40 g L^{-1} (Table 7.11) (Checa-Fernández, Santos et al. 2022, ART. 5). **179**

Figure 7.43. Influence of US power on (a) α-HCH and β-HCH conversion and TCBs'/HCH_0 ratio and (b) COCs conversion, dechlorination degree (Cl^-/Cl_0) and chlorine balance. T_{3h} = temperature reached at final reaction time. Operational conditions: $C_{HCHs,0}$ = 404 mg kg^{-1} (TS L2), W_S = 15 g, V_L/W_S = 2, molar NaOH:PS = 2, C_{PS} = 40 g L^{-1} (Table 7.11) (Checa-Fernández, Santos et al. 2022, ART. 5). **180**

Figure 7.44. Influence of initial C_{PS} on PS conversion. Operational conditions: $C_{HCHs,0}$ = 404 mg kg^{-1} (TS L2), W_S = 15 g, V_L/W_S = 2, molar NaOH:PS = 2, US power = 165 W (Table 7.11). Temperature at final reaction time (3 h), 67 ºC (Checa-Fernández, Santos et al. 2022, ART. 5). **182**

Figure 7.45. Influence of initial PS concentration on α-HCH and β-HCH conversion and TCBs'/HCH_0 degradation (a) and COCs conversion and dechlorination degree (Cl^-/Cl_0) (b). Operational conditions: $C_{HCHs,0}$ = 404 mg kg^{-1} (TS L2), W_S = 15 g, V_L/W_S = 2, molar NaOH:PS = 2, US power = 165 W (Table 7.11). T_{3h} = temperature reached at final reaction time, 67 ºC (Checa-Fernández, Santos et al. 2022, ART. 5). **183**

Figure 7.46. Effect of surfactants on COCs solubilization and $K_{d,COCs}$ (Eq. (7.20)) at pH = 7 (a and c) and pH > 12 (b and d, C_{NaOH} = 13.5 g L^{-1}). Final pH values (•). $C_{HCHs,0}$ = 373 mg kg^{-1} (TS L2). 15 g of soil and 30 g of aqueous phase. $C_{surfactant}$ = 10 g L^{-1} (Table 7.12) (Checa-Fernández, Santos et al. 2023, ART. 6). **187**

Figure 7.47. Effect of surfactants on COCs distribution (n_i in mmol) in soil and aqueous phases at a-c) pH_0 = 7 and d-f) pH_0 > 12. $C_{HCHs,0}$ = 373 mg kg^{-1} (TS L2). $C_{surfactant}$ = 10 g L^{-1} (Table 7.12) (Checa-Fernández, Santos et al. 2023, ART. 6). **189**

Figure 7.48. Effect of alkali concentration on COCs solubilization and $K_{d,COCs}$ (Eq. (7.20)) when using SDS (a-b), E3 (c-d), and T80 (e-f). Initial pH > 12 in all runs. Final pH values (•). $C_{HCHs,0}$ = 373 mg kg^{-1} (TS L2). C_{surf} = 10 g L^{-1} (Table 7.12) (Checa-Fernández, Santos et al. 2023, ART. 6). **190**

Figure 7.49. Effect of surfactant concentration on COCs solubilization and $K_{d,COCs}$ (Eq. (7.20)) when using SDS (a-b) and E3 (c-d). Final pH values (•). $C_{HCHs,0}$ = 373 mg kg^{-1} (TS L2). C_{NaOH} = 4 g L^{-1} (Table 7.12) (Checa-Fernández, Santos et al. 2023, ART. 6). **191**

Figure 7.50. Effect of successive solubilization cycles and V_L/W_S in the percentage of COCs removed from the soil with SDS (a) and E3 (b). $K_{d,COCs}$ (Eq. (7.20)) are included. Operational conditions summarized in Table 7.12 (Checa-Fernández, Santos et al. 2023, ART. 6). **193**

Figure 7.51. Evolution of COCs (mainly TCBs) (a), PS (b) conversion and pH (c) with reaction time when treating PEs (Table 7.13). C_{PS} = 40 g L^{-1}, NaOH:PS = 2, T = 40 ºC. (Checa-Fernández, Santos et al. 2023, ART. 6). **197**

Figure 7.52. Conversion of α-HCH, β-HCH and COCs, dechlorination degree (Cl^-/Cl_0) and PS consumption for remediation treatments (PS/T) and (PS/NaOH/T) applied on sample TS L2 (C_{HCHs} = 409 mg kg^{-1}). Operational conditions: C_{PS} = 60 g L^{-1}, T = 50 ºC, V_L/W_S = 2. PS/T = 17 days. PS/NaOH/T = 11 days (molar NaOH:PS = 2). **200**

Figure 7.53. pH values at initial and final reaction time in PS/T and PS/NaOH/T treatments. Operational conditions: C_{PS} = 60 g L^{-1}, T = 50 ºC, V_L/W_S = 2. PS/T = 17 days. PS/NaOH/T = 11 days (molar NaOH:PS = 2). **202**

Figure 7.54. Toxicity ($1/EC_{50,}$ Microtox® mBSPT) of the soil phase of the (a) reference (TS L0, Ref), polluted (TS L2) and soils treated by PS/T and PS/NaOH/T, and (b) the reference (Ref) soil before and after contact with NaOH (Ref+NaOH) (NaOH effect), and after the PS/NaOH/T treatment. **204**

Figure 7.55. Toxicity of aqueous phases (reaction supernatants and elutriates, BT) before (reference (TS L0) and polluted (TS L2) soils) and after applying the remediation processes (PS/T and PS/NaOH/T). ND: toxicity not detected. **205**

Figure 7.56. Toxicity of organic phases (aOSSST) of the reference topsoil (TS L0), polluted soil (TS L2) and treated soils after applying the remediation processes (PS/T and PS/NaOH/T). ND: toxicity not detected. **206**

Figure 7.57. Soil toxicity ($1/EC_{50,}$ Microtox® mBSPT) of the unpolluted, polluted and treated soils (Santos, García-Cervilla et al. 2022, ART. 7). **211**

Figure 7.58. Soil organic extract toxicity ($1/EC_{50}$, Microtox® aOSSST) (a) and COCs concentration (mg kg_{soil}^{-1}) (b) of the unpolluted, polluted, and treated soils (Santos, García-Cervilla et al. 2022, ART. 7). **213**

CHAPTER 9. ONGOING AND FUTURE WORK 229

Figure 9.1. Contaminant (HCH particles) addition to soil samples. **231**

Figure 9.2. Experimental device for treatment of soils P1, P2 and P3. **232**

Figure 9.3. Conversion of oxidant and HCH isomers when treating P1, P2 and P3 soils. **232**

Figure 9.4. Eggs (Artemio Pur®, left) and live (right) *Artemia salina*. **234**

Figure 9.5. Multiwell plate on a light table employed for Daphnia magna test. **235**

Figure 9.6. Synthesis of the bimetals Fe-Cu by mixing Fe and Cu microparticles (a) and subsequent disk milled (b). **237**

LIST OF ACRONYMS, ABBREVIATIONS, AND SYMBOLS

AOPs	advanced oxidation processes
BT	Basic test
BTEX	benzene, toluene, etilbenzene, xilene
C	coarse (soil particles)
CB	chlorobenzene
CHCs	chlorinated hydrocarbons
CI	confidence interval
CMC	critic micellar concentration
COC	chlorinated organic compound
DCB	Dichlorobenzene
DNAPL	dense non aqueous phase liquid
E3	surfactant E-Mulse® 3
EC_{50}	effective nominal concentration of toxicant that reduces the intensity of light emission by 50%
ECD	electron capture detector
EPA	Environmental Protection Agency
Eq	Equation
ESDAC	European Soil Data Center
F	fine (soil particles)
Fe-Cu	bimetallic particles
FID	flame ionization detector
GC	gas chromatography
HCH	Hexachlorocyclohexane
HeptaCH	Heptachlorocyclohexane
HCX	Hexachlorocyclohexene
HOC	hydrophobic organic compound
HP	hydrogen peroxide
I	light emitted by the bioluminescent bacteria
IC	ionic carbon
IC_{50}	sample dilution ratio that yields a 50% reduction of bacteria light emission
ISCO	in situ chemical Oxidation
ISTD	internal standard
L	pollution level
LNAPL	light non aqueous phase liquid
MAC	maximum allowable concentration
mBSPT	modified Basic Solid-Phase Test
MS	mass selective detector
NAPL	non aqueous phase liquid

ND	not detectable
OAS	osmotic adjustment solution
Ox	Oxidant
Ox/Ox_{stc}	ratio between the concentration of oxidant and the stoichiometric concentration of oxidant theoretically required for the COCs mineralization
PCB	Pentachlorobenzene
PCX	Pentachlorocyclohexene
PFAS	Polyfluoroalkylishigher-than-normal substances
PM	particulate matter
PMS	Peroxymonosulfate
POP	persistent organic pollutants
PS	Persulfate
PTFE	polytetrafluoroethylene, Teflon®
PV	pore volumen
SARGA	Sociedad Aragonesa de Gestión Agroambiental
SDS	surfactant sodium dodecyl sulfate
SE	soil elutriate
SEAR	surfactant enhanced aquifer remediation
S-ISCO	surfactant enhanced in situ chemical oxidation
SOE	soil organic extract
stc	Stoichiometric
SS	Subsoil
T	temperature (°C)
T80	surfactant Tween® 80
TC	total carbon
TCB	Trichlorobenzene
TCE	Trichloroethylene
TetraCB	Tetrachlorobenzene
TOC	total organic carbon
TS	Topsoil
TPH	total petroleum hydrocarbon
TUs	toxicity units
US	Ultrasounds
UV	ultra-violet
V_L	mass of aqueous phase (g)
V_L/W_S	mass ratio of aqueous phase/soil (g/g)
W_S	mass of solid phase (g)
X	Conversion
ZVI	zero-valent iron microparticles

Chapter 1.

STRUCTURE OF THE DOCTORAL THESIS

This Doctoral Thesis consists of the following chapters; the most relevant aspects discussed are detailed below.

i) **Summary**
ii) **Articles compounding the Doctoral Thesis**
iii) **Introduction**
iv) **Scopes and Aims**
v) **Materials and Methods**
vi) **Results and Discussion**
vii) **Conclusions**
viii) **Ongoing and Future work**
ix) **References**
x) **Appendices**

Detailed information about the **seven articles compounding the Doctoral Thesis** is summarized in the third chapter.

The **Introduction** aims to contextualize the current soil pollution problem, including different types of contamination and pollutants. Special attention has been paid to soils polluted with chlorinated organic compounds (COCs). Additionally, various existing alternatives for soil remediation are discussed. Particular relevance is given to chemical oxidation processes, including Advanced Oxidation Processes (AOPs).

Under these premises, the interest of this Doctoral Thesis is justified, and the main and specific objectives of the research are discussed in the **Scopes and Aims** section.

The reagents used are listed in the **Materials and Methods** chapter. Real soil samples and soil contaminants (HCH particulate matter and DNAPL samples) are also described. The experimental procedures used in this research are detailed. Finally, the analytical methods employed for soil and aqueous phases characterization are summarized.

In the **Results and Discussion** section, the main results obtained in the research conducted during the development of this Doctoral Thesis are summarized. This chapter is organized into three sections. i) Characterization of soil samples (topsoil (TS) and subsoil (SS)) and soil contaminants (HCH particulate matter and DNAPL). ii) Application of different oxidation treatments for the remediation of polluted TS. First, the application of different oxidants and activators has been evaluated. Subsequently, the intensification of the

alkaline activation of persulfate (PS/NaOH) treatment was studied by applying temperature, ultrasounds, and surfactants. iii) Acute toxicity evaluation of the treated soils.

In the **Conclusions** chapter, the original contributions of this Doctoral Thesis are summarized.

Ongoing and future work is detailed, including the work in progress and future challenges for the practical implementation of the technologies. The **references** are included in the last chapter.

Finally, two **Appendices** complete this study.

- **Appendix I** includes *other publications*, such as articles and book chapters, derived from this Doctoral Thesis and not included in the Results and Discussion section.
- **Appendix II** includes the *contributions to congresses* from the research performed.

Chapter 2.

SUMMARY/RESUMEN

2.1. Summary

This work is part of a broader research topic on developing effective remediation technologies for soils and groundwater contaminated with lindane wastes. It has been carried out in the labs of the **INPROQUIMA** Research Group (Department of Chemical Engineering and Materials at the Complutense University of Madrid).

The intensive use of **organochlorine pesticides** (OCPs) for agricultural pest control in the second half of the 20th century and the inadequate management of their wastes is a huge environmental problem. It has been progressively demonstrated their adverse effects on non-target organisms. Therefore, the Stockholm Convention banned the production and use of many OCPs. The characteristics of these compounds, such as high lipophilicity, bioaccumulation, and slow degradation, have resulted in water and soil contamination. Consequently, the awareness of the importance of soil pollution has increased in recent decades, and increasing research has been conducted on the remediation of polluted sites with OCPs. One of the most used OCPs was lindane (γ-Hexachlorocyclohexane (γ-HCH)), produced by the chlorination of benzene with UV. The **lindane production** during the last century has generated huge volumes of solid and liquid wastes, causing hot points of soil and groundwater contamination.

A noticeable case of lindane waste pollution is in the province of Huesca (Sabiñánigo, Spain), in the **Sardas and Bailín landfills**. In these sites, the company INQUINOSA discharged more than 100,000 tons of solid and liquid wastes illegally with a high content of HCHs and other organochlorine compounds, contaminating soil and groundwater in the surrounding. The discharge of solid wastes (**technical HCH**) caused the pollution of surface soil (**topsoil** (TS)), in which HCHs are found in the form of particulate matter and/or adsorbed onto soil particles. On the other hand, the lindane liquid waste was composed of more than 28 chlorinated organic compounds (COCs), from chlorobenzene to heptachlorocyclohexanes, forming a Dense Non-Aqueous Phase Liquid (DNAPL). The **DNAPL** dump in the landfill percolated by gravity through the subsoil, being adsorbed during this migration, generating **subsoil** (SS) and groundwater pollution.

Addressing these contamination cases requires a comprehensive long-term approach, including assessment, remediation, and prevention strategies. In this context, it is necessary to identify the type, location, and extent of the pollution and develop appropriate remediation technologies to mitigate the risks.

This Doctoral Thesis aims to evaluate the remediation of soils contaminated with COCs by applying different **chemical oxidation treatments**. This work has focused on surface soils (topsoil (TS)) polluted by solid lindane wastes from the old Bailín landfill (Sabiñánigo, Huesca, Spain). TS remediation by different on-site treatments has been proposed and validated. The **acute toxicity** of TS before and after applying these treatments has been deeply studied. Additionally, it has been assessed how different in situ oxidation treatments (previously selected) for subsoil (SS) remediation affected the SS acute toxicity.

Firstly, the **characterization of real polluted matrices** (Subsection 7.1), including i) polluted soils (TS and SS), ii) different sources of pollution (HCH particulate matter (TS) and DNAPL (SS)), and iii) aqueous phases in contact with the soils after partitioning equilibrium (simulating leachates (TS) and groundwater (SS)) have been performed. The physico-chemical composition, pollution level, and acute toxicity were evaluated, providing valuable information for future field applications of selected remediation treatments at the site.

Concerning physico-chemical properties, TS and SS were moderately alkaline soils with buffer capacity due to the significant content of carbonates (such as calcium carbonate). The content of metals (Fe, Ca, Na, and Al), which can contribute to the decomposition of oxidants, especially hydrogen peroxide, was not negligible. In TS samples, only a low percentage of total organic carbon (TOC) measured corresponds to COCs, the rest of the organic matter being attributable to natural organic matter as humic acid-like compounds. On the contrary, in SS samples, the TOC was mainly due to the COCs content.

In addition, the sources of contamination (HCH particulate matter and DNAPL) and the concentration of contaminants in TS and SS samples have been characterized. The solid wastes generated during lindane manufacturing (HCH particulate matter) were mainly composed of α-HCH (83%) and β-HCH (9%), whereas low concentrations of the other HCHs isomers (Σγ, δ, ε-HCH (8%)) were measured. TS samples were mainly polluted by HCHs isomers, with a distribution of 75% of α-HCH and 22% of β-HCH, with a total HCHs concentration ranging from 40 to 1150 mg kg_{soil}^{-1}. These results confirmed that the TS pollution was primarily due to the presence of HCH particulate matter, with a small contribution of these pollutants adsorbed into the soil. The concentration of HCHs in the elutriates (leachates) ranged from 0.1 to 10.9 mg L^{-1} and increased with increasing COCs concentration in soil, although the low solubility of these compounds limited this value.

The liquid waste (DNAPL) was composed of more than 28 COCs, from chlorobenzene to heptachlorocyclohexanes, and the same COCs were present in the SS samples, with significantly higher concentration (500-9500 mg kg^{-1}) than in TS. Following the same trend, SS elutriates (simulating groundwater) presented a higher value of COCs solubilized (40-50 mg L^{-1}) due to the higher solubility of COCs from DNAPL than HCH particulate matter.

The acute toxicity of all the polluted matrices has been evaluated by applying three complementary Microtox® tests (developed or modified in this Doctoral Thesis) i) Basic Test (BT) for aqueous samples, ii) modified Basic Solid-Phase Test (mBSPT), for solid samples, and iii) adapted Organic Solvent Sample Solubilization test (aOSSST) for organic extracts. Thus, a complete overview of the acute toxicity of these polluted sites was obtained. Soil samples (TS and SS) presented high acute toxicity in the Microtox® mBSPT, increasing with higher COCs concentration in the soil. In the same way, the toxicity of soil elutriates (Microtox® BT) was well correlated to dissolved COCs. In line with the higher COCs presence, SS elutriates (simulated groundwater) presented higher acute toxicity than those corresponding to TS (simulated surface leachates). The results obtained when analyzing the organic extracts (Microtox® aOSSST) represented more plainly the acute toxicity of these soils, as this method is not limited by COCs solubility in water.

Different **on-site oxidation treatments** were evaluated for the remediation of contaminated TS (Subsection 7.2). It should be highlighted that bioremediation cannot be applied due to the high contamination levels in TS in the most polluted areas of the Bailín landfill (C_{HCHs} > 400 mg kg_{soil}^{-1}), and other technologies must be used as the first steps.

First, the **oxidant** system has been selected considering its effectiveness in COCs removal and its stability in the soil system studied (Subsection 7.2.1). For that purpose, a comprehensive understanding of the variables influencing the rate of chemical reactions involved in the oxidation processes occurring in both aqueous and soil phases has been performed. Thus, the evolution of parent pollutants, byproducts, and oxidants over reaction time has been analyzed. Considering the physico-chemical characteristics of the soil (high carbonate content) and the pollutants nature, hydrogen peroxide (**HP**) was discarded due to excessive unproductive consumption of the oxidant and iron precipitation. Persulfate (**PS**) was the oxidizing agent selected due to its high aqueous solubility, lower affinity for natural soil organic compounds, higher stability in the soil system studied, ease of handling, etc.

To enhance the COCs oxidation, applying different **PS activations** such as **alkali** (NaOH, 20 ºC) and **temperature** (40 ºC), which increase the generation of radicals (sulfate, hydroxyl, and superoxyl radicals, depending on the activation method), was evaluated (Subsection 7.2.2). The thermal activation of PS (PS/T, 40ºC) led to moderate COCs conversions due to the low HCHs solubility and their refractoriness towards oxidation by $SO_4^{\bullet-}$. The increase in reaction temperature (from 20 to 80 ºC) and oxidant concentration (from 10 to 80 g L^{-1}) played a fundamental role in the PS/T treatment, increasing the production of sulfate radicals and decreasing the chlorinated byproducts. Under the selected treatment conditions (55 °C, C_{PS} = 80 g L^{-1}, V_L/W_S = 2/1, 100 rpm and 9 days) a degradation of HCHs around 83% was achieved in the absence of chlorinated by-products (chlorine balance ≈ 100%).

Under alkaline conditions (pH > 12, PS/NaOH system), HCHs were dehydrochlorinated to a mixture of trichlorobenzenes (TCBs). The TCBs generated have a higher solubility in water than HCHs and are more easily oxidable. Consequently, the conversion of COCs increased significantly under these conditions. The β-HCH isomer was more recalcitrant to dehydrochlorination than α-HCH, being the limiting step of the process. Thus, the reaction times required to achieve acceptable COC conversion were high. Different alternatives for the **intensification of the PS/NaOH treatment** have been studied (Subsection 7.2.3): i) temperature (PS/NaOH/T), ii) ultrasound (PS/NaOH/US), and iii) surfactant (S/PS/NaOH/T). A comprehensive approach has been extensively conducted to assess the influence of the main operating conditions (reagent addition order, temperature or US power, aqueous/soil ratio, initial concentration of PS, and stirring rate) on the COCs degradation efficiency.

In the case of the PS/NaOH treatment intensification by **temperature** application, the selected conditions imply a simultaneous addition of reagents (PS and NaOH), T = 50 °C, C_{PS} = 40 g L^{-1}, V_L/W_S = 2, pH > 12, achieving 100% and 81% of α-HCH and β-HCH conversion (3 days), 94% of dechlorination degree and COCs conversion (no chlorinated byproducts) and 29% of PS consumption. The intensification of PS/NaOH by temperature application resulted in a promising option to reduce the reaction time considerably.

The PS/NaOH intensification by **US** application increased the efficiency of the process due to i) the enhanced desorption of the pollutants from the soil to the aqueous phase, ii) the increase in radical production, and iii) the improved oxidation kinetics. When increasing the US power and the initial concentration of PS, the degradation of HCHs and dechlorination increased. At selected operating conditions (V_L/W_S = 2, C_{PS} = 60 g L^{-1},

NaOH/PS = 2, 165 W), a conversion and dechlorination degree of pollutants of 94% and 74% were achieved in only 3 h of reaction time, significantly reducing the reaction time required.

To conclude evaluating different possibilities for the intensification of the PS/NaOH treatment, the **surfactant** (SDS, E3 and T80) application has been assessed. pH conditions, NaOH, and surfactant concentration remarkably affected the pollutants solubilization efficiency, obtaining the highest COCs solubilization at alkaline conditions (pH > 12), moderate NaOH concentration (4 g L^{-1}), and high surfactant concentration (10 g L^{-1}). By applying optimal solubilization conditions (SDS or E3 (5 g L^{-1}), pH > 12, simultaneous addition of reagents, V_L/W_S = 2 and 3 successive solubilization cycles of 24 h), more than 80% of COCs were extracted from the soil. The resulting emulsion has been treated by the PS/NaOH/T (C_{PS} = 40 g L^{-1}, NaOH: PS = 2, and T = 40 ºC). COCs conversions of 96% were achieved in 72 h when SDS emulsions were treated, highlighting the suitability of the integrated surfactant-enhanced solubilization and emulsion treatment process.

Finally, the possible adverse effects of the on-site treatments applied for soil remediation on **acute toxicity** (associated with high concentrations of reagents, generation of by-products, etc.) have been assessed. In this regard, the acute toxicity of TS after the application of PS/T and PS/NaOH/T treatments and SS after ISCO (PS/NaOH) and S-ISCO (S/PS/NaOH) treatments have been evaluated using Microtox® bioassay (subsection 7.3). After the thermal activation of PS (PS/T), the acute toxicity of the TS (Microtox® mBST) was reduced to the minimum level. Additionally, neither the reaction supernatant nor its aqueous leachate (Microtox® BT) exhibited toxicity. Similarly, a significant soil organic extract toxicity (Microtox® aOSSST) reduction was obtained after the remediation treatment. The soil organic matter, mainly attributable to humic acid-type compounds, was resistant to the oxidation treatment and the pH remained unaltered. Thus, the application of a bioremediation post-treatment after the chemical process seems feasible.

The PS/NaOH/T treatment did not contribute to the acute toxicity of TS, with similar values before and after treatment (Microtox® mBSPT). Since a high conversion of COCs was obtained (X_{COCs} = 98%), the fact that this is not reflected in a reduction of the acute toxicity may be attributed to the high NaOH concentration used (and the V_L/W_S ratio). Thus, a more thorough washing of the soils after alkaline treatment would be necessary from the acute toxicity point of view. The aqueous reaction supernatant (PS/NaOH/T treatment) presented a non-negligible toxicity level, justified by the presence of TCBs

(compounds more soluble and with higher acute toxicity than HCHs). However, the toxicity of this soil elutriate was low (low TCBs concentration).

In the case of SS treated by ISCO and S-ISCO, the soil acute toxicity significantly decreased. Neither the application of the surfactant (E3) nor its concentration (within the concentration range studied) generates acute toxicity in the treated soil. Thus, the proposed in situ treatments (ISCO or S-ISCO, with alkaline activation of PS) could be suitable for a full-scale application.

It should be highlighted that further research should be conducted to assess the toxicity in the presence of other organisms and trophic levels (such as *Artemia salina*, *Daphnia magna*, etc.) and biodegradability assays to obtain a more representative conclusion before practical implementation.

2.2. Resumen

Este trabajo forma parte de una extensa línea de investigación centrada en el desarrollo de tecnologías eficaces para la remediación de suelos y aguas subterráneas contaminados con residuos procedentes de la fabricación de lindano. Se ha llevado a cabo en los laboratorios del Grupo de Investigación **INPROQUIMA** (Departamento de Ingeniería Química y de Materiales, de la Universidad Complutense de Madrid).

El intensivo uso de **pesticidas organoclorados** (OCPs) durante la segunda mitad del siglo XX, así como la inadecuada gestión de sus residuos, ha generado un gran problema medioambiental. Los efectos adversos de estos compuestos en la salud humana han sido recientemente demostrados. Por ello, con el fin de proteger el medio ambiente y la salud humana, el Convenio de Estocolmo prohibió tanto la producción como el uso de muchos de estos pesticidas. Las características de estos compuestos, como su baja solubilidad, potencial bioacumulación, alta persistencia y baja biodegradabilidad, han provocado la contaminación de grandes volúmenes de aguas y suelos. En este contexto, la investigación llevada a cabo para la remediación de emplazamientos contaminados con OCPs ha aumentado significativamente en las últimas décadas. Uno de los pesticidas organoclorados más empleado fue el lindano (γ-Hexaclorociclohexano (γ-HCH)), producido mediante la cloración del benceno con UV. El proceso de **producción de lindano** es muy ineficiente, por lo que se generaron miles de toneladas de residuos, sólidos y líquidos. El vertido incontrolado de estos residuos durante las últimas décadas ha generado importantes focos de contaminación, tanto del suelo, como de las aguas subterráneas.

Uno de los casos de contaminación por residuos de la fabricación de lindano más notorios de Europa se encuentra en la provincia de Huesca (Sabiñánigo, España), en los **vertederos de Sardas y Bailín**. En estos emplazamientos, la empresa INQUINOSA vertió ilegalmente más de 100.000 toneladas de residuos sólidos y líquidos con un alto contenido en HCHs y otros compuestos organoclorados, provocando la contaminación de amplias superficies de suelo y agua subterránea. El vertido de residuos sólidos (**HCH técnico**) provocó la contaminación del **suelo superficial** (*topsoil* (TS)), en el que la contaminación se encuentra en forma de materia particulada de HCHs y/o adsorbida en el suelo. Por otra parte, los residuos líquidos (generados en reacciones fallidas y en las colas de destilación del proceso de purificación) están constituidos por un total de 28 compuestos orgánicos clorados (COCs), desde

clorobenceno hasta heptaclorociclohexanos, de baja solubilidad, formando una fase densa líquida no acuosa (DNAPL). El **DNAPL** se filtró por acción de la gravedad a través del subsuelo, siendo adsorbido durante esta migración, y generando la contaminación del **subsuelo** (SS) y, por lo tanto, de las aguas subterráneas de estos emplazamientos.

Abordar estos complejos casos de contaminación requiere un enfoque global a largo plazo, que incluya estrategias de evaluación, remediación y prevención. En este contexto, es necesario identificar el tipo, la ubicación y el alcance de la contaminación y desarrollar tecnologías de remediación adecuadas para mitigar los riesgos.

Esta Tesis Doctoral tiene como principal objetivo evaluar la remediación de suelos y sedimentos contaminados con COCs mediante la aplicación de diferentes **tratamientos de oxidación química**. La tesis se ha centrado en la descontaminación de suelos superficiales (*topsoil* (TS)) procedentes del antiguo vertedero de Bailín (Sabiñánigo, Huesca, España) contaminados por residuos sólidos de la fabricación del lindano. Se ha propuesto y validado la remediación de los suelos mediante diferentes tratamientos de oxidación on-site. Por otro lado, se ha estudiado la **toxicidad aguda** (Microtox®) del suelo antes y tras la aplicación de los tratamientos de remediación seleccionados como más adecuados. Finalmente, se ha evaluado la toxicidad aguda de los suelos tras la aplicación de diferentes tratamientos de oxidación in situ previamente seleccionados para la remediación del subsuelo (SS).

En primer lugar, se ha llevado a cabo la **caracterización** de todas las **matrices reales** implicadas (subsección 7.1), incluyendo i) los suelos contaminados (TS y SS), ii) las diferentes fuentes de contaminación (partículas de HCH (TS) y DNAPL (SS)), y iii) las fases acuosas en contacto con los suelos tras el equilibrio de partición (simulando lixiviados y aguas subterráneas del emplazamiento contaminado). Esta caracterización evalúa la composición fisicoquímica, el nivel de contaminación y la toxicidad aguda, proporcionando información relevante para la futura aplicación de los tratamientos de remediación seleccionados en el emplazamiento.

En cuanto a las propiedades fisicoquímicas, TS y SS son suelos moderadamente alcalinos con capacidad buffer, debido al importante contenido de carbonatos (principalmente en forma de carbonato cálcico) que presentan. La concentración en metales (Fe, Ca, Na, y Al), no fue despreciable. Cabe destacar que éstos son potencialmente activos en la descomposición de oxidantes, especialmente el peróxido de hidrógeno. En el caso de TS, sólo un bajo porcentaje del carbono orgánico total

(COT) medido corresponde a los COCs presentes en el suelo, siendo el resto atribuible a su contenido en materia orgánica natural (ácidos húmicos, etc.). Por el contrario, en el caso de SS, el COT medido es atribuible principalmente al contenido de COCs.

Además, se han caracterizado las fuentes de contaminación (materia particulada de HCHs y DNAPL) y la concentración de COCs de los diferentes niveles de contaminación de los suelos. Los residuos sólidos generados en la fabricación de lindano (materia particulada de HCH) están compuestos principalmente de α-HCH (83%), β-HCH (9%), y bajas concentraciones de otros isómeros HCH (Σγ,δ,ε-HCH (8%)). Los distintos niveles de contaminación de las muestras de TS presentaron una distribución de contaminantes del 75% de α-HCH y 22% de β-HCH, con una concentración total de HCHs que osciló entre 40 y 1150 mg kg_{suelo}^{-1}. Estos resultados confirman que la contaminación del TS se debe principalmente a la presencia de partículas de HCH, con una pequeña contribución de estos contaminantes adsorbidos en el suelo. La concentración de HCHs en los elutriatos (lixiviados) osciló entre 0.1 y 10.9 mg L^{-1}, aumentando al aumentar la concentración de HCHs en el suelo.

Los COCs identificados en el DNAPL fueron también detectados en las muestras de SS, con una concentración de contaminantes (500-9500 mg kg^{-1}) significativamente mayor que en el caso del TS. Siguiendo la misma tendencia, los elutriados del SS (simulando la composición de las aguas subterráneas del emplazamiento) presentaron una mayor concentración de COCs (40-50 mg L^{-1}) que los del TS debido a la mayor solubilidad de los COCs presentes en el DNAPL que en las partículas de HCH.

Para completar la caracterización de todas las matrices en estudio se ha evaluado su **toxicidad aguda** mediante el método de **Microtox®**, aplicando tres ensayos complementarios (desarrollados o adaptados en la presente investigación): i) "basic test" (BT), para muestras líquidas ii) "modified Basic Solid Phase Test" (mBSPT), para muestras sólidas y iii) "adapted Organic Solvent Sample Solubilization Test" (aOSSST) para extractos orgánicos. Las muestras de suelo (TS y SS) presentaron una elevada toxicidad aguda (Microtox® mBSPT), aumentando ésta al aumentar la concentración de COCs en el suelo. Del mismo modo, la toxicidad de los elutriados del suelo (Microtox® BT) se correlacionó con la concentración de COCs disueltos. En consonancia con la mayor presencia de COCs en SS, los elutriados de este suelo (agua subterránea simulada) presentaron una toxicidad aguda mayor que los correspondientes a TS (lixiviados superficiales simulados). La toxicidad de los extractos orgánicos (metanol) confirmó los resultados anteriores y resultó ser el método más

fiable para determinar la toxicidad de suelos contaminados con compuestos orgánicos hidrófobos.

Posteriormente, se han evaluado diferentes **tratamientos de oxidación on-site** para la remediación de TS contaminados con HCHs (subsección 7.2). Cabe destacar que debido a los altos niveles de contaminación del TS en las zonas más contaminadas del vertedero de Bailín (C_{HCHs} > 400 mg kg_{suelo}^{-1}), no podría aplicarse directamente un tratamiento de biorremediación, siendo necesario utilizar tecnologías químicas.

En primer lugar, se ha seleccionado el **oxidante** (peróxido de hidrógeno (**HP**) y persulfato de sodio (**PS**)), teniendo en cuenta su eficacia en la eliminación de COCs y su estabilidad en el suelo (subsección 7.2.1). Para ello, se ha llevado a cabo un estudio exhaustivo de las variables implicadas en los procesos de oxidación que tienen lugar tanto en fase acuosa como en el suelo. Se ha analizado la evolución a lo largo del tiempo de reacción de los contaminantes, los intermedios de reacción generados y la concentración de oxidante. Considerando las características físico-químicas del suelo (alto contenido en carbonatos) y la naturaleza de los contaminantes, se descartó el uso del peróxido de hidrógeno (activado por Fe, proceso Fenton) debido al excesivo consumo improductivo del oxidante y a la precipitación de hierro (asociada al pH). Se seleccionó como oxidante más adecuado el persulfato (PS) debido a su alta solubilidad acuosa, mayor estabilidad en el suelo, facilidad de manejo, etc.

Para aumentar el grado de degradación de los COCs se evaluaron diferentes alternativas para **activar el PS**, como la adición de **álcali** (NaOH, 20 ºC) y la aplicación de **temperatura** (40 ºC). La activación del PS aumenta la generación de radicales (sulfato, hidroxilo y superóxido, en función del tipo de activación), especies capaces de degradar los compuestos orgánicos (subsección 7.2.2). La activación térmica de persulfato condujo a una conversión moderada de COCs debido principalmente a la baja solubilidad de los HCHs y a su refractariedad a la oxidación por los radicales $SO_4^{\bullet-}$. Tanto la temperatura de reacción (de 20 a 80 ºC), como la concentración de oxidante (de 10 a 80 g L^{-1}) jugaron un papel fundamental en el tratamiento PS/T, aumentando la producción de radicales sulfato y disminuyendo la concentración de intermedios de reacción. Bajo las condiciones de tratamiento seleccionadas (55 ºC, C_{PS} = 80 g L^{-1}, V_L/W_S = 2/1, 100 rpm y 9 días) se consiguió una degradación de HCHs en torno al 83% en ausencia de subproductos clorados (balance de cloro ≈ 100%).

En condiciones alcalinas (pH > 12, sistema PS/NaOH), se produce la hidrodecloración de los HCHs a triclorobencenos (TCBs). Los TCBs generados presentan mayor solubilidad en agua que los HCHs y son más fácilmente oxidables, por lo que la conversión de COCs aumenta significativamente en estas condiciones. El isómero β-HCH es más recalcitrante a la hidrodecloración que α-HCH, siendo la etapa limitante del proceso. De este modo, los tiempos de reacción necesarios para alcanzar conversiones de COCs aceptables fueron elevados. Por este motivo se han estudiado diferentes alternativas de **intensificación del tratamiento PS/NaOH** (subsección 7.2.3): i) temperatura (PS/NaOH/T), ii) ultrasonidos (PS/NaOH/US) y iii) surfactante (S/PS/NaOH/T). Se ha llevado a cabo un estudio exhaustivo para evaluar la influencia de las principales condiciones de operación en la degradación de COCs tales como el orden de adición de los reactivos, temperatura o potencia de US, relación fase acuosa/suelo, concentración inicial de PS y velocidad de agitación, entre otras.

En el caso de la intensificación del tratamiento PS/NaOH mediante la aplicación de **temperatura**, las condiciones seleccionadas implican una adición simultánea de reactivos (PS y NaOH), T = 50 °C, C_{PS} = 40 g L^{-1}, V_L/W_S = 2 y pH > 12, consiguiendo un 100% y 81% de conversión de α-HCH y β-HCH, respectivamente, un 94% de degradación de COCs y decloración y una conversión de COCs (ausencia de intermedios de reacción) y un 29% de consumo de PS (3 días de tratamiento). De este modo, la intensificación del proceso PS/NaOH con temperatura resultó ser una opción prometedora, con resultados atractivos desde el punto de vista de eliminación de contaminantes y tiempos de reacción asumibles.

La intensificación del proceso PS/NaOH mediante la aplicación de **US** aumentó la eficiencia del proceso debido a que i) la desorción de los COCs (principalmente TCBs) del suelo a la fase acuosa se ve favorecida, ii) se produce un aumento de la producción de radicales, y iii) se mejora la cinética de oxidación. Al aumentar la potencia de US y la concentración de PS, mejora la degradación de los HCHs y el grado de decloración. En las condiciones de operación seleccionadas (V_L/W_S = 2, C_{PS} = 60 g L^{-1}, NaOH/PS = 2, 165 W), se alcanzó una conversión y decloración de contaminantes del 94% y 74%, respectivamente, en tan sólo 3 h de reacción, reduciendo significativamente el tiempo de tratamiento requerido.

Para concluir la intensificación del tratamiento PS/NaOH, se ha evaluado la aplicación de **surfactantes** (SDS, E3 y T80) con el fin de solubilizar los COCs del suelo y tratar posteriormente las emulsiones contaminadas. El pH y la concentración de

NaOH y surfactante afectaron notablemente a la eficiencia de solubilización de los COCs, obteniéndose la mayor solubilización de contaminantes al trabajar a pH alcalino (>12), con una concentración moderada de NaOH (pH>12, 4 g L^{-1}) y una elevada concentración de surfactante (10 g L^{-1}). Bajo las condiciones óptimas de solubilización (SDS o E3 (5 g L^{-1}), pH > 12, adición simultánea de reactivos, V_L/W_S = 2 y 3 ciclos sucesivos de solubilización de 24 h), se consiguió solubilizar más del 80% de los COCs presentes en el suelo. La emulsión resultante se trató mediante el proceso PS/NaOH/T (C_{PS} = 40 g L^{-1}, NaOH: PS = 2, y T = 40 °C). Se alcanzaron conversiones de COCs > 95% (72 h) en el caso de las emulsiones de SDS, lo que pone de manifiesto la idoneidad del proceso integrado de mejora de la solubilización de COCs mediante aplicación de surfactante y el posterior tratamiento de la emulsión.

Por último, se ha evaluado el posible efecto adverso de los tratamientos aplicados (asociados a la elevada concentración de reactivos, la generación de intermedios de oxidación, etc.), en la **toxicidad aguda de los suelos**. En este sentido, se ha evaluado la toxicidad aguda del TS tras los tratamientos PS/T y PS/NaOH/T y del SS tras los tratamientos ISCO (PS/NaOH) y S-ISCO (S/PS/NaOH) mediante el bioensayo Microtox® (subsección 7.3). La toxicidad del TS (Microtox® mBSPT) se redujo a valores equivalentes a los correspondientes con el suelo limpio tras la activación térmica del PS (PS/T). Además, ni el sobrenadante de la reacción ni su lixiviado acuoso (Microtox® BT) mostraron toxicidad. De forma similar, se obtuvo una reducción significativa de la toxicidad del extracto orgánico del suelo tras el tratamiento de remediación (Microtox® aOSSST). La materia orgánica del suelo, atribuible principalmente a compuestos de tipo ácido húmico, fue resistente al tratamiento de oxidación y el pH del suelo no se modificó. Por lo tanto, la aplicación de un tratamiento de biorremediación posterior al tratamiento químico parece factible.

El tratamiento PS/NaOH/T no aportó toxicidad aguda al suelo, obteniéndose valores similares antes y después del tratamiento (Microtox® mBSPT). Dado que se obtuvo una elevada conversión de COCs (X_{COCs} = 98%), el hecho de que esto no se refleje en una reducción de la toxicidad aguda puede atribuirse a la elevada concentración de NaOH empleada (y la relación V_L/W_S). Así, desde el punto de vista de la toxicidad aguda, sería necesario un lavado más exhaustivo de los suelos después del tratamiento alcalino. El sobrenadante acuoso de reacción (tratamiento PS/NaOH/T) presentó un nivel de toxicidad no despreciable, justificado por la presencia de TCBs

(compuestos más solubles y con mayor toxicidad aguda que los HCHs). Sin embargo, la toxicidad del elutriado de este suelo fue baja (baja concentración de TCBs).

Los tratamientos ISCO (PS/NaOH) y S-ISCO (E3/PS/NaOH) del subsoil (SS) condujeron a una reducción significativa de la toxicidad aguda (Microtox® mBSPT). Se puede concluir que ni la aplicación del surfactante empleado (E3) ni su concentración (dentro del rango estudiado) generan toxicidad aguda en el suelo tratado. Así pues, los tratamientos in situ propuestos (ISCO o S-ISCO) resultan adecuados para la remediación a gran escala de los suelos contaminados con DNAPL.

Cabe destacar que deberían realizarse medidas adicionales para evaluar la toxicidad de los suelos (así como sus elutriados y extractos orgánicos) en presencia de otros organismos y niveles tróficos (*Artemia salina*, *Daphnia magna*, etc.) y ensayos de biodegradabilidad para obtener una conclusión más representativa previa a la aplicación a escala real de los procesos de remediación estudiados.

Chapter 3.

ARTICLES COMPOUNDING THE DOCTORAL THESIS

This doctoral Thesis is presented as a Compendium of Publications in the PhD Program. **Seven papers** related to the topic presented in the Thesis Research Plan and approved by the Academic Committee of the Chemical Engineering Doctoral Program have been published in JCR-indexed journals. The information (title, authors, journal name, cites, year of publication, DOI, and quartile) and the first and last page of each article are detailed below.

ARTICLE 1

Title: Comprehensive study of acute toxicity using Microtox® bioassay in soils contaminated by lindane wastes
Authors: C. M. Domínguez, P. Ventura, **A. Checa-Fernández**, A. Santos.
Journal: Science of The Total Environment
Publication year: 2023
Volume, Page: 856, 159146
DOI: 10.1016/j.scitotenv.2022.159146
Quartile (Area): Q1 (Environmental Engineering)
Cited by (SCOPUS): 4

Science of the Total Environment 856 (2023) 159146

Contents lists available at ScienceDirect

Science of the Total Environment

journal homepage: www.elsevier.com/locate/scitotenv

Comprehensive study of acute toxicity using Microtox® bioassay in soils contaminated by lindane wastes

Carmen M. Domínguez *, Paula Ventura, Alicia Checa-Fernández, Aurora Santos

Dpto. Ingeniería Química y de Materiales, Facultad de Ciencias Químicas, Universidad Complutense Madrid, Ciudad Universitaria S/N, 28040 Madrid, Spain

HIGHLIGHTS

- Acute toxicity evaluation of soils contaminated with lindane wastes.
- Three Microtox ® bioassays: Soils, soil elutriates and soil organic extracts.
- The higher the concentration of the pollutants, the higher toxicity.
- Acute toxicity caused by DNAPL (subsoil) is greater than that of HCHs (topsoil).
- Soils, organic extracts, and subsoil elutriates presented high toxicity.

GRAPHICAL ABSTRACT

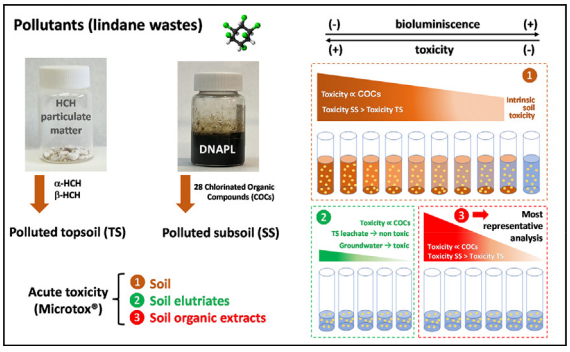

ARTICLE INFO

Editor: Frederic Coulon

Keywords:
HCHs
DNAPL
Lindane wastes
Ecotoxicity
Polluted soil

ABSTRACT

This research studies the acute toxicity of real contaminated soils (topsoil and subsoil) with hazardous chlorinated organic compounds (COCs) from lindane manufacturing wastes. The Microtox® bioassay was used to determine the toxicity of soils (*modified Basic Solid Phase Test*), soil elutriates (*Basic Test*), and organic extracts (*adapted Organic Solvent Sample Solubilization Test*), in which hydrophobic organic compounds are soluble. The acute toxicity of these persistent contaminants (hexachlorocyclohexanes, HCH isomers, as particulate matter in topsoil, and COCs, from dense non-aqueous phase liquid, DNAPL, in subsoil) and the commercial compounds were also measured. Soils tested showed different contaminant levels (topsoil: 0.9–1149 mg/kg and subsoil: 20–9528 mg/kg). Soil contaminants distribution, concentration and acute toxicity were highly related to the contamination source (HCHs or DNAPL). Soils, organic extracts, and subsoil elutriates presented high toxicity, highlighting the need for remediation of these sites. EC_{50} was calculated in the three-test applied for the soils tested. EC_{50} vs. COCs concentration in soils and soil elutriates showed an asymptotic trend, explained by the low pollutants solubility in the aqueous phase. Contrarily, EC_{50} vs. soil COCs concentration was more linear in the case of the organic extracts. This test was the most reliable from statistical analysis. The three methods reveal interesting and complementary information and are necessary for a complete overview of the acute toxicity of contaminated soils.

1. Introduction

Lindane (the gamma isomer of 1,2,3,4,5,6-hexachlorocyclohexane, γ-HCH) was a broad-spectrum insecticide extensively produced in Europe during the second half of the 20th century (Vega et al., 2016). For each tonne of lindane produced, approximately 6–10 t of other waste HCH-isomers without insecticidal properties were generated (mainly α-HCH and β-HCH). These wastes were usually dumped in the vicinity of production sites, originating an environmental problem of great magnitude (Santos et al., 2018a, 2018b). One of the most severe cases of lindane waste pollution is located in the province of Huesca (Sabiñánigo, Spain), in Sardas

* Corresponding author.
E-mail address: carmdomi@ucm.es (C.M. Domínguez).

http://dx.doi.org/10.1016/j.scitotenv.2022.159146
Received 15 August 2022; Received in revised form 26 September 2022; Accepted 27 September 2022
Available online 01 October 2022

Appendix A. Supplementary data

Supplementary data to this article can be found online at https://doi.org/10.1016/j.scitotenv.2022.159146.

References

Baran, A., Tarnawski, M., Koniarz, T., Szara, M., 2019. Content of nutrients, trace elements, and ecotoxicity of sediment cores from Rożnów reservoir (Southern Poland). Environ. Geochem. Health 41 (6), 2929–2948.

Bond, G.P., Martin, J., 2005. Microtox. In: Wexler, P. (Ed.), Encyclopedia of Toxicology, Second edition Elsevier, New York, pp. 110–111.

Campisi, T., Abbondanzi, F., Casado-Martinez, C., DelValls, T., Guerra, R., Iacondini, A., 2005. Effect of sediment turbidity and color on light output measurement for Microtox® Basic Solid-Phase Test. Chemosphere 60 (1), 9–15.

Checa-Fernández, A., Santos, A., Romero, A., Domínguez, C.M., 2021. Remediation of real soil polluted with hexachlorocyclohexanes (α-HCH and β-HCH) using combined thermal and alkaline activation of persulfate: optimization of the operating conditions. Sep. Purif. Technol. 270, 118795.

Checa-Fernández, A., Santos, A., Conte, L.O., Romero, A., Domínguez, C.M., 2022. Enhanced remediation of a real HCH-polluted soil by the synergetic alkaline and ultrasonic activation of persulfate. Chem. Eng. J. 440, 135901.

Corporation, M., 1995. Microtox® Acute Toxicity Basic Test Procedures Carlsbad, CA.

Čvančarová, M., Křesinová, Z., Cajthaml, T., 2013. Influence of the bioaccessible fraction of polycyclic aromatic hydrocarbons on the ecotoxicity of historically contaminated soils. J. Hazard. Mater. 254–255, 116–124.

Doe, K., Jackman, P., Scroggins, R., McLeay, D., Wohlgeschaffen, G., 2005. Solid-phase test for sediment toxicity using the luminescent bacterium, Vibrio fischeri. Small-scale Freshwater Toxicity Investigations. Springer, pp. 107–136.

Doherty, F.G., 2001. A review of the Microtox® toxicity test system for assessing the toxicity of sediments and soils. Water Qual.Res.J. 36 (3), 475–518.

Dominguez, C.M., Checa-Fernandez, A., Romero, A., Santos, A., 2021. Degradation of HCHs by thermally activated persulfate in soil system: effect of temperature and oxidant concentration. J.Environ.Chem.Eng. 9 (4), 105668.

Dominguez, C.M., Romero, A., Checa-Fernandez, A., Santos, A., 2021. Remediation of HCHs-contaminated sediments by chemical oxidation treatments. Sci. Total Environ. 751, 141754.

Fernández, J., Arjol, M.A., Cacho, C., 2013. POP-contaminated sites from HCH production in Sabiñánigo, Spain. Environ. Sci. Pollut. Res. 20 (4), 1937–1950.

García-Cervilla, R., Santos, A., Romero, A., Lorenzo, D., 2020. Remediation of soil contaminated by lindane wastes using alkaline activated persulfate: kinetic model. Chem. Eng. J. 393, 124646.

Garcia-Cervilla, R., Santos, A., Romero, A., Lorenzo, D., 2021. Partition of a mixture of chlorinated organic compounds in real contaminated soils between soil and aqueous phase using surfactants: influence of pH and surfactant type. J.Environ.Chem.Eng. 9 (5), 105908.

Garcia-Cervilla, R., Santos, A., Romero, A., Lorenzo, D., 2022. Abatement of chlorobenzenes in aqueous phase by persulfate activated by alkali enhanced by surfactant addition. J. Environ. Manag. 306, 114475.

Garg, N., Lata, P., Jit, S., Sangwan, N., Singh, A.K., Dwivedi, V., Niharika, N., Kaur, J., Saxena, A., Dua, A., Nayyar, N., Kohli, P., Geueke, B., Kunz, P., Rentsch, D., Holliger, C., Kohler, H.-P.E., Lal, R., 2016. Laboratory and field scale bioremediation of hexachlorocyclohexane (HCH) contaminated soils by means of bioaugmentation and biostimulation. Biodegradation 27 (2), 179–193.

ISO, W., 1998. Determination of the inhibitory effect of water samples on the light emission of vibrio fischeri (luminescent bacteria test). Iso 11348-1, 2 and 3, 1-21.

Kaiser, K.L., Palabrica, V.S., 1991. Photobacterium phosphoreum toxicity data index. Water Qual.Res.J. 26 (3), 361–431.

Kwan, K., Dutka, U.B., 1990. Simple two-step sediment extraction procedure for use in genotoxicity and toxicity bioassays. Toxic. Assess. 5 (4), 395–404.

Kwan, K.K., Dutka, B.J., 1995. Comparative assessment of two solid-phase toxicity bioassays: the direct sediment toxicity testing procedure (DSTTP) and the microtox® solid-phase test (SPT). Bull. Environ. Contam. Toxicol. 55 (3), 338–346.

Libralato, G., Annamaria, V.G., Francesco, A., 2010. How toxic is toxic? A proposal for wastewater toxicity hazard assessment. Ecotoxicol. Environ. Saf. 73 (7), 1602–1611.

Lorenzo, D., García-Cervilla, R., Romero, A., Santos, A., 2020. Partitioning of chlorinated organic compounds from dense non-aqueous phase liquids and contaminated soils from lindane production wastes to the aqueous phase. Chemosphere 239, 124798.

Marugán, J., Bru, D., Pablos, C., Catalá, M., 2012. Comparative evaluation of acute toxicity by Vibrio fischeri and fern spore based bioassays in the follow-up of toxic chemicals degradation by photocatalysis. J. Hazard. Mater. 213–214, 117–122.

Parvez, S., Venkataraman, C., Mukherji, S., 2006. A review on advantages of implementing luminescence inhibition test (Vibrio fischeri) for acute toxicity prediction of chemicals. Environ. Int. 32 (2), 265–268.

Roig, N., Nadal, M., Sierra, J., Ginebreda, A., Schuhmacher, M., Domingo, J.L., 2011. Novel approach for assessing heavy metal pollution and ecotoxicological status of rivers by means of passive sampling methods. Environ. Int. 37 (4), 671–677.

Ruiz, M.J., López-Jaramillo, L., Redondo, M.J., Font, G., 1997. Toxicity assessment of pesticides using the microtox test: application to environmental samples. Bull. Environ. Contam. Toxicol. 59 (4), 619–625.

Santos, A., Fernandez, J., Guadano, J., Lorenzo, D., Romero, A., 2018. Chlorinated organic compounds in liquid wastes (DNAPL) from lindane production dumped in landfills in Sabinanigo (Spain). Environ. Pollut. 242, 1616–1624.

Santos, A., Fernández, J., Guadaño, J., Lorenzo, D., Romero, A., 2018. Chlorinated organic compounds in liquid wastes (DNAPL) from lindane production dumped in landfills in Sabiñanigo (Spain). Environ. Pollut. 242, 1616–1624.

Santos, A., Domínguez, C.M., Lorenzo, D., García-Cervilla, R., Lominchar, M.A., Fernández, J., Gómez, J., Guadaño, J., 2019. Soil flushing pilot test in a landfill polluted with liquid organic wastes from lindane production. Heliyon 5 (11), e02875.

Semple, K.T., Morriss, A.W.J., Paton, G.I., 2003. Bioavailability of hydrophobic organic contaminants in soils: fundamental concepts and techniques for analysis. Eur. J. Soil Sci. 54 (4), 809–818.

Svenson, A., 1996. Microtox Toxicity in Soil. 1249. IVL-publ. B.

Svenson, A., Edsholt, E., Ricking, M., Remberger, M., Röttorp, J., 1996. Sediment contaminants and microtox toxicity tested in a direct contact exposure test. Environ.Toxicol. Water Qual. 11 (4), 293–300.

Vega, M., Romano, D., Uotila, E., 2016. Lindane (persistent organic pollutant) in the EU E. P. s. P. D. f. C. R. a. C. Affairs.

Wacławek, S., Silvestri, D., Hrabák, P., Padil, V.V.T., Torres-Mendieta, R., Wacławek, M., Černík, M., Dionysiou, D.D., 2019. Chemical oxidation and reduction of hexachlorocyclohexanes: a review. Water Res. 162, 302–319.

Wentworth, C.K., 1922. A scale of grade and class terms for clastic sediments. J. Geol. 30 (5), 377–392.

ARTICLE 2

Title: Remediation of HCHs-contaminated sediments by chemical oxidation treatments.
Authors: C. M. Domínguez, A. Romero, **A. Checa-Fernández**, A. Santos
Journal: Science of the Total Environment
Publication year: 2021
Volume, Page: 751, 141754
DOI: 10.1016/j.scitotenv.2020.141754
Quartile (Area): Q1 (Environmental Engineering)
Cited by (SCOPUS): 24

Science of the Total Environment 751 (2021) 141754

Contents lists available at ScienceDirect

Science of the Total Environment

journal homepage: www.elsevier.com/locate/scitotenv

Remediation of HCHs-contaminated sediments by chemical oxidation treatments

Carmen M. Dominguez, Arturo Romero, Alicia Checa-Fernandez, Aurora Santos *

Dpto. Ingeniería Química y de Materiales, Facultad de Ciencias Químicas, Universidad Complutense Madrid, Ciudad Universitaria S/N, 28040 Madrid, Spain

HIGHLIGHTS

- The abatement of α and β-HCH in real soils has been studied by chemical oxidation.
- The high NOD of H_2O_2 of the treated soil make the Fenton process unsuitable.
- PS activated by T[a] at neutral pH is limited by the low solubility of HCHs.
- At pH > 12, α-HCH was faster dehydrochlorinated to TCBs than β-HCH.
- With PS activated by NaOH (pH > 12), the abatement of TCBs formed was enhanced by T[a].

GRAPHICAL ABSTRACT

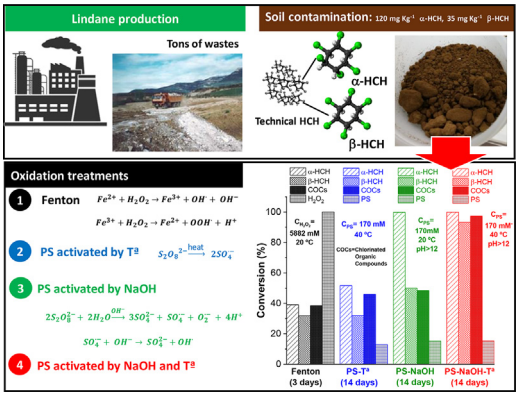

ARTICLE INFO

Article history:
Received 22 May 2020
Received in revised form 23 July 2020
Accepted 15 August 2020
Available online 18 August 2020

Editor: Vitor Jorge Vilar

Keywords:
HCHs
Remediation
Persulfate
Thermal activation
Alkaline activation
Fenton

ABSTRACT

The intensive use of organochlorine pesticides, such as lindane (γ-HCH), and the inadequate management of their wastes, is a huge environmental problem. The lindane production during the last century has generated huge volumes of solid wastes of other HCH isomers, causing hot points of soil and groundwater contamination. The soil treated in this work was obtained from a landfill located in the nearby of an old lindane factory, containing α-HCH and β-HCH as main contaminants. This study addresses for the first time the application of different chemical oxidation treatments, *viz.* Fenton process (H_2O_2 + Fe), persulfate (PS) activated by temperature (20 and 40 °C), by alkali (NaOH) and by the combination of alkali and temperature (NaOH, 40 °C) for the remediation of HCH-polluted soils (C_{HCHs} = 155 mg kg^{-1}). The intrinsic characteristics of the soil (high carbonate content) led to high consumption of H_2O_2 ($X_{H2O2} \approx 100\%$ at 24 h) and complete iron precipitation, making unappropriated the application of the Fenton process. The efficiency of thermal PS was limited by the low solubility of HCH isomers in the aqueous phase, the high refractoriness of these compounds towards oxidation, and the presence of the contaminants in the form of particulate matter. After 25 days of treatment, a conversion of chlorinated organic compounds (COCs) of 50% was achieved (V_L/W_{soil} = 2, C_{PS} = 40 g L^{-1}, 40 °C), whereas the application of PS activated by alkali and temperature (40 °C) led to promising results. At pH above 12, HCHs were dehydrochlorinated to trichlorobenzenes, which were further oxidized by hydroxyl radicals. The hydrolysis rate of β-HCH was the limiting step of the process, and it was favored by increasing the reaction temperature. At 40 °C, a conversion of COCs above 95% was achieved (V_L/W_{soil} = 2, C_{PS} = 40 g L^{-1}, C_{NaOH} = 13.5 g L^{-1}, 14 days) with low oxidant consumption (X_{PS} = 30%).

* Corresponding author.
E-mail address: aursan@ucm.es (A. Santos).

https://doi.org/10.1016/j.scitotenv.2020.141754
0048-9697/

Baciocchi, R., Boni, M.R., D'Aprile, L., 2004. Application of H_2O_2 lifetime as an indicator of TCE Fenton-like oxidation in soils. J. Hazard. Mater. 107 (3), 97–102.

Banerjee, S., 1984. Solubility of organic mixtures in water. Environ. Sci. Technol. 18 (8), 587–591.

Blus, L.J., 2003. Organochlorine pesticides. Handbook of Ecotoxicology. vol. 2, pp. 313–340.

Buser, H.-R., Mueller, M.D., 1995. Isomer and enantioselective degradation of hexachlorocyclohexane isomers in sewage sludge under anaerobic conditions. Environ. Sci. Technol. 29 (3), 664–672.

Chiou, C.T., Schmedding, D.W., Manes, M., 2005. Improved prediction of octanol-water partition coefficients from liquid-solute water solubilities and molar volumes. Environ. Sci. Technol. 39 (22), 8840–8846.

Concha-Grana, E., Turnes-Carou, M., Muniategui-Lorenzo, S., Lopez-Mahia, P., Prada-Rodriguez, D., Fernández-Fernández, E., 2006. Evaluation of HCH isomers and metabolites in soils, leachates, river water and sediments of a highly contaminated area. Chemosphere 64 (4), 588–595.

Dominguez, C.M., Rodriguez, S., Lorenzo, D., Romero, A., Santos, A.J.W., Air, and S. Pollution, 2016. Degradation of Hexachlorocyclohexanes (HCHs) by Stable Zero Valent Iron (ZVI) Microparticles. vol. 227 p. 446 (12).

Dominguez, C.M., Romero, A., Fernandez, J., Santos, A., 2018. In situ chemical reduction of chlorinated organic compounds from lindane production wastes by zero valent iron microparticles. J. Water Process Eng. 26, 146–155.

Dominguez, C.M., Rodriguez, V., Montero, E., Romero, A., Santos, A., 2019a. Methanol-enhanced degradation of carbon tetrachloride by alkaline activation of persulfate: kinetic model. Sci. Total Environ. 666, 631–640.

Dominguez, C.M., Romero, A., Santos, A., 2019b. Selective removal of chlorinated organic compounds from lindane wastes by combination of nonionic surfactant soil flushing and Fenton oxidation. Chem. Eng. J. 376, 120009.

Dominguez, C.M., Rodriguez, V., Montero, E., Romero, A., Santos, A., 2020a. Abatement of dichloromethane using persulfate activated by alkali: a kinetic study. Sep. Purif. Technol. 241, 116679.

Dominguez, C.M., Romero, A., Lorenzo, D., Santos, A., 2020b. Thermally activated persulfate for the chemical oxidation of chlorinated organic compounds in groundwater. J. Environ. Manag. 261, 110240.

Eisenberg, G., 1943. Colorimetric determination of hydrogen peroxide. Ind. Eng. Chem. Anal. Ed. 15 (5), 327–328.

Elliott, D.W., Lien, H.-L., Zhang, W.-x., 2008. Zerovalent iron nanoparticles for treatment of ground water contaminated by hexachlorocyclohexanes. J. Environ. Qual. 37 (6), 2192–2201.

Elliott, D.W., Lien, H.-L., Zhang, W.-X., 2009. Degradation of lindane by zero-valent iron nanoparticles. J. Environ. Eng. 135 (5), 317–324.

EPA, U, 2003. Integrated Risk Information System 2003.

Fernandez, J., Arjol, M.A., Cacho, C., 2013. POP-contaminated sites from HCH production in Sabinanigo, Spain. Environ. Sci. Pollut. Res. 20 (4), 1937–1950.

García-Cervilla, R., Santos, A., Romero, A., Lorenzo, D., 2020. Remediation of soil contaminated by lindane wastes using alkaline activated persulfate: kinetic model. Chem. Eng. J. 393.

Gayer, K., Woontner, L., 1956. The solubility of ferrous hydroxide and ferric hydroxide in acidic and basic media at 25. J. Phys. Chem. 60 (11), 1569–1571.

Gupta, A., Kaushik, C., Kaushik, A., 2001. Degradation of hexachlorocyclohexane isomers by two strains of Alcaligenes faecalis isolated from a contaminated site. Bull. Environ. Contam. Toxicol. 66 (6), 794–800.

Haag, W.R., Yao, C.D., 1992. Rate constants for reaction of hydroxyl radicals with several drinking water contaminants. Environ. Sci. Technol. 26 (5), 1005–1013.

Huang, K.-C., Zhao, Z., Hoag, G.E., Dahmani, A., Block, P.A., 2005. Degradation of volatile organic compounds with thermally activated persulfate oxidation. Chemosphere 61 (4), 551–560.

Ike, I.A., Linden, K.G., Orbell, J.D., Duke, M., 2018. Critical review of the science and sustainability of persulphate advanced oxidation processes. Chem. Eng. J. 338, 651–669.

Jayaraj, R., Megha, P., Sreedev, P., 2016. Organochlorine pesticides, their toxic effects on living organisms and their fate in the environment. Interdiscip. Toxicol. 9 (3–4), 90–100.

Joo, S.H., Zhao, D., 2008. Destruction of lindane and atrazine using stabilized iron nanoparticles under aerobic and anaerobic conditions: effects of catalyst and stabilizer. Chemosphere 70 (3), 418–425.

Karlaganis, G., Marioni, R., Sieber, I., Weber, A., 2001. The elaboration of the 'Stockholm convention' on persistent organic pollutants (POPs): a negotiation process fraught with obstacles and opportunities. Environ. Sci. Pollut. Res. 8 (3), 216–221.

Liang, C., Huang, C.-F., Mohanty, N., Kurakalva, R.M., 2008. A rapid spectrophotometric determination of persulfate anion in ISCO. Chemosphere 73 (9), 1540–1543.

Lominchar, M.A., Rodriguez, S., Lorenzo, D., Santos, N., Romero, A., Santos, A., 2017. Phenol abatement using persulfate activated by nZVI, H_2O_2 and NaOH and development of a kinetic model for alkaline activation. Environ. Technol. 1–9.

Lorenzo, D., García-Cervilla, R., Romero, A., Santos, A., 2020. Partitioning of chlorinated organic compounds from dense non-aqueous phase liquids and contaminated soils from lindane production wastes to the aqueous phase. Chemosphere 239, 124798.

Ma, J., Li, H., Chi, L., Chen, H., Chen, C., 2017. Changes in activation energy and kinetics of heat-activated persulfate oxidation of phenol in response to changes in pH and temperature. Chemosphere 189, 86–93.

Madaj, R., Sobiecka, E., Kalinowska, H., 2018. Lindane, kepone and pentachlorobenzene: chloropesticides banned by Stockholm convention. Int. J. Environ. Sci. Technol. 15 (2), 471–480.

Matzek, L.W., Carter, K.E., 2016. Activated persulfate for organic chemical degradation: a review. Chemosphere 151, 178–188.

Mertens, B., Blothe, C., Windey, K., De Windt, W., Verstraete, W., 2007. Biocatalytic dechlorination of lindane by nano-scale particles of Pd (0) deposited on Shewanella oneidensis. Chemosphere 66 (1), 99–105.

Mueller, N.C., Braun, J., Bruns, J., Černík, M., Rissing, P., Rickerby, D., Nowack, B., 2012. Application of nanoscale zero valent iron (NZVI) for groundwater remediation in Europe. Environ. Sci. Pollut. Res. 19 (2), 550–558.

Pardo, F., Rosas, J.M., Santos, A., Romero, A., 2014. Remediation of a biodiesel blend-contaminated soil by using a modified Fenton process. Environ. Sci. Pollut. Res. 21 (21), 12198–12207.

Peng, L., Deng, D., Guan, M., Fang, X., Zhu, Q., 2015. Remediation HCHs POPs-contaminated soil by activated persulfate technologies: feasibility, impact of activation methods and mechanistic implications. Sep. Purif. Technol. 150, 215–222.

Phillips, T.M., Lee, H., Trevors, J.T., Seech, A.G., 2006. Full-scale in situ bioremediation of hexachlorocyclohexane-contaminated soil. J. Chem. Technol. Biotechnol. 81 (3), 289–298.

Ranc, B., Faure, P., Croze, V., Simonnot, M., 2016. Selection of oxidant doses for in situ chemical oxidation of soils contaminated by polycyclic aromatic hydrocarbons (PAHs): a review. J. Hazard. Mater. 312, 280–297.

Ricking, M., Schwarzbauer, J., 2008. HCH residues in point-source contaminated samples of the Teltow Canal in Berlin, Germany. Environ. Chem. Lett. 6 (2), 83–89.

Romero, A., Santos, A., Vicente, F., Rodriguez, S., Lafuente, A.L., 2009. In situ oxidation remediation technologies: kinetic of hydrogen peroxide decomposition on soil organic matter. J. Hazard. Mater. 170 (2–3), 627–632.

Sandell, E.B., 1959. Colorimetric Determination of Traces of Metals.

Santos, A., Rosas, J.M., 2016. In situ chemical oxidation (ISCO). Soil Remediation: Applications and New Technologies, p. 75.

Santos, A., Fernandez, J., Rodriguez, S., Dominguez, C.M., Lominchar, M.A., Lorenzo, D., Romero, A., 2018. Abatement of chlorinated compounds in groundwater contaminated by HCH wastes using ISCO with alkali activated persulfate. Sci. Total Environ. 615, 1070–1077.

Shiu, W.Y., Ma, K.C., Mackay, D., Seiber, J.N., Wauchope, R.D., 1990. Solubilities of pesticide chemicals in water. 1. Environmental physical-chemistry. Rev. Environ. Contam. Toxicol. 116, 1–13.

Siegrist, R.L., Crimi, M., Simpkin, T.J., 2011. In Situ Chemical Oxidation for Groundwater Remediation. Springer Science & Business Media.

Singh, R., Singh, A., Misra, V., Singh, R.P., 2011. Degradation of lindane contaminated soil using zero-valent iron nanoparticles. J. Biomed. Nanotechnol. 7 (1), 175–176.

Srivastava, V., Srivastava, T., Kumar, M.S., 2019. Fate of the persistent organic pollutant (POP)Hexachlorocyclohexane (HCH) and remediation challenges. Int. Biodeterior. Biodegradation 140, 43–56.

Teel, A.L., Finn, D.D., Schmidt, J.T., Cutler, L.M., Watts, R.J., 2007. Rates of trace mineral-catalyzed decomposition of hydrogen peroxide. J. Environ. Eng. 133 (8), 853–858.

Torres, J., Fróes-Asmus, C., Weber, R., Vijgen, J., 2013. HCH contamination from former pesticide production in Brazil—a challenge for the Stockholm Convention implementation. Environ. Sci. Pollut. Res. 20 (4), 1951–1957.

Tsai, K.P., Chen, C.Y., 2007. An algal toxicity database of organic toxicants derived by a closed-system technique. Environ. Toxicol. Chem. 26 (9), 1931–1939.

Usman, M., Tascone, O., Faure, P., Hanna, K., 2014. Chemical oxidation of hexachlorocyclohexanes (HCHs) in contaminated soils. Sci. Total Environ. 476-477, 434–439.

Usman, M., Hanna, K., Haderlein, S., 2016. Fenton oxidation to remediate PAHs in contaminated soils: a critical review of major limitations and counter-strategies. Sci. Total Environ. 569, 179–190.

Vega, M., Romano, D., Uotila, E., 2016. Lindane (persistent organic pollutant) in the EU. Directorate General for Internal Policies. Policy Department C: Citizens' Rights and Constitutional Affairs. Petitions (PETI), p. 571 PE.

Vicente, F., Rosas, J.M., Santos, A., Romero, A., 2011. Improvement soil remediation by using stabilizers and chelating agents in a Fenton-like process. Chem. Eng. J. 172 (2), 689–697.

Vijgen, J., Abhilash, P.C., Li, Y.F., Lal, R., Forter, M., Torres, J., Singh, N., Yunus, M., Tian, C., Schaeffer, A., Weber, R., 2011. Hexachlorocyclohexane (HCH) as new Stockholm Convention POPs-a global perspective on the management of Lindane and its waste isomers. Environ. Sci. Pollut. Res. 18 (2), 152–162.

Wacławek, S., Silvestri, D., Hrabák, P., Padil, V.V., Torres-Mendieta, R., Wacławek, M., Černík, M., Dionysiou, D.D., 2019. Chemical oxidation and reduction of hexachlorocyclohexanes: a review. Water Res. 162, 302–319.

Wang, J., Wang, S., 2018. Activation of persulfate (PS) and peroxymonosulfate (PMS) and application for the degradation of emerging contaminants. Chem. Eng. J. 334, 1502–1517.

Wang, Z., Deng, D., Yang, L., 2014. Degradation of dimethyl phthalate in solutions and soil slurries by persulfate at ambient temperature. J. Hazard. Mater. 271, 202–209.

Watts, R.J., Teel, A.L., 2005. Chemistry of modified Fenton's reagent (catalyzed H_2O_2 propagations–CHP) for in situ soil and groundwater remediation. J. Environ. Eng. 131 (4), 612–622.

Watts, R.J., Teel, A.L., 2006. Treatment of contaminated soils and groundwater using ISCO. Practice Periodical of Hazardous, Toxic, and Radioactive Waste Management. vol. 10 (1), pp. 2–9.

Watts, R.J., Haeri-McCarroll, T.M., Teel, A.L., 2008. Effect of contaminant hydrophobicity in the treatment of contaminated soils by catalyzed H_2O_2 propagations (modified Fenton's reagent). J. Adv. Oxid. Technol. 11 (2), 354–361.

Wycisk, P., Stollberg, R., Neumann, C., Gossel, W., Weiss, H., Weber, R., 2013. Integrated methodology for assessing the HCH groundwater pollution at the multi-source contaminated mega-site Bitterfeld/Wolfen. Environ. Sci. Pollut. Res. 20 (4), 1907–1917.

Xiao, H., Li, N.Q., Wania, F., 2004. Compilation, evaluation, and selection of physical-chemical property data for alpha-, beta-, and gamma-hexachlorocyclohexane. J. Chem. Eng. Data 49 (2), 173–185.

Zhang, Y., Zhou, M., 2019. A critical review of the application of chelating agents to enable Fenton and Fenton-like reactions at high pH values. J. Hazard. Mater. 362, 436–450.

ARTICLE 3

Title: Degradation of HCHs by thermally activated persulfate in soil system. Effect of temperature and oxidant concentration

Authors: C. M. Domínguez, **A. Checa-Fernández**, A. Romero and A. Santos.

Journal: Journal of Environmental Chemical Engineering
Publication year: 2021
Volume, Page: 9, 105668
DOI: 10.1016/j.jece.2021.105668
Quartile (Area): Q1 (Chemical Engineering)
Cited by (SCOPUS): 26

Journal of Environmental Chemical Engineering 9 (2021) 105668

Contents lists available at ScienceDirect

Journal of Environmental Chemical Engineering

journal homepage: www.elsevier.com/locate/jece

Degradation of HCHs by thermally activated persulfate in soil system: Effect of temperature and oxidant concentration

Carmen M. Dominguez *, Alicia Checa-Fernandez, Arturo Romero, Aurora Santos

Departamanto Ingeniería Química y de Materiales, Facultad de Ciencias Químicas, Universidad Complutense Madrid, Ciudad Universitaria S/N, 28040 Madrid, Spain

ARTICLE INFO

Editor: V. Victor

Keywords:
Hexachlorocyclohexanes (HCHs)
Soil remediation
Persulfate
Thermal activation
Sulfate radicals
Temperature intensification

ABSTRACT

Soils contaminated with hexachlorocyclohexanes (HCHs) are a legacy of the heavy use of lindane during the 20th century. This pesticide production generated large amounts of residues of other HCH isomers, which were habitually mismanaged. The sediments treated in this work (coming from an old lindane landfill) are an example of this environmental problem of global dimensions. The efficient remediation of these sediments, mainly contaminated with β-HCH (99 mg kg^{-1}) and α-HCH (254 mg kg^{-1}) isomers, is still a challenge. The thermal activation of persulfate (PS) required excessive reaction times, which could be reduced by optimizing the variables of the process. This study aims to explore the effect of using higher reaction temperatures (35, 45, and 55 ºC) and initial oxidant concentrations (10, 20, 40, 60, and 80 g L^{-1}). Batch experiments (liquid/soil = 2/1, 100 rpm) were performed to evaluate the influence of these two variables in HCHs abatement, dechlorination degree, generation of intermediate compounds, and oxidant consumption. An increase in the reaction temperature accelerates the pollutant oxidation and dechlorination rate and decreases the concentration of chlorinated byproducts. The initial PS concentration also plays a crucial role in HCHs degradation. At selected operating conditions (55 ºC, PS = 80 g L^{-1}), a conversion of HCHs around 83% was achieved, without chlorinated byproducts (chlorine balance ≈ 100%) at only 9 days of treatment. A plausible pathway for the degradation of HCHs-polluted soils by thermally activated PS has been proposed from the identified species, involving a scheme of series-parallel reactions.

1. Introduction

Lindane (γ-hexachlorocyclohexane, γ-HCH), an organochlorine pesticide (OCP), was intensely used on a worldwide scale during the second half of the 20th century [1]. The production of lindane (photochemical chlorination of benzene) was an inefficient process, generating large volumes of the other HCH isomers (mainly α-, β- and δ-HCH) without insecticidal properties [2]. The HCH generated-wastes were inappropriately dumped during decades in the vicinity of the production sites, resulting in environmental contamination with global dimensions [3–7]. Due to their high toxicity and persistence in the environment [8], the Environmental Protection Agency has classified HCHs as possible human carcinogens [9]. Moreover, the isomers α-HCH, β-HCH and γ-HCH have been included in the list of persistent organic pollutants (POPs) by the Stockholm Convention [10]. Although lindane production and use have been banned in most countries, many landfills remain contaminated by HCH-wastes today.

One of the HCHs-polluted sites that has aroused great interest due to its complexity and risk associated with the proximity of a river and reservoir is that of the Bailín landfill, near Sabiñánigo (Aragon, Spain). The company INQUINOSA operated from 1975 to 1988 [5], discharging more than one hundred thousand tons of wastes during this period (http://www.stoplindano.es/). Consequently, these landfills are contaminated by solid HCHs-wastes, mainly α-HCH and β-HCH, in the form of particulate matter and/or adsorbed in the soil particles [5,11].

There are several studies in the literature focused on the remediation of HCHs in the aqueous phase [7,12], where different oxidation (ozonation [13], photo-Fenton [13], electrochemical oxidation process [14–16], sonolysis [17], PS activated by temperature [18] and alkali [19]) and reduction (zero-valent iron microparticles [20]) treatments have been studied. However, only a few works concerning the remediation of soils contaminated by HCHs-wastes were performed. They consist of applying chemical oxidation with permanganate, Fenton process, and different ways of activated PS (Fe, temperature, and alkali) [11,21–23]. Although exciting results were obtained with soils artificially contaminated with HCHs [21] or a real soil polluted with lindane

* Corresponding author.
E-mail address: carmdomi@ucm.es (C.M. Dominguez).

https://doi.org/10.1016/j.jece.2021.105668
Received 18 February 2021; Received in revised form 20 April 2021; Accepted 9 May 2021
Available online 18 May 2021

[16] C.M. Dominguez, N. Oturan, A. Romero, A. Santos, M.A. Oturan, Removal of lindane wastes by advanced electrochemical oxidation, Chemosphere 202 (2018) 400–409, https://doi.org/10.1016/j.chemosphere.2018.03.124.
[17] M. Kida, S. Ziembowicz, P. Koszelnik, Removal of organochlorine pesticides (OCPs) from aqueous solutions using hydrogen peroxide, ultrasonic waves, and a hybrid process, Sep. Purif. Technol. 192 (2018) 457–464, https://doi.org/10.1016/j.seppur.2017.10.046.
[18] C.M. Dominguez, A. Romero, D. Lorenzo, A. Santos, Thermally activated persulfate for the chemical oxidation of chlorinated organic compounds in groundwater, J. Environ. Manag. 261 (2020), 110240.
[19] A. Santos, J. Fernandez, S. Rodriguez, C.M. Dominguez, M.A. Lominchar, D. Lorenzo, A. Romero, Abatement of chlorinated compounds in groundwater contaminated by HCH wastes using ISCO with alkali activated persulfate, Sci. Total Environ. 615 (2018) 1070–1077, https://doi.org/10.1016/j.scitotenv.2017.09.224.
[20] C.M. Dominguez, A. Romero, J. Fernandez, A. Santos, In situ chemical reduction of chlorinated organic compounds from lindane production wastes by zero valent iron microparticles, J. Water Process Eng. 26 (2018) 146–155.
[21] L. Peng, D. Deng, M. Guan, X. Fang, Q. Zhu, Remediation HCHs POPs-contaminated soil by activated persulfate technologies: feasibility, impact of activation methods and mechanistic implications, Sep. Purif. Technol. 150 (2015) 215–222, https://doi.org/10.1016/j.seppur.2015.07.002.
[22] R. García-Cervilla, A. Santos, A. Romero, D. Lorenzo, Remediation of Soil contaminated by lindane wastes using alkaline activated persulfate: kinetic model, Chem. Eng. J. 393 (2020), 124646, https://doi.org/10.1016/j.cej.2020.124646.
[23] M. Usman, O. Tascone, P. Faure, K. Hanna, Chemical oxidation of hexachlorocyclohexanes (HCHs) in contaminated soils, Sci. Total Environ. 476–477 (2014) 434–439, https://doi.org/10.1016/j.scitotenv.2014.01.027.
[24] I.A. Ike, K.G. Linden, J.D. Orbell, M. Duke, Critical review of the science and sustainability of persulphate advanced oxidation processes, Chem. Eng. J. 338 (2018) 651–669, https://doi.org/10.1016/j.cej.2018.01.034.
[25] C.Y. Zhu, F.X. Zhu, D.D. Dionysiou, D.M. Zhou, G.D. Fang, J. Gao, Contribution of alcohol radicals to contaminant degradation in quenching studies of persulfate activation process, Water Res. 139 (2018) 66–73, https://doi.org/10.1016/j.watres.2018.03.069.
[26] J. Deng, Y. Shao, N. Gao, Y. Deng, S. Zhou, X. Hu, Thermally activated persulfate (TAP) oxidation of antiepileptic drug carbamazepine in water, Chem. Eng. J. 228 (2013) 765–771.
[27] I.A. Ike, J.D. Orbell, M. Duke, Feasibility, mechanisms, and optimisation of organic pollutant degradation by thermally activated persulphate, Chem. Eng. Res. Des. 136 (2018) 304–314, https://doi.org/10.1016/j.cherd.2018.05.041.
[28] D. Zhao, X. Liao, X. Yan, S.G. Huling, T. Chai, H. Tao, Effect and mechanism of persulfate activated by different methods for PAHs removal in soil, J. Hazard. Mater. 254–255 (2013) 228–235, https://doi.org/10.1016/j.jhazmat.2013.03.056.
[29] Z. Wang, D. Deng, L. Yang, Degradation of dimethyl phthalate in solutions and soil slurries by persulfate at ambient temperature, J. Hazard. Mater. 271 (2014) 202–209.
[30] X. Chen, M. Murugananthan, Y. Zhang, Degradation of p-Nitrophenol by thermally activated persulfate in soil system, Chem. Eng. J. 283 (2016) 1357–1365.
[31] F. Vicente, J.M. Rosas, A. Santos, A. Romero, Improvement soil remediation by using stabilizers and chelating agents in a Fenton-like process, Chem. Eng. J. 172 (2) (2011) 689–697, https://doi.org/10.1016/j.cej.2011.06.036.
[32] J.M. Rosas, F. Vicente, A. Santos, A. Romero, Soil remediation using soil washing followed by Fenton oxidation, Chem. Eng. J. 220 (2013) 125–132, https://doi.org/10.1016/j.cej.2012.11.137.
[33] Y. Liu, S. Wang, Y. Wu, H. Chen, Y. Shi, M. Liu, W. Dong, Degradation of ibuprofen by thermally activated persulfate in soil systems, Chem. Eng. J. 356 (2019) 799–810.
[34] K.-C. Huang, Z. Zhao, G.E. Hoag, A. Dahmani, P.A. Block, Degradation of volatile organic compounds with thermally activated persulfate oxidation, Chemosphere 61 (4) (2005) 551–560.
[35] L.W. Matzek, K.E. Carter, Activated persulfate for organic chemical degradation: a review, Chemosphere 151 (2016) 178–188.
[36] J. Ma, Y. Yang, X. Jiang, Z. Xie, X. Li, C. Chen, H. Chen, Impacts of inorganic anions and natural organic matter on thermally activated persulfate oxidation of BTEX in water, Chemosphere 190 (2018) 296–306.
[37] J. Wang, S. Wang, Activation of persulfate (PS) and peroxymonosulfate (PMS) and application for the degradation of emerging contaminants, Chem. Eng. J. 334 (2018) 1502–1517, https://doi.org/10.1016/j.cej.2017.11.059.
[38] A. Santos, J. Fernández, J. Guadaño, D. Lorenzo, A. Romero, Chlorinated organic compounds in liquid wastes (DNAPL) from lindane production dumped in landfills in Sabiñanigo (Spain), Environ. Pollut. 242 (2018) 1616–1624, https://doi.org/10.1016/j.envpol.2018.07.117.
[39] C. Liang, C.-F. Huang, N. Mohanty, R.M. Kurakalva, A rapid spectrophotometric determination of persulfate anion in ISCO, Chemosphere 73 (9) (2008) 1540–1543.
[40] R. Anderson, E. Rasor, F. Van Ryn, Particle size separation via soil washing to obtain volume reduction, J. Hazard. Mater. 66 (1) (1999) 89–98, https://doi.org/10.1016/S0304-3894(98)00210-6.
[41] E. Concha-Grana, M. Turnes-Carou, S. Muniategui-Lorenzo, P. Lopez-Mahia, D. Prada-Rodriguez, E. Fernández-Fernández, Evaluation of HCH isomers and metabolites in soils, leachates, river water and sediments of a highly contaminated area, Chemosphere 64 (4) (2006) 588–595.
[42] T.M. Phillips, H. Lee, J.T. Trevors, A.G. Seech, Full-scale in situ bioremediation of hexachlorocyclohexane-contaminated soil, J. Chem. Technol. Biotechnol.: Int. Res. Process, Environ. Clean. Technol. 81 (3) (2006) 289–298.
[43] A. Santos, C. Domínguez, D. Lorenzo, HCH-Contaminated Soils and Remediation Technologies, 2020. https://doi.org/10.5772/intechopen.93405.
[44] D. Lorenzo, R. García-Cervilla, A. Romero, A. Santos, Partitioning of chlorinated organic compounds from dense non-aqueous phase liquids and contaminated soils from lindane production wastes to the aqueous phase, Chemosphere 239 (2020), 124798, https://doi.org/10.1016/j.chemosphere.2019.124798.
[45] S. Wacławek, V. Antoš, P. Hrabák, M. Černík, Remediation of hexachlorocyclohexanes by cobalt-mediated activation of peroxymonosulfate, Desalin. Water Treat. 57 (54) (2016) 26274–26279, https://doi.org/10.1080/19443994.2015.1119757.
[46] S. Khan, X. He, J.A. Khan, H.M. Khan, D.L. Boccelli, D.D. Dionysiou, Kinetics and mechanism of sulfate radical-and hydroxyl radical-induced degradation of highly chlorinated pesticide lindane in UV/peroxymonosulfate system, Chem. Eng. J. 318 (2017) 135–142.
[47] J. Senthilnathan, L. Philip, Photocatalytic degradation of lindane under UV and visible light using N-doped TiO2, Chem. Eng. J. 161 (1) (2010) 83–92, https://doi.org/10.1016/j.cej.2010.04.034.
[48] J. Cao, W.-X. Zhang, D.G. Brown, D. Sethi, Oxidation of lindane with Fe (II)-activated sodium persulfate, J. Environ. Eng. Sci. 25 (2) (2008) 221–228.
[49] C.M. Dominguez, A. Romero, A. Santos, Selective removal of chlorinated organic compounds from lindane wastes by combination of nonionic surfactant soil flushing and Fenton oxidation, Chem. Eng. J. 376 (2019), 120009.
[50] D. Lorenzo, A. Santos, A. Sánchez-Yepes, L.Ó. Conte, C.M. Domínguez, Abatement of 1, 2, 4-trichlorobencene by wet peroxide oxidation catalysed by goethite and enhanced by visible LED light at neutral pH, Catalysts 11 (1) (2021) 139.
[51] P.D. Goulden, D.H.J. Anthony, Kinetics of uncatalyzed peroxydisulfate oxidation of organic material in fresh water, Anal. Chem. 50 (7) (1978) 953–958, https://doi.org/10.1021/ac50029a032.
[52] I.M. Kolthoff, I.K. Miller, The chemistry of persulfate. I. The kinetics and mechanism of the decomposition of the persulfate ion in aqueous medium1, J. Am. Chem. Soc. 73 (7) (1951) 3055–3059, https://doi.org/10.1021/ja01151a024.
[53] C. Liang, H.-W. Su, Identification of sulfate and hydroxyl radicals in thermally activated persulfate, Ind. Eng. Chem. Res. 48 (11) (2009) 5558–5562, https://doi.org/10.1021/ie9002848.
[54] F. Vicente, A. Santos, A. Romero, S. Rodriguez, Kinetic study of diuron oxidation and mineralization by persulphate: effects of temperature, oxidant concentration and iron dosage method, Chem. Eng. J. 170 (1) (2011) 127–135, https://doi.org/10.1016/j.cej.2011.03.042.
[55] K.-C. Huang, R.A. Couttenye, G.E. Hoag, Kinetics of heat-assisted persulfate oxidation of methyl tert-butyl ether (MTBE), Chemosphere 49 (4) (2002) 413–420, https://doi.org/10.1016/S0045-6535(02)00330-2.
[56] C.J. Liang, C.J. Bruell, M.C. Marley, K.L. Sperry, Thermally activated persulfate oxidation of trichloroethylene (TCE) and 1,1,1-trichloroethane (TCA) in aqueous systems and soil slurries, Soil Sediment Contam. Int. J. 12 (2) (2003) 207–228, https://doi.org/10.1080/713610970.
[57] R.H. Waldemer, P.G. Tratnyek, R.L. Johnson, J.T. Nurmi, Oxidation of chlorinated ethenes by heat-activated persulfate: kinetics and products, Environ. Sci. Technol. 41 (3) (2007) 1010–1015, https://doi.org/10.1021/es062237m.

ARTICLE 4

Title: Remediation of real soil polluted with hexachlorocyclohexanes (α-HCH and β-HCH) using combined thermal and alkaline activation of persulfate: Optimization of the operating conditions

Authors: **A. Checa-Fernández**, A. Santos, A. Romero, C. M. Domínguez

Journal: Separation and Purification Technology
Publication year: 2021
Volume, Page: 270, 118795
DOI: 10.1016/j.seppur.2021.118795
Quartile (Area): Q1 (Analytical Chemistry)
Cited by (SCOPUS): 17

Separation and Purification Technology 270 (2021) 118795

Contents lists available at ScienceDirect

Separation and Purification Technology

journal homepage: www.elsevier.com/locate/seppur

Remediation of real soil polluted with hexachlorocyclohexanes (α-HCH and β-HCH) using combined thermal and alkaline activation of persulfate: Optimization of the operating conditions

Alicia Checa-Fernández, Aurora Santos, Arturo Romero, Carmen M. Domínguez *

Dpto. Ingeniería Química y de Materiales, Facultad de Ciencias Químicas, Universidad Complutense Madrid, Ciudad Universitaria S/N, 28040 Madrid, Spain

ARTICLE INFO

Keywords:
HCHs
Soil remediation
Persulfate
Alkali
Temperature intensification

ABSTRACT

Contamination of organic pollutants such as hexachlorocyclohexane (HCH) isomers poses a significant threat to human health and the environment. The alkaline activation of persulfate (PS) intensified by temperature to remediate surface sediments contaminated with HCH-wastes dumped by a lindane producing company (mainly α-HCH = 254 mg kg^{-1} and β-HCH = 99 mg kg^{-1}) has been optimized. The treatment leads to promising results at 40 °C. Batch experiments were carried out to evaluate the influence of reagent addition order (simultaneous or sequential), reaction temperature (40–60 °C), liquid/soil ratio (V_L/W_S = 1 and 2), PS concentration (20–60 g L^{-1}) and stirring rate (10–100 rpm) on chlorinated compound abatement. The reagent addition order did not affect the efficiency of the process. Raising either temperature or PS concentration significantly accelerates the hydrolysis rate of β-HCH and the generated trichlorobenzenes (TCBs) oxidation rate. Increasing the V_L/W_S ratio also accelerated the pollutant oxidation rate. At the selected operating conditions (pH > 12, simultaneous addition of PS and NaOH, 50 °C, PS = 40 g L^{-1}, V_L/W_S = 2, NaOH/PS = 2 and 100 rpm), a conversion of α-HCH and β-HCH of 100% and 81%, and a dechlorination degree of 94% were achieved in 3 days. PS consumption was 29%; thus, the aqueous solution could be reused in a new batch of soil remediation, the separation of the aqueous and the soil phases being a rapid sedimentation step.

1. Introduction

Contamination of soils by hexachlorocyclohexane (HCH) isomers is a severe ongoing problem worldwide [54]. Among the HCHs isomers, lindane (γ-HCH) was one of the most used pesticides until the 1990s [3]. Lindane production implied the generation of vast amounts of wastes of other HCHs isomers, generally α-, β-, γ-, δ-, ε-HCH [61]. Specifically, each ton of lindane generated 8–12 tons of other HCH isomers without insecticidal properties [1]. The uncontrolled disposal of these wastes has resulted in very significant environmental contamination of large areas. Based on their environmental properties, α-HCH, β-HCH, and γ-HCH were listed as persistent organic pollutants (POPs) in Annex A of the Stockholm Convention in 2009 [49,53]. Lindane was produced in Spain at four production sites: two in the Basque Country, one in Galicia, and another, in Aragon. INQUINOSA, established in Sabiñánigo (Aragon), generated approximately 6800 ton $year^{-1}$ of solid wastes and 300–1500 ton $year^{-1}$ of liquid wastes [14], which were dumped in the landfills of Bailín and Sardas. This site's environmental risk increases due to the Gállego river's proximity and, therefore, requires efficient remediation strategies.

Advanced oxidation processes (AOPs) constitute a promising technology for the safe remediation of soils contaminated with high levels of POPs [5,56]. Chemical oxidation can be applied *in situ* (*in situ* chemical oxidation, ISCO), injecting an oxidant in the subsurface, or *ex situ*, where the affected soil is removed from its original location. When the contamination is located at the surface, the affected soil can also be treated on-site, avoiding dangerous and costly soil displacement out of the contaminated site. The oxidants most used include hydrogen peroxide (H_2O_2) catalyzed by Fe (Fenton process), permanganate (PM, MnO_4^-), and persulfate (PS, $S_2O_8^{2-}$) [5,46,62,65]. The Fenton process has shown significant limitations when applied to the remediation of real HCHs-contaminated soils [10,51]. The initial acidification required (pH = 3) is costly and impractical due to the buffering capacity of soils with high carbonate content [50], as is the current case (>38% of $CaCO_3$). Furthermore, excessive unproductive consumption of H_2O_2 and iron precipitation was reported when treating the sediments coming from

* Corresponding author.
E-mail address: carmdomi@ucm.es (C.M. Domínguez).

https://doi.org/10.1016/j.seppur.2021.118795
Received 28 January 2021; Received in revised form 13 April 2021; Accepted 14 April 2021
Available online 20 April 2021

Romero: Funding acquisition, Resources, Supervision. **Carmen M. Domínguez:** Conceptualization, Methodology, Investigation, Writing - review & editing.

Declaration of Competing Interest

The authors declare that they have no known competing financial interests or personal relationships that could have appeared to influence the work reported in this paper.

Acknowledgments

The authors acknowledge the financial support from SARGA (project ref. 5507001-182), the Regional Government of Madrid (CARESOIL project, S2018/EMT-4317) and the Spanish Ministry of Science (projects CTM2016-77151-C2-1-R and PID2019-105934RB-I00). The authors thank SARGA and the Department of Climate Change and Environmental Education, Government of Aragon, for their support during this work.

Appendix A. Supplementary material

Supplementary data to this article can be found online at https://doi.org/10.1016/j.seppur.2021.118795.

References

[1] G. Bodenstein, Lindane, monograph of an insecticide, Chapter Disposal Wastes From Lindane Manufacture 134 (1972) 1972.
[2] I. Bouzid, J. Maire, F. Laurent, M. Broquaire, N. Fatin-Rouge, Controlled treatment of a high velocity anisotropic aquifer model contaminated by hexachlorocyclohexanes, Environ. Pollut. 268 (2021), 115678.
[3] K. Breivik, J.M. Pacyna, J. Münch, Use of alpha-, beta- and gamma-hexachlorocyclohexane in Europe, 1970–1996, Sci Total Environ 239 (1–3) (1999) 151–163.
[4] L. Chen, X. Hu, T. Cai, Y. Yang, R. Zhao, C. Liu, A. Li, C. Jiang, Degradation of Triclosan in soils by thermally activated persulfate under conditions representative of in situ chemical oxidation (ISCO), Chem. Eng. J. 369 (2019) 344–352.
[5] M. Cheng, G. Zeng, D. Huang, C. Lai, P. Xu, C. Zhang, Y. Liu, Hydroxyl radicals based advanced oxidation processes (AOPs) for remediation of soils contaminated with organic compounds: A review, Chem. Eng. J. 284 (2016) 582–598.
[6] Y. Deng, R. Zhao, Advanced Oxidation Processes (AOPs) in Wastewater Treatment, Current Pollution Reports 1 (3) (2015) 167–176.
[7] C.M. Dominguez, N. Oturan, A. Romero, A. Santos, M.A. Oturan, Removal of organochlorine pesticides from lindane production wastes by electrochemical oxidation, Environ. Sci. Pollut. Res. 25 (35) (2018) 34985–34994.
[8] C.M. Dominguez, V. Rodriguez, E. Montero, A. Romero, A. Santos, Methanol-enhanced degradation of carbon tetrachloride by alkaline activation of persulfate: Kinetic model, Sci. Total Environ. 666 (2019) 631–640.
[9] C.M. Dominguez, V. Rodriguez, E. Montero, A. Romero, A. Santos, Abatement of dichloromethane using persulfate activated by alkali: A kinetic study, Sep. Purif. Technol. 241 (2020), 116679.
[10] C.M. Dominguez, A. Romero, A. Checa-Fernandez, A. Santos, Remediation of HCHs-contaminated sediments by chemical oxidation treatments, Sci. Total Environ. 751 (2021), 141754.
[11] C.M. Dominguez, A. Romero, D. Lorenzo, A. Santos, Thermally activated persulfate for the chemical oxidation of chlorinated organic compounds in groundwater, J. Environ. Manage. 261 (2020), 110240.
[12] C.M. Dominguez, A. Romero, A. Santos, Selective removal of chlorinated organic compounds from lindane wastes by combination of nonionic surfactant soil flushing and Fenton oxidation, Chem. Eng. J. 376 (2019) 120009, https://doi.org/10.1016/j.cej.2018.09.170.
[13] A. Enell, F. Reichenberg, G. Ewald, P. Warfvinge, Desorption kinetics studies on PAH-contaminated soil under varying temperatures, Chemosphere 61 (10) (2005) 1529–1538.
[14] J. Fernandez, M.A. Arjol, C. Cacho, POP-contaminated sites from HCH production in Sabinanigo, Spain, Environ. Sci. Pollut. Res. 20 (4) (2013) 1937–1950.
[15] O.S. Furman, A.L. Teel, R.J. Watts, Mechanism of Base Activation of Persulfate, Environ. Sci. Technol. 44 (16) (2010) 6423–6428.
[16] A. Gabet, H. Métivier, C. de Brauer, G. Mailhot, M. Brigante, Hydrogen peroxide and persulfate activation using UVA-UVB radiation: Degradation of estrogenic compounds and application in sewage treatment plant waters, J. Hazard. Mater. 405 (2021), 124693.
[17] R. García-Cervilla, A. Santos, A. Romero, D. Lorenzo, Remediation of soil contaminated by lindane wastes using alkaline activated persulfate: Kinetic model, Chem. Eng. J. 124646 (2020).
[18] P.D. Goulden, D.H.J. Anthony, Kinetics of uncatalyzed peroxydisulfate oxidation of organic material in fresh water, Anal. Chem. 50 (7) (1978) 953–958.
[19] W.R. Haag, C.C.D. Yao, Rate constants for reaction of hydroxyl radicals with several drinking water contaminants, Environ. Sci. Technol. 26 (5) (1992) 1005–1013.
[20] M. Hayyan, M.A. Hashim, I.M. AlNashef, Superoxide Ion: Generation and Chemical Implications, Chem. Rev. 116 (5) (2016) 3029–3085.
[21] M. Homolková, P. Hrabák, M. Kolář, M. Černík, Degradability of hexachlorocyclohexanes in water using ferrate (VI), Water Sci. Technol. 71 (3) (2014) 405–411.
[22] K.-C. Huang, R.A. Couttenye, G.E. Hoag, Kinetics of heat-assisted persulfate oxidation of methyl tert-butyl ether (MTBE), Chemosphere 49 (4) (2002) 413–420.
[23] I.A. Ike, K.G. Linden, J.D. Orbell, M. Duke, Critical review of the science and sustainability of persulphate advanced oxidation processes, Chem. Eng. J. 338 (2018) 651–669.
[24] Y. Ji, C. Dong, D. Kong, J. Lu, Q. Zhou, Heat-activated persulfate oxidation of atrazine: Implications for remediation of groundwater contaminated by herbicides, Chem. Eng. J. 263 (2015) 45–54.
[25] R.L. Johnson, P.G. Tratnyek, R.O.B. Johnson, Persulfate Persistence under Thermal Activation Conditions, Environ. Sci. Technol. 42 (24) (2008) 9350–9356.
[26] I.M. Kolthoff, I.K. Miller, The Chemistry of Persulfate. I. The Kinetics and Mechanism of the Decomposition of the Persulfate Ion in Aqueous Medium1, J. Am. Chem. Soc. 73 (7) (1951) 3055–3059.
[27] C. Liang, C.-F. Huang, N. Mohanty, R.M. Kurakalva, A rapid spectrophotometric determination of persulfate anion in ISCO, Chemosphere 73 (9) (2008) 1540–1543.
[28] C. Liang, H.-W. Su, Identification of Sulfate and Hydroxyl Radicals in Thermally Activated Persulfate, Ind. Eng. Chem. Res. 48 (11) (2009) 5558–5562.
[29] C. Liang, Z.-S. Wang, C.J. Bruell, Influence of pH on persulfate oxidation of TCE at ambient temperatures, Chemosphere 66 (1) (2007) 106–113.
[30] C.J. Liang, C.J. Bruell, M.C. Marley, K.L. Sperry, Thermally Activated Persulfate Oxidation of Trichloroethylene (TCE) and 1,1,1-Trichloroethane (TCA) in Aqueous Systems and Soil Slurries, Soil Sediment Contaminat.: Int. J. 12 (2) (2003) 207–228.
[31] J.L. Liu, Z.H. Liu, F.J. Zhang, X.S. Su, C. Lyu, Thermally activated persulfate oxidation of NAPL chlorinated organic compounds: effect of soil composition on oxidant demand in different soil-persulfate systems, Water Sci. Technol. 75 (8) (2017) 1794–1803.
[32] M.A. Lominchar, S. Rodríguez, D. Lorenzo, N. Santos, A. Romero, A. Santos, Phenol abatement using persulfate activated by nZVI, H2O2 and NaOH and development of a kinetic model for alkaline activation, Environ. Technol. 39 (1) (2018) 35–43.
[33] M.A. Lominchar, A. Santos, E. de Miguel, A. Romero, Remediation of aged diesel contaminated soil by alkaline activated persulfate, Sci. Total Environ. 622 (2018) 41–48.
[34] D. Lorenzo, R. García-Cervilla, A. Romero, A. Santos, Partitioning of chlorinated organic compounds from dense non-aqueous phase liquids and contaminated soils from lindane production wastes to the aqueous phase, Chemosphere 239 (2020) 124798, https://doi.org/10.1016/j.chemosphere.2019.124798.
[35] S. Mandal, Reaction rate constants of hydroxyl radicals with micropollutants and their significance in advanced oxidation processes, J. Adv. Oxid. Technol 21 (178) (2018), e195.
[36] L.W. Matzek, K.E. Carter, Activated persulfate for organic chemical degradation: A review, Chemosphere 151 (2016) 178–188.
[37] P. Neta, R.E. Huie, A.B. Ross, Rate constants for reactions of inorganic radicals in aqueous solution, J. Phys. Chem. Ref. Data 17 (3) (1988) 1027–1284.
[38] F. Pardo, J.M. Rosas, A. Santos, A. Romero, Remediation of a Biodiesel Blend-Contaminated Soil with Activated Persulfate by Different Sources of Iron, Water Air Soil Pollut. 226 (2) (2015), https://doi.org/10.1007/s11270-014-2267-4.
[39] L. Peng, D. Deng, M. Guan, X. Fang, Q. Zhu, Remediation HCHs POPs-contaminated soil by activated persulfate technologies: Feasibility, impact of activation methods and mechanistic implications, Sep. Purif. Technol. 150 (2015) 215–222.
[40] X. Ren, G. Zeng, L. Tang, J. Wang, J. Wan, Y. Liu, J. Yu, H. Yi, S. Ye, R. Deng, Sorption, transport and biodegradation – An insight into bioavailability of persistent organic pollutants in soil, Sci. Total Environ. 610–611 (2018) 1154–1163.
[41] A. Santos, C. Domínguez, D. Lorenzo, HCH-Contaminated Soils and 818 Remediation Technologies. IntechOpen, 2020 (10.5772/intechopen.93405).
[42] A. Santos, J. Fernández, J. Guadaño, D. Lorenzo, A. Romero, Chlorinated organic compounds in liquid wastes (DNAPL) from lindane production dumped in landfills in Sabiñanigo (Spain), Environ. Pollut. 242 (2018) 1616–1624.
[43] A. Santos, J. Fernandez, S. Rodriguez, C.M. Dominguez, M.A. Lominchar, D. Lorenzo, A. Romero, Abatement of chlorinated compounds in groundwater contaminated by HCH wastes using ISCO with alkali activated persulfate, Sci Total Environ 615 (2018) 1070–1077.
[44] A. Santos, D. Lorenzo, C.M. Dominguez, Electrochemically assisted remediation of contaminated soils: fundamentals, technologies, combined processes and pre-pilot and scale-up applications. Chapter 10: Persulfate in the remediation of soil and groundwater contaminated by organic compounds. SpringerNature, 2021.
[45] T. Siddique, B.C. Okeke, M. Arshad, W.T. Frankenberger, Temperature and pH Effects on Biodegradation of Hexachlorocyclohexane Isomers in Water and a Soil Slurry, J. Agric. Food. Chem. 50 (18) (2002) 5070–5076.
[46] R.L. Siegrist, M. Crimi, T.J. Simpkin, In Situ Chemical Oxidation for Groundwater Remediation, Springer-Verlag, New York, New York, 2011.
[47] Y. Tao, O. Monfort, M. Brigante, H. Zhang, G. Mailhot, Phenanthrene decomposition in soil washing effluents using UVB activation of hydrogen peroxide and peroxydisulfate, Chemosphere 263 (2021), 127996.

ARTICLE 5

Title: Enhanced remediation of a real HCH-polluted soil by the synergetic alkaline and ultrasonic activation of persulfate.
Authors: **A. Checa-Fernández**, A. Santos, L. O. Conte, A. Romero, C. M. Domínguez.
Journal: Chemical Engineering Journal
Publication year: 2022
Volume, Page: 440, 135901
DOI: 10.1016/j.cej.2022.135901
Quartile (Area): Q1 (Chemical Engineering)
Cited by (SCOPUS): 14

Chemical Engineering Journal 440 (2022) 135901

Contents lists available at ScienceDirect

Chemical Engineering Journal

journal homepage: www.elsevier.com/locate/cej

Enhanced remediation of a real HCH-polluted soil by the synergetic alkaline and ultrasonic activation of persulfate

Alicia Checa-Fernández [a], Aurora Santos [a], Leandro O. Conte [a,b], Arturo Romero [a], Carmen M. Domínguez [a,*]

[a] Dpto. Ingeniería Química y de Materiales, Facultad de Ciencias Químicas, Universidad Complutense Madrid. Ciudad Universitaria S/N. 28040, Madrid, Spain
[b] Instituto de Desarrollo Tecnológico para la Industria Química (INTEC), Consejo Nacional de Investigaciones Científicas y Técnicas (CONICET) and Universidad Nacional del Litoral (UNL), Santa Fe, Argentina

ARTICLE INFO

Keywords:
HCHs
Soil remediation
Ultrasound
Persulfate
Alkaline activation

ABSTRACT

The desorption of hydrophobic organic compounds (HOCs) and limited mass transfer in soil systems is a significant challenge for efficient soil remediation by oxidation treatments. The utilization of sonochemistry is a promising technology to enhance the decontamination of HOCs-polluted soils. In this work, ultrasound (US) was coupled to NaOH for activating persulfate (PS) to enhance the remediation of a real soil polluted with hexachlorocyclohexanes (HCHs) (Σ_{HCHs} = 404 mg kg^{-1}). Batch experiments (mass aqueous/soil ratio, V_L/W_S = 2) were performed to evaluate the effect of US on HOCs desorption and oxidation. Moreover, the influence of US power (0–245 W, corresponding to 0–91 W L^{-1} of US power density) and the initial oxidant concentration (C_{PS} = 10–60 g L^{-1}) on pollutants abatement, dechlorination degree, and oxidant consumption have been studied. Scanning electron microscopy (SEM) images verified that the US facilitates the breakdown of soil aggregates, enhancing the desorption of trichlorobenzenes (TCBs) (generated from HCHs alkaline hydrolysis) from the soil. Moreover, their subsequent oxidation is favouring because of higher radical species concentrations and the temperature rise. An increase in the US power up to 165 W accelerates the production rate of radicals, improving the pollutants' degradation. The difference between pollutant oxidation and dechlorination decreases with increasing US power, associated with a lower concentration of intermediate chlorinated compounds. In the same way, the initial oxidant concentration plays a fundamental role in the remediation treatment. At the selected operating conditions (C_{PS} = 60 g L^{-1}, NaOH/PS = 2, 165 W), a pollutants degradation and dechlorination of 0.94 and 0.74, respectively, were achieved in just 3 h of reaction time.

1. Introduction

Among soil contaminants, persistent organic pollutants (POPs) are of particular concern because of their long half-life in the environment and high toxicity [1]. Recently, some hexachlorocyclohexane (HCH) isomers (α-, β-, and γ-HCH) have been added to the POPs list, regulated by the Stockholm Convention [2]. γ-HCH, also known as lindane, has been extensively used as a wide-spectrum pesticide during the last 5 decades, resulting in global environmental contamination. Regrettably, lindane production entailed the generation of other HCH isomers (α-, β-, ε-, and δ-HCH) without insecticidal properties, representing around 85–90% of the total volume [3]. Usually, these compounds were uncontrollably dumped near the production sites, becoming hazardous wastes [4]. HCHs are hydrophobic organic contaminants (HOCs) that have high persistence in soil and water systems and are considered toxic and carcinogenic compounds [5]. Although lindane production and use have been banned in most countries, many sites around the planet remain contaminated by its wastes nowadays. Thus, to ensure the protection of human health and the environment, there is an urgent need for further assessments and remediation of HCH-polluted sites. The lindane legacy is of great significance in Europe, where most of HCHs waste (63%) is concentrated [2]. One of the most relevant cases is found in Sabiñánigo (Huesca, Spain), where the Sardas and Bailín landfills are located. On this site, the company INQUINOSA discharged>7,000 tons of HCH-solid waste per year, generating large quantities of superficial soil pollution [4]. This solid waste was mainly constituted by α-, β-, δ-, and ε-HCH isomers (lindane was separated by distillation from the other HCH isomers for its commercialization) [4].

* Corresponding author.
E-mail address: carmdomi@ucm.es (C.M. Domínguez).

https://doi.org/10.1016/j.cej.2022.135901
Received 17 December 2021; Received in revised form 14 March 2022; Accepted 16 March 2022
Available online 18 March 2022

[7] M. Usman, O. Tascone, P. Faure, K. Hanna, Chemical oxidation of hexachlorocyclohexanes (HCHs) in contaminated soils, Science of The Total Environment 476–477 (2014) 434–439.

[8] L. Peng, D. Deng, M. Guan, X. Fang, Q. Zhu, Remediation HCHs POPs-contaminated soil by activated persulfate technologies: Feasibility, impact of activation methods and mechanistic implications, Separation and Purification Technology 150 (2015) 215–222.

[9] C.M. Dominguez, A. Checa-Fernandez, A. Romero, A. Santos, Degradation of HCHs by thermally activated persulfate in soil system: Effect of temperature and oxidant concentration, Journal of Environmental Chemical Engineering 9 (4) (2021), 105668.

[10] A. Checa-Fernández, A. Santos, A. Romero, C.M. Domínguez, Remediation of real soil polluted with Hexachlorocyclohexanes (α-HCH and β-HCH) using combined thermal and alkaline activation of persulfate: Optimization of the operating conditions, Separation and Purification Technology 270 (2021) 118795.

[11] S. Waclawek, H.V. Lutze, K. Grubel, V.V.T. Padil, M. Cernik, D.D. Dionysiou, Chemistry of persulfates in water and wastewater treatment: A review, Chem. Eng. J. 330 (2017) 44–62, https://doi.org/10.1016/j.cej.2017.07.132.

[12] Z. Zhou, X. Liu, K. Sun, C. Lin, J. Ma, M. He, W. Ouyang, Persulfate-based advanced oxidation processes (AOPs) for organic-contaminated soil remediation: A review, Chemical Engineering Journal 372 (2019) 836–851.

[13] D. Lorenzo, R. García-Cervilla, A. Romero, A. Santos, Partitioning of chlorinated organic compounds from dense non-aqueous phase liquids and contaminated soils from lindane production wastes to the aqueous phase, Chemosphere 239 (2020), 124798.

[14] A. Santos, J. Fernandez, S. Rodriguez, C. Dominguez, M. Lominchar, D. Lorenzo, A. Romero, Abatement of chlorinated compounds in groundwater contaminated by HCH wastes using ISCO with alkali activated persulfate, Science of the Total Environment 615 (2018) 1070–1077.

[15] A.J. Effendi, M. Wulandari, T. Setiadi, Ultrasonic application in contaminated soil remediation, Current Opinion in Environmental Science & Health 12 (2019) 66–71.

[16] Y.-J. Lei, Y. Tian, C. Fang, W. Zhan, L.-C. Duan, J. Zhang, W. Zuo, X.-W. Kong, Insights into the oxidation kinetics and mechanism of diesel hydrocarbons by ultrasound activated persulfate in a soil system, Chemical Engineering Journal 378 (2019), 122253.

[17] Y.-J. Lei, J. Zhang, Y. Tian, J. Yao, Q.-S. Duan, W. Zuo, Enhanced degradation of total petroleum hydrocarbons in real soil by dual-frequency ultrasound-activated persulfate, Science of The Total Environment 748 (2020), 141414.

[18] S. Wang, N. Zhou, Removal of carbamazepine from aqueous solution using sono-activated persulfate process, Ultrasonics Sonochemistry 29 (2016) 156–162.

[19] Z. Wei, F.A. Villamena, L.K. Weavers, Kinetics and Mechanism of Ultrasonic Activation of Persulfate: An in Situ EPR Spin Trapping Study, Environmental Science & Technology 51 (6) (2017) 3410–3417, https://doi.org/10.1021/acs.est.6b05392.

[20] X. Luo, H. Gong, Z. He, P. Zhang, L. He, Recent advances in applications of power ultrasound for petroleum industry, Ultrasonics Sonochemistry 70 (2021), 105337.

[21] D. Deng, X. Lin, J. Ou, Z. Wang, S. Li, M. Deng, Y. Shu, Efficient chemical oxidation of high levels of soil-sorbed phenanthrene by ultrasound induced, thermally activated persulfate, Chemical Engineering Journal 265 (2015) 176–183.

[22] Y.-T. Li, D. Li, L.-J. Lai, Y.-H. Li, Remediation of petroleum hydrocarbon contaminated soil by using activated persulfate with ultrasound and ultrasound/Fe, Chemosphere 238 (2020), 124657.

[23] A. Goi, M. Viisimaa, Integration of ozonation and sonication with hydrogen peroxide and persulfate oxidation for polychlorinated biphenyls-contaminated soil treatment, Journal of Environmental Chemical Engineering 3 (4) (2015) 2839–2847.

[24] Y.-J. Lei, Y. Tian, Z. Sobhani, R. Naidu, C. Fang, Synergistic degradation of PFAS in water and soil by dual-frequency ultrasonic activated persulfate, Chemical Engineering Journal 388 (2020), 124215.

[25] P.D. Goulden, D.H.J. Anthony, Kinetics of uncatalyzed peroxydisulfate oxidation of organic material in fresh water, Analytical Chemistry 50 (7) (1978) 953–958, https://doi.org/10.1021/ac50029a032.

[26] I.M. Kolthoff, I.K. Miller, The Chemistry of Persulfate. I. The Kinetics and Mechanism of the Decomposition of the Persulfate Ion in Aqueous Medium1, Journal of the American Chemical Society 73(7) 73 (7) (1951) 3055–3059.

[27] J.M. Monteagudo, H. El-taliawy, A. Durán, G. Caro, K. Bester, Sono-activated persulfate oxidation of diclofenac: Degradation, kinetics, pathway and contribution of the different radicals involved, Journal of Hazardous Materials 357 (2018) 457–465.

[28] O.S. Furman, A.L. Teel, M. Ahmad, M.C. Merker, R.J. Watts, Effect of basicity on persulfate reactivity, Journal of Environmental Engineering 137 (4) (2011) 241–247.

[29] Y. Liu, S. Wang, Y. Wu, H. Chen, Y. Shi, M. Liu, W. Dong, Degradation of ibuprofen by thermally activated persulfate in soil systems, Chemical Engineering Journal 356 (2019) 799–810.

[30] L.W. Matzek, K.E. Carter, Activated persulfate for organic chemical degradation: a review, Chemosphere 151 (2016) 178–188.

[31] J. Ma, Y. Yang, X. Jiang, Z. Xie, X. Li, C. Chen, H. Chen, Impacts of inorganic anions and natural organic matter on thermally activated persulfate oxidation of BTEX in water, Chemosphere 190 (2018) 296–306.

[32] J. Wang, S. Wang, Activation of persulfate (PS) and peroxymonosulfate (PMS) and application for the degradation of emerging contaminants, Chemical Engineering Journal 334 (2018) 1502–1517.

[33] R.A. Shrestha, T.D. Pham, M. Sillanpää, Effect of ultrasound on removal of persistent organic pollutants (POPs) from different types of soils, Journal of Hazardous Materials 170 (2) (2009) 871–875.

[34] A. Tor, M.E. Aydin, S. Ozcan, Ultrasonic solvent extraction of organochlorine pesticides from soil, Analytica Chimica Acta 559 (2) (2006) 173–180, https://doi.org/10.1016/j.aca.2005.11.078.

[35] A. Santos, J. Fernández, J. Guadaño, D. Lorenzo, A. Romero, Chlorinated organic compounds in liquid wastes (DNAPL) from lindane production dumped in landfills in Sabiñanigo (Spain), Environmental Pollution 242 (2018) 1616–1624.

[36] R. García-Cervilla, A. Santos, A. Romero, D. Lorenzo, Remediation of soil contaminated by lindane wastes using alkaline activated persulfate: kinetic model, Chemical Engineering Journal 393 (2020), 124646.

[37] C. Liang, C.-F. Huang, N. Mohanty, R.M. Kurakalva, A rapid spectrophotometric determination of persulfate anion in ISCO, Chemosphere 73 (9) (2008) 1540–1543.

[38] O. Hamdaoui, E. Naffrechoux, L. Tifouti, C. Pétrier, Effects of ultrasound on adsorption–desorption of p-chlorophenol on granular activated carbon, Ultrasonics Sonochemistry 10 (2) (2003) 109–114.

[39] S. He, X. Tan, X. Hu, Y. Gao, Effect of ultrasound on oil recovery from crude oil containing sludge, Environmental Technology 40 (11) (2019) 1401–1407, https://doi.org/10.1080/09593330.2017.1422553.

[40] S. Waclawek, D. Silvestri, P. Hrabak, V.V.T. Padil, R. Torres-Mendieta, M. Waclawek, M. Cernik, D.D. Dionysiou, Chemical oxidation and reduction of hexachlorocyclohexanes: A review, Water Research 162 (2019) 302–319, https://doi.org/10.1016/j.watres.2019.06.072.

[41] Y.-T. Li, J.-J. Zhang, Y.-H. Li, J.-L. Chen, W.-Y. Du, Treatment of soil contaminated with petroleum hydrocarbons using activated persulfate oxidation, ultrasound, and heat: A kinetic and thermodynamic study, Chemical Engineering Journal 428 (2022), 131336.

[42] W. Song, J. Li, W. Zhang, X. Hu, L. Wang, An experimental study on the remediation of phenanthrene in soil using ultrasound and soil washing, Environmental Earth Sciences 66 (5) (2012) 1487–1496, https://doi.org/10.1007/s12665-011-1388-y.

[43] C.M. Dominguez, A. Romero, D. Lorenzo, A. Santos, Thermally activated persulfate for the chemical oxidation of chlorinated organic compounds in groundwater, Journal of Environmental Management 261 (2020), 110240.

[44] C.J. Liang, C.J. Bruell, M.C. Marley, K.L. Sperry, Thermally Activated Persulfate Oxidation of Trichloroethylene (TCE) and 1,1,1-Trichloroethane (TCA) in Aqueous Systems and Soil Slurries, Soil and Sediment Contamination: An International Journal 12 (2) (2003) 207–228, https://doi.org/10.1080/713610970.

[45] R.H. Waldemer, P.G. Tratnyek, R.L. Johnson, J.T. Nurmi, Oxidation of Chlorinated Ethenes by Heat-Activated Persulfate: Kinetics and Products, Environmental Science & Technology 41 (3) (2007) 1010–1015, https://doi.org/10.1021/es062237m.

[46] C. Liang, H.-W. Su, Identification of Sulfate and Hydroxyl Radicals in Thermally Activated Persulfate, Industrial & Engineering Chemistry Research 48 (11) (2009) 5558–5562, https://doi.org/10.1021/ie9002848.

ARTICLE 6

Title: Remediation of real soils polluted with pesticides by activated persulfate and surfactant addition
Authors: **A. Checa-Fernández**, A. Santos, A. Romero, C. M. Domínguez
Journal: Journal of Water Process Engineering
Publication year: 2023
Volume, Page: 53, 103829
DOI: 10.1016/j.jwpe.2023.103829
Quartile (Area): Q1 (Water Science and Technology)
Cited by (SCOPUS): 0

Journal of Water Process Engineering 53 (2023) 103829

Contents lists available at ScienceDirect

Journal of Water Process Engineering

journal homepage: www.elsevier.com/locate/jwpe

Remediation of real soils polluted with pesticides by activated persulfate and surfactant addition

Alicia Checa-Fernández, Aurora Santos, Arturo Romero, Carmen M. Domínguez *

Dpto. Ingeniería Química y de Materiales, Facultad de Ciencias Químicas, Universidad Complutense Madrid, Ciudad Universitaria S/N, 28040 Madrid, Spain

ARTICLE INFO

Keywords:
Remediation
HCHs
Surfactants
Partition coefficient
Activated persulfate

ABSTRACT

The existence of soils contaminated with organochlorine pesticides represents a serious environmental problem. In this work, a real soil contaminated with hexachlorocyclohexanes (ΣHCH = 373 mg kg^{-1}), persistent organic pollutants included in the Stockholm Convention, was remediated. Surfactants were used to enhance the pollutants solubilization and activated persulfate (PS) oxidation to degrade the pollutants. Solubilization experiments were performed to evaluate the effect of surfactant (sodium dodecyl sulfate (SDS), Emulse-3® (E3) and Tween-80® (T80)), pH, reagents addition order and concentration ($C_{surfactant}$ = 0–10 g L^{-1}, C_{NaOH} = 0–13.5 g L^{-1}). Surfactants selection was performed attending to their ability to solubilize chlorinated organic compounds (COCs). The use of surfactants improved COCs solubilization, especially at pH > 12; conditions at which HCHs hydrolyze to trichlorobenzenes (TCBs), with higher solubility. The higher the surfactant concentration, the higher the COCs concentration in the emulsion. COCs solubilization of 83 % and 89 % were achieved in three surfactant consecutive cycles at highly alkaline conditions using SDS and E3, respectively (T80 was unstable). The resulting emulsions were treated by PS activated by alkali and intensified by temperature. COCs conversion of 30 % and 96 % were achieved when treating E3 and SDS-emulsions (72 h), respectively, highlighting the suitability of SDS for the integrated process.

1. Introduction

In the last decades, industrial activities have generated vast quantities of soil polluted with hydrophobic organic compounds (HOCs), becoming a major environmental problem [1]. One of the most serious cases is the pollution caused by lindane wastes, the gamma isomer of hexachlorocyclohexane (γ-HCH), a polychlorinated pesticide globally used in the second half of the 20th [2]. The lindane manufacture generated large quantities of other HCH isomers (namely α-, β, ε-, and δ-HCH) without insecticidal properties, leading to large deposits of HCH wastes worldwide [3]. Three HCHs (α-, β-, and γ-HCH) have been included in the list of persistent organic pollutants (POPs) in the Stockholm Convention [4] because of their high refractoriness and adverse effects on the ecosystem and human beings. Thus, owing to its toxicity and health implications, the production and use of lindane have been banned in most European countries, the USA, and Canada. In this sense, feasible degradation technologies are required to remediate the sites polluted with these wastes and implement the abovementioned convention.

Advanced oxidation processes (AOPs) can be a feasible option for the remediation of HCHs-polluted soils. Among the AOPs tested (using H_2O_2 and persulfate (PS) as oxidants), PS-based treatments led to better results [5,6] due to the high stability, aqueous solubility, and low cost of this oxidant [7,8]. The degradation power of PS is usually increased activating this oxidant by metal cations, alkali (NaOH), heat, or other energy sources, such as ultrasound, ultraviolet, etc., generating different radicals species [9–15]. Among these systems, PS activated by temperature [5,16], NaOH [10,17], the combination of NaOH and temperature [10,17] and the intensification of NaOH with US [9] have recently been studied for the remediation of HCH-polluted soils. The main limitations found are the high HCHs adsorption onto the soil particles and their low solubility. Thus, their transfer into the aqueous phase, where the degradation process takes mainly place [17–19], is restricted. This limitation can be overcome by the use of surfactants, amphiphilic-nature substances able to reduce the surface tension of water [20], enhancing HOCs solubilization [21]. In this context, the use of surfactants [1,22] and the treatment of the resulting emulsions [23,24] for the remediation of soils contaminated with HOCs has received increasing attention in the

* Corresponding author.
E-mail address: carmdomi@ucm.es (C.M. Domínguez).

https://doi.org/10.1016/j.jwpe.2023.103829
Received 15 February 2023; Received in revised form 10 April 2023; Accepted 11 May 2023

[2] J. Fernández, M. Arjol, C. Cacho, POP-contaminated sites from HCH production in Sabiñánigo, Spain, Environ. Sci. Pollut. Res. 20 (4) (2013) 1937–1950.
[3] J. Vijgen, B. de Borst, R. Weber, T. Stobiecki, M. Forter, HCH and lindane contaminated sites: European and global need for a permanent solution for a long-time neglected issue, Environ. Pollut. 248 (2019) 696–705.
[4] J. Vijgen, P.C. Abhilash, Y.F. Li, R. Lal, M. Forter, J. Torres, N. Singh, M. Yunus, C. Tian, A. Schäffer, R. Weber, Hexachlorocyclohexane (HCH) as new Stockholm convention POPs—a global perspective on the management of Lindane and its waste isomers, Environ. Sci. Pollut. Res. 18 (2) (2011) 152–162.
[5] C.M. Dominguez, A. Checa-Fernandez, A. Romero, A. Santos, Degradation of HCHs by thermally activated persulfate in soil system: effect of temperature and oxidant concentration, J. Environ. Chem. Eng. 9 (4) (2021), 105668.
[6] M. Usman, O. Tascone, P. Faure, K. Hanna, Chemical oxidation of hexachlorocyclohexanes (HCHs) in contaminated soils, Sci. Total Environ. 476-477 (2014) 434–439.
[7] S. Wacławek, D. Silvestri, P. Hrabák, V.V.T. Padil, R. Torres-Mendieta, M. Wacławek, M. Černík, D.D. Dionysiou, Chemical oxidation and reduction of hexachlorocyclohexanes: a review, Water Res. 162 (2019) 302–319.
[8] Z. Zhou, X. Liu, K. Sun, C. Lin, J. Ma, M. He, W. Ouyang, Persulfate-based advanced oxidation processes (AOPs) for organic-contaminated soil remediation: a review, Chem. Eng. J. 372 (2019) 836–851.
[9] A. Checa-Fernández, A. Santos, L.O. Conte, A. Romero, C.M. Domínguez, Enhanced remediation of a real HCH-polluted soil by the synergetic alkaline and ultrasonic activation of persulfate, Chem. Eng. J. 440 (2022), 135901.
[10] C.M. Dominguez, A. Romero, A. Checa-Fernandez, A. Santos, Remediation of HCHs-contaminated sediments by chemical oxidation treatments, Sci. Total Environ. 751 (2021), 141754.
[11] A. Gabet, H. Métivier, C. de Brauer, G. Mailhot, M. Brigante, Hydrogen peroxide and persulfate activation using UVA-UVB radiation: degradation of estrogenic compounds and application in sewage treatment plant waters, J. Hazard. Mater. 405 (2021), 124693.
[12] L.W. Matzek, K.E. Carter, Activated persulfate for organic chemical degradation: a review, Chemosphere 151 (2016) 178–188.
[13] Y. Tao, O. Monfort, M. Brigante, H. Zhang, G. Mailhot, Phenanthrene decomposition in soil washing effluents using UVB activation of hydrogen peroxide and peroxydisulfate, Chemosphere 263 (2021), 127996.
[14] A. Tsitonaki, B. Petri, M. Crimi, H. Mosbaek, R.L. Siegrist, P.L. Bjerg, In situ chemical oxidation of contaminated soil and groundwater using persulfate: a review, Crit. Rev. Environ. Sci. Technol. 40 (1) (2010) 55–91.
[15] S. Wacławek, H.V. Lutze, K. Grübel, V.V.T. Padil, M. Černík, D.D. Dionysiou, Chemistry of persulfates in water and wastewater treatment: a review, Chem. Eng. J. 330 (2017) 44–62.
[16] L. Peng, D. Deng, M. Guan, X. Fang, Q. Zhu, Remediation HCHs POPs-contaminated soil by activated persulfate technologies: feasibility, impact of activation methods and mechanistic implications, Sep. Purif. Technol. 150 (2015) 215–222.
[17] A. Checa-Fernández, A. Santos, A. Romero, C.M. Domínguez, Remediation of real soil polluted with hexachlorocyclohexanes (α-HCH and β-HCH) using combined thermal and alkaline activation of persulfate: optimization of the operating conditions, Sep. Purif. Technol. 270 (2021), 118795.
[18] R. García-Cervilla, A. Santos, A. Romero, D. Lorenzo, Remediation of soil contaminated by lindane wastes using alkaline activated persulfate: kinetic model, Chem. Eng. J. 393 (2020), 124646.
[19] L. Wang, L. Peng, L. Xie, P. Deng, D. Deng, Compatibility of surfactants and thermally activated persulfate for enhanced subsurface remediation, Environ. Sci. Technol. 51 (12) (2017) 7055–7064.
[20] S. Wang, C.N. Mulligan, An evaluation of surfactant foam technology in remediation of contaminated soil, Chemosphere 57 (9) (2004) 1079–1089.
[21] M. Cheng, G. Zeng, D. Huang, C. Yang, C. Lai, C. Zhang, Y. Liu, Advantages and challenges of Tween 80 surfactant-enhanced technologies for the remediation of soils contaminated with hydrophobic organic compounds, Chem. Eng. J. 314 (2017) 98–113.
[22] J. Liu, L. Zhao, Q. Liu, J. Li, Z. Qiao, P. Sun, Y. Yang, A critical review on soil washing during soil remediation for heavy metals and organic pollutants, Int. J. Environ. Sci. Technol. 19 (1) (2022) 601–624.
[23] C.M. Dominguez, A. Romero, A. Santos, Selective removal of chlorinated organic compounds from lindane wastes by combination of nonionic surfactant soil flushing and Fenton oxidation, Chem. Eng. J. 376 (2019), 120009.
[24] R. García-Cervilla, A. Santos, A. Romero, D. Lorenzo, Compatibility of nonionic and anionic surfactants with persulfate activated by alkali in the abatement of chlorinated organic compounds in aqueous phase, Sci. Total Environ. 751 (2021), 141782.
[25] I. Bouzid, J. Maire, E. Brunol, S. Caradec, N. Fatin-Rouge, Compatibility of surfactants with activated-persulfate for the selective oxidation of PAH in groundwater remediation, J. Environ. Chem. Eng. 5 (6) (2017) 6098–6106.
[26] R. Garcia-Cervilla, A. Santos, A. Romero, D. Lorenzo, Simultaneous addition of surfactant and oxidant to remediate a polluted soil with chlorinated organic compounds: slurry and column experiments, J. Environ. Chem. Eng. 10 (3) (2022), 107625.
[27] C. Trellu, N. Oturan, Y. Pechaud, E.D. van Hullebusch, G. Esposito, M.A. Oturan, Anodic oxidation of surfactants and organic compounds entrapped in micelles – selective degradation mechanisms and soil washing solution reuse, Water Res. 118 (2017) 1–11.
[28] V. Srivastava, M. Puri, T. Srivastava, P.V. Nidheesh, M.S. Kumar, Integrated soil washing and bioreactor systems for the treatment of hexachlorocyclohexane contaminated soil: a review on enhanced degradation mechanisms, and factors affecting soil washing and bioreactor performances, Environ. Res. 208 (2022), 112752.
[29] B. Bartolo, N.M. Elena, R.-L. Elvira, Enhanced desorption of lindane from an agricultural soil assisted by cyclodextrin aqueous solutions, in: Proceedings of the World Congress on Engineering and Computer Science, 2008.
[30] M.B. Carboneras, J. Villaseñor, F.J. Fernández, M.A. Rodrigo, P. Cañizares, Selection of anodic material for the combined electrochemical-biological treatment of lindane polluted soil washing effluents, J. Hazard. Mater. 384 (2020), 121237.
[31] M. Muñoz-Morales, M. Braojos, C. Sáez, P. Cañizares, M.A. Rodrigo, Remediation of soils polluted with lindane using surfactant-aided soil washing and electrochemical oxidation, J. Hazard. Mater. 339 (2017) 232–238.
[32] J. Wan, D. Meng, T. Long, R. Ying, M. Ye, S. Zhang, Q. Li, Y. Zhou, Y. Lin, Simultaneous removal of lindane, lead and cadmium from soils by rhamnolipids combined with citric acid, PLoS One 10 (6) (2015), e0129978.
[33] E.R. Bandala, F. Aguilar, L.G. Torres, Surfactant-enhanced soil washing for the remediation of sites contaminated with pesticides, Land Contamination & Reclamation 18 (2) (2010) 2.
[34] R. García-Cervilla, A. Romero, A. Santos, D. Lorenzo, Surfactant-enhanced Solubilization of chlorinated organic compounds contained in DNAPL from Lindane waste: effect of surfactant type and pH, Int. J. Environ. Res. Public Health 17 (12) (2020).
[35] R. Garcia-Cervilla, A. Santos, A. Romero, D. Lorenzo, Partition of a mixture of chlorinated organic compounds in real contaminated soils between soil and aqueous phase using surfactants: influence of pH and surfactant type, J. Environ. Chem. Eng. 9 (5) (2021), 105908.
[36] C.M. Domínguez, P. Ventura, A. Checa-Fernández, A. Santos, Comprehensive study of acute toxicity using Microtox® bioassay in soils contaminated by lindane wastes, Sci. Total Environ. 159146 (2022).
[37] A. Santos, J. Fernández, J. Guadaño, D. Lorenzo, A. Romero, Chlorinated organic compounds in liquid wastes (DNAPL) from lindane production dumped in landfills in Sabiñanigo (Spain), Environ. Pollut. 242 (2018) 1616–1624.
[38] C. Liang, C.-F. Huang, N. Mohanty, R.M. Kurakalva, A rapid spectrophotometric determination of persulfate anion in ISCO, Chemosphere 73 (9) (2008) 1540–1543.
[39] D. Lorenzo, R. García-Cervilla, A. Romero, A. Santos, Partitioning of chlorinated organic compounds from dense non-aqueous phase liquids and contaminated soils from lindane production wastes to the aqueous phase, Chemosphere 239 (2020), 124798.
[40] E. Mousset, D. Huguenot, E.D. van Hullebusch, N. Oturan, G. Guibaud, G. Esposito, M.A. Oturan, Impact of electrochemical treatment of soil washing solution on PAH degradation efficiency and soil respirometry, Environ. Pollut. 211 (2016) 354–362.
[41] J. Wan, S. Yuan, K. Mak, J. Chen, T. Li, L. Lin, X. Lu, Enhanced washing of HCB contaminated soils by methyl-β-cyclodextrin combined with ethanol, Chemosphere 75 (6) (2009) 759–764.
[42] T.D. Pham, M. Kobayashi, Y. Adachi, Adsorption of anionic surfactant sodium dodecyl sulfate onto alpha alumina with small surface area, Colloid Polym. Sci. 293 (1) (2015) 217–227.
[43] O. Iglesias, M.A. Sanromán, M. Pazos, Surfactant-enhanced solubilization and simultaneous degradation of phenanthrene in marine sediment by electro-Fenton treatment, Ind. Eng. Chem. Res. 53 (8) (2014) 2917–2923.
[44] M. Abouseoud, A. Yataghene, A. Amrane, R. Maachi, Effect of pH and salinity on the emulsifying capacity and naphthalene solubility of a biosurfactant produced by Pseudomonas fluorescens, J. Hazard. Mater. 180 (1–3) (2010) 131–136.
[45] E. Congiu, J.-J. Ortega-Calvo, Role of desorption kinetics in the rhamnolipid-enhanced biodegradation of polycyclic aromatic hydrocarbons, Environ. Sci. Technol. 48 (18) (2014) 10869–10877.
[46] S. Lamichhane, K.C. Bal Krishna, R. Sarukkalige, Surfactant-enhanced remediation of polycyclic aromatic hydrocarbons: a review, J. Environ. Manag. 199 (2017) 46–61.
[47] K. Yang, L. Zhu, B. Xing, Enhanced soil washing of phenanthrene by mixed solutions of TX100 and SDBS, Environ. Sci. Technol. 40 (13) (2006) 4274–4280.
[48] W. Zhou, L. Zhu, Distribution of polycyclic aromatic hydrocarbons in soil–water system containing a nonionic surfactant, Chemosphere 60 (9) (2005) 1237–1245.
[49] T. Pan, T. Deng, X. Zeng, W. Dong, S. Yu, Extractive biodegradation and bioavailability assessment of phenanthrene in the cloud point system by Sphingomonas polyaromaticivorans, Appl. Microbiol. Biotechnol. 100 (2016) 431–437.
[50] S. Peng, W. Wu, J. Chen, Removal of PAHs with surfactant-enhanced soil washing: influencing factors and removal effectiveness, Chemosphere 82 (8) (2011) 1173–1177.
[51] S. Paria, K.C. Khilar, A review on experimental studies of surfactant adsorption at the hydrophilic solid–water interface, Adv. Colloid Interf. Sci. 110 (3) (2004) 75–95.
[52] C.M. Dominguez, A. Romero, D. Lorenzo, A. Santos, Thermally activated persulfate for the chemical oxidation of chlorinated organic compounds in groundwater, J. Environ. Manag. 261 (2020), 110240.
[53] F. Chen, Z. Luo, G. Liu, Y. Yang, S. Zhang, J. Ma, Remediation of electronic waste polluted soil using a combination of persulfate oxidation and chemical washing, J. Environ. Manag. 204 (2017) 170–178.
[54] Y. Qiu, M. Xu, Z. Sun, H. Li, Remediation of PAH-contaminated soil by combining surfactant enhanced soil washing and Iron-activated persulfate oxidation process, Int. J. Environ. Res. Public Health 16 (3) (2019) 441.
[55] M.A. Lominchar, D. Lorenzo, A. Romero, A. Santos, Remediation of soil contaminated by PAHs and TPH using alkaline activated persulfate enhanced by

ARTICLE 7

Title: Acute Toxicity Evaluation of Lindane-Waste Contaminated Soils Treated by Surfactant-Enhanced ISCO

Authors: A. Santos, R. García-Cervilla, **A. Checa-Fernández**, C. M. Domínguez, D. Lorenzo

Journal: Molecules

Publication year: 2022

Volume, Page: 27, 2985

DOI: 10.3390/molecules27248965

Quartile (Area): Q1 (Pharmaceutical science)

Cited by (SCOPUS): 0

molecules

MDPI

Article

Acute Toxicity Evaluation of Lindane-Waste Contaminated Soils Treated by Surfactant-Enhanced ISCO

Aurora Santos *, Raúl García-Cervilla, Alicia Checa-Fernández, Carmen M. Domínguez and David Lorenzo

Departamento de Ingeniería Química y de Materiales, Ingeniería Química y de Materiales, Facultad de Ciencias Químicas, Universidad Complutense Madrid, Ciudad Universitaria S/N, 28040 Madrid, Spain
* Correspondence: aursan@quim.ucm.es

Abstract: The discharge of lindane wastes in unlined landfills causes groundwater and soil pollution worldwide. The liquid waste generated (a mixture of 28 chlorinated organic compounds, COCs) constitutes a dense non-aqueous phase liquid (DNAPL) that is highly persistent. Although in situ chemical oxidation (ISCO) is effective for degrading organic pollutants, the low COCs solubility requires high reaction times. Simultaneous injection of surfactants and oxidants (S-ISCO) is a promising technology to solve the limitation of ISCO treatment. The current work studies the remediation of highly polluted soil (COCs = 3682 mg/kg) obtained at the Sardas landfill (Sabiñáñigo, Spain) by ISCO and S-ISCO treatments. Special attention is paid to acute soil toxicity before and after the soil treatment. Microtox®, modified Basic Solid-Phase Test (mBSPT) and adapted Organic Solvent Sample Solubilization Test (aOSSST) were used for this scope. Persulfate (PS, 210 mM) activated by alkali (NaOH, 210 mM) was used in both ISCO and S-ISCO runs. A non-ionic and biodegradable surfactant selected in previous work, Emulse®3 (E3, 5, and 10 g/L), was applied in S-ISCO experiments. Runs were performed in soil columns filled with 50 g of polluted soil, with eight pore volumes (Pvs) of the reagents injected and 96 h between successive Pv injections. The total treatment time was 32 days. The results were compared with those corresponding without surfactant (ISCO). After remediation treatments, soils were water-washed, simulating the conditions of groundwater flux in the subsoil. The treatments applied highly reduced soil toxicity (final soil toxicity equivalent to that obtained for non-contaminated soil, mBSPT) and organic extract toxicity (reduction > 95%, aOSSST). Surfactant application did not cause an increase in the toxicity of the treated soil, highlighting its suitability for full-scale applications.

Keywords: ecotoxicity; soil remediation; DNAPL; persulfate; ISCO; S-ISCO; chlorinated organic compounds

Citation: Santos, A.; García-Cervilla, R.; Checa-Fernández, A.; Domínguez, C.M.; Lorenzo, D. Acute Toxicity Evaluation of Lindane-Waste Contaminated Soils Treated by Surfactant-Enhanced ISCO. *Molecules* **2022**, *27*, 8965. https://doi.org/10.3390/molecules27248965

Academic Editor: Gavino Sanna

Received: 30 November 2022
Accepted: 14 December 2022
Published: 16 December 2022

1. Introduction

Lindane (γ-hexachlorocyclohexane, γ-HCH) was used as a broad-spectrum pesticide during the second half of the 20th century. It was manufactured by benzene photochlorination, yielding a mixture of isomers (α-, β-, γ-, δ-, ε-HCH) known as technical HCH. γ-HCH is the only isomer with insecticidal properties, and the HCHs mixture requires purification by distillation with solvents and fractional crystallization [1]. This process was highly inefficient, and for each tonne of lindane, approximately 6–10 tonnes of other HCH isomers were generated [2]. Solid and liquid wastes from lindane production were usually dumped in the vicinity of the production sites, resulting in significant soil and groundwater pollution. Due to its danger, the production and use of lindane were banned in most countries. Nevertheless, there are many HCH-polluted spots around the world requiring urgent remedial actions. One particular case is that of Sabiñánigo (Huesca, Spain), where the company INQUINOSA dumped more than 140,000 tonnes of HCH waste in two unfilled landfills: Sardas and Bailín [3].

37. Mowat, F.S.; Bundy, K.J. Experimental and mathematical/computational assessment of the acute toxicity of chemical mixtures from the Microtox® assay. *Adv. Environ. Res.* **2002**, *6*, 547–558. [CrossRef]
38. Joly, P.; Bonnemoy, F.; Charvy, J.-C.; Bohatier, J.; Mallet, C. Toxicity assessment of the maize herbicides S-metolachlor, benoxacor, mesotrione and nicosulfuron, and their corresponding commercial formulations, alone and in mixtures, using the Microtox® test. *Chemosphere* **2013**, *93*, 2444–2450. [CrossRef]
39. Chen, C.-Y.; Lu, C.-L. An analysis of the combined effects of organic toxicants. *Sci. Total Environ.* **2002**, *289*, 123–132. [CrossRef]
40. Campisi, T.; Abbondanzi, F.; Casado-Martinez, C.; DelValls, T.A.; Guerra, R.; Iacondini, A. Effect of sediment turbidity and color on light output measurement for Microtox® Basic Solid-Phase Test. *Chemosphere* **2005**, *60*, 9–15. [CrossRef]
41. Čvančarová, M.; Křesinová, Z.; Cajthaml, T. Influence of the bioaccessible fraction of polycyclic aromatic hydrocarbons on the ecotoxicity of historically contaminated soils. *J. Hazard. Mater.* **2013**, *254–255*, 116–124. [CrossRef]
42. Dominguez, C.M.; Checa-Fernandez, A.; Romero, A.; Santos, A. Degradation of HCHs by thermally activated persulfate in soil system: Effect of temperature and oxidant concentration. *J. Environ. Chem. Eng.* **2021**, *9*, 105668. [CrossRef]
43. Dominguez, C.M.; Romero, A.; Fernandez, J.; Santos, A. In situ chemical reduction of chlorinated organic compounds from lindane production wastes by zero valent iron microparticles. *J. Water Process Eng.* **2018**, *26*, 146–155. [CrossRef]
44. Kaiser, K.L.E.; Palabrica, V.S. Photobacterium phosphoreum toxicity data index. *Water Pollut. Res. J. Can.* **1991**, *26*, 361–431. [CrossRef]
45. Kwan, K.K.; Dutka, B.J. Comparative assessment of two solid-phase toxicity bioassays: The direct sediment toxicity testing procedure (DSTTP) and the microtox® solid-phase test (SPT). *Bull. Environ. Contam. Toxicol.* **1995**, *55*, 338–346. [CrossRef]

Chapter 4.

INTRODUCTION

4.1. Soil pollution

4.1.1. Types of soil pollution attending the contamination source

4.1.2. Main soil pollutants

4.2. Remediation of soils polluted by organic compounds

4.3. Lindane wastes pollution: a case study

4.1. Soil pollution

Soil pollution refers to the presence of a chemical or substance at a higher-than-normal concentration, which has adverse effects on non-targeted organisms (FAO 2015). Industrialization, mining, and intensification in agriculture have left a legacy of contaminated soils around the world (Rodríguez-Eugenio 2018). Soil pollution is an alarming issue and has been identified as the third most crucial threat to soil functions in Europe (FAO 2015). In the European Economic Area, there are more than one million potentially polluted sites, referred to as sites where unacceptable soil contamination is suspected, and detailed investigations need to be carried out to verify whether there is an unacceptable risk (EEA 2007). According to Figure 4.1, around 1200000 sites have been identified in Europe, and more than 127000 are classified as contaminated. However, only 45% of these were remediated until 2011 (Panagos, Van Liedekerke et al. 2013).

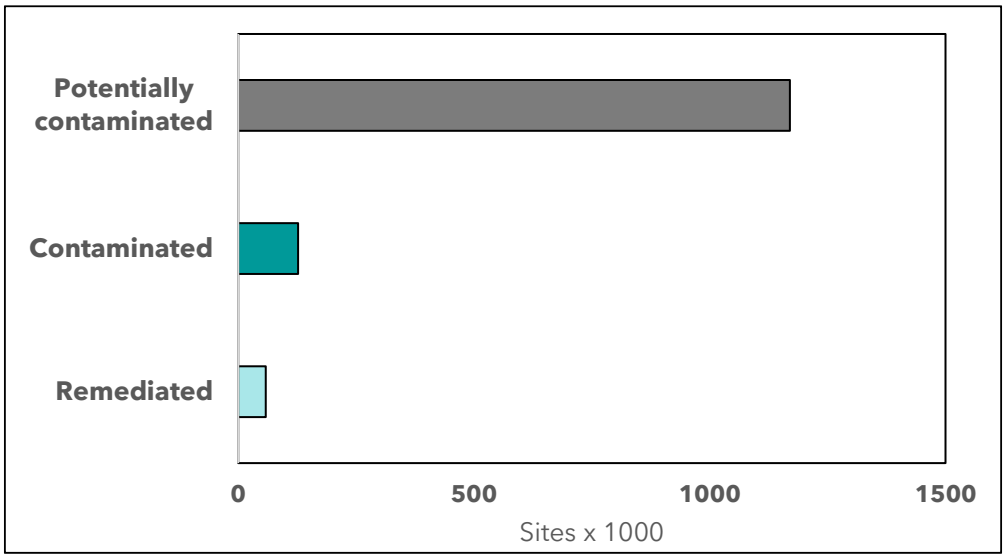

Figure 4.1. Number of identified remediated, potentially contaminated, and contaminated sites reported in Europe (Panagos, Van Liedekerke et al. 2013).

Fortunately, the awareness of the importance of soil pollution has increased in recent decades, and increasing research has been conducted on the remediation of soil pollution (Rodríguez-Eugenio 2018). The scientific productivity of articles and reviews related to polluted soils and their treatment published from 2012 to 2022 is shown in Figure 4.2. There is evidence of an increase in publications by up to four times in the last two decades, highlighting the scientific community interest in this topic.

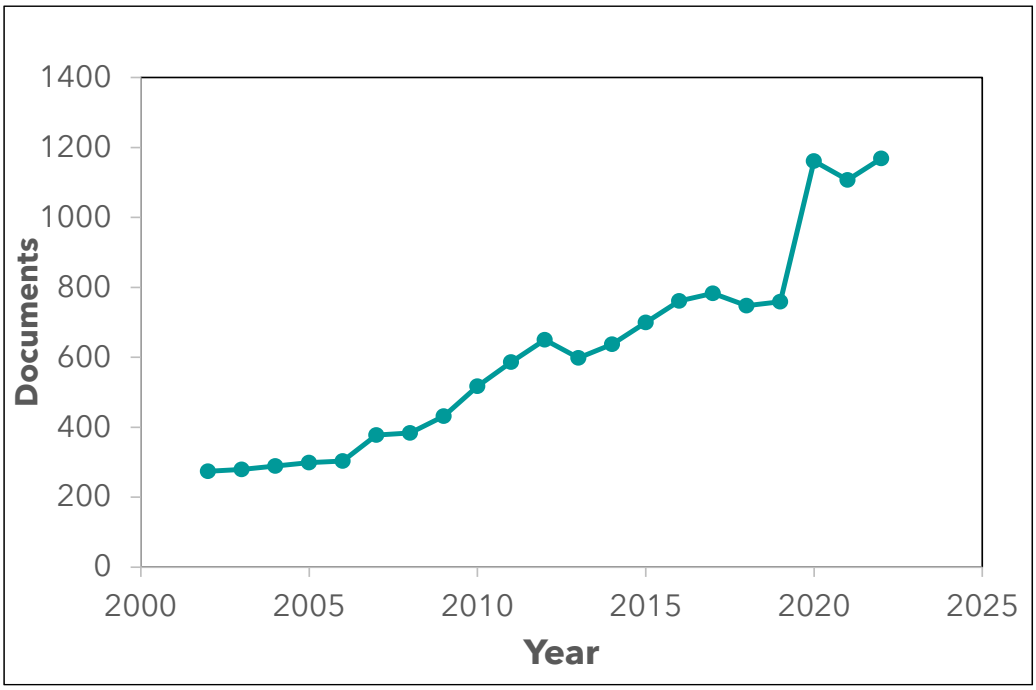

Figure 4.2. Annual number of publications in Web of Science on soil pollution from 2002 to 2022.

Similarly, social and political awareness of soil has risen since, in 2001, the 6th Environment Action Programme (EAP) of the European Union established that soil protection was a priority for Europe (Rodríguez and Payá Pérez 2017). The strategy for soil protection was launched by the European Commission in 2006 (Rodríguez and Payá Pérez 2017, Panagos and Montanarella 2018), recognizing the need to prevent soil degradation. Consequently, some steps have been taken to approve several legal approaches to implement a European governance framework to ensure soil protection (Panagos and Montanarella 2018). However, due to the lack of a specific common framework in Europe, several Member States have developed legislation to protect their soils, prevent further contamination, and regulate procedures for treating soil pollution (Rodríguez and Payá Pérez 2017). Although the legal background for addressing soil contamination varies considerably from one country to another (Figure 4.3) (Rodríguez and Payá Pérez 2017), the adoption of long-term objectives (2030-2050 timeframe) demonstrates the growing awareness in the political and social spheres for polluted soil management (Montanarella and Panagos 2021). Recently, the European Commission presented an ambitious package of measures within the Biodiversity Strategy 2030 (Montanarella and Panagos 2021), including actions to protect our soils (EU Soil Strategy for 2030).

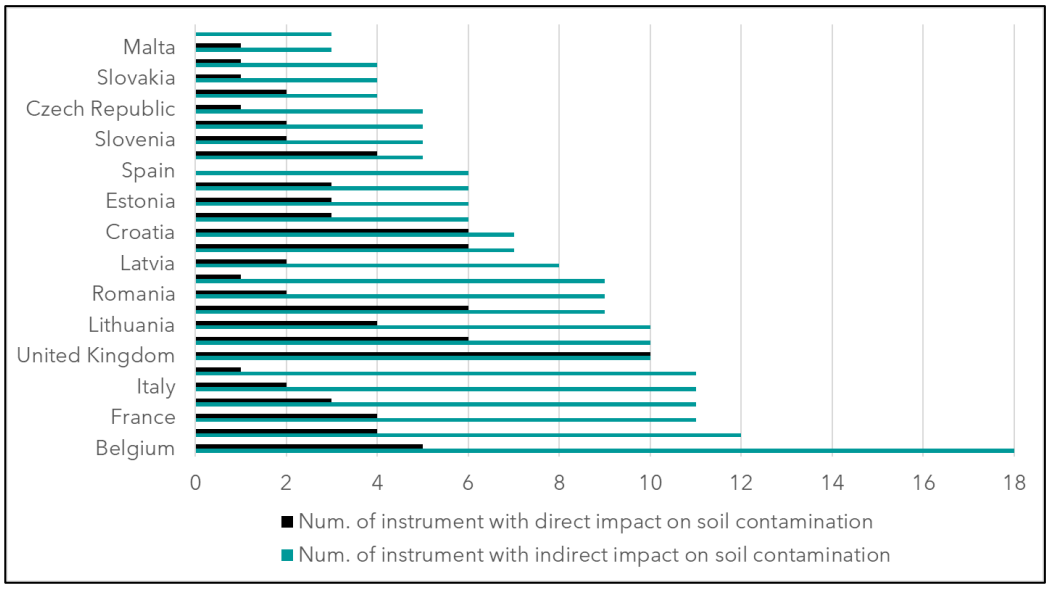

Figure 4.3. Number of national policies that explicitly (directly) or indirectly address soil contamination (Rodríguez and Payá Pérez 2017).

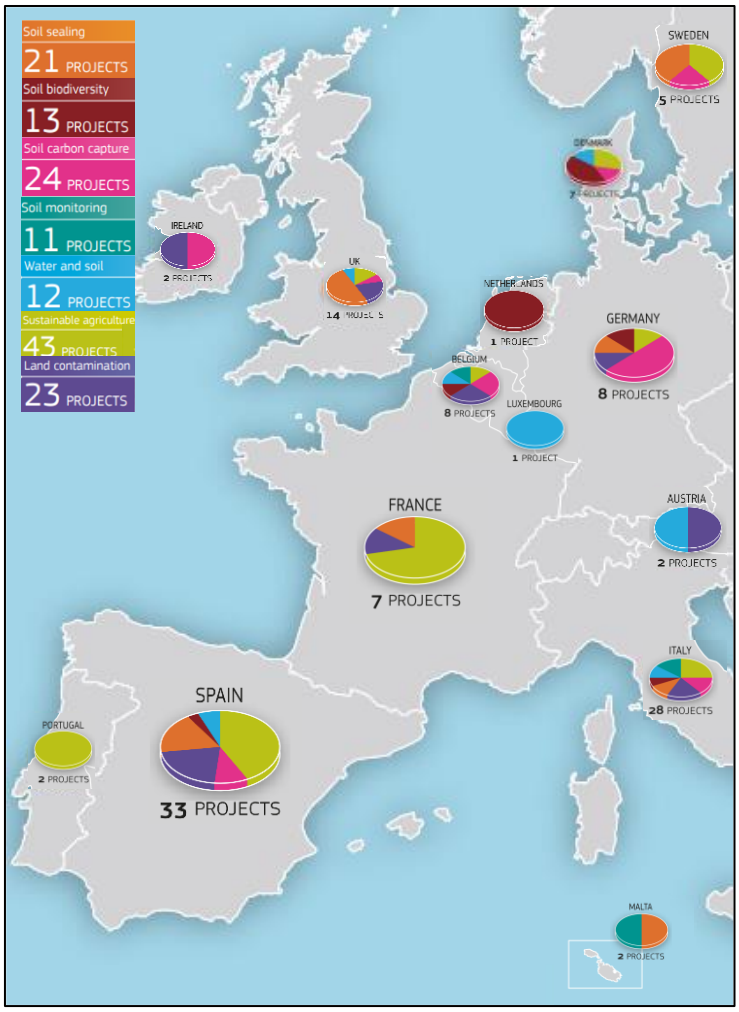

Figure 4.4. Distribution of soil-related LIFE projects (Camarsa, Sliva et al. 2014).

In recent years, the European Commission has funded research and innovation projects to restore and protect the health of soils in Europe, as is the case of the Horizon Europe and LIFE projects. Figure 4.4 shows the distribution of LIFE projects related to European soil (Camarsa, Sliva et al. 2014). These projects facilitate collaboration between public institutions and businesses, contributing to policy support, research, and raising awareness.

4.1.1. Types of soil pollution attending the contamination source

Considering the source of contamination, soil pollution can be either local or diffuse (Figure 4.5):

- **Local pollution** is caused by inadequate waste disposal within a particular area in which contaminants are released into the soil, and the source of pollution is easily identified. Examples of local soil pollution include former factory sites, inadequate waste and wastewater disposal, uncontrolled landfills (where waste is not disposed of correctly or according to its toxicity), and excessive application of agrochemicals, among others (Rodríguez-Eugenio 2018).
- **Diffuse pollution** is spread over extensive areas and does not have a single or easily identified source (FAO 2015). Diffuse pollution involves the transport of pollutants via air, soil, and water systems. Consequently, it is difficult to delimit the spatial extent of this type of pollution (Geissen, Mol et al. 2015). Many contaminants that cause local pollution may subsequently contribute to diffuse pollution.

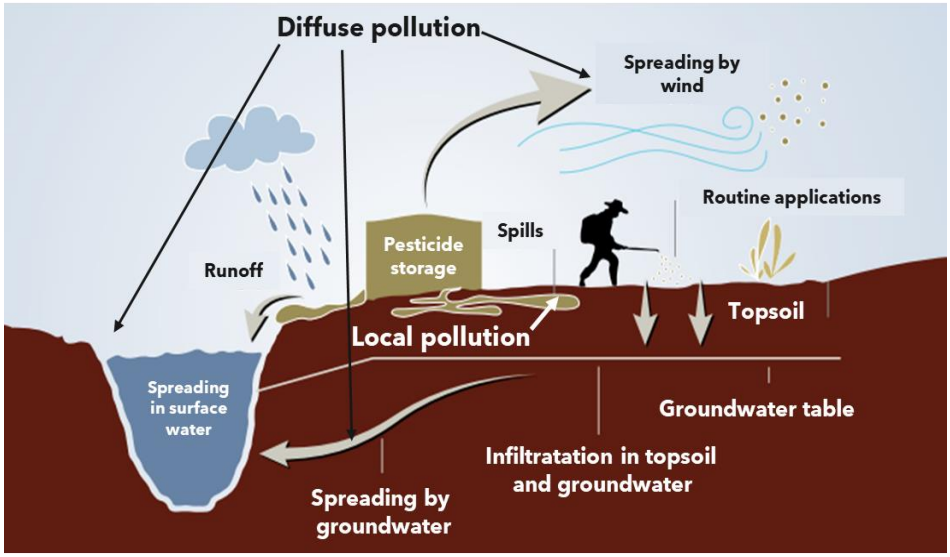

Figure 4.5. Types of soil pollution and their transport pathway in the environment. Adapted from (Rodríguez and Payá Pérez 2017).

4.1.2. Main soil pollutants

This section discusses the most common pollutants that affect the soil. To determine the contaminants to investigate in this study, examining the current situation of contaminated sites in European countries is necessary. The European Soil Data Center (ESDAC) reviewed the distribution of the main soil and groundwater contaminants in various EU countries (Panagos, Van Liedekerke et al. 2013), as summarized in Figure 4.6. **Heavy metals** contribute the most to soil contamination in Europe. The presence of **organic pollutants** is also significant. Particularly highlights the presence of **BTEX** (benzene, toluene, ethylbenzene, and xylene), polycyclic aromatic hydrocarbons (**PAHs**, such as naphthalene and anthracene), as well as chlorinated hydrocarbons (**CHCs**), such as trichloroethylene (**TCE**), dichlorobenzene (**DCB**), polychlorinated biphenyls (**PCBs**) and hexachlorocyclohexanes (**HCHs**). In this context and considering their significant impact on soil contamination, this Thesis focuses on the remediation of soils polluted with **chlorinated organic compounds**.

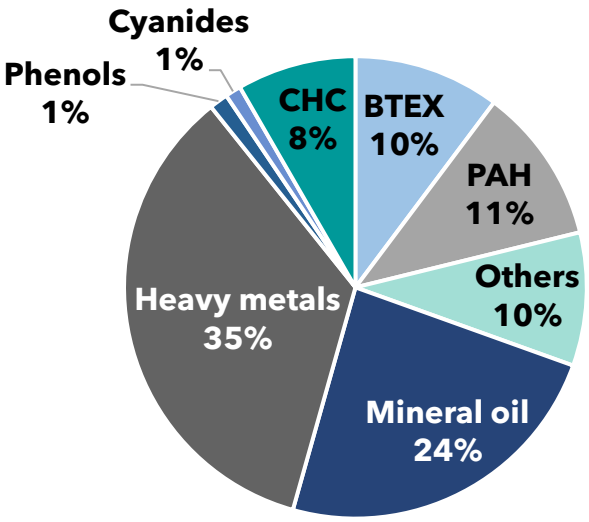

Figure 4.6. Distribution of contaminants affecting soil in European countries (Panagos, Van Liedekerke et al. 2013).

Most organic pollutants are hydrophobic organic compounds (HOCs). Owing to their limited solubility in water and hydrophobicity (Huo, Liu et al. 2020), the dumping of hydrophobic organic liquid phases into the environment results in a separate liquid phase, named Non-Aqueous Phase Liquids (NAPLs). They are also characterized by a strong tendency to adsorb onto soil organic fractions (Verginelli, Capobianco et al. 2017), making them a significant environmental issue. Depending on whether their density is lower or higher than that of water, they are classified as Light-NAPLs (LNAPLs) and Dense-NAPLs

(DNAPLs), respectively (Ciampi, Esposito et al. 2021). LNAPLs typically include petroleum hydrocarbons, and DNAPLs, chlorinated organic compounds (Javanbakht, Arshadi et al. 2017). After a contamination event, LNAPLs are usually found in the unsaturated zone or flooding over the water table owing to their low density (Amanat, Barbati et al. 2022) (Figure 4.7-a). In contrast, owing to their higher density, DNAPLs migrate through the saturated zone, generating pools in the non-permeable layers (Figure 4.7-b).

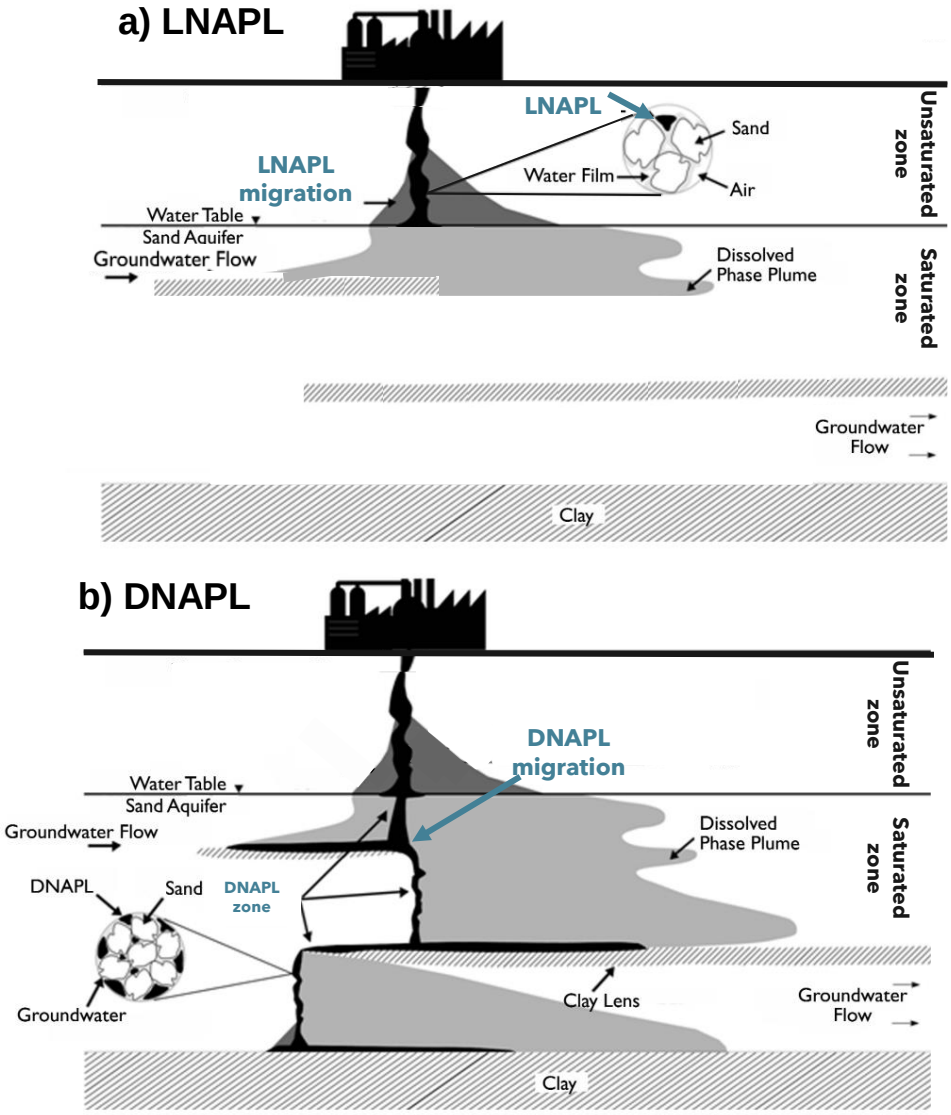

Figure 4.7. Conceptualization of NAPLs migration in the subsurface, (a) LNAPL and (b) DNAPL. Adapted from (Jackson 2004).

During the percolation of these phases through the soil, part of the organic fraction is retained between the pore spaces, leading to soil contamination (Barbati, Lorini et al. 2023). This leads to a long-term persistent source of pollution of groundwater since, due to their low solubility, the contaminants dissolve slowly, generating a contamination plume

and making their removal challenging, especially when using traditional remediation techniques (Ciampi, Esposito et al. 2021, Amanat, Barbati et al. 2022).

In this scenario, attending to their considerable impact on soil contamination, the present Thesis focuses on developing practical techniques for the remediation of soils polluted with **chlorinated organic compounds (COCs)** from both the surface and saturated zone.

4.2. Remediation of soils polluted by organic compounds

Remediation techniques (as opposed to containment or confinement techniques) seek to reduce the concentration of contaminants. Remediation processes can be divided into three main groups depending on the operation mode:

- **Ex situ**: excavation of contaminated soil from its original location and subsequent transport for treatment off the site. This operating mode is selected if on-site and in situ treatments cannot be applied.
- **On-site**: soil extraction and treatment at the site, without transporting. Once treated, soil is usually returned to its original location.
- **In situ**: treatment of polluted soil at its original location. When possible, in situ remediation is often preferred due to minimal site disturbance, safety, simplicity, and cost-effectiveness.

The advantages and disadvantages of the ex situ, on-site, and in situ technologies are summarized in Table 4.1. The type of operation mode selected will depend on different factors such as i) the type of pollution (local or diffuse), ii) the nature of the pollutant, and iii) its location (surface, unsaturated or saturated zone).

The most traditionally used method for remediating contaminated aquifers is the **Pump&Treat**, consisting of the extraction and subsequent on-site treatment of groundwater (Teramoto, Pede et al. 2020). However, the physico-chemical characteristics of NAPLs, such as low aqueous solubility and hydrophobicity, as well as the presence of pollutants trapped in the soil pores, are responsible for considerably lengthening remediation times, low removal rates, and high costs, making the Pump&Treat inefficient (Kavanaugh, Suresh et al. 2003, McGuire, McDade et al. 2006). Significant efforts have been made to overcome these limitations by developing efficient remediation technologies to maximize NAPLs mobilization and eliminate chlorinated organic compounds (Barbati, Lorini et al. 2023).

Table 4.1. Summary of advantages and disadvantages of ex situ, on-site, and in situ technologies (Adapted from (UNEP 2021)).

	Advantages	Disadvantages
Ex situ	• Remediation processes are quicker	• Cost of excavation • Cost of transportation • Soil structure and biodiversity are harder to re-establish
On-site	• Easier to control • Easier to monitor	• Cost of excavation • Cost of manipulation on-site • Soil structure and biodiversity are harder to re-establish
In situ	• Excavation costs avoided • Soil structure and biodiversity rehabilitates more quickly	• Longer time to reach remediation objective • More challenging to control remediation processes • More difficult to monitor

Remediation options include: i) **physical** (incineration, thermal desorption, vapor extraction, etc.), ii) **chemical** (augmentation, oxidation, reduction, etc.), iii) **biological** (bioaugmentation, biostimulation, phytodegradation, etc.), and **combined** treatments, as presented in Figure 4.8.

Physical remediation methods use physical and mechanical barriers to immobilize, isolate, and separate contaminants from the soil (Thomé, Reginatto et al. 2019, Ossai, Ahmed et al. 2020), and depending on the type of technique can be applied ex situ, on-site or in situ. Some examples include **incineration** (on-site or ex situ), in which excavated soil is transferred to a contained facility and heated under controlled conditions. Organic pollutants are vaporized, collected, or destroyed through pyrolysis (Lombi and Hamon 2005). **Thermal desorption** (in situ) consists of heating (90~560°C) the contaminated soil using steam, microwave, or infrared radiation to volatilize the pollutants (Michael-Igolima, Abbey et al. 2022). However, physical methods are usually labour-intensive, time-consuming, expensive, and in many cases, need further treatment of the gases produced during remediation (Michael-Igolima, Abbey et al. 2022, Rajendran, Priya et al. 2022). All this has consequently led to an increasing interest in alternative technologies, such as chemical and biological treatments.

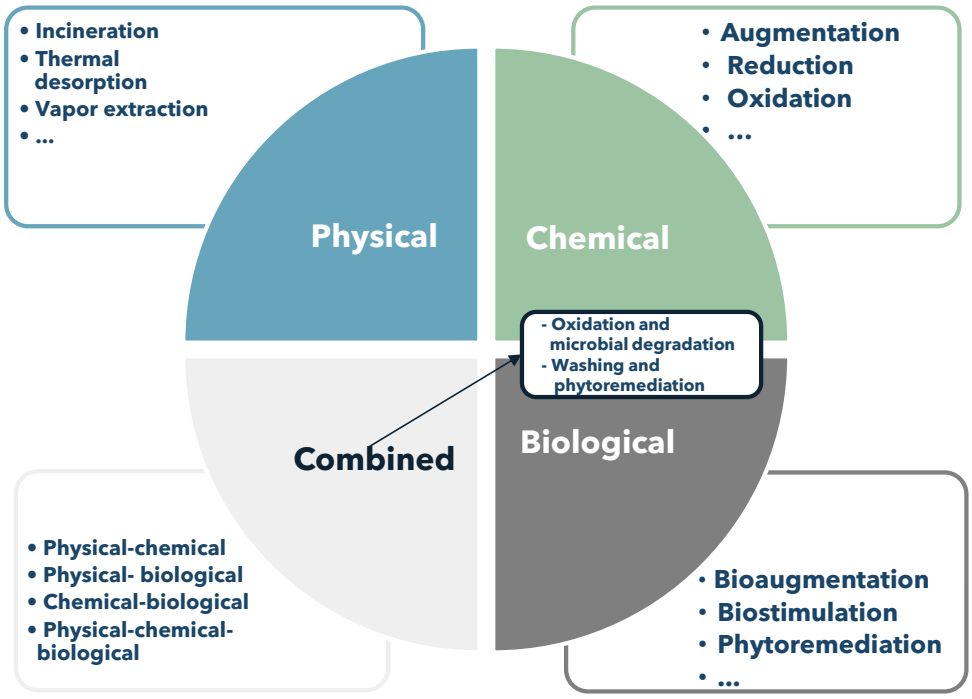

Figure 4.8. Categorization of methods for the remediation of soils and sediments contaminated with organic pollutants.

Chemical treatments can offer an attractive rapid, and aggressive alternative (Michael-Igolima, Abbey et al. 2022). These remediation technologies consist of applying the chemical and degrading the organic pollutants in soil and groundwater and can be used ex situ, on-site, or in situ (Brebbia 2013, Besha, Bekele et al. 2018). Chemical methods include augmentation, reduction, and oxidation (De Albergaria J.T.V.S. 2016). **Chemical augmentation** consists of adding chemicals (such as phosphoric acid, potassium phosphate, sulfuric acid, hydrogen chloride, etc.) to the soil to stimulate the activities of degrading microorganisms in the soil. **Chemical reduction**, mainly using zero-valent iron in the form of nano or microparticles (injected or as permeable reactive barriers into the subsurface), has turned out to be a promising alternative for the pollutant degradation (Dominguez, Parchao et al. 2016, Dominguez, Romero et al. 2018). However, it has significant limitations when pollutants are adsorbed on the soil or even found as hydrophobic particulate matter due to transport limitations (Mueller, Braun et al. 2012). Therefore, remediation studies applying zero valent iron nanoparticles to polluted soils at real scale are minimal.

Among **chemical oxidation** treatments involving oxidants, **Advanced Oxidation Processes (AOPs)** are well-established technologies for decontaminating polluted soils. AOPs typically involve the generation of highly reactive radical species, such as hydroxyl

($OH^{\bullet}$), sulfate ($SO_4^{\bullet-}$), and superoxide ($O_2^{\bullet-}$) radicals, which are strong oxidants capable of breaking down a wide range of contaminants (Cheng, Zeng et al. 2016, Zhou, Liu et al. 2019, Wang, Brigante et al. 2020). The most used oxidants are **hydrogen peroxide** (H_2O_2) catalyzed by Fe (Fenton process), which generates hydroxyl and hydroperoxyl radicals (Eqs. (4.1) and (4.2)), and **persulfate** (PS, $S_2O_8^{2-}$) (Siegrist, Crimi et al. 2011, Cheng, Zeng et al. 2016, Zhang, Liu et al. 2020).

$$Fe^{2+} + H_2O_2 \rightarrow Fe^{3+} + OH^{\cdot} + OH^{-} \quad (4.1)$$

$$Fe^{3+} + H_2O_2 \rightarrow Fe^{2+} + OOH^{\cdot} + H^{+} \quad (4.2)$$

The selection of the oxidant should consider a balance between its chemical effectiveness in removing the pollutants and its stability in the soil. In this regard, the application of the **Fenton** process in soil remediation is limited by: i) the high unproductive consumption of hydrogen peroxide due to the characteristics of the soil and ii) the precipitation of Fe (III) to $Fe(OH)_3$ at near-neutral pH. The last one provokes removing Fe (III) from the catalytic cycle (Santos and Rosas 2016, Checa-Fernández, Santos et al. 2021). Soluble inorganic or organic ligands (**chelating agents**) can overcome these limitations (Checa-Fernández, Santos et al. 2021). Chelating agents form complexes with Fe(II)/Fe(III) at neutral pH, keeping it soluble. Thus, the production of oxidative species is enhanced, and the applicability of Fenton oxidation is extended to a wider pH range (Zhang and Zhou 2019, Ahile, Wuana et al. 2020).

In recent years, the use of persulfate (**PS**) has significantly increased in soil remediation processes owning to its attractive properties (high aqueous solubility, high stability in water and/or soil, applicability in a high pH range, a lower affinity for natural soil organic compounds and therefore, longer lifetime and higher radius of influence than H_2O_2, ease of handling, etc.) (Matzek and Carter 2016, Ike, Linden et al. 2018, Santos, Fernandez et al. 2018, García-Cervilla, Santos et al. 2020). **PS** can be **activated** to generate free radicals using **heat** (or other energy sources) (Eq. (4.3)), **alkaline** substances such as NaOH (Eqs. (4.4) and (4.5)), or by the addition of **transition metals** such as iron (Eq. (4.6)).

$$S_2O_8^{2-} \xrightarrow{\text{heat}} 2\, SO_4^{\cdot-} \quad (4.3)$$

$$2\, S_2O_8^{2-} + 2\, H_2O \xrightarrow{OH^-} 3\, SO_4^{2-} + SO_4^{\cdot-} + O_2^{\cdot-} + 4\, H^{+} \quad (4.4)$$

$$SO_4^{\cdot-} + OH^- \rightarrow SO_4^{2-} + {\cdot}OH \quad (4.5)$$

$$S_2O_8^{2-} + Fe^{2+} \rightarrow Fe^{3+} + SO_4^{2-} + SO_4^{\cdot-} \quad (4.6)$$

Recently, **ultrasounds** (US) have been used to enhance pollutant desorption from soil (Effendi, Wulandari et al. 2019) and to activate PS *via* cavitation and thermal activation (Lei, Tian et al. 2019, Lei, Zhang et al. 2020), decreasing the reaction time required to degrade the pollutants. Eqs. (4.7)-(4.8) show the main reactions involved in the US-activated PS system, where "))))" refers to the US irradiation (Wang and Zhou 2016). US application involves the production of localized hot spots, reaching temperatures and pressures above 5000 K and 500 atm, respectively (Wei, Villamena et al. 2017, Luo, Gong et al. 2021). These extreme conditions result in water thermolysis, generating radical species such as $OH^{\bullet}$ and $H^{\bullet}$ (Eq. (4.7)) (Wang and Zhou 2016). Under these conditions, PS can generate sulfate radicals ($SO_4^{\bullet-}$) (Eq. (4.8)). Moreover, the rapid temperature rise caused by the breakage of cavitation bubbles enhances the thermal activation of PS generating sulfate radicals (Eq. (4.3)).

$$H_2O \xrightarrow{))))} OH^{\bullet} + H^{\bullet} \quad (4.7)$$

$$S_2O_8^{2-} \xrightarrow{))))} 2SO_4^{\bullet-} \quad (4.8)$$

The selection of the PS activation method will depend on the nature and concentration of contaminants and their location (surface or saturated zone). If the contamination is in the surface (named sediments or **topsoil**), applying a wider range of PS activations (temperature, US, alkali, etc.) for the **on-site** treatment of soils is possible.

In the case of **subsoil** (and, therefore, groundwater) pollution, applying some PS activation methods, such as temperature or US for in situ chemical oxidation (ISCO) processes, is technologically complex or economically unfeasible. The alkaline activation of PS could be the most convenient method (Devi, Das et al. 2016, Santos, Lorenzo et al. 2021). However, when sites are polluted with significant residual NAPL mass (containing hydrophobic organics compounds; HOCs), ISCO technology is not sufficiently effective in achieving decontamination goals at reasonable times and costs (Hoag and Collins 2011, Wang, Hoag et al. 2013). This is mainly due to the limitation of the pollutants transfer into the aqueous phase, where the degradation occurs (Wang, Peng et al. 2017, García-Cervilla, Santos et al. 2020). This limitation can be overcome by using **surfactants**,

amphiphilic-nature substances able to reduce the surface tension of water (Wang and Mulligan 2004), enhancing HOCs solubilization and/or mobilization (Cheng, Zeng et al. 2017).

In this context, the application of surfactants has gained interest as it improves the remediation of NAPLs-contaminated sources in less time and with lower costs. The application of surfactant solutions can be in situ (soil flushing) or ex situ (soil washing) processes (Karaoglu, Copty et al. 2019). Soil washing involves the excavation of a polluted matrix followed by enhanced solubilization of pollutants by surfactant addition. This treatment is mainly applied to remediate the unsaturated zone (Mao, Jiang et al. 2015). Contrary, in soil flushing treatment (also named **SEAR**, Surfactant Enhanced Aquifer Remediation), surfactant solution is injected through specific wells into the aquifer, passing through the polluted area of the saturated zone to solubilize/mobilize NAPLs (Dominguez, Romero et al. 2019). The simultaneous injection of oxidant and surfactant (S-ISCO) has also emerged as an interesting alternative for the in situ treatment of the NAPLs-polluted sites.

Microbial degradation of pollutants has recently attracted increasing attention as a less expensive and more environmentally friendly alternative to conventional chemical treatment methods (Zhang, Lin et al. 2020). **Biological** remediation methods can remove organic pollutants in the soil by using living organisms such as microorganisms and plants (Michael-Igolima, Abbey et al. 2022). Biological treatments include **biostimulation** (addition of nutrients or organic matter to stimulate microbial activity), **bioaugmentation** (introduction of degrading microbes or organic amendments containing active microorganisms), and **phytoremediation** (plants are used to detoxify contaminated soils), among others (Ren, Zeng et al. 2018). However, biological treatments also pose some limitations, such as the longer clean-up time and difficulty degrading high concentrations and recalcitrant contaminants (Michael-Igolima, Abbey et al. 2022).

In this context, it is interesting to use **combined treatments**, which integrate the strength of two or more methods, thereby limiting their individual weaknesses. By optimizing the interactions between different remediation methods, it is possible to achieve high degradation efficiency while minimizing toxicity. Some examples include physical-chemical, physical-biological, chemical-biological, and physical-chemical-biological methods. Notably, in the case of the on-site treatment of polluted TS, chemical-biological and physical-biological combined methods may serve as polishing agents after

applying physical or chemical processes, restoring the functionality of contaminated soil. Similarly, considering the heterogeneity of contamination in the subsoils, a train of subsequent technologies, as the concentration of the pollutant is reduced, can be applied (Figure 4.9, (Domínguez, Checa-Fernández et al. 2023)). The technologies train begins with the direct extraction of the dense phase, followed by SEAR, combined or not with further on-site oxidation processes of the resultant emulsion, in situ chemical oxidation processes enhanced by surfactants (S-ISCO) followed by in situ oxidation processes for the treatment of the contamination plume (ISCO) (Domínguez, Checa-Fernández et al. 2023), and finally, the application of a bioremediation treatment.

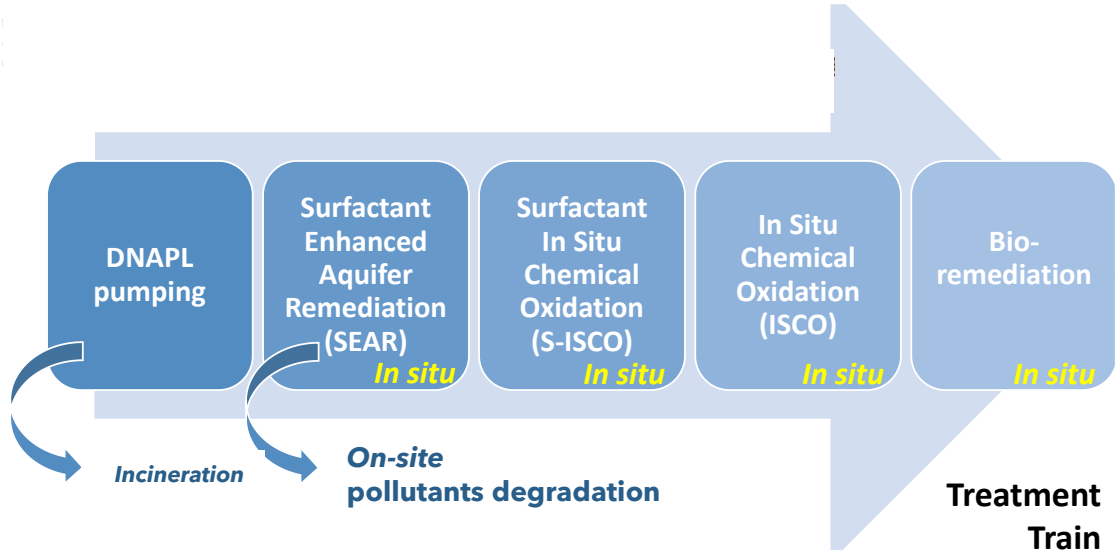

Figure 4.9. Treatment train typically carried out for subsoil remediation. Adapted from (Domínguez, Checa-Fernández et al. 2023).

In conclusion, it is essential to note that the selection of remediation treatment and the operating mode (ex situ, on-site, or in situ) should consider the lithological and mineralogical characteristics of the polluted site, the type and concentration of contaminants, their location (surface or saturated zone), and the technical and economic reality of the contaminated area (Swartjes 2011). Thus, the need to analyze all these aspects when remediating each practical case is emphasized.

4.3. Lindane wastes pollution: a case study

An actual case study of great interest within soil polluted by chlorinated organic pollutants is the problem of contamination by **lindane wastes**. Lindane (the gamma isomer of 1,2,3,4,5,6-hexachlorocyclohexane, γ-HCH) was a broad-spectrum insecticide extensively produced in Europe during the second half of the 20th century (Vega, Romano et al. 2016). Thus, this compound (and other HCH isomers) is one of the most frequently detected chlorinated contaminants in the environment (Bhatt, Kumar et al. 2009). The synthesis of lindane, schematized in Figure 4.10, consists of the photochemical chlorination of benzene with ultraviolet (UV) light, producing a mixture of HCH isomers called technical HCH. However, lindane is the only isomer with insecticidal properties. Thus, technical HCH undergoes a purification stage. For each tonne of lindane produced, approximately 6-10 tonnes of other wastes were generated, including two types: i) liquid wastes coming from the chlorination failed reaction and distillation tails, which constitute a DNAPL, and ii) solid HCH-wastes (consisting of a mixture of HCH isomers without insecticidal properties) (Figure 4.10).

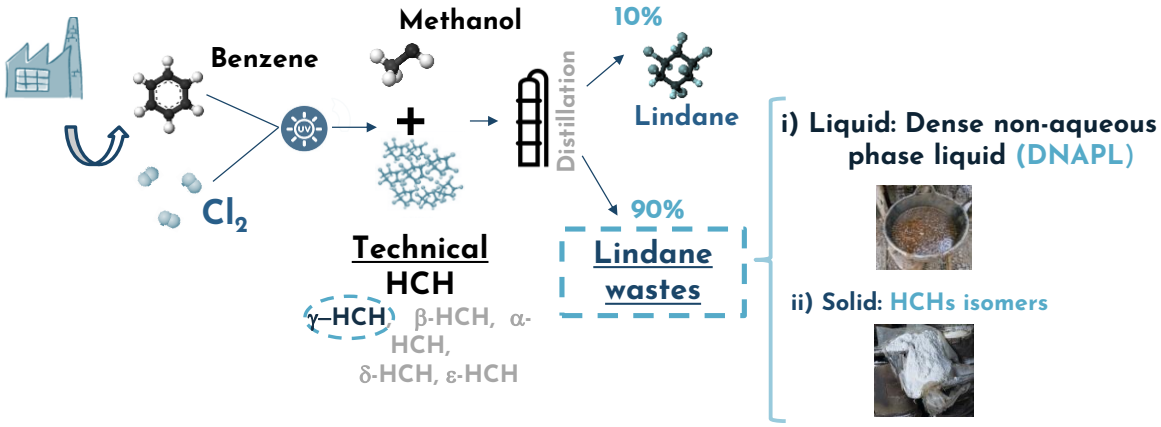

Figure 4.10. Scheme of lindane production process and types of wastes produced.

These wastes were usually dumped near production sites, originating an environmental problem of great magnitude (Santos, Fernandez et al. 2018). Thus, it is estimated that there are between 4 and 7 million tons of waste from lindane production spread throughout the world, leading to the globe largest POP stockpile (Vijgen, Abhilash et al. 2011, Fernández, Arjol et al. 2013) in which 63% of the total waste is concentrated in Europe. The location of these polluted sites and the estimated quantity of HCH waste dumped in those places is shown in Figure 4.11.

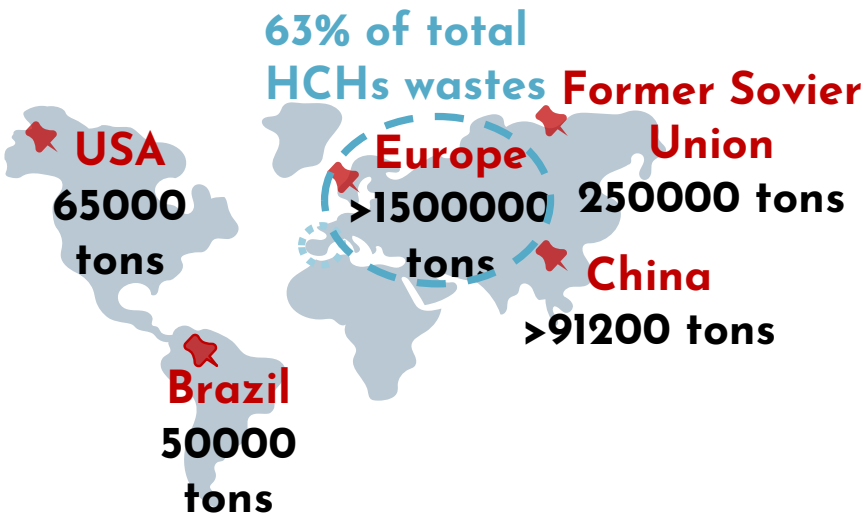

Figure 4.11. Location and quantities of stored/dumped HCH wastes around the world. Adapted from (Vijgen, Abhilash et al. 2011).

α- and β-HCH isomers, as well as lindane (γ-HCH), have been classified as possible human carcinogens by the United States Environmental Protection Agency (EPA 2003) and included in the list of persistent organic pollutants (POPs) by the Stockholm Convention. Consequently, lindane production and use are forbidden in most countries.

One of the most severe cases of lindane waste pollution is located in the province of Huesca (Sabiñánigo, Spain), in Sardas and Bailín landfills, where the company INQUINOSA discharged approximately 115,000 tons of waste with a high content of HCHs and other organochlorine compounds (Fernández, Arjol et al. 2013), resulting in the contamination of soil and groundwater. These contaminated sites have aroused great interest because of their complexity and the risks associated with their proximity to the Gállego River (Santos, Fernandez et al. 2018). The disposal of lindane wastes (as solid and liquid waste) in these landfills and the consequent types of associated pollution (topsoil (TS), leachates, subsoil (SS), and groundwater) are schematized in Figure 4.12. TS pollution is derived from the discharge of solid HCH wastes (Figure 4.12). This type of pollution is found in the form of particulate matter and/or adsorbed onto soil particles (Fernández, Arjol et al. 2013). The effect of rain on contaminated topsoil causes leachate contamination (Domínguez, Checa-Fernández et al. 2023). SS contamination was mainly originated from the dumping of liquid wastes (DNAPL), which consist of a mixture of 28 Chlorinated Organic Compounds (COCs) from chlorobenzene to heptachlorocyclohexane (Santos, Fernandez et al. 2018). Because of its high density (1.5-1.8 g mL^{-1}), this phase migrated through the saturated zone until impermeable bedrock, causing a contaminant plume (Figure 4.12).

Considering the risks posed by this site, there is an urgent need to develop effective remediation techniques. COCs concentration of the real soil phases (surface and saturated zone) from the Sardas and Bailín landfills must be characterized before and after the treatments. The physico-chemical characteristics of the soil and the pollutants nature affect the oxidation system selected. The level of contamination in landfill soil is very heterogeneous and changes with location and depth, as well as with the contaminant type (DNAPL or technical-HCH), highlighting the need to completely characterize all the real matrices involved.

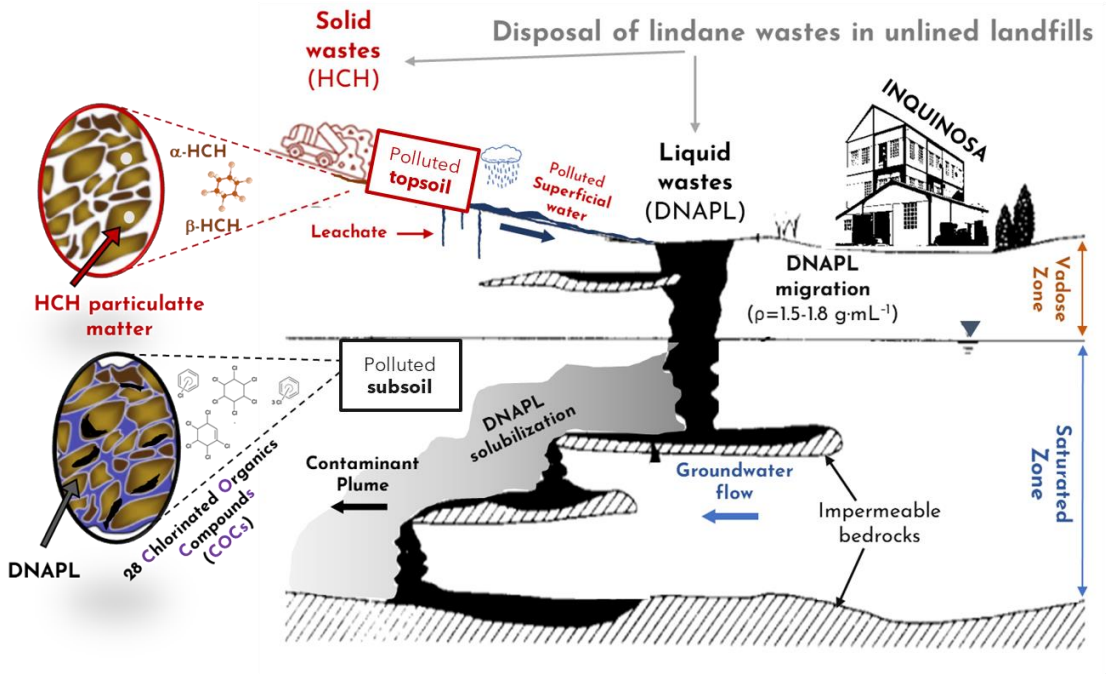

Figure 4.12. Schematization disposal of lindane wastes by INQUINOSA and the further dispersion of contaminants in the topsoil and subsoil (Domínguez, Ventura et al. 2023, **ART. 1**).

Subsoils and their source of contamination (DNAPL) have been characterized in previous studies. Santos, Fernandez et al. (2018) evaluated the composition of six DNAPL samples obtained from Sardas and Bailín landfills. Additionally, subsoil samples of Sardas alluvial impacted by DNAPL, as well as the partitioning equilibrium of COCs between the DNAPL or soil and the aqueous phases, have been studied extensively (García-Cervilla, Romero et al. 2020, Lorenzo, García-Cervilla et al. 2020, Garcia-Cervilla, Santos et al. 2021). However, the **characterization of topsoils** (sediments from the surface) of the Bailín landfill, contaminated by the disposal of the solid technical-HCH, needs more study. Thus, the current study will determine topsoil characterization (physicochemical properties and COCs concentration). Soil samples were obtained from the Bailín landfill

(Sabiñanigo, Spain) in cooperation with the Aragon Government and companies, such as EMGRISA and SARGA.

Additionally, the **acute toxicity of all real polluted matrices involved** (topsoil (TS), leachate, subsoil (SS), and groundwater) is unknown. Thus, the acute toxicity of the i) polluted soils (TS and SS), ii) different sources of pollution (HCH particulate matter (TS) and DNAPL (SS)), and iii) aqueous phases in contact with the soils after partitioning equilibrium (simulating leachates and groundwater from the polluted emplacement) will be determined for the first time. This information would provide valuable information for the toxicity characterization of these real matrices, an essential aspect for future field applications of selected remediation treatments at the site.

Regarding the application of different remediation technologies, several studies have focused on the COCs abatement in the aqueous phase by on-site treatments (Wacławek, Silvestri et al. 2019, Adithya, Jayaraman et al. 2021), by applying oxidation (ozonation (Cruz-González, Julcour et al. 2018), photo-Fenton (Cruz-González, Julcour et al. 2018), electrochemical oxidation process (Wacławek, Antoš et al. 2016, Dominguez, Oturan et al. 2018), sonolysis (Kida, Ziembowicz et al. 2018), PS activated by temperature (Dominguez, Romero et al. 2020) and alkali (Santos, Fernandez et al. 2018)), and reduction (zero-valent iron microparticles (Dominguez, Rodriguez et al. 2016, Dominguez, Romero et al. 2018) treatments. Likewise, subsoil remediation through the application of ISCO (PS activated by alkali) and S-ISCO (E-Mulse® 3 as the surfactant, and PS activated by alkali as the oxidant) treatments has been deeply studied (Santos, Fernandez et al. 2018, García-Cervilla, Romero et al. 2020, García-Cervilla, Santos et al. 2020, Lorenzo, García-Cervilla et al. 2020, Garcia-Cervilla, Santos et al. 2021, García-Cervilla, Santos et al. 2021, Garcia-Cervilla, Santos et al. 2022, García-Cervilla, Santos et al. 2022).

However, only a few studies have focused on the application of oxidation technologies for the remediation of HCHs-polluted topsoil, applying chemical oxidation (permanganate, Fenton process, and different methods of activated PS: Fe, temperature, and alkali) (Usman, Tascone et al. 2014, Peng, Deng et al. 2015). Exciting results were obtained with soils artificially contaminated with HCHs (Peng, Deng et al. 2015) or real soil polluted with lindane (Usman, Tascone et al. 2014). However, the behavior of other HCH isomers (α- and β-HCH, the primary pollutants of the Bailín landfill topsoils) towards chemical oxidation has not been previously studied. Moreover, the influence of treating real polluted soil (with aged contamination and particulate matter) instead of spiked soil remains a challenge for the scientific community. In this context, the application of

chemical oxidation treatments to the remediation of real HCHs-polluted topsoils was evaluated in this Doctoral Thesis for the first time.

In addition to high COCs degradation efficiency, remediation treatments must meet low toxicity and minimal impact on the soil ecosystem (Trellu, Mousset et al. 2016, Garcia-Cervilla, Santos et al. 2022). In this regard, it must be highlighted that although the use of chemicals (oxidants, activators, and/or surfactants) in soil remediation has grown in recent years, there is limited information regarding their intrinsic toxicity, especially about their interaction with the soil and how their use affects soil toxicity, which is decisive for the remediation treatments implementation.

In this context, the effect of selected treatments for the remediation of TS and SS on acute soil toxicity using Microtox® bioassays was evaluated. For this purpose, the acute toxicity of polluted and treated soils was determined. To the best of our knowledge, this is the first study that evaluates the toxicity of soils after remediation treatments, including the effect of soil alkalinization, oxidant, and surfactant addition, providing practical information for a full-scale application.

Chapter 5.

SCOPES AND AIMS

The presence of hydrophobic organic compounds (HOCs), as is the case for most chlorinated organic compounds (COCs) in soil, has become a major environmental challenge due to their high persistence and toxicity. In this context, the main objective of this Doctoral Thesis is the **remediation of soils contaminated with chlorinated organic compounds by applying different chemical oxidation treatments**.

The following partial objectives were established to achieve this global aim:

1. **Characterization of polluted samples.** Initial characterization is required to determine the efficiency of further oxidation treatments. Real soil samples polluted by lindane wastes obtained from the Bailín and Sardas landfills (topsoil (TS) and subsoil (SS), respectively) will be characterized. Soil lithology, chemical-physical composition, COCs type, and COCs concentration are decisive factors when selecting an oxidation treatment. Characterization of the pollution sources (HCHs particulate matter (TS) and DNAPL (SS)) will also be performed. Finally, the Microtox® bioassay will be used to comprehensively assess the initial acute toxicity of soil samples and their corresponding elutriates. This study is presented in Subsection 7.1.

2. **Topsoil (TS) oxidation treatments.** Different oxidation treatments (Fenton and PS activated) for the on-site remediation of HCHs-polluted TS will be evaluated.

   2.1. Oxidant and activator evaluation. The oxidant system will be selected considering the balance between its chemical effectiveness in COCs removal and its stability in the soil under study. The application of different oxidants (hydrogen peroxide (HP) and persulfate (PS)) and activators (Fe, NaOH, and temperature) will be tested. Notably, oxidation reactions in complex systems such as soils often involve multiple interactions with soil components, making the determination of reaction rates more challenging. A comprehensive understanding of the variables influencing the rate of chemical reactions involved in the oxidation processes occurring in both aqueous and soil phases is necessary to implement the treatment on a real scale. Thus, the evolution of parent pollutants, by-products, and oxidants over reaction time will be analyzed. This study is presented in Subsections 7.2.1. and 7.2.2.

   2.2. Intensification of PS/NaOH. Identifying the most cost-effective and time-saving treatment for successful soil remediation is essential. Based on the previously obtained results, the intensification of the PS/NaOH treatment by the application of temperature

(PS/NaOH/**T**), ultrasound (PS/NaOH/**US**), and surfactants (**S**/PS/NaOH) will be evaluated. Therefore, a comprehensive approach will be extensively conducted to assess the influence of the main operating conditions (reagent addition order, temperature or US power, aqueous/soil ratio, initial concentration of PS, and stirring rate) on the COCs degradation efficiency. Particular attention will be paid to evaluating the pollutants dechlorination degree and identifying intermediate COCs under the tested operating conditions. This study is faced in Subsection 7.2.3.

3. **Acute toxicity evaluation.** When selecting soil remediation treatments, it is essential to consider not only the COCs degradation efficiency but also must meet both low ecotoxicity and minimal impact on the soil ecosystem. This involves assessing the possible adverse effects of the treatment on soil organisms. In this regard, the toxicity of **TS** after the application of PS/T and PS/NaOH/T treatments and **SS** after ISCO (PS/NaOH) and S-ISCO (S/PS/NaOH) treatments will be evaluated using Microtox® bioassay (Subsections 7.3.1 and 7.3.2, respectively).

Chapter 6.

MATERIALS AND METHODS

6.1. Materials

6.1.1. Reagents

6.1.2. Soil samples

6.1.3. Soil contaminants (HCH particulate matter and DNAPL)

6.2. Experimental procedures for soil remediation

6.2.1. Topsoil (TS) oxidation treatments

6.2.2. Subsoil (SS) oxidation treatments

6.3. Analytical methods

6.3.1. Soil phase

6.3.1.1. Chlorinated Organic Compounds (COCs)

6.3.1.2. Metals

6.3.1.3. pH

6.3.1.4. Total organic carbon

6.3.1.5. Scanning electron microscopy (SEM) and elemental energy dispersive analysis (EDS)

6.3.1.6. Acute toxicity

6.3.2. Aqueous phase

6.3.2.1. Chlorinated Organic Compounds (COCs)

6.3.2.2. Oxidants

6.3.2.3. Iron

6.3.2.4. Chlorides

6.3.2.5. pH

6.3.2.6. Surfactants

6.3.2.7. Acute toxicity

6.1. Materials

All reagents used in the experimental procedures and the analytical methods are summarized in this section. The soils (topsoil and subsoil) samples and soil contaminants (HCH particulate matter and DNAPL) used in the experiments are also described below.

6.1.1. Reagents

The reagents used in the experiments, the suppliers, and applications are listed in Table 6.1. Hydrogen peroxide (HP) and sodium persulfate (PS) were used as oxidants. Iron (II) sulfate (Fe_2SO_4) and sodium citrate ($Na_3C_6H_5O_7$) have been used as activator and chelating agent, respectively, in the Fenton treatment. Sodium hydroxide (NaOH) was used as PS activator. Three commercial surfactants were used for soil washing experiments: two nonionic surfactants, E-Mulse®-3 (E3) and Tween®-80 (T80, $C_{64}H_{124}O_{26}$), and one anionic surfactant, sodium dodecyl sulfate (SDS, $C_{12}H_{25}NaO_4S$). Commercially available chlorinated organic compounds (COCs: chlorobenzene (CB), 1,2-dichlorobenzene (1,2-DCB), 1,3 - dichlorobenzene (1,3-DCB), 1,4-dichlorobenzene (1,4-DCB), 1,2,3-trichlorobenzene (1,2,3-TCB), 1,2,3,4-tetrachlorobenzene (1,2,3,4-TetraCB), 1,2,3,5-tetrachlorobenzene (1,2,3,5-TetraCB), and 1,2,3,4-tetrachlorobenzene (1,2,3,4-TetraCB), HCHs (α-, β-, γ- and δ-HCH), all of them supplied by Sigma-Aldrich were used for calibration curves. All the reagents were of analytical grade. Aqueous solutions were prepared using high-purity water from a Millipore Direct-Q system with a resistivity > 18 MΩ cm (25 °C).

Table 6.1. Reagents employed in this Doctoral Thesis.

Compound	Molecular formula	Supplier	Application
Hydrogen peroxide (HP)	H_2O_2	Sigma-Aldrich	Oxidant
Persulfato sódico (PS)	$Na_2S_2O_8$	Sigma-Aldrich	Oxidant
Iron (II) sulfate	Fe_2SO_4	Sigma-Aldrich	HP catalyst
Sodium citrate	$Na_3C_6H_5O_7$	Sigma-Aldrich	Chelating agent
Sodium hydroxide	NaOH	Riedel-de Haën	PS activator
E-Mulse®-3 (E3)	-	EthicalChem	Surfactant
Tween®-80 (T80)	$C_{64}H_{124}O_{26}$	Sigma-Aldrich	Surfactant
Sodium dodecyl sulfate (SDS)	$NaC_{12}H_{25}SO_4$	Sigma-Aldrich	Surfactant
Methanol	CH_3OH	Fisher Chemical	COCs extraction (soil phase)

Compound	Molecular formula	Supplier	Application
n-Hexane	C_6H_{14}	Honeywell	COCs extraction (aqueous phase)
Bicyclohexyl	$C_{12}H_{22}$	Sigma-Aldrich	ISTD GC/FID analyses
Tetrachloroethane	$C_2H_2Cl_4$	Sigma-Aldrich	ISTD GC/ECD analyses
Nitric acid	HNO_3	Sigma-Aldrich	Soil digestion
Hydrochloric acid	HCl	Sigma-Aldrich	Soil digestion
Phosphoric acid	H_3PO_4	Fisher	Inorganic carbon determination
Potassium hydrogen phthalate	$C_8H_5KO_4$	Sigma-Aldrich	TOC calibration
Potassium iodide	KI	Fisher-Chemical	PS quantification
Sodium hydrogen carbonate	$NaHCO_3$	Panreac	PS quantification
Titanium oxisulfate	$TiOSO_4$	Sigma-Aldrich	HP quantification
1,10-Phenantroline	$C_{12}H_8N_2$	Sigma-Aldrich	Iron quantification
Sodium acetate	$C_2H_3NaO_2$	Sigma-Aldrich	Iron quantification
Sodium carbonate anhydrous	Na_2CO_3	Panreac	Mobile phase IC analyses
Sulfuric acid	H_2SO_4	Fisher	Regenerating solution IC analyses
Acetone	C_3H_6O	Fisher	Regenerating solution IC analyses
Oxalic acid	$C_2H_2O_4$	Riedel-de Haën	Regenerating solution IC analyses
Microtox® Acute Reagent	-	ModernWater Inc.	Toxicity determination
Reconstitution Solution	-	ModernWater Inc.	Toxicity determination
Sodium chloride	NaCl	Sigma-Aldrich	Osmotic adjustment toxicity determination
Sodium thiosulfate pentahydrate	$Na_2S_2O_3{\cdot}5H_2O$	Sigma-Aldrich	PS removal
Phenol	C_6H_6O	Riedel-de Haën	Control compound toxicity determination
COCs	-	Sigma-Aldrich	COCs calibration curves

COCs=Chlorinated organic compounds, TOC=total organic carbon, ISTD= Internal standard, GC=gas chromatography, FID= flame ionization detector, ECD= electron capture detector, IC=ionic chromatography

6.1.2. Soil samples

Two types of soils polluted with lindane wastes, **topsoil (TS)** and **subsoil (SS),** were collected at different points from the Bailín and Sardas landfills (Sabiñánigo, Spain), respectively. The locations of the sampling sites are shown in Figure 6.1, and the depth, pollutant type (HCH particulate matter or DNAPL), particle size, pollution level, acronym, and the experimental tests performed are summarized in Table 6.2.

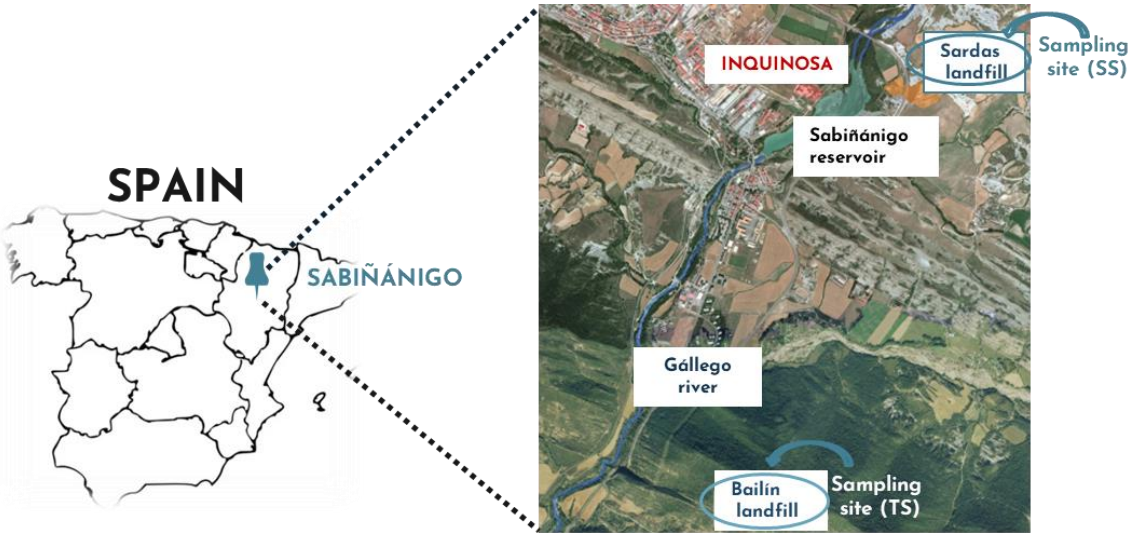

Figure 6.1. Location of sampling sites of TS and SS samples, in Bailín and Sardas landfills, respectively.

TS samples provided by SARGA (Sociedad Aragonesa de Gestión Agroambiental) were taken at different points and a depth between 0 and 0.3 m. Samples were collected and milled in the landfill facilities, and stored in plastic bags (4 °C, darkness) until analysis (15-30 days). For the on-site treatment of TS, the coarser particles of the soil (with low adsorption capacity) are usually removed by sieving, density, or gravity (Benschoten, Matsumoto et al. 1997). Thus, received TS samples (around 20 lots of at least 4 kg each) were sieved using an electromagnetic sieve shaker (BA-200-N), and the fraction from 0.02 to 2 mm (around 95% of total TS) was selected for further experimentation.

SS samples were obtained from boreholes (drilled by the company EMGRISA) from one of the most contaminated areas in the Sardas landfill (Figure 6.1). The soil corresponds to the permeable layer located at 12.5–15.5 m below ground level. Samples were dried (48 h at room temperature, 22 °C), stored in glass jars (4°C, darkness, <30 days), and sieved. The fraction with a particle size between 0.25 and 2 mm was named "coarse" (C),

and the fraction <0.25 mm, which corresponds with fine sand and clay (Wentworth classification (Wentworth 1922)), was named "fine" (F).

COCs concentration in the different samples of TS and SS was analysed and classified according to their pollution level (L) based on an arbitrary scale. L1 corresponds to the soil sample with the lowest COCs concentration among the measured samples, and increasing numbers (L2, L3, etc.) were used as COCs concentration increased for both TS and SS. From the analyzed samples, those with significantly different COCs concentrations were selected for the study: 4 levels for TS and 3 levels for SS coarse and SS fine (Table 6.2).

The distinction between physical interference and the effect of target pollutants on toxicity tests is usually achieved using reference soil samples (Doherty 2001). For this reason, additional soil samples with physicochemical characteristics equivalent to each soil type (topsoil (TS), subsoil coarse (SS-C), and subsoil fine (SS-F)) but with a significantly lower pollutant concentration were used. These reference samples were collected from the vicinity of the landfills (Bailín and Sardas), outside the perimeter of the contaminated areas at depths similar to those used for the respective polluted soils and denoted by pollution level "L0".

The pollution level selected for the **oxidation treatments** for the **on-site remediation of TS** (and measurement of toxicity after selected treatments) was **TS L2** since it was the most representative level of contamination (the most common concentration of HCHs in the received samples). In the case of **SS**, **SS-C L2** was the sample selected to evaluate soil toxicity after ISCO (PS/NaOH) and S-ISCO (E3/PS/NaOH) treatments. These soils have been highlighted in bold type in Table 6.2.

Table 6.2. Soil samples used in oxidation treatments and toxicity evaluation.

Soil	Depth (m)	Pollutants type	Particle size (mm)	Pollution level	Acronym	Testing
Topsoil (TS)	0-0.3	HCH particulate matter	0.02-2	L0	TS L0	- Acute toxicity - Unproductive oxidant consumption
				L1	TS L1	Acute toxicity
				L2	**TS L2**	**- TS oxidation treatments** **- Toxicity before and after treatments**
				L3	TS L3	Acute toxicity
				L4	TS L4	Acute toxicity
Subsoil (SS)	12.5-15.5	DNAPL (Σ_{COCs}=28)	0.25-2 Coarse (C)	L0	SS-C L0	Acute toxicity
				L1	SS-C L1	Acute toxicity
				L2	**SS-C L2**	**Toxicity before and after treatments**
				L3	SS-C L3	Acute toxicity
			< 0.25 Fine (F)	L0	SS-F L0	Acute toxicity
				L1	SS-F L1	Acute toxicity
				L2	SS-F L2	Acute toxicity
				L3	SS-F L3	Acute toxicity

6.1.3. Soil contaminants (HCH particulate matter and DNAPL)

Soil contaminants: real samples of **HCH particulate matter** (TS) and **DNAPL** (SS) were employed in this study. Soil contaminants were collected at the same locations as the respective soil samples, Bailín (HCH particulate matter) and Sardas (DNAPL) landfills, respectively (Figure 6.1). A photograph of the soil samples and the pollution sources, HCH particulate matter and DNAPL, is shown in Figure 6.2. HCH particulate matter was obtained by manually separating it from the received TS. The company EMGRISA and the Aragon Government provided the DNAPL sample.

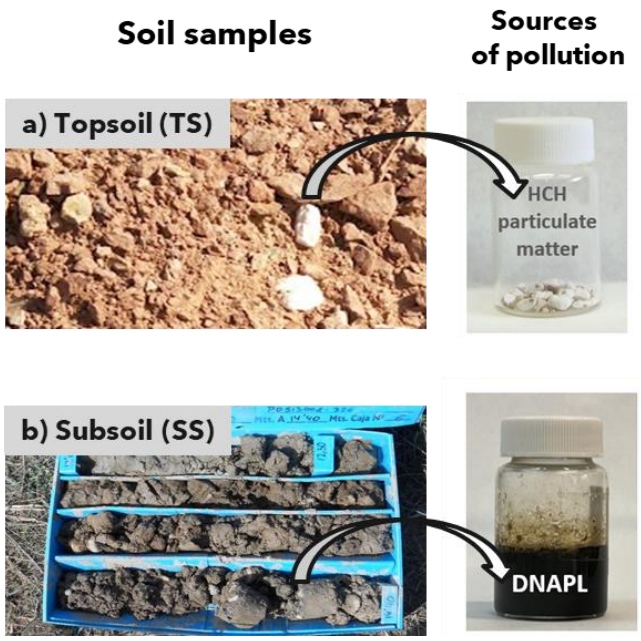

Figure 6.2. Photograph of soil samples and their respective sources of pollution: (a) topsoil and HCH particulate matter, (b) subsoil core obtained from a borehole and DNAPL.

6.2. Experimental procedures for soil remediation

This section describes the experimental methodology applied to evaluate the efficiency of different chemical oxidation treatments for the remediation of polluted TS.

6.2.1. Topsoil (TS) oxidation treatments

On-site remediation of topsoil has been evaluated by different chemical oxidation treatments using two oxidants: hydrogen peroxide (HP) activated by iron and persulfate (PS) activated by different methods:

- Fenton process (HP/Fe)
- Persulfate (PS)
- Alkali-activated persulfate (PS/NaOH)
- Temperature-activated persulfate (PS/T)
- Alkali-activated persulfate intensified by temperature (PS/NaOH/T)
- Alkali-activated persulfate intensified with ultrasound (PS/NaOH/US)
- Surfactant-enhanced solubilization and oxidation of the polluted emulsion (S/PS/NaOH/T)

Table 6.3 summarizes the oxidation treatments studied, the range of variables evaluated, and the abbreviation assigned for each set of runs (detailed in subsequent sections). The efficiency of different Oxidants (HP and PS, runs "O") and Activators (NaOH and temperature, runs "A") was evaluated. The intensification of the selected system, PS/NaOH, was studied by the application of i) Temperature (PS/NaOH/T, runs "T"), ii) Ultrasounds (PS/NaOH/US, runs "U"), and iii) Surfactants (S/PS/NaOH/T, Runs "S"). The influence of the main operating conditions (oxidant concentration, NaOH:PS molar ratio, soil/aqueous phase ratio (V_L/W_S), stirring rate, reagents addition order, temperature, ultrasound power, and treatment time) was evaluated for each treatment as appropriate.

Table 6.3. Summary of the oxidation treatments studied for on-site TS (TS L2, Table 6.2) remediation.

Main objective	Treatment studied	Variables studied	Equipment used	Run code
Oxidant evaluation	- Fenton (**HP**/Fe) - **PS**	- C_{HP} = 12-200 g L^{-1} - T = 25 ºC	Rotatory agitator (Figure 6.3-a)	**O**
PS activator evaluation	-PS/**NaOH** -PS/**T**	-NaOH:PS = 2 - T = 35-55 ºC - C_{PS} = 10-80 g L^{-1}	Constant temperature bath (Figure 6.3-b)	**A**
Intensification of PS/NaOH	-PS/NaOH/**T**	- Reagents addition order - T = 40-60 ºC - V_L/W_S ratio = 1-2 - C_{PS} = 20-60 g L^{-1} - Stirring rate = 10-100 rpm	Constant temperature bath (Figure 6.3-b)	**T**
	- PS/NaOH/**US**	- US power density = 0-91 W L^{-1} - C_{PS} = 10-60 g L^{-1}	US bath and prove (Figure 6.3-c and d)	**U**
	- **S**/PS/NaOH/T)	- S = T80, E3, SDS - C_{NaOH} = 0-13.5 - $C_{surfactant}$ = 2-10 g L^{-1} - Solubilization cycles = 1-3 - V_L/W_S ratio = 2-6	Rotatory agitator (Figure 6.3-a) and heating stirrer plate (Figure 6.5)	**S**

As previously stated, the soil sample selected to carry out the oxidation experiments was TS L2. TS sample was crushed and sieved (< 0.25 mm) before conducting remediation tests to increase the analyses representativeness and reproducibility. The reactors were filled with 15 g of polluted soil and 30 mL of the aqueous solution containing the desired concentration of reagents (oxidant, alkali, and/or surfactant). Three commercial surfactants were used in the S/PS/NaOH/T treatment, two nonionic: E-Mulse®-3 (E3) and Tween®-80 (T80), and one anionic, sodium dodecyl sulfate (SDS).

The reactors were shaken and/or heated in different equipment depending on the conditions applied (temperature, stirring rate, US, etc.). The experiments carried out to evaluate the oxidant (runs "O") were performed in a rotatory agitator (LBX RR80) (Figure 6.3-a). In contrast, those performed to evaluate the activator (runs "A") were carried out in a constant-temperature bath (UNITRONIC-ORBITAL) equipped with a digital electronic regulator of temperature, time, and stirring rate (Figure 6.3-b). The same experimental device was used to carry out PS/NaOH/T experiments.

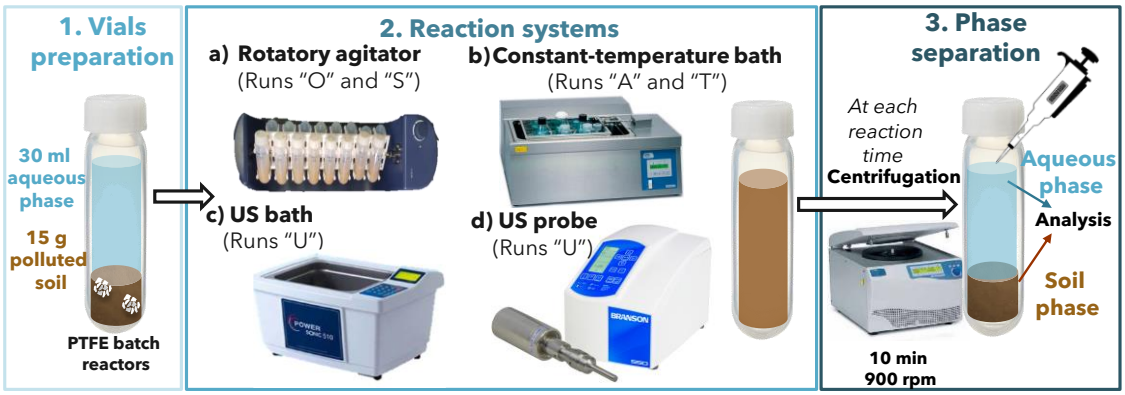

Figure 6.3. Schematic diagram of the experimental procedures carried out for "O", "A", "T", and "U" runs. Equipment employed in reaction systems: (a) rotatory agitator (LBX), (b) constant-temperature orbital bath (Unitronic), (c) US bath (Power sonic 505), (d) US probe (Branson Digital Sonifier SFX 550).

Two experimental devices have been employed to carry out the experiments intensified by US. First, an experiment was carried out at isothermal conditions (22 ± 2°C) using a US bath (Figure 6.3-c, 40 kHz, 2.56 L, 350 W, 137 W L^{-1}) to evaluate the US effect. A circulatory water bath was used to maintain a constant temperature. The water level inside the bath (volume of 2.5 L) was adjusted to cover the volume occupied by the soil-aqueous phase suspension of the Teflon reactors (2 reactors of 30 mL each), giving a total sonicated volume of 2.56 L. The effect of US power and PS concentration have been studied by using a US probe, which provides greater versatility than the US bath, with a 3/4" diameter ultrasonic horn operating at 20 kHz (Figure 6.3-d). The sonicator was conducted using the pulse mode of 4 s "on" and 1 s "off". The ultrasonic horn was immersed in a bath (2.5 L of water), and 6 reactors were homogeneously placed around the horn at a 2 cm distance (total sonicated volume of 2.68 L). A schematic diagram of the experimental setup is shown in Figure 6.4. It should be noted that the experimental device was acoustically and thermally isolated. The solution temperature of the water bath (equivalent to that of the slurry inside the Teflon reactors) was monitored by a thermocouple thermometer (DeltaOHM HD 2108.2).

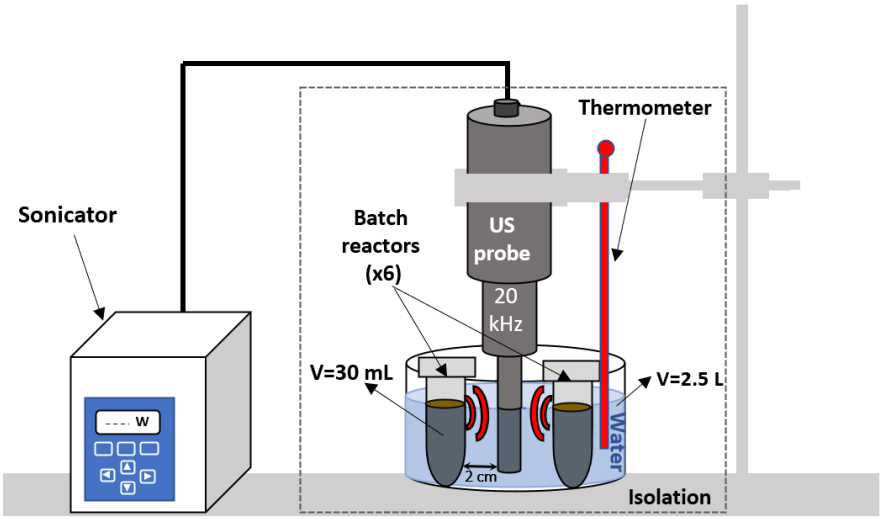

Figure 6.4. Schematic diagram of the US probe experimental setup (20 kHz, total volume = 2.68 L) (Checa-Fernández, Santos et al. 2022, **ART. 5**).

At the selected reaction times, the vials were sacrificed. The reactors were centrifuged (10 min, 9000 rpm, MEDTRONIC-BL-S, JP SELECTA®), and the aqueous phase was separated from the solid phase by decantation (Figure 6.3), and both were analyzed (Subsection 6.3).

The main steps of the experimental procedure followed for the surfactant-enhanced solubilization experiments (S/PS/NaOH/T, runs "S") are schematized in Figure 6.5. As previously mentioned, the reactors were filled with 15 g of polluted soil and 30 mL of the aqueous solution containing the desired concentration of reagents when appropriate (surfactant and/or alkali). The reactors were shaken at 80 rpm in a rotatory agitator (Figure 6.5-a) at ambient temperature for 24 h. This time was enough to reach the pollutants equilibrium between the aqueous and solid phases (Checa-Fernández, Santos et al. 2022, **ART. 5**). At this time, vials were centrifuged (10 min, 90 rpm), aqueous and solid phases were analyzed (Subsection 6.3), and the resulting polluted emulsions (PEs) were subsequently treated by the alkaline activation of PS intensified by temperature (PS/NaOH/T). Oxidation runs were carried out in thermostatted closed cylindrical glass vials (10 mL) without head-space to minimize COCs volatilization. The solution was magnetically stirred (80 rpm) and heated (40 °C) using a TechRADLEYS heating stirrer plate (Figure 6.5). A volume of 10 mL of the PEs was added to the vial. The oxidation experiments started once PS was added as a pure solid (40 g L^{-1}). Additionally, the corresponding concentration of NaOH was added to achieve a molar ratio of NaOH:PS = 2.

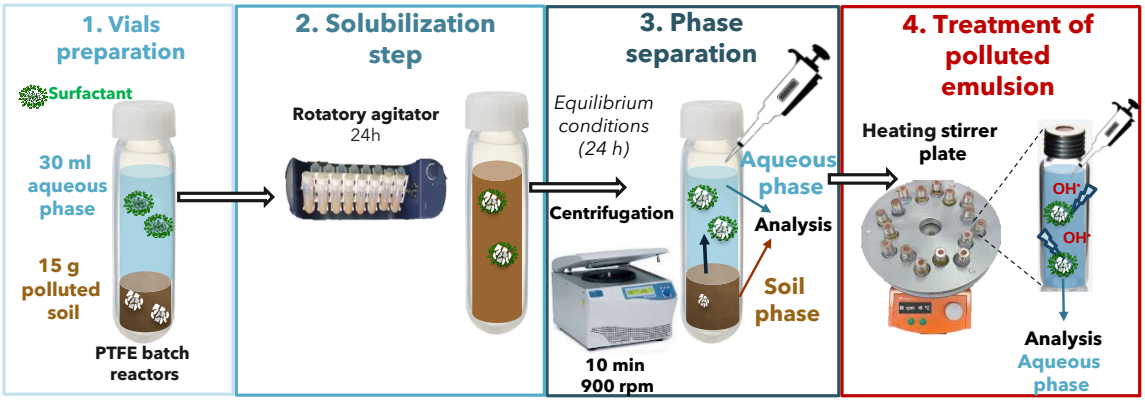

Figure 6.5. Schematic diagram of the experimental procedure carried out for runs "S", including the surfactant-enhanced solubilization step and the subsequent treatment of the polluted emulsion.

All remediation experiments have been carried out at least duplicated, being the standard deviation always less than 10%.

6.2.2. Subsoil (SS) oxidation treatments

The ISCO and S-ISCO experiments were carried out in glass columns (diameter = 3 cm) with two side ports (4.7 cm between them). The column characteristics have been summarized in Table 6.4, and a scheme of the column assembly is shown in Figure 6.6. Three columns were prepared: one for ISCO treatment and two for S-ISCO treatments. The columns were filled with approximately 50 g of polluted soil (SS-C L2, Table 6.2). Firstly, one pore volume (Pv) of Milli-Q water was injected into the columns to achieve pore water saturation (0.3 mL min^{-1}, 35 min approx.) using a peristaltic pump (Spetec Perimax 12). Then, the alkaline pretreatment was applied (2 Pvs, NaOH solution (210 mM)).

After that, 8 Pvs (containing the desired oxidant/activator/surfactant concentration, see Table 6.4) were successively injected into each column (0.3 mL min^{-1}) with a time elapsed between each pore volume injection of 96 h. The total time the oxidant injected in the successive pore volumes remained in the column was approximately 32 days. The ISCO run used an oxidant/activator solution (oxidant and NaOH concentration of 210 mM, NaOH:PS = 1), and the surfactant E3 (5 and 10 g L^{-1}) was fed to the S-ISCO columns. Operational conditions were selected from previous work (Garcia-Cervilla, Santos et al. 2022). The experiments were performed at room temperature (22 ± 2 °C). Pvs eluted from the columns were collected and stored.

After the 8 Pvs with the reagents, 8 Pvs of tap water were successively injected into the columns, simulating the groundwater flow in the subsoil after the chemical treatment.

The effluents were collected and analyzed. Finally, the columns were disassembled, homogenized, and dried at room temperature before studying the COCs and acute toxicity of the treated soils.

Table 6.4. Experimental conditions in column runs. The flow rate used in all Pv injections was 0.3 mL min^{-1}. Soil sample: SS-C L2 (Table 6.2) (Santos, García-Cervilla et al. 2022, **ART. 7**).

Soil Columns	**ISCO**	**S-ISCO**	**S-ISCO**
Soil height (cm)	4.7	4.7	4.7
Soil mass (g)	53	51	52
Pv (mL)	11.2	10.7	10.9
Alkaline Pretreatment			
C_{NaOH} (mM)	210	210	210
nº Pvs injected	2	2	2
Time between next Pv injection (h)	24	24	24
Reagents injected			
$C_{surfactant}$ (g L^{-1})	0	5	10
C_{PS} (mM)	210	210	210
C_{NaOH} (mM)	210	210	210
nº Pvs injected	8	8	8
Time between next Pv injection (h)	96	96	96
Washing with tap water			
nº Pvs injected	8	8	8
Time between next Pv injection (h)	0.5	0.5	0.5

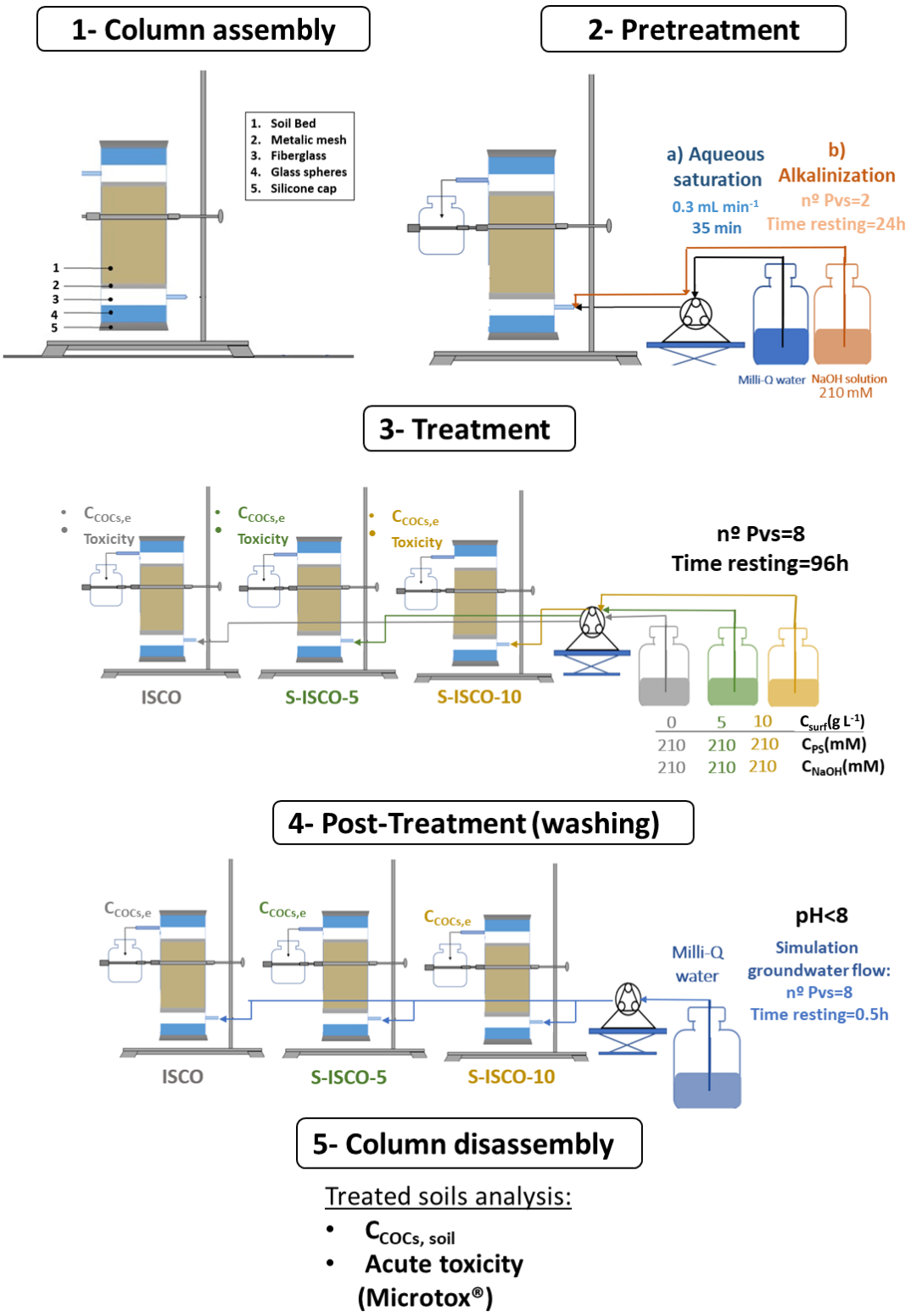

Figure 6.6. Scheme of the different stages followed in the remediation experiments. Experimental conditions are summarized in Table 6.4 (Santos, García-Cervilla et al. 2022, **ART. 7**).

6.3. Analytical methods

Soil samples (TS and SS) and the aqueous phases in contact with the corresponding soil after partitioning equilibrium was reached (called elutriates) were characterized. Moreover, the soil and aqueous phases resulting from the soil remediation treatments at different reaction times were analyzed. The analytical methods used to characterize soil and aqueous phases are detailed below.

6.3.1. Soil phase

6.3.1.1. Chlorinated Organic Compounds (COCs)

Firstly, **COCs extraction** from soil was performed by mixing 15 g of soil with 30 mL of methanol in 40 mL-PTFE sealed vials. The sample was introduced in an ultrasound bath (Power Sonic 505) at 45 °C for 180 min. The PTFE vials were cooled (room temperature) and centrifuged (10 min, 9000 rpm, MEDTRONIC-BL-S, JP SELECTA®); the organic phase was analyzed. This extraction method was optimized to select soil-solvent ratio, energy source (US, microwave), extraction time, soil-solvent separation procedure (centrifugation, filtering), etc. (Dominguez, Checa-Fernandez et al. 2021, **ART. 3,** Checa-Fernández, Santos et al. 2021, **ART. 4,** Domínguez, Ventura et al. 2023, **ART. 1**). Following this procedure, a percentage between 95-98% of COCs in soil are extracted to the organic phase with very reproducible results.

COCs identification in the organic phase was performed by **gas chromatography** (**GC**, Agilent 6890) coupled with a mass spectrometry detector (**GC-MSD**). In contrast, their quantification was accomplished by GC coupled with a flame ionization detector (**FID**) and electron capture detector (**ECD**) (Figure 6.7). Helium (2.8 mL min^{-1}) was used as the carrier gas for the chromatographic analyses. The sample injection volume was 2 mL, and the GC injection port temperature was 250 °C. The temperature program started at 80 °C; after that, a 10 °C min^{-1} ramp temperature up to 180 °C was applied and held constant at this temperature for 15 min. The exit of the column (HP-5-MS, 30 m × 0.25 mm i.d., 5% phenyl methyl siloxane) was split (1:1) to both FID and ECD detectors and simultaneously measured.

COCs quantification was accomplished obtaining calibration curves from standard commercial COCs: chlorobenzene (CB), 1,2-dicholorobenzene (1,2-DCB), 1,3-dicholorobenzene (1,3-DCB), 1,4-dicholorobenzene (1,4-DCB), 1,2,3-trichlorobenzene (1,2,3-TCB), 1,2,3,4-tetrachlorobenzene (1,2,3,4-TetraCB), 1,2,3,5-tetrachlorobenzene

(1,2,3,5-TetraCB), and 1,2,3,4-tetrachlorobenzene (1,2,3,4-TetraCB), and HCHs (α-, β-, γ-, and δ-HCH). Other non-commercial COCs such as pentachlorocyclohexenes (PentaCXs), hexacholorocylohexenes (HexaCXs), and heptachlorocyclohexanes (HeptaCHs) were identified and quantified by using real DNAPL samples (Santos, Fernandez et al. 2018). The quantification of HCH isomers when their concentration was < 5 mg L^{-1} was performed by GC-ECD (due to the higher sensibility of this detector for high-chlorine compounds), while in all other cases, by GC-FID. Bicyclohexyl and tetrachloroethane were used as internal standard compounds (ISTDs) for FID and ECD, minimizing experimental errors.

Figure 6.7. Gas chromatograph (GC).

As an example, the GC-FID chromatograms of the soil pollution sources (HCH particulate matter and DNAPL) are shown in Figure 6.8-a and -b, respectively. In the case of HCHs isomers with a low concentration (γ-, δ-, and ε-HCH), an inset of the corresponding GC-ECD chromatogram has been added. As can be seen, HCH particles mainly comprise α- and β-HCH isomers and lower concentrations of the other HCH isomers (see inset of Figure 6.8-a). However, in the case of DNAPL, more than 20 COCs are present.

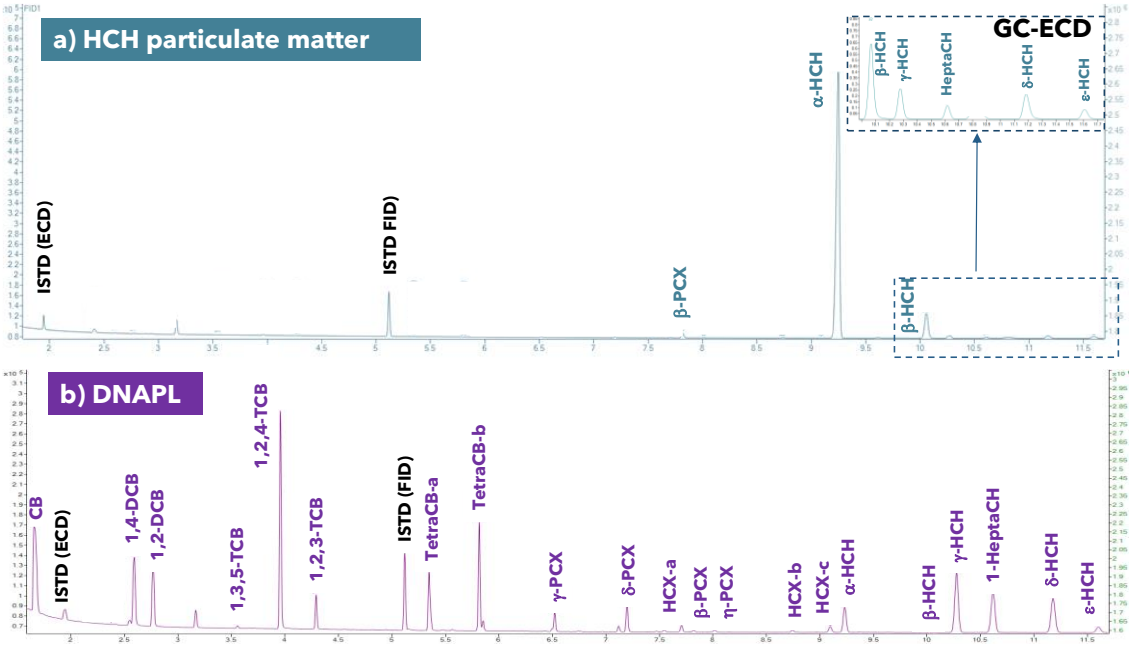

Figure 6.8. GC-FID and GC-ECD (inset) chromatograms of the sources of soil pollution: (a) HCH particulate matter and (b) DNAPL.

6.3.1.2. Metals

Firstly, the soil samples (0.5 g) were placed in a microwave extraction device (Milestone Ethos One) and digested using a mixture of nitric acid (9 mL, 70%) and hydrochloric acid (3 mL, 37%), following the EPA 3051A method. An initial temperature ramp from ambient temperature to 175 °C was applied for 5.5 min, and then, this temperature was kept constant for 4.5 min. The resulting aqueous phase was filtrated with a 0.45 µm filter and measured.

After the acid digestion, metal cations were quantified in soil samples using a **microwave plasma atomic emission spectrometer** (4100 **MP-AES**, Agilent, Figure 6.9). A multi-element standard solution IV (Supelco) compounded with 23 elements (1000 mg L^{-1}) diluted in nitric acid was used for the calibration curves. The positioning view, the nebulizer pressure, and the weight length for each metal were fixed according to previous work (García-Cervilla, Santos et al. 2020).

Figure 6.9. Microwave plasma atomic emission spectrometer (MP-AES).

6.3.1.3. pH

The **pH** of soil samples was measured following the EPA METHOD 9045D. A Basic 20-CRISON **pH electrode** was used to determine the pH from a soil-water suspension (aqueous phase/soil ratio equal to 1). The suspension is continuously stirred for 5 min. Subsequently, the soil suspension is centrifuged, and the pH of the resulting phase is measured.

6.3.1.4. Total organic carbon

The total carbon (TC) of soil samples was measured with a Shimadzu **TOC-V_{CSH} analyzer** by oxidative combustion at 680 °C using an infrared detector equipped with an **SSM-5000A solid sampler** (EN 15936:2012) (Figure 6.10). The soil sample was placed in a crucible and inserted into the SSM-5000A solid sampler.

Figure 6.10. TOC-V CSH analyser (left) and SSM 5000 solid sampler (right).

The **inorganic carbon** (IC) of solid samples was quantified in the same equipment using synthetic air and after the acidification of the sample with phosphoric acid (35%) at 200 °C. The **total organic carbon** (TOC) of the soil was calculated as the difference between TC and IC. Calibrates with potassium hydrogen phthalate and sodium carbonate were performed to quantify the TC and IC, respectively.

6.3.1.5. *Scanning electron microscopy (SEM) and elemental energy dispersive analysis*

The soil morphology was characterized by **scanning electron microscopy** (SEM) (JEOL JSM 6335F INT). Moreover, a qualitative elemental **energy dispersive analysis** (EDS) was also performed (Oxford Instruments, model: X-Max 80 mm^2). Analyses and imaging were performed at 20 kV. Due to the non-conductive nature of samples, graphite coating (also compatible with EDS analysis) was applied. SEM and EDS analyses were conducted at the Spanish National Centre for Electron Microscopy (ICTS).

6.3.1.6. *Acute toxicity*

The **acute toxicity** of samples was determined by the **Microtox®** bioassay, which is based on measuring the natural luminescence emitted by the marine bacteria *Vibrio fischeri* (ISO 11348-3, 1998). The exposure of these bacteria to toxic substances disrupts the bacteria respiratory processes, reducing the emitted light (Bond and Martin 2005). The sample dilution ratio that yields a 50% reduction of bacteria light emission is named IC_{50} (Eq. (6.1)):

$$IC_{50}(\%) = \frac{V_{sample}}{V_{total}} 100 \qquad (6.1)$$

where V_{sample} is the volume of the polluted sample in the total volume (V_{total}) that cause 50% inhibition of the light emitted at standard conditions (15 ºC and corresponding time). The total volume is the sum of the sample volume, the diluent, and the bacteria.

Toxicity Units (TUs) are calculated with Eq. (6.2) (Santos, Yustos et al. 2004):

$$TUs = \frac{100}{IC_{50}(\%)} \qquad (6.2)$$

If the polluted sample contains only one contaminant of known concentration, the effective nominal concentration of toxicant that reduces the intensity of light emission by 50% (EC_{50}) can be calculated following Eq. (6.3):

$$EC_{50_i}(mg\ L^{-1}) = \frac{C_i}{TUs} = \frac{IC_{50}}{100} C_i \qquad (6.3)$$

where C_i is the contaminant concentration in the polluted sample (mg L^{-1}).

The TUs of a mixture of known composition and EC_{50_i} values can be estimated with Eq. (6.4) (Santos, Yustos et al. 2004):

$$TUs = \sum \frac{C_i}{EC_{50_i}} \quad (6.4)$$

where C_i is the concentration of each compound in the aqueous phase (mg L^{-1}), and $EC_{50\,i}$ the corresponding effective nominal concentration (mg L^{-1}). TUs estimated by Eq. (6.4) can be higher or lower than those obtained by Eq. (6.2) due to synergistic (positive or negative effects) or to the presence of non-identified compounds or unknown EC_{50_i} values (Chen and Lu 2002, Mowat and Bundy 2002, Joly, Bonnemoy et al. 2013).

Acute toxicity assessments were performed in triplicate using a **Microtox® M500 Analyzer** (Microbics Corporation, USA) (Figure 6.11). Negative and positive controls were diluent (NaCl, 2%) and phenol (100 mg L^{-1}, EC_{50} = 13-26 mg L^{-1}). The criteria for judging the quality of the data obtained in a particular test followed the guidelines: i) the variation coefficient of the light readings for the control solutions must be less than 12%, ii) light loss decreases as test concentration decreases (approximately monotonic), and iii) the coefficient of determination (R^2) must be greater than 0.9. If these conditions were not fulfilled, the test was discarded, and the sample was analysed again. In the current work, samples have been considered nontoxic when bioluminescence inhibition did not exceed 20% during analysis time, following the recommendations found in the literature (Baran, Tarnawski et al. 2019).

Figure 6.11. Microtox® M500 Analyzer (Microbics Corporation, USA) (left) and *Vibrio fischeri* bacteria (right).

Different sample preparation procedures and protocols have been used to measure the acute toxicity of the **soil** samples, and due to the low solubility of the contaminants, their corresponding **soil organic extracts** have also been analysed. The fractions of soils with particle diameter above 0.25 mm (TS and SS-C) were crushed and sieved (< 0.25 mm) before determining their toxicity and preparing the organic extracts to increase the

representativeness and reproducibility of the analyses. The pH of the samples is crucial for toxicity analysis since the bacterial reagent is sensitive to pH (the effect is minimal between 6.0 and 8.0 (Microbics Corporation 1995)). Thus, before toxicity analyses, pH adjustment was performed (when required) to be in the acceptable range.

Toxicity of Soil by modified Basic Solid-Phase Test

Soil toxicity was evaluated with the *modified Basic Solid-Phase Test* (**mBSPT**), proposed by Campisi, Abbondanzi et al. (2005), based on the analysis of an aqueous soil suspension (Slurry). The detailed procedure used in the mBSPT analysis, including the preparation of the soil suspension, has been summarized in Figure 6.12. Soil suspensions (slurries) were prepared by mixing 7 g of soil (< 0.25 mm) with 35 mL of a saline solution (diluent, NaCl 2%) for 10 min under magnetic stirring. The concentration of soil in the slurry was 200 g L^{-1}. For each slurry, 9 dilutions and 3 blanks were analyzed. When evaluating the toxicity after applying different oxidation treatments, residual PS was removed with thiosulfate (TiS) from reaction samples to avoid oxidant interference with the toxicity results. The stoichiometric amount of TiS (2 moles of TiS per mole of PS) was added to the aqueous phase, and 24 h was required for the complete oxidant removal (Olmez-Hanci et al., 2014). pH of soils treated with NaOH was neutralized before toxicity analyses by washing with HCl (pH = 2.5).

Light emitted (I) by the bioluminescent bacteria was measured without filtration, so turbidity and colour effects on light emission must be considered (Doherty 2001). In the mBSPT, these aspects are considered by recording the initial bacterial light emission ($I_{0,\,soil}$) immediately after adding the sample. Following the mBSTP procedure, the sample was added at different concentrations to the bacteria vials, where the reconstituted bacterial reagent (1 vial of Microtox® Acute Reagent mixed with 1 mL of the Reconstitution Solution, stored at 5 °C in the "Reagent well") is mixed with NaCl, 2% (Figure 6.12). The maximum concentration of soil in the analysis cuvette after the addition of the soil suspension (200 g L^{-1}) with the diluent and the reconstituted bacterial reagent was 99 $g_{soil}\,L^{-1}$ (9.9% mass), with each successive dilution being 50% of the previous one. The soil concentration was normalized for the sample moisture content, less than 10% (dry-weight basis). The bioluminescence inhibition of *Vibrio fischeri* was measured after 30 min of sample exposure ($I_{30,\,soil}$). Toxicity results have been expressed as $EC_{50,\,soil}$ (g L^{-1}), which indicates the concentration of soil in the cuvette (in g L^{-1}) that yields 50% of light inhibition (Eq. (6.5)).

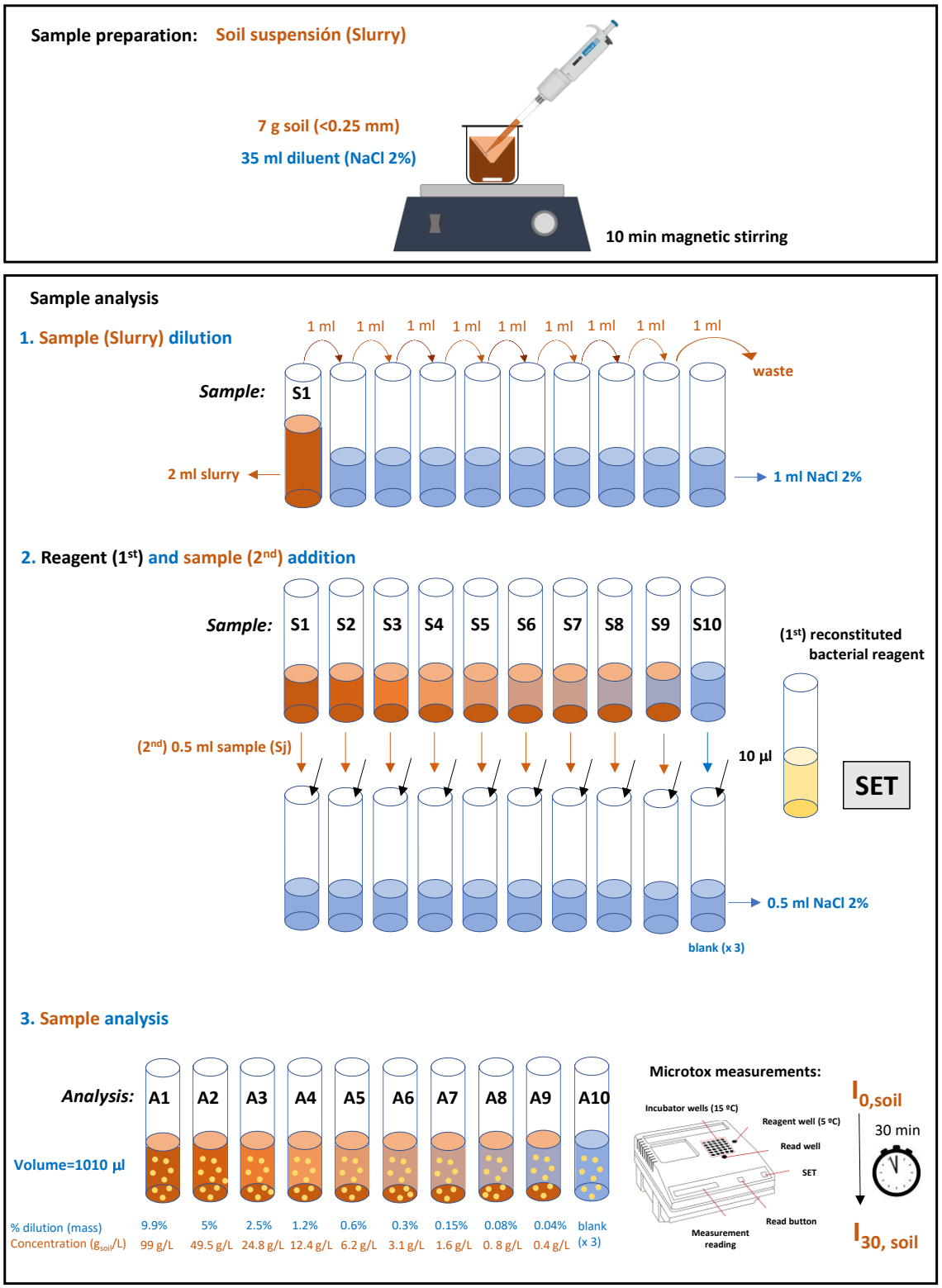

Figure 6.12. Soil phase toxicity determination: modified Basic Solid-Phase Test (mBSPT) (Domínguez, Ventura et al. 2023, **ART. 1**).

$$EC_{50,\ soil}\ (g_{soil}\ L^{-1}) = \frac{mass_{soil}}{V_{total}} \qquad (6.5)$$

Toxicity of Soil extracts by Organic Solvent Sample Solubilization Test

Hydrophobic organic compounds (HOCs), like most of the COCs present in the studied soils, are poorly soluble in the aqueous phase. To overcome this limitation, the *Organic Solvent Sample Solubilization Test* (OSSST) (Microbics Corporation 1995) dissolve (or extract) organic solvent-soluble compounds from soils and determine the toxicity of this organic extract. The Microbics Corporation (1995) manual recommended solvents are ethanol, methanol, and dimethyl sulfoxide. Methanol has been chosen in this study since this solvent is efficient in COCs extraction from these soils (García-Cervilla, Santos et al. 2020, Dominguez, Romero et al. 2021, **ART. 2,** Dominguez, Checa-Fernandez et al. 2021, **ART. 3,** Checa-Fernández, Santos et al. 2021, **ART. 4**).

The detailed procedure for soil organic extracts toxicity analysis (*adapted Organic Solvent Sample Solubilization Test, aOSSST*), including the protocol followed to prepare the soil organic extracts, has been summarized in Figure 6.14. COCs extraction was performed using the following procedure: 15 g of soil (crushed and sieved) were put in contact with 15 g of methanol (soil/solvent mass ratio = 1/1) in 40 mL-PTFE sealed vials in an ultrasound bath (180 min, 45 °C, Power sonic 505). The PTFE vials were cooled (room temperature) and centrifuged (10 min, 9000 rpm, MEDTRONIC-BL-S, JP SELECTA®), the supernatant organic phase constituting the soil organic extract (SOE).

The bacterial reagent is sensitive to organic solvents. Therefore, the organic solvent maximum allowable concentration (MAC) in the solution in contact with the microorganism has been previously determined to ensure a null effect of the solvent on the measured toxicity (Kwan and Dutka 1990). A sensitivity analysis was conducted to determine the MAC of methanol with the Microtox® *Basic Test*. The toxicity threshold is the lowest concentration of contaminant to exhibit a percentage of inhibition more significant than the negative control (James, Dindal et al. 2003). In this work, it has been considered that no toxicity was detected if the bioluminescence inhibition did not exceed 20%. In this work, the concentration of methanol that causes bioluminescence inhibition higher than 15% was considered as the toxicity threshold being conservative. Figure 6.13 shows the percentage of inhibition as a function of the volume concentration of methanol. The toxicity threshold is 4.25%v of methanol. Hence, considering the immediate lower integer, the maximum allowable concentration (MAC) of methanol was 4%, which agrees with that previously reported in the literature (Kwan and Dutka 1990)

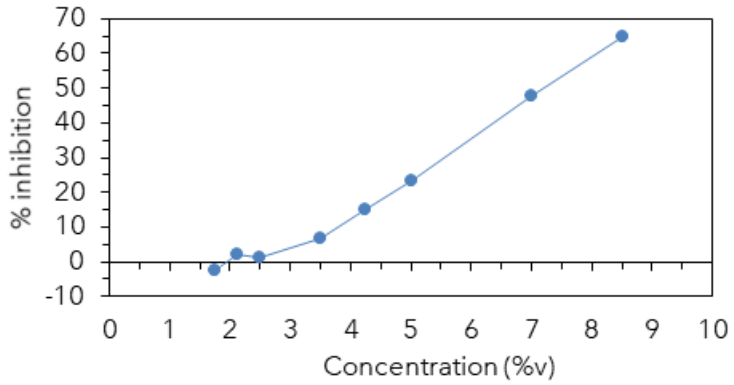

Figure 6.13. Percentage of inhibition of the luminescence of the bacterium Vibrio fischeri vs. concentration of methanol (in volume) after 30 minutes of exposure (Domínguez, Ventura et al. 2023, **ART. 1**).

The solution used to prepare the progressive dilutions of this sample (5 dilutions including the blank), named "DS solution", should also contain 4% of methanol (so that all dilutions have the same percentage of methanol and differences in toxicity can be only attributed to organic contaminants). Therefore, the DS solution was prepared by mixing 4 volumes of methanol and 96 volumes of eluent (NaCl, 2%). To acclimatize the bacteria to methanol, the bacterial reagent in this protocol (adapted bacterial reagent) was prepared using the DS solution and stored in the read well (see Figure 6.14). The initial bacteria light emission ($I_{0,organic}$) is measured after adding 100 µL of the adapted reconstituted bacteria to 2 mL of DS solution. The diluted samples (0.9 mL) were added to the vials with the reconstituted bacteria, and the bioluminescence inhibition of *Vibrio fischeri* was measured after 15 min ($I_{15,\ organic}$). In this protocol, sample preparation and dilution (step 3 in Figure 6.14) were performed in bigger vials and outside the Microtox® device at the same temperature conditions (15 °C).

The dilution ratio of the organic extract that yields a 50% reduction of bacteria light emission is $IC_{50,\ organic.}$ Toxicity results have been expressed as $EC_{50,\ organic}$ ($g_{soil}\ L^{-1}$), being calculated by Eq. (6.6), which considers the soil/methanol mass ratio (1000 g kg^{-1}) used for SOE preparation and the methanol density ($\rho_{methanol}$ = 0.792 kg L^{-1}).

$$EC_{50,organic}\ (g_{soil}L_{MeOH}^{-1}) = \frac{IC_{50,organic}\ (\%)}{100} \cdot \frac{mass_{soil}}{mass_{methanol}} \cdot \rho_{methanol} \qquad (6.6)$$

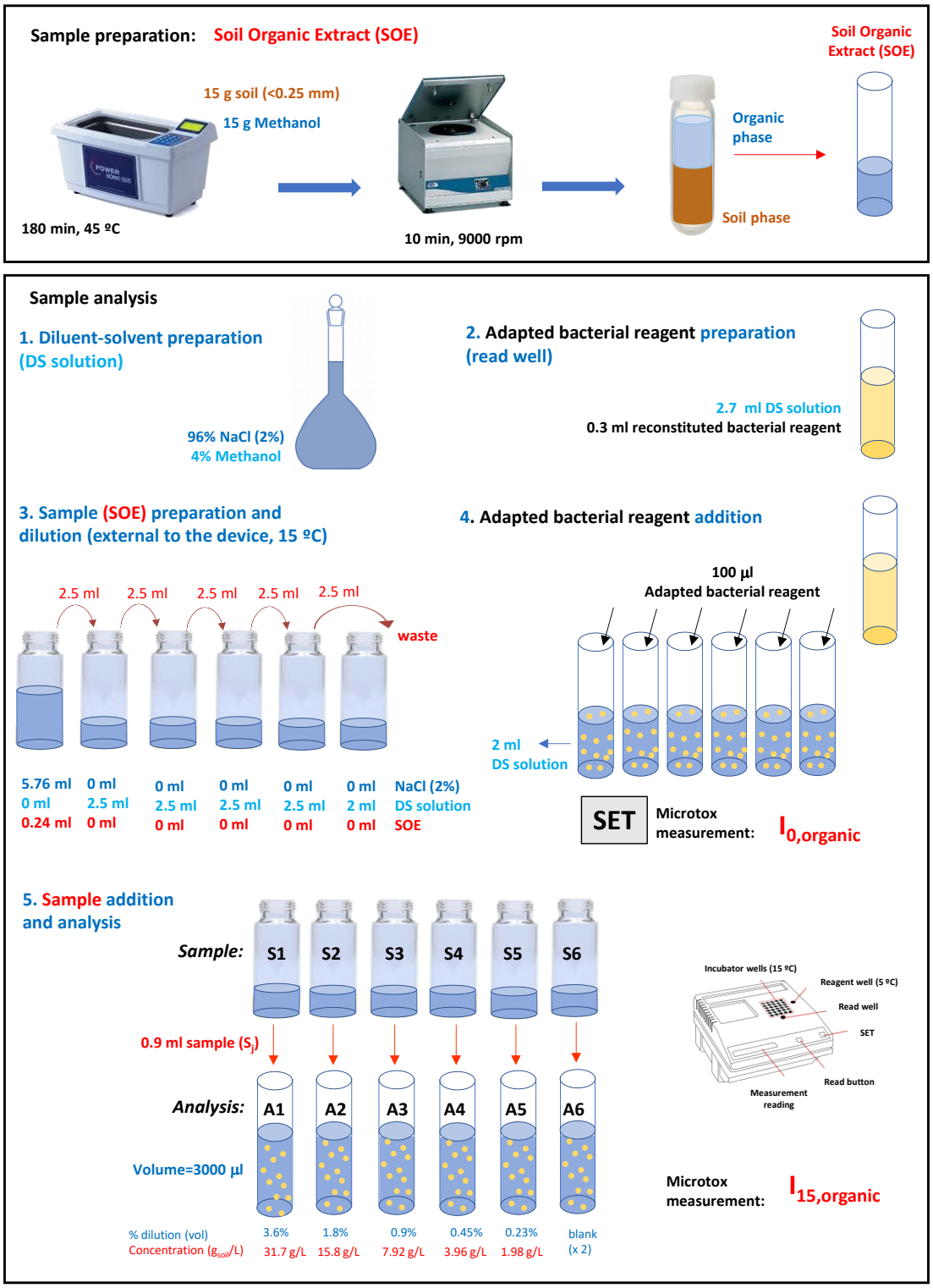

Figure 6.14. Soil extracts: adapted Organic Solvent Sample Solubilization Test (Domínguez, Ventura et al. 2023, **ART. 1**).

6.3.2. Aqueous phase

6.3.2.1. Chlorinated Organic Compounds (COCs)

The pollutants measurement method differs depending on whether an aqueous phase (without surfactant) or an emulsion (with ionic or nonionic surfactants) was analyzed.

Without surfactant

COCs extraction from aqueous phases was performed using n-hexane as an organic solvent (1/1 mass ratio). The biphasic mixture was vigorously agitated, and the organic supernatant was analyzed by **GC/FID/ECD**, as described in Subsection 6.3.1.1. The extraction with hexane stops the reaction if an oxidant is present in the aqueous phase.

With ionic surfactant

In the case of ionic surfactants (SDS), the emulsion was broken before extraction by adding NaCl. The emulsion was vigorously agitated, and the surfactant precipitated (Garcia-Cervilla, Santos et al. 2021). After that, COCs in the aqueous phase were extracted with hexane (1/1 mass ratio, as previously stated), and the organic supernatant was analyzed by **GC/FID/ECD** (Subsection 6.3.1.1.).

With nonionic surfactant

In the case of the nonionic surfactants E3 and T80, the emulsion cannot be broken, and therefore, the extraction of COCs cannot be performed. Thus, the aqueous emulsion was diluted with a soluble organic solvent: methanol (1/10 volume ratio) and analyzed by **GC/FID/ECD** (Subsection 6.3.1.1.). In the case of reaction samples, if the oxidant remained in the aqueous phase, the reaction was stopped due to MeOH addition (sulfate and hydroxyl radical react with methanol and are rapidly consumed).

6.3.2.2. Oxidants

Hydrogen peroxide (HP) concentration in solution was determined by a **colorimetric method** using the titanium oxisulfate method (Eisenberg 1943). Titanium oxysulfate reacts with the HP present in the reaction sample, forming a yellow peroxocomplex, whose absorbance was measured using a BOECO S-20 UV-VIS spectrophotometer (Figure 6.15) at 410 nm. Figure 6.16-a shows the calibration curve obtained, ranging from 0.05 to 3.00 g L^{-1}.

Figure 6.15. Spectrophotometer (BOECO S-20 UV-VIS).

Persulfate (PS) concentration in the aqueous phase was determined by a **colorimetric method** using a water/KI/$NaHCO_3$ solution (Liang, Huang et al. 2008). The yellow iodine colour formed, proportional to PS concentration, was measured using a BOECO S-20 UV-VIS spectrophotometer (Figure 6.15) at 352 nm. Figure 6.16-b shows the calibration curve obtained, ranging from 0.01 to 1 g L^{-1}.

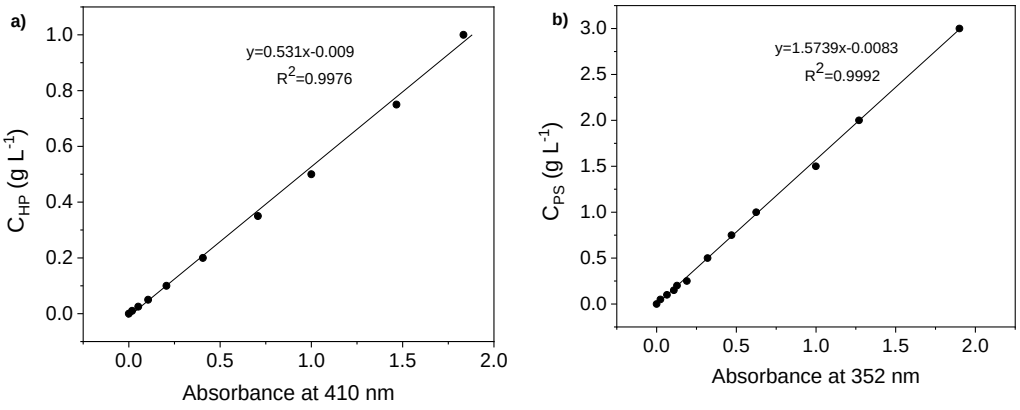

Figure 6.16. Calibration curves for quantifying (a) HP at 410 nm and (b) PS at 352 nm.

6.3.2.3. Iron

Iron in solution was determined by a **colorimetric method** using the *o*-phenanthroline method (Sandell 1945). This method is based on the formation of a red-orange iron (II) complex with o-phenanthroline, whose absorbance is measured at 510 nm (BOECO S-20 UV-VIS spectrophotometer) (Figure 6.15). Figure 6.17 shows the calibration curve obtained, ranging from 2 to 20 mg L^{-1}.

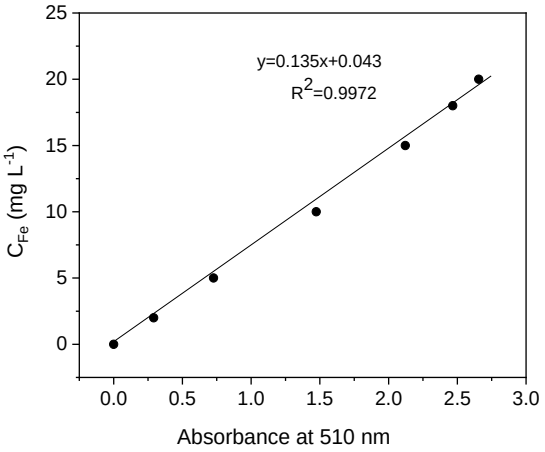

Figure 6.17. Calibration curve for the quantification of Fe at 510 nm.

6.3.2.4. Chlorides

The pollutants dechlorination degree was evaluated in terms of chlorides released to the liquid phase, quantified by **ion chromatography** with chemical suppression using a conductivity detector (Figure 6.18, Metrohm 761 Compact IC). A Metrosep A SUPP5 5-250 column (25 cm length, 4 mm diameter) was used as the stationary phase, and an aqueous solution of 3.2 mM Na2CO3 and 1 mM $NaHCO_3$ as the mobile phase (0.7 mL min^{-1}). Sample injection (250 µL) included an online filtering system (0.45 µm). A sulfuric acid, acetone, and oxalic acid solution was used to regenerate the ionic resins.

Figure 6.18. Ion chromatograp (Metrohm 761 Compact IC).

6.3.2.5. pH

The **pH** of the aqueous samples was measured using a pH Metrohm 914 portable coupled with a 20-CRISON **pH electrode**.

6.3.2.6. Surfactants

The initial and remanent **surfactant concentration** in the emulsions after COCs solubilization experiments (in the absence of oxidants) for the **TS remediation experiments** was determined by **TOC**. TOC was measured by a Shimadzu **TOC-V CSH analyzer** (Figure 6.10) using synthetic air as a carrier gas and a furnace temperature of 900 ºC. For surfactant concentration determination it has been considered the carbon content in SDS, E3, and T80, respectively (0.50, 0.58, and 0.60 g_C g_{surf}^{-1}, calculated from the molecular weight (SDS) and experimentally (E3 and T80)), and subtracted the TOC contribution of COCs in the aqueous phase (previously quantified by GC-FID/ECD).

The surfactant concentration in the aqueous phase of the column effluent for the **SS remediation experiments** was determined as Equivalent Surfactant Concentration (ESC) (García-Cervilla, Santos et al. 2021). In a glass vial, a volume of the aqueous sample was added. Then, a mass of a synthetic DNAPL with the same composition as those obtained under alkaline conditions was added. Once the chlorobenzenes were solubilized, the emulsion was centrifuged. Finally, the supernatant was analyzed by GC-FID/ECD. The ESC value was calculated by Eq. (6.7):

$$\mathrm{ESC} = \frac{\sum \mathrm{COC_j}_{\mathrm{solubilized}}}{\mathrm{WSR}} \qquad (6.7)$$

ESC (g L^{-1}) is the surfactant concentration with the same solubilization capacity that the aqueous surfactant solution analyzed. The solubilization capacity of E3 is represented by the Mass Solubilization Ratio (WSR) (mg_{COCs} $g_{surfactant}^{-1}$). WSR of E3 for a mixture of chlorobenzenes under alkaline conditions (1005 mg g^{-1}) was obtained elsewhere (García-Cervilla, Romero et al. 2020).

6.3.2.7. Acute toxicity

The **acute toxicity** of the aqueous phase after the partitioning equilibrium soil-water was reached (elutriates) was evaluated with the **Microtox® *Basic Test*,** according to the standard operating procedure (Microbics Corporation 1995). The detailed technique used for elutriates toxicity analysis, including the protocol followed to prepare the aqueous elutriates from TS and SS samples, has been included in Figure 6.19.

Soil elutriates (SE) were obtained after mixing 15 g of soil (< 0.25 mm) and 30 g of Milli Q water in 40 mL-PTFE vials for 24 h (22º C, 80 rpm, rotary agitator, RR80, LBX®), enough time to reach COCs desorption equilibrium between the soil and the aqueous

phases (Garcia-Cervilla, Santos et al. 2021, Checa-Fernández, Santos et al. 2022, **ART. 5**). The vials were centrifuged (10 min, 9000 rpm, MEDTRONIC-BL-S, JP SELECTA®) to separate both phases, the aqueous phase constituting the Microtox® test sample: SE. Additionally, the toxicity of the aqueous reaction supernatants of the different treatments was analyzed. Before measurement, the remanent PS was removed (as described in Subsection 6.3.1.6), and the pH was adjusted (6-8).

The osmotic control of the initial SE (2.5 mL) was reached by adding 250 mL of OAS (NaCl, 22%). For each SE, 4 dilutions and a blank (without SE) were analysed. Vials with the bacteria reagent were prepared by mixing 0.5 mL of the diluent and 10 mL of the reconstituted bacteria reagent, and the initial bacteria light emission ($I_{0,\ elutriate}$) was measured. The diluted samples (0.5 mL) were added to the vials with the reconstituted bacteria. The maximum concentration of SE in the analysis cuvettes is 45%, being the concentration 50% of the previous one with each successive dilution. The SE dilution ratio that yields a 50% reduction of bacteria light emission is $IC_{50,\ elutriate}$. The bioluminescence inhibition of *Vibrio fischeri* was measured at 15 min of exposure ($I_{15,\ elutriate}$). Toxicity results have been expressed as $EC_{50,\ elutriate}$ ($g_{soil}\ L^{-1}$), which considers the soil/water ratio used (500 g L^{-1}) in elutriates preparation (Eq. (6.8)):

$$EC_{50,elutriate}\ (g_{soil}L^{-1}) = \frac{IC_{50,elutriate}\ (\%)}{100} \cdot \frac{mass_{soil}}{V_{water}} \qquad (6.8)$$

Thus, the soil concentration in this test ranges from 28.2 to 225 $g_{soil}\ L^{-1}$, in addition to the blank (without SE).

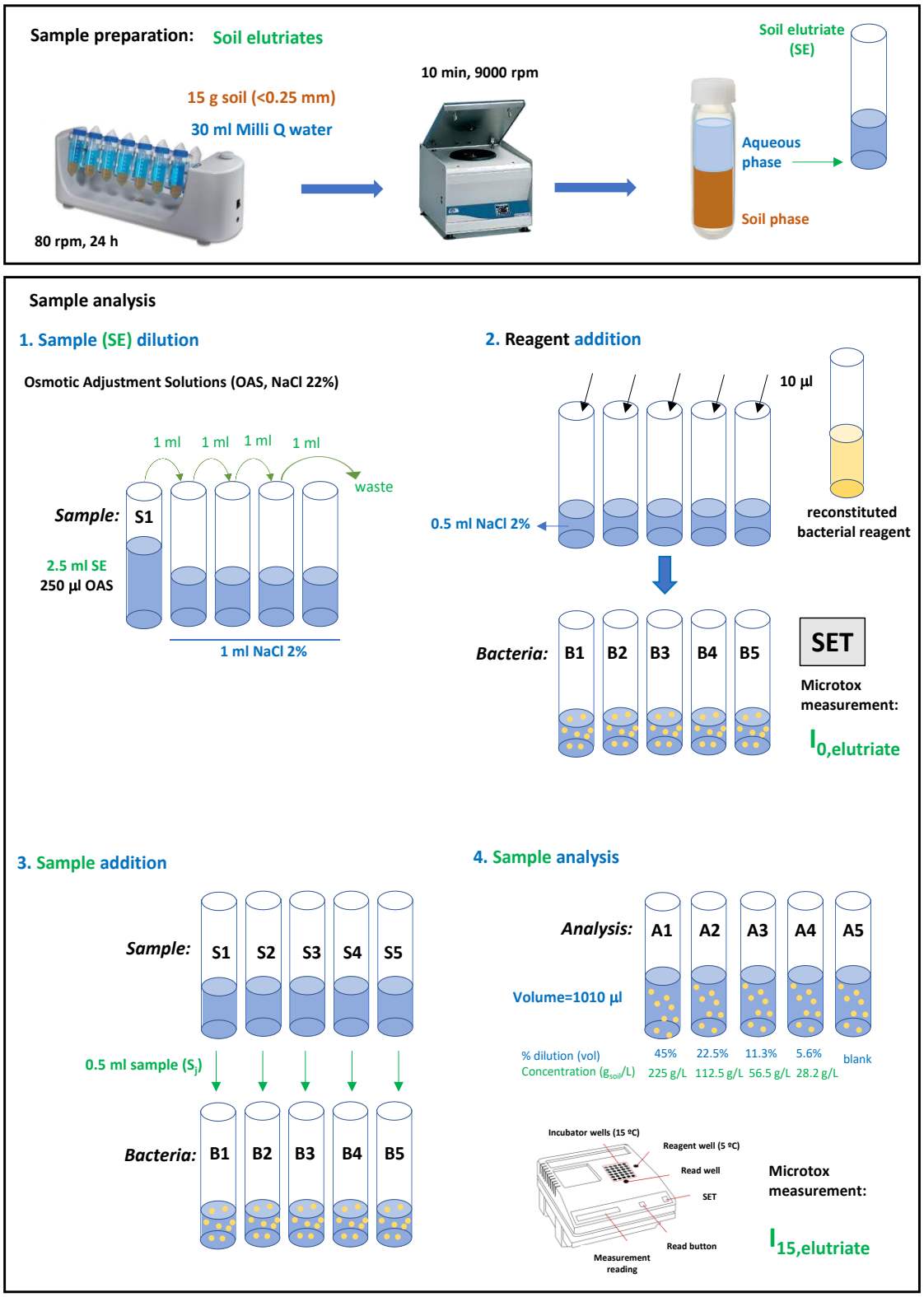

Figure 6.19. Elutriates (aqueous phase): Basic Test (Domínguez, Ventura et al. 2023, **ART. 1**).

Chapter 7.

RESULTS AND DISCUSSION

7.1. Soils characterization

7.1.1. Physico-chemical composition and pollutant concentration

7.1.2. Acute toxicity

7.1.2.1. Acute toxicity of soils

7.1.2.2. Acute toxicity of soil elutriates

7.1.2.3. Acute toxicity of soil organic extracts

7.2. Topsoil (TS) oxidation treatments

7.2.1. Oxidant evaluation: HP and PS

7.2.1.1. Hydrogen peroxide (HP/Fe, Fenton process)

7.2.1.2. Persulfate (PS)

7.2.2. PS activation evaluation: NaOH and T

7.2.3. Intensification of PS/NaOH

7.2.3.1. PS/NaOH/T

7.2.3.2. PS/NaOH/US

7.2.3.3. S/PS/NaOH/T

7.3. Acute toxicity of treated soils

7.3.1. Remediated Topsoil

7.3.2. Remediated Subsoil

This chapter compiles the results obtained in this Doctoral Thesis based on the publications previously detailed in Chapter 3. It has been structured in three blocks, the first one focused on soil characterization, the second on topsoil (TS) remediation treatments, and the third one on how these treatments affect soil toxicity.

- **Characterization** of polluted topsoil (TS) and subsoil (SS) samples and their corresponding elutriates, including physico-chemical properties, chlorinated organic compounds (COCs) concentration, and toxicity. Additionally, the sources of soil pollution (HCH particulate matter (PM) in the case of TS and DNAPL in the case of SS) have been characterized.
- **Evaluation of TS oxidation treatments**. The application of different oxidants (hydrogen peroxide and persulfate) and activators (iron salts, temperature, and NaOH) and further intensification of PS/NaOH treatment (temperature, US, and surfactants) for TS remediation was thoroughly studied.
- **Toxicity evaluation** after applying the selected treatments (PS/T and PS/NaOH/T for TS and ISCO (PS/NaOH) and S-ISCO (E3/PS/NaOH) for SS).

7.1. Soils characterization

This section describes the i) physico-chemical composition, ii) pollution level, and iii) toxicity of **soil samples** (topsoil (**TS**) and subsoil (**SS**)) and their corresponding **elutriates**. The respective sources of pollution, HCH particulate matter, and DNAPL, have also been characterized.

7.1.1. Physico-chemical composition and pollutant concentration

The inorganic characterization of the soil samples of the landfills (TS (Bailín landfill), SS-C, and SS-F (Sardas landfill)) is summarized in Table 7.1. It should be noted that in the case of SS, two fractions were characterized: fine (SS-F) and coarse (SS-C), attending the Wentworth classification (Wentworth 1922)), as previously summarized in Table 6.2. As can be seen, the inorganic composition did not depend on the contamination level of the soil (TS and SS) samples.

According to the measured pH (7.2 - 7.8), they are moderately alkaline soils with buffer capacity due to the significant content of carbonates (≈ 40%, as calcium carbonate). The content of metals, such as Fe, Ca, Na and Al, is not negligible. Particular attention

should be paid to Fe and Mn concentration since these metals can contribute to the decomposition of the oxidants, especially hydrogen peroxide (Teel, Finn et al. 2007).

Table 7.1. Topsoil (TS) and subsoil (SS) inorganic characterization (mean ± standard deviation).

	TS[a]	SS-C[b]	SS-F[b]
IC (%)	4.6 ± 0.2	5.4 ± 0.4	5.2 ± 0.3
$CaCO_3$ (%)	38.3 ± 1.8	45.0 ± 3.3	43.2 ± 2.5
pH	7.4 ± 0.2	7.5 ± 0.3	7.5 ± 0.1
Metal concentration (mg kg^{-1})			
Fe	21099 ± 1581	30563 ± 1554	32345 ± 1038
Mg	11704 ± 698	6428 ± 11	7603 ± 307
Ca	168796 ± 6141	180352 ± 3607	172982 ± 2619
Cu	ND	35 ± 11	48 ± 8
Mn	392 ± 21	550 ± 32	530 ± 15
Na	1533 ± 1925	1491 ± 218	1273 ± 154
Al	17076 ± 1759	15588 ± 633	17653 ± 542
K	5545 ± 459	3185 ± 186	4207 ± 219

ND = not detected. [a]TS L2 sample, [b]Mean obtained for all pollution levels (L1-L4) (Table 6.2).

The concentration of COCs, the TOC measured, and the ratio between the TOC of COCs and TOC measured ($TOC_{COCs,\ soil}/TOC_{measured,\ soil}$) in the different levels of contamination of both types of soils (TS and SS) together with the concentration of contaminants determined in the respective elutriates are included in Table 7.2. As can be seen, only a small percentage of TOC measured in TS samples corresponds to chlorinated organic compounds. The rest of the organic matter is attributable to the presence of natural organic matter as humic acid-like compounds (Dominguez, Romero et al. 2021, **ART. 2**). On the contrary, in SS samples the TOC is mainly due to the COCs content.

Table 7.2. COCs concentration, TOC measured, and the percentage ratio between $TOC_{COCs,soil}$ /$TOC_{measured,soil}$ in soils and COCs in soils elutriates (V_L/W_S = 2).

Soil	Acronym Sample	$COCs_{soil}$ (mg kg_{soil}^{-1})	$TOC_{measured,soil}$ (mg kg_{soil}^{-1})	$TOC_{COCs,soil}$/ $TOC_{measured,soil}$ (%)	$COCs_{,elutriate}$ (mg L_{water}^{-1})
Topsoil (TS)	TS L0	1	15000±2000 (1.5±0.2%)	<0.1	0.07
	TS L1	42		0.1	0.05
	TS L2	155 - 409		0.3-0.7	3.15 - 4.74
	TS L3	802		1.3	4.68
	TS L4	1147		1.9	10.92
Subsoil (SS)	SS-C L0	20	6	83.3	0.06
	SS-C L1	518	150	83.3	31.30
	SS-C L2	3682	1000 (0.1%)	90.9	56.90
	SS-C L3	6372	1720	90.9	41.00
	SS-F L0	33	10	76.9	0.07
	SS-F L1	1042	280	90.9	33.10
	SS-F L2	3024	880	83.3	36.50
	SS-F L3	9528	2820	83.3	48.60

The samples employed for the remediation treatments have been highlighted in bold type and blue. In the case of TS L2, a range of COCs concentrations is included as different lots of contaminated soil were used (slightly varying the initial concentration).

TS samples were mainly polluted with HCH isomers. TS pollution was present as particulate matter of HCHs and adsorbed into the soil (Figure 7.1).

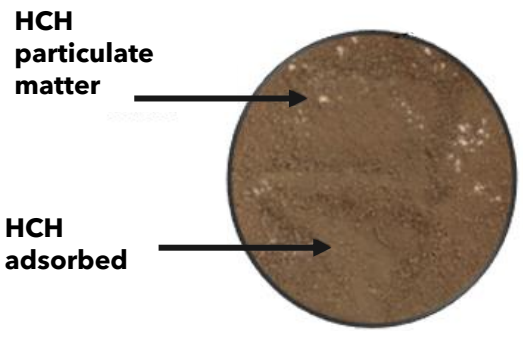

Figure 7.1. Photograph of contaminated TS.

The COCs distribution in TS samples (pollution levels L1-L4) is shown in Figure 7.2 (total COCs concentration is included in the legend). The pollution level L0 has not been included since its low COCs concentration (< 1 mg kg^{-1}) would lead to an erroneous interpretation of the results. COCs distribution was similar for all the pollutant levels studied, and it mainly corresponds to HCH isomers (the sum of other compounds such as

β-PCX represents less than 1%). The HCH isomers in a higher proportion were α-HCH (80-85%) and β-HCH (10-15%), except for L1 sample in which the ratio between these compounds was reversed. This can be explained because in TS L1 no particulate matter was visible to the naked eye. Thus, can be assumed that most of the contamination was due to adsorbed HCHs. The enrichment in β-HCH isomer (the most recalcitrant and stable HCH isomer) in adsorbed contamination was described in the literature (Semple, Morriss et al. 2003). Low concentrations of the other HCH isomers were also detected in TS samples (Σγ-,δ-,ε-HCH = 3 ± 1%).

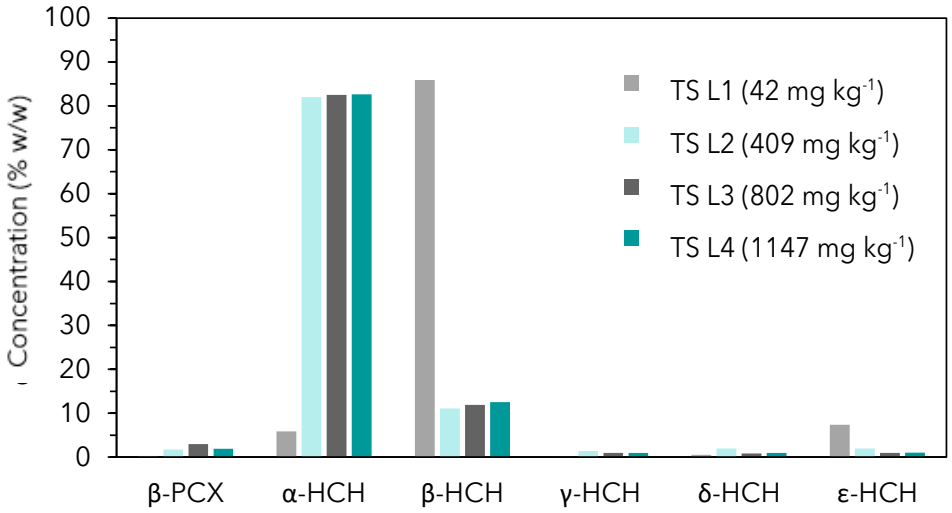

Figure 7.2. COCs distribution in TS samples (total COCs concentration is included in the legend) (Domínguez, Ventura et al. 2023, **ART. 1**).

The distribution of COCs for **SS-C and SS-F** is depicted in Figure 7.3-a and b, respectively. As can be seen, COCs concentration in SS samples was significantly higher than in TS (Table 7.2), which is attributed to the different sources of soil contamination (particulate matter of HCHs for topsoil and DNAPL for subsoil). COCs composition is very variable in the coarse fraction (the contribution of γ-HCH is especially high in L1). In contrast, in fraction F, pollutants distribution was similar regardless of the contamination level (γ-HCH percentage increases with COCs concentration).

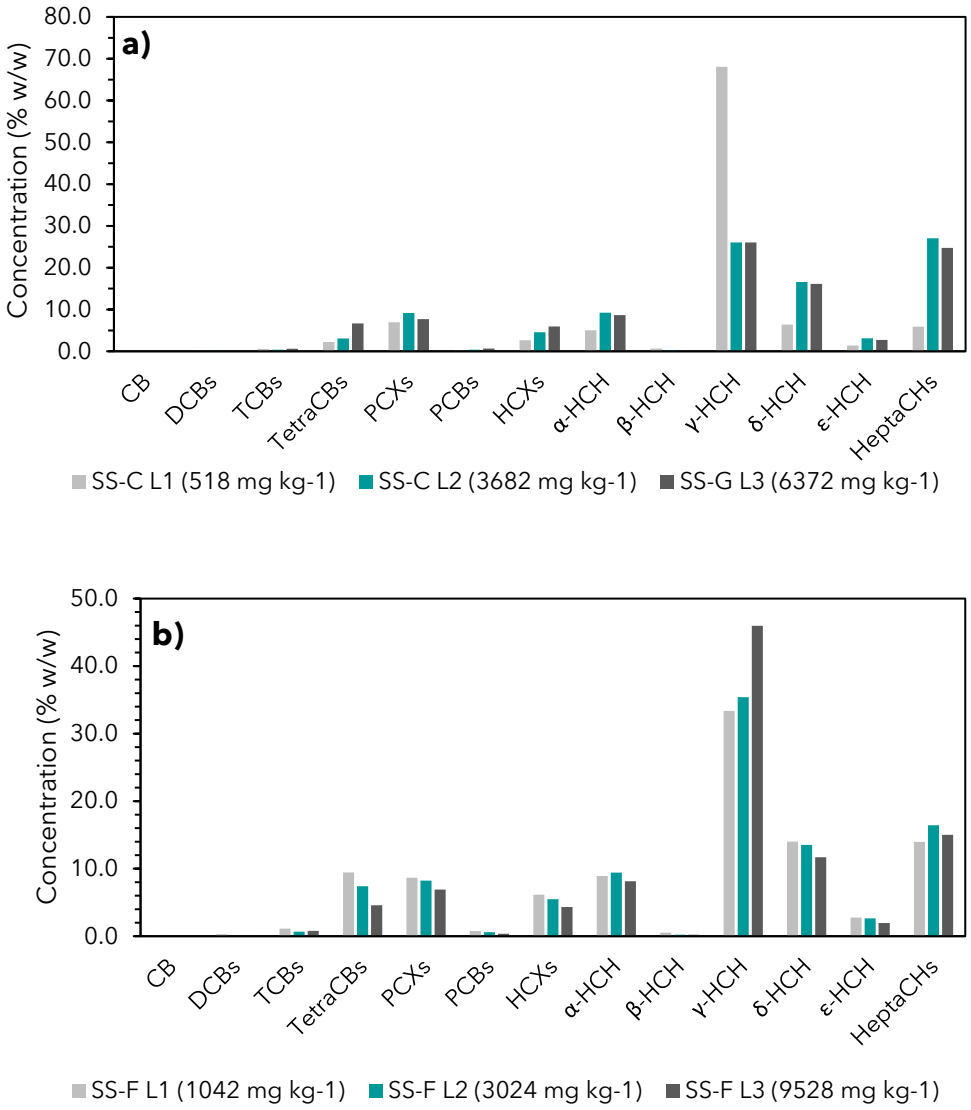

Figure 7.3. COCs distribution in SS-C (a) and SS-F (b) samples (COCs concentration is included in the legend) (Domínguez, Ventura et al. 2023, **ART. 1**).

As previously stated, the concentration of COCs in TS and SS **elutriates** is included in Table 7.2. To facilitate interpretation, COCs concentration in the elutriates has been represented vs. COCs concentration in the soil for the three types of soils: TS, SS-C, and SS-F (Figure 7.4).

As expected, as COCs concentration in the soil increases, COCs concentration in the elutriates also increases. It should be noted that this increase was not linear. In the case of subsoil elutriates (SS-C and SS-F), a maximum value of COCs solubilized of around 40-50 mg L^{-1} was reached (asymptotic trend), which can be attributed to the saturation of COCs in the aqueous phase caused by the high pollutant concentration in this soil. The asymptotic trend was similar in both SS soils (SS-C and SS-F). However, it was not reached

in the case of topsoil. For equal COCs concentration in the soils (≈400-500 mg kg^{-1}), TS elutriates presented a significantly lower COCs concentration than SS elutriates (*i.e.* TS L2 (4.74 mg L^{-1}) *vs.* SS-C L1 (31.30 mg L^{-1}), Table 7.2). The origin of this result lies in the contamination source. HCH isomers (topsoil) are poorly soluble in water, while DNAPL (subsoil) contains a mixture of chlorinated organic compounds (among them, chlorobenzenes) with higher water solubility, as detailed below.

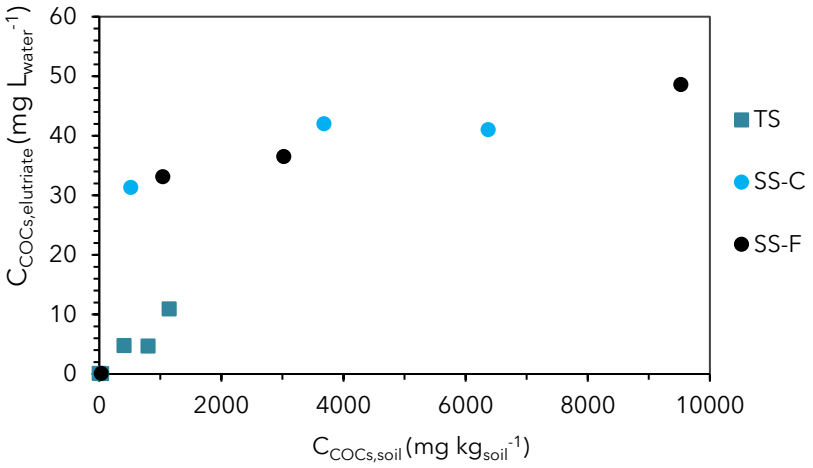

Figure 7.4. COCs concentration in the elutriates (V_L/W_S=2) *vs.* soils (Domínguez, Ventura et al. 2023, **ART. 1**).

COCs distribution in HCH particulate matter and DNAPL is depicted in Figure 7.5-a and-b, respectively. The composition of HCH particulate matter can be explained by attending to the lindane (γ-HCH) manufacturing process. The distribution of HCH isomers in the technical-HCH was: α = 55-80%, β = 5-14%, γ = 10-15%, δ = 2-16%, ε = 3–5% (Fernández, Arjol et al. 2013, Wacławek, Silvestri et al. 2019). Consequently, after the lindane purification process, the solid residue (HCH particulate matter) was mainly composed of α-HCH, followed by β-HCH. In the analyzed samples (Figure 7.5-a), the percentage of these isomers was 83.4 and 8.7%, respectively. As expected, γ-HCH, the product of interest (the only isomer with pesticide properties), was found in a smaller proportion (1.8%) due to the purification of the technical HCH mixture. Moreover, it should be highlighted that the percentage of α-HCH found in HCHs particles was only slightly higher than that noticed in TS samples (83.4% *vs.* 80-82%), confirming that the contamination of the TS mainly was due to the presence of particulate HCHs, with a small contribution of these pollutants adsorbed into the soil.

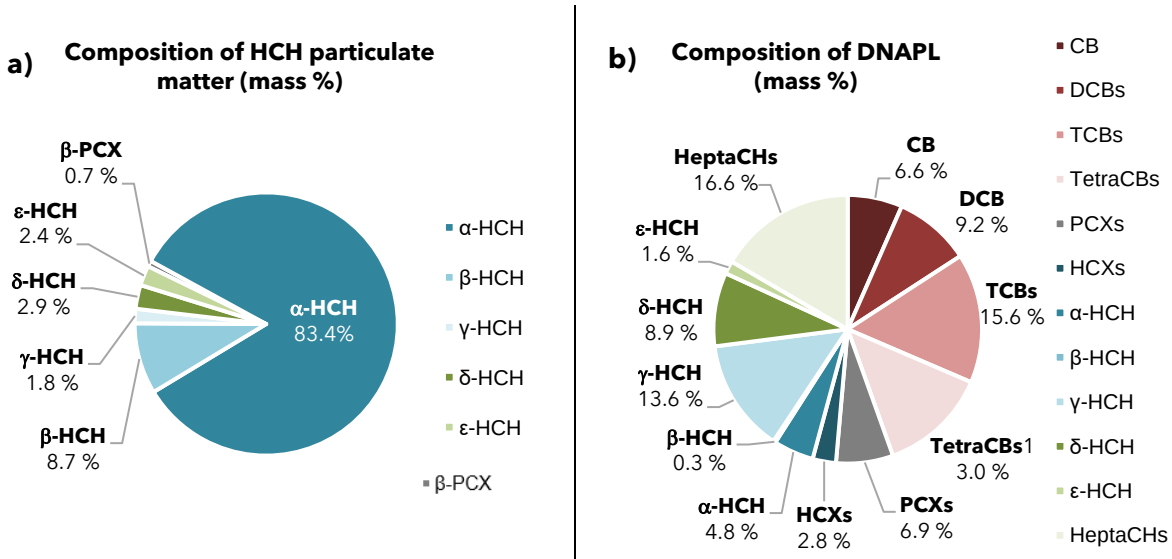

Figure 7.5. COCs distribution in (a) HCH particulate matter and (b) DNAPL (Domínguez, Ventura et al. 2023, **ART. 1**).

In the case of DNAPL, more than 20 COCs have been identified (see GC-FID chromatograms, Figure 6.8-b), as previously reported (Santos, Fernandez et al. 2018). Pollutants have been grouped by isomer families: chlorobenzene (CB), dichlorobenzenes (DCBs), trichlorobenzenes (TCBs), tetrachlorobenzenes (TetraCBs), pentachlorocyclohexenes (PCXs), hexachlorocyclohexenes (HCXs) and heptachlorocyclohexanes (HeptaCHs), whereas HCH isomers (α, β, γ, δ, ε-HCH) have been considered separately due to their interest (Figure 7.5-b). The main DNAPL compounds were HCHs (29%), being lindane the major HCH isomer present (13.6%), followed by δ-, α-, and ε-HCH, whereas β-HCH was the HCH isomer found in the lowest concentration (0.3%). The percentage of the rest of COCs was: HeptaCHs (17%) > TCBs (16%) > TetraCBs (13%) > DCBs (9%) > CB ≈ PCXs (7%) > HCXs (3%). These results agree with those obtained in a previous study, in which different DNAPLs from Sabiñánigo landfills were characterized (Santos, Fernandez et al. 2018).

7.1.2. Acute toxicity

The Microtox® bioassay has been used to comprehensively assess the acute toxicity of real soil samples highly polluted with lindane wastes (TS and SS) following three different procedures. The results obtained are supported by statistical analysis.

The **modified Basic Solid-Phase Test** (mBSPT, Subsection 6.3.1.6) has been applied to analyze the toxicity of an **aqueous slurry of polluted soils** in water at standard conditions. The **Basic Test** procedure (Subsection 6.3.2.7) has been used to study the toxicity of an aqueous phase in contact with the soil after partitioning equilibrium was reached (called **elutriates**). Measuring soil elutriates toxicity is necessary to know the toxicity risk associated with the waters in contact with the polluted soils (leachates or groundwaters). Finally, the **Organic Solvent Sample Solubilization Test** (aOSSST, Subsection 6.3.2.7) has been adapted to measure the acute toxicity of **organic extracts from soils** after all the hydrophobic organic compounds in soil were dissolved in this extract. Measuring the toxicity of the organic extracts is essential in the case of hydrophobic soil pollutants, such as HCHs. Therefore, all three measures are necessary for a complete overview of the acute toxicity of contaminated soils under study.

7.1.2.1. Acute toxicity of soils

Soil toxicity values ($EC_{50,soil}$, Microtox® mBSPT) with the confidence interval (CI) and the concentration of COCs of each sample are given in Table 7.3. According to the classification proposed by Kwan and Dutka (1995): $EC_{50} > 10$ g L^{-1} nontoxic sample, 5 g $L^{-1} < EC_{50} \leq 10$ g L^{-1} moderately toxic sample, and $EC_{50} \leq 5$ g L^{-1} very toxic sample, soils collected from Sardas and Bailín landfills are highly toxic ($EC_{50} \leq 5$ g L^{-1}). The fact that the reference samples (L0), with low COCs concentration, exhibit intrinsic toxicity would indicate that there are toxic compounds for the bacteria used in the test (*Vibrio fischeri*) in the soil matrix.

The relationship between soil toxicity (expressed as $1/EC_{50,\,soil}$, in L g_{soil}^{-1}) and COCs concentration for each type of soil (TS, SS-C, and SS-F) and pollution level has been represented in Figure 7.6-a (COCs concentration has been considered as a single compound to simplify).

It is also noticed that at similar values of COCs concentration, soil toxicity differed depending on its origin: SS-C > TS > SS-F (Figure 7.6-a). The fact that fraction fine (F) toxicity was lower than fraction coarse (C) toxicity for the same soil type (SS) could be

justified based on the contaminant bioavailability concept. Contaminants are more strongly adsorbed to the soil in fraction F and are less accessible to bacteria, resulting in lower toxicity. Secondly, the more significant toxicity of SS compared to TS for the same particle size (C) and COCs concentration could be associated with the contaminants type (DNAPL and HCH particulate matter), as will be further discussed.

Table 7.3. Acute toxicity measured by Microtox® modified Basic Solid-Phase Test (a), Basic Test (b), and adapted Organic Solvent Sample Solubilization Test (c) for soils, soils elutriates, and soils organic extracts, respectively (Domínguez, Ventura et al. 2023, **ART. 1**).

	Soil (a)			**Soil elutriate (b)**			**Soil organic extract (c)**		
Sample	**$EC_{50,soil}$ (g_{soil} L_{slurry}^{-1})**	**CI**	**$C_{COCs,soil}$ (mg kg_{soil}^{-1})**	**$EC_{50,elutriate}$ (g_{soil} L^{-1})**	**CI**	**$C_{COCs,elutriate}$ (mg L_{water}^{-1})**	**$EC_{50,organic}$ (g_{soil} L_{MeOH}^{-1})**	**CI**	**$C_{COCs,soil}$ (mg kg_{soil}^{-1})**
TS L0	2.22	0.12	<1	ND	-	0.07	ND	-	<1
TS L1	1.95	0.32	42	ND	-	0.05	ND	-	42
TS L2	1.29	0.25	409	306.5	18.95	4.74	16.66	3.56	409
TS L3	1.03	0.21	802	312	29.05	4.68	19.23	4.63	802
TS L4	0.94	0.26	1147	125	26.55	10.92	8.49	2.49	1147
SS-C L0	1.62	0.12	20	ND	-	0.06	27.80	3.94	20
SS-C L1	0.70	0.01	518	56.5	9.6	31.30	3.79	0.21	518
SS-C L2	0.66	0.07	3682	29	0.35	56.90	0.55	0.04	3682
SS-C L3	0.65	0.02	6372	31	3.15	41.00	0.44	0.02	6372
SS-F L0	3.30	0.04	33	ND	-	0.07	29.53	0.98	33
SS-F L1	1.34	0.18	1042	67	9.5	33.10	1.31	0.06	1042
SS-F L2	1.10	0.13	3024	47.5	12.25	36.50	0.48	0.01	3024
SS-F L3	0.96	0.06	9528	29.5	4.6	48.60	0.38	0.08	9528

**$C_{COCs,\ soil}$ ($mg\ kg_{soil}^{-1}$) of soil (a), and soil organic extract (c) correspond to the same samples and measurement procedure. ND: toxicity not detected. CI: confidence interval, 95%.*

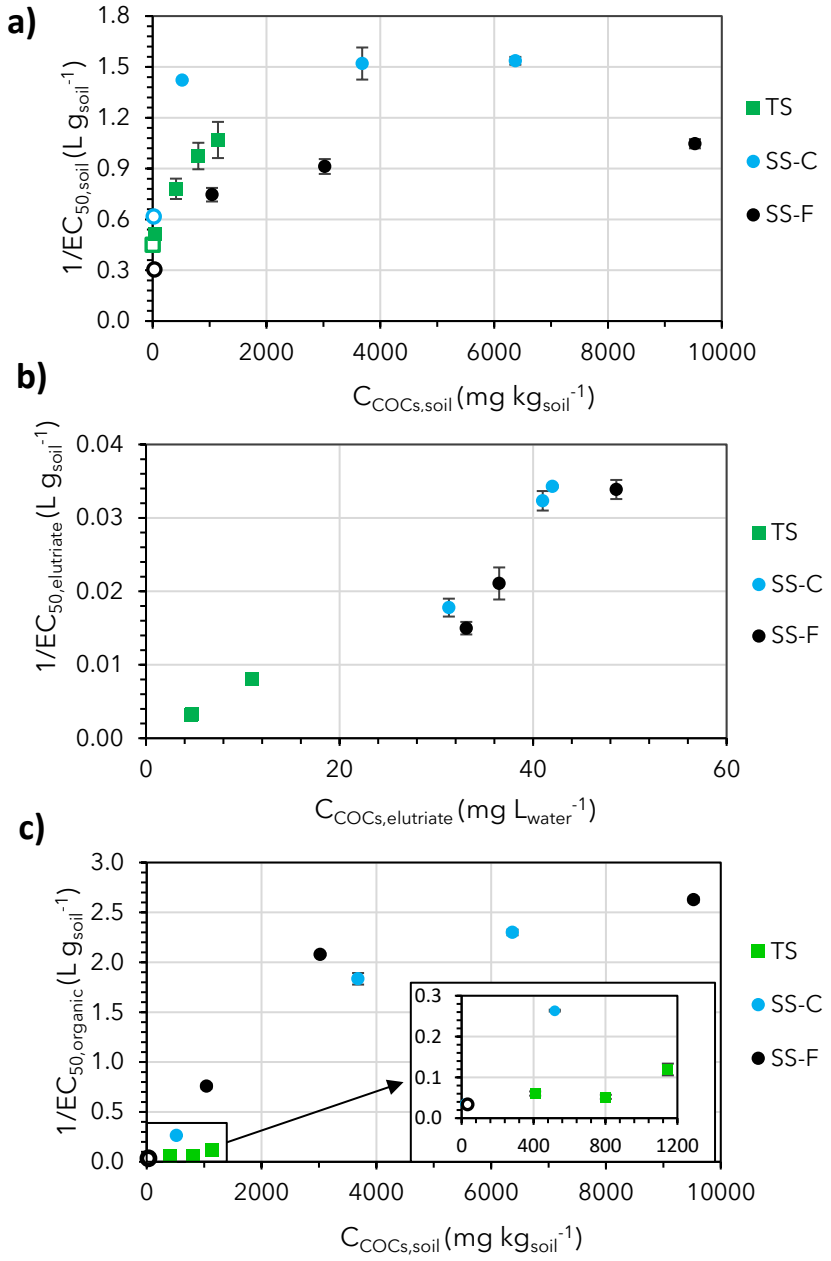

Figure 7.6. (a) Soil toxicity ($1/EC_{50,\ soil}$, Microtox® mBSPT), (b) Elutriate toxicity ($1/EC_{50,\ elutriate}$, Microtox® BT), and (c) Soil organic extract toxicity ($1/EC_{50,\ organic}$, Microtox® aOSSST) *vs.* COCs concentration. The unfilled markers denote the reference soil samples (L0) (Domínguez, Ventura et al. 2023, **ART. 1**).

7.1.2.2. Acute toxicity of soil elutriates

The measurement of soil elutriates acute toxicity is necessary to know the toxicity risk associated with the waters in contact with the polluted soils (leachates or groundwaters), and it is of particular relevance when there are superficial waters in the vicinity of the contaminated site.

Elutriate toxicity results ($EC_{50,\ elutriate}$, Microtox® *Basic Test*), the confidence interval (CI), and COCs concentration are given in Table 7.3-b. The calculation of toxicity values that would require soil elutriates dilutions below 45% (maximum concentration measured in this protocol) has been obtained by extrapolation. The toxicity evaluation has been carried out according to the classification proposed by Libralato, Annamaria et al. (2010): EC_{50} > 100 g L^{-1} low toxicity sample, 10 g $L^{-1} \leq EC_{50} \leq$ 100 g L^{-1} moderately toxic sample, EC_{50} < 10 g L^{-1} very toxic sample. As seen in Table 7.3, topsoil (TS) elutriates presented low acute toxicity, which could indicate that the possible leachates from the surface soil of the landfills are not an environmental issue in terms of acute toxicity. However, subsoil fraction elutriates, C-SS and F-SS, exhibited moderate acute toxicity from pollution level L1 (reference levels toxicity (L0) was not detectable), meaning that groundwater in contact with contaminated subsoil (C_{COCs} > 500 mg kg^{-1}) would imply a moderate but significant environmental risk in terms of acute toxicity.

Elutriate toxicity is expected to be related to solubilized compounds from soil: COCs, other organic compounds (if any), and inorganic species, such as metals, present in the soil (Čvančarová, Křesinová et al. 2013). Elutriate reference samples (L0) did not exhibit toxicity (Table 7.3), and metals concentration does not vary with the contamination level. Thus, it can be inferred that these species do not contribute to elutriate toxicity. Elutriate toxicity results (expressed as $1/EC_{50,\ elutriate}$ in L g_{soil}^{-1}) for each soil type (TS, SS-C, and SS-F) and pollution level have been plotted *vs.* COCs concentration in these aqueous phases (Figure 7.6-b) (COCs concentration has been considered as a single compound to simplify). Regardless of soil type, an approximately linear trend can be observed.

The concentration of COCs (C_{COCs}) and the effective nominal concentration (EC_{50}, Eq. (6.3)) of HCH particulate matter (HCH PM) and DNAPL (as a single compound) in the saturated aqueous phase (Microtox® Basit Test) are shown in Table 7.4. Moreover, the concentration and EC_{50} values of the pure compounds with higher content in HCH PM and DNAPL have also been measured in saturated aqueous phases, and values are summarized in Table 7.4. Additionally, solutions with solved pollutants were prepared in

MeOH, and the EC_{50} was determined using the Microtox® adapted organic Solvent Sample Solubilization Test (detailed in Subsection 7.1.2.3).

Table 7.4. Concentration and EC_{50} of HCH PM, DNAPL, and pure commercial contaminants in saturated aqueous solutions (Microtox® BT) and organic (MeOH) phases (Microtox® aOSSST) (Domínguez, Ventura et al. 2023, **ART. 1**).

	C_{COCs} saturated aqueous phase (mg kg_{water}^{-1})	**EC_{50} (mg L_{water}^{-1})** (Microtox® BT)	**EC_{50} (mg L_{MeOH}^{-1})** (Microtox® aOSSST)
HCH PM	7.75	ND	39.43
DNAPL	41.8	4.41	4.23
α-HCH	1.2	ND	ND
β-HCH	0.2	ND	ND
γ-HCH	7.2	8.34	4.23
δ-HCH	10.5	3.50	9.37
1,2,3-TCB	7.7	0.82	4.96
1,2,4-TCB	30.0	3.44	7.82
1,2,3,4-TetraCB	2.1	0.61	4.23

ND = not detected.

HCH particulates exhibited increased bioluminescence at the minimum concentration of the measured sample (Figure 7.7-a), meaning that the inhibition percentage reached a negative value. This behaviour is due to hormesis, a phenomenon of response to potentially toxic agents characterized by stimulation at low doses and inhibition at higher doses, following a hyperbolic trend (Kwan and Dutka (1990)).

α-HCH and β-HCH did not present acute toxicity toward the bacterium *Vibrio fischeri*, as occurred with HCH particulate matter (the maximum bioluminescence inhibition of the aqueous phase saturated in these pollutants did not reach 20%, results shown in Table 7.4). The fact that these compounds represent around 90% of the HCH particulate matter (Figure 7.5-a) would justify that no toxicity response had been detected in the aqueous phase for this source of contamination (the concentration of COCs in HCH particulate matter was 7.75 mg kg^{-1}, Table 7.4). Contrarily, the aqueous phases of γ- and δ-HCH, and especially chlorobenzenes (1,2,3-TCB, 1,2,4-TCB, and 1,2,3,4-TetraCB), which practically represent 50% of the DNAPL composition, exhibited considerable acute toxicity, which would justify the high acute toxicity of DNAPL ($EC_{50,\ DNAPL}$ = 4.41 mg L^{-1}, the concentration of COCs in this aqueous solution was 41.8 mg kg^{-1}, Table 7.4).

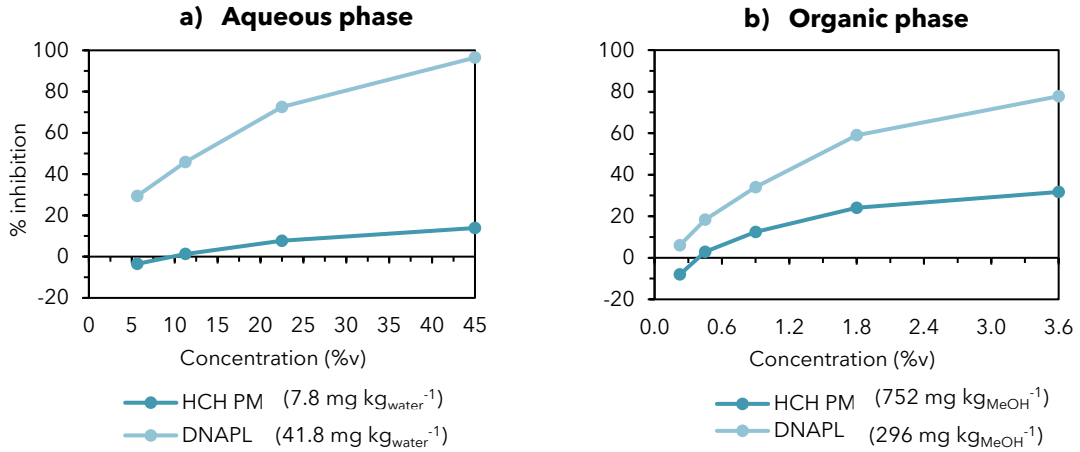

Figure 7.7. Inhibition (%) of *Vibrio fischeri* bioluminescence *vs.* the concentration of HCH PM and DNAPL (a) in the Basic Test and b) in the adapted Organic Solvent Sample Solubilization Test (b). The absolute concentration of the contaminant is included in the legend (Domínguez, Ventura et al. 2023, **ART. 1**).

The results obtained here are in agreement with those found in the literature. Svenson, Edsholt et al. (1996) analyzed the acute toxicity of sediments contaminated with chlorinated pesticides, including α-HCH. According to their results, this compound was not potentially toxic to the bacteria tested. Garg, Lata et al. (2016) studied the toxicity of β-HCH and δ-HCH in saturated aqueous solutions. A bioluminescence reduction was not detected for these compounds. Still, in the case of δ-HCH, negative inhibition (hormesis) was observed, indicating that this isomer exhibits acute toxicity at higher concentrations. Finally, Kaiser and Palabrica (1991) collected about 1350 acute toxicity data of individual organic compounds for the *Vibrio fischeri* bacterium. The EC_{50} ranges (or exact values) for γ-HCH, 1,2,4-TCB, 1,2,3-TCB, and 1,2,3,4-TetraCB were 5.67-11.1, 3.01-3.70, 2.50-2.62, and 1.88 mg L^{-1}, respectively. The acute toxicity reported for γ-HCH and 1,2,4-TCB agrees with that obtained in the present study (8.34 and 3.44 mg L^{-1}, respectively (Table 7.4)), while in the case of 1,2,3-TCB and 1,2,3,4-TetraCB, the EC_{50} values found in the literature were slightly higher than those obtained in the present study (0.82 and 0.61 mg L^{-1}, respectively. The low solubility of α-HCH and β-HCH in the aqueous phase makes the measurement of EC_{50} by the Microtox® Basic Test impossible. On the contrary, determining the toxicity of poorly water-soluble compounds in an organic matrix is recommended (Microbics Corporation (1995), Ruiz, López-Jaramillo et al. (1997)).

7.1.2.3. Acute toxicity of soil organic extracts

Determining the acute toxicity of soil organic extracts ensures the total availability of the pollutants from soil (Čvančarová, Křesinová et al. 2013). These results ($EC_{50,\ organic}$, Microtox® *adapted Organic Solvent Sample Solubilization Test*), the confidence interval (CI), and the corresponding COCs concentration are given in Table 7.3-c. The calculation of acute toxicity values that would require concentrations of soil organic extract above 3.6% (maximum study concentration in this protocol) has been obtained by extrapolation. To the best of our knowledge, there is no toxicity classification in the literature regarding the organic extract samples.

Acute toxicity results of soil organic extracts ($1/EC_{50,\ organic}$, expressed in L g_{soil}^{-1}) for each soil type (TS, SS-C, and SS-F) and pollution level have been plotted *vs.* COCs concentration (Figure 7.6-c, COCs concentration has been considered as a single compound to simplify). An inset of the plot on the range of low COCs concentrations was zoomed in to facilitate the interpretation of the results.

The higher the soil COCs concentration, the higher the acute toxicity of the organic extract (Figure 7.6-c). Values obtained for F and C subsoil samples suggest a logarithmic trend between toxicity and contaminants concentration. This corresponds to the logarithmic relationship between bacteria inhibition and the sample concentration studied. The toxicity of similar COCs concentration values differs depending on the soil origin (TS or SS): SS-C≈SS-F > TS. The similar COCs composition of C-SS and F-SS explains the similar toxicity values with COCs concentrations obtained for these soils. The fact that the TS organic extracts are considerably less toxic than the SS fractions (SS-C and SS-F) can be explained again by attending to the different contaminant types (HCH particles in TS and DNAPL in SS).

The effective nominal concentration (EC_{50}, Eq. (6.3)) of HCH particulates and DNAPL (as a single compound) and the most representative COCs (commercially available) of these contaminants solved in methanol have been determined (Microtox® *adapted Organic Solvent Sample Solubilization Test*, Table 7.4). Since COCs solubility in methanol is significantly higher than in water, the analysis of the organic phase allows for determining their acute toxicity at higher concentrations. The EC_{50} of HCH PM obtained was 39.43 mg L^{-1}. As can be seen, the DNAPL concentration that induces 50% of bioluminescence inhibition was significantly lower (4.23 mg L^{-1}), highlighting the higher acute toxicity of compounds in DNAPL. This finding explains the higher toxicity values

obtained for the organic extracts in the case of SS (contaminated by DNAPL) than TS (contaminated by HCH particulates) (Figure 7.6-c).

The low acute toxicity of HCH particulate matter in this test can be explained again by attending to its composition. The average EC_{50} values (mg L^{-1}) obtained in the Microtox® test for the organic phase showed that α-HCH and β-HCH (≈ 90% of HCH particulates, Figure 7.5-a) did not present acute toxicity toward the bacterium *Vibrio fischeri* either, despite being in much higher concentration than in the aqueous phase (Table 7.4).

Soil organometallic compounds soluble in methanol pass into organic extracts (Roig, Nadal et al. 2011). Additionally, the concentration of these species is not affected by the pollutant level and is similar for the three soil types Table 7.1. Thus, the results corresponding to reference samples (L0), with negligible pollutants concentration, would indicate if these organometallic compounds participated in the toxicity response. Since TS L0, with a COCs concentration < 1 mg kg^{-1}, does not exhibit toxicity, the soil metals effect can be ruled out. Hence, the toxicity values obtained for samples SS-C L0 and SS-F L0 (EC_{50} = 27.80 and 29.53 mg L_{MeOH}^{-1}) are attributable to COCs concentration (20 and 33 mg_{COCs} kg_{soil}^{-1}).

Finally, soil organic extracts toxicity values have been plotted *vs.* those corresponding to soils (Figure 7.8). The results obtained for low COCs concentrations indicate that soils exhibited more significant toxicity than their organic extracts, which was especially notable for topsoil samples. As can be seen, this behaviour was reversed as the concentration of COCs increased. Soil organic extracts toxicity increased exponentially with soil toxicity for subsoil samples. This phenomenon would confirm that: i) contaminant-free soil has non-negligible intrinsic acute toxicity, and ii) the mBSPT test considers the bioavailability of contaminants, although the solubility equilibrium limits it. Finally, it should be highlighted that the *Microtox® adapted Organic Solvent Sample Solubilization Test* resulted in the most reliable test for evaluating the toxicity of these types of soils, considering the lower standard deviation of $1/EC_{50}$ values obtained (Table 7.5).

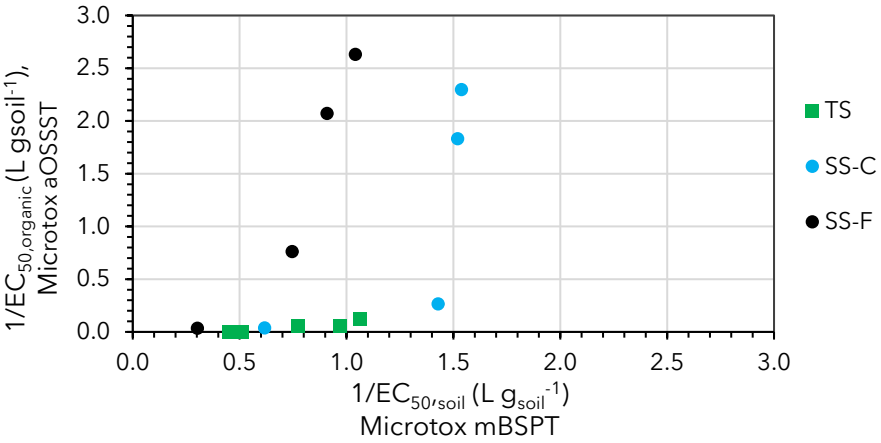

Figure 7.8. Soil organic extract toxicity ($1/EC_{50,\ organic}$, Microtox® adapted Organic Solvent Sample Solubilization Test) *vs.* soil toxicity ($1/EC_{50,\ soil}$, Microtox® mBSPT) (Domínguez, Ventura et al. 2023, **ART. 1**).

Table 7.5. Pearson and Spearman correlation coefficients obtained between EC_{50} and COCs concentration (Domínguez, Ventura et al. 2023, **ART. 1**).

	Soil		**Soil elutriates**		**Soil organic extracts**	
Coefficient:	Pearson	Spearman	Pearson	Spearman	Pearson	Spearman
TS	0.98	1.00	1.00	0.97	0.78	0.87
SS-C	0.63	0.80	1.00	1.00	0.88	1.00
SS-F	0.63	0.80	0.85	1.00	0.98	1.00

The Pearson coefficient obtained for TS soils and elutriates was higher than those corresponding to SS-C and SS-F. Since topsoil presents a lower COCs concentration than subsoil, the contaminants solubility limit was not reached; therefore, the points were in the range of linear dependence, which is not the case for subsoil. Spearman coefficient values were close to +1.00 in all cases, confirming a positive association between the toxicity of the samples and the concentration of the pollutant. Thus, considering the statistical analysis, the discussion of previous results obtained can be corroborated.

Therefore, it can be concluded that the three methods used reveal interesting and complementary information. The measurement of soil toxicity provides information on the contaminants present in the soil and the intrinsic toxicity of the soil, so it should be carried out in each case study (different soil characteristics). The measurement of soil elutriates

toxicity provides information about the acute toxicity of the solubilized pollutants in leachates or groundwaters, and it is of particular relevance when there are superficial waters in the vicinity of the contaminated site. Finally, measuring the acute toxicity of the organic extracts adds valuable information in the case of having hydrophobic compounds as soil pollutants, such as HCHs. Therefore, all three measures are necessary to achieve a complete overview of the acute toxicity of contaminated soils.

7.2. Topsoil (TS) oxidation treatments

On-site remediation of **topsoil** has been evaluated by different **chemical oxidation treatments**, using hydrogen peroxide and persulfate as oxidants.

Firstly, the stoichiometric concentration of oxidant (Ox_{stc}) required for the mineralization of pollutants (HCHs) is calculated considering: i) the moles of the main radical generated per mol of oxidant, ii) the stoichiometry of HCHs mineralization by the generated radicals, iii) the aqueous to solid phase ratio used (V_L/W_S) where V_L is the volume of the aqueous phase and W_S the mass of soil used, and iv) the initial HCHs concentration in the soil.

In the case of the **Fenton process**, 1 mol of H_2O_2 gives 1 mol of OH• and 1 mol of •OOH (Eqs. (4.1) and (4.2), Subsection 4.2), both considered active in the oxidation of HCHs (Eq. (7.1)).

$$Fe^{2+} + H_2O_2 \rightarrow Fe^{3+} + OH^{\cdot} + OH^{-} \quad (4.1)$$

$$Fe^{3+} + H_2O_2 \rightarrow Fe^{2+} + OOH^{\cdot} + H^{+} \quad (4.2)$$

$$C_6H_6Cl_6 + 12\,H_2O_2 \xrightarrow{Fe} 6\,CO_2 + 12\,H_2O + 6\,HCl \quad (7.1)$$

In the thermal activation of PS (**PS/T**), 1 mol of PS gives 2 mol of sulfate radicals (Eq. (4.3), Subsection 4.2), whereas, in the alkaline activation of PS (**PS/NaOH**), 2 mol of this oxidant gives 1 mol of OH• (Eqs. (4.4) and (4.5), Subsection 4.2).

$$S_2O_8^{2-} \xrightarrow{heat} 2\,SO_4^{\cdot -} \quad (4.3)$$

$$2\,S_2O_8^{2-} + 2\,H_2O \xrightarrow{OH^-} 3\,SO_4^{2-} + SO_4^{\cdot -} + O_2^{\cdot -} + 4\,H^{+} \quad (4.4)$$

$$SO_4^{\cdot -} + OH^{-} \rightarrow SO_4^{2-} + {\cdot}OH \quad (4.5)$$

The stoichiometry considered for the HCHs mineralization in the PS/T and PS/NaOH systems by the generated sulfate and hydroxyl radicals is shown in Eqs. (7.2) and (7.3), respectively.

$$C_6H_6Cl_6 + 24\ SO_4^{\cdot-} + 12H_2O \rightarrow 6\ CO_2 + 24\ SO_4H^- + 6\ HCl \quad (7.2)$$

$$C_6H_6Cl_6 + 24\ OH^{\cdot} \rightarrow 6\ CO_2 + 12\ H_2O + 6\ HCl \quad (7.3)$$

The efficiency of the remediation treatments has been evaluated considering the conversion of the different species involved in the reactions (pollutants and oxidant) (X_i), defined in Eq. (7.4). It has been determined considering the initial concentration ($C_{i,0}$) and that corresponding to the different reaction times (C_i).

$$X_i(\%) = \left(1 - \frac{C_i}{C_{i,0}}\right) \cdot 100 \quad (7.4)$$

The HCHs oxidation could generate dechlorinated compounds and eventually carbon dioxide, water, and chlorides. The dechlorination degree ($Cl^-/Cl_{HCH,soil0}$,%)) has been calculated as the ratio of chloride concentration in the liquid phase (Cl^-, mg L^{-1}) to the value expected if the initial concentration of HCHs in the soil phase were fully dechlorinated ($Cl_{HCH,soil0}$, mg kg^{-1}), as described in Eq. (7.5). Additionally, the chlorine balance (%) has been determined by Eq. (7.6). The aqueous phase/soil ratio used (V_L/W_S) has been considered for calculating the dechlorination degree and the chlorine balance. Finally, the efficiency of PS at the different experimental conditions tested ($PS_{efficiency}$) has been calculated by Eq. (7.7).

$$\text{Dechlorination degree}(\%) = \left(\frac{Cl^-(\text{mg L}^{-1})}{Cl_{HCHs,soil,0}(\text{mg kg}^{-1})} \cdot \frac{V_L\,(L)}{W_S\,(kg)}\right) \cdot 100 \quad (7.5)$$

$$\text{Chlorine balance}\ (\%) = \frac{(Cl^-(\text{mg L}^{-1}) + Cl_{COCs,aqueous}(\text{mg L}^{-1})) \cdot \frac{V_L(L)}{W_S\,(kg)} + Cl_{COCs,soil}(\text{mg kg}^{-1})}{Cl_{HCHs,soil,0}\ (\text{mg kg}^{-1})} \quad (7.6)$$

$$PS_{efficiency} = \frac{\text{COCs removed (mg)}}{\text{PS consumed (g)}} \quad (7.7)$$

7.2.1. Oxidant evaluation: HP and PS

The on-site application of different oxidants (**hydrogen peroxide** (HP/Fe, Fenton process) and **persulfate** (PS)) to the remediation of HCHs-polluted TS has been evaluated. The experimental conditions of the different oxidants tested are listed in Table 7.6**.** This table includes the run number, the type of oxidant and its concentration, the catalyst concentration (when appropriate), and the ratio between the oxidant concentration employed and the stoichiometric concentration theoretically required for the HCHs mineralization (Ox/Ox_{stc}).

Table 7.6. Operational conditions of the remediation experiments for the oxidant evaluation (Soil sample: $C_{HCHs,0}$ = 155 mg kg^{-1} (TS L2), W_S = 10 g, V_L/W_S = 2, T = 20 ºC).

Run	Oxidant	$C_{oxidant}$ (g L^{-1})	C_{Fe} (g L^{-1})	Ox/Ox_{stc}
O1	HP (Fenton)	12	0.5	110
O2		200	0.5	1800
O3	PS	40	-	26

7.2.1.1. Hydrogen peroxide (HP/Fe, Fenton process)

The conversion of hydrogen peroxide and the remaining concentration of iron with reaction time in Fenton experiments is depicted in Figure 7.9.

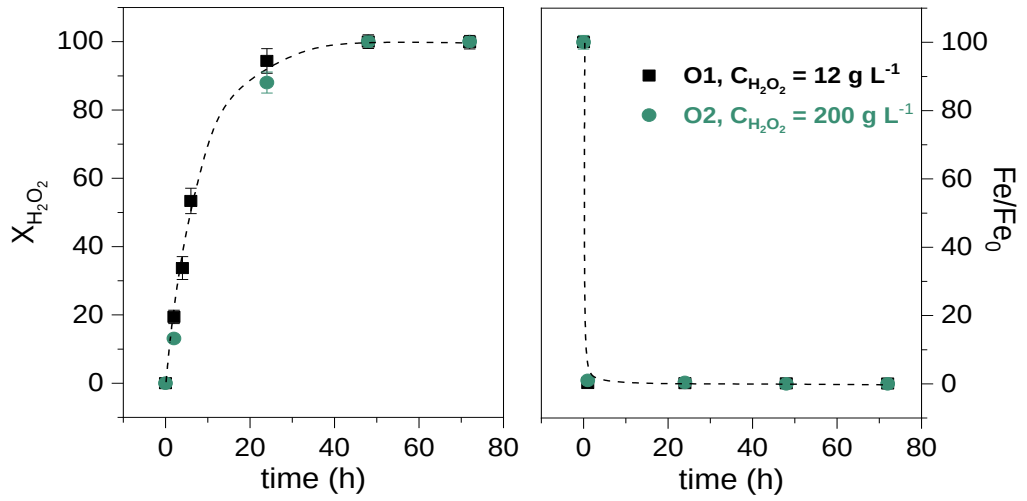

Figure 7.9. Hydrogen peroxide conversion and remaining iron in solution with reaction time in Fenton experiments (O1 and O2, Table 7.6). Experimental conditions: V_L/W_S = 2, 20 ºC, $C_{HCHs,0}$ = 155 mg kg^{-1} (TS L2), pH ≈ 7, C_{Fe} = 0.5 g L^{-1} (Dominguez, Romero et al. 2021, **ART. 2**).

As can be seen, hydrogen peroxide decomposition was too fast, regardless of the initial concentration of this reagent (12 and 200 g L^{-1}). The conversion of the oxidant was almost complete at 24 h reaction time, which can be related to its unproductive decomposition in the presence of soil, generating water and oxygen, as often noticed in the literature (Baciocchi, Boni et al. 2004, Romero, Santos et al. 2009). The use of stabilizers such as phosphate would be needed to minimize this unproductive reaction and increase the stability of hydrogen peroxide (Baciocchi, Boni et al. 2003, Baciocchi, Boni et al. 2004, Vicente, Rosas et al. 2011).

The high consumption of H_2O_2 was not associated with a substantial degradation of the pollutants attending to the results shown in Figure 7.10, where the conversion of α-HCH, β-HCH, and total HCHs in the solid is represented. When using an oxidant concentration of 12 g L^{-1}, a negligible removal of the contaminants (≈2%) was obtained. Working with a significantly higher concentration of H_2O_2 (200 g L^{-1}), the conversion of COCs increased but not enough (40% of total COCs removal at 100% conversion of the oxidant). These discouraging results are in accordance with those previously reported in the literature (Usman, Tascone et al. 2014).

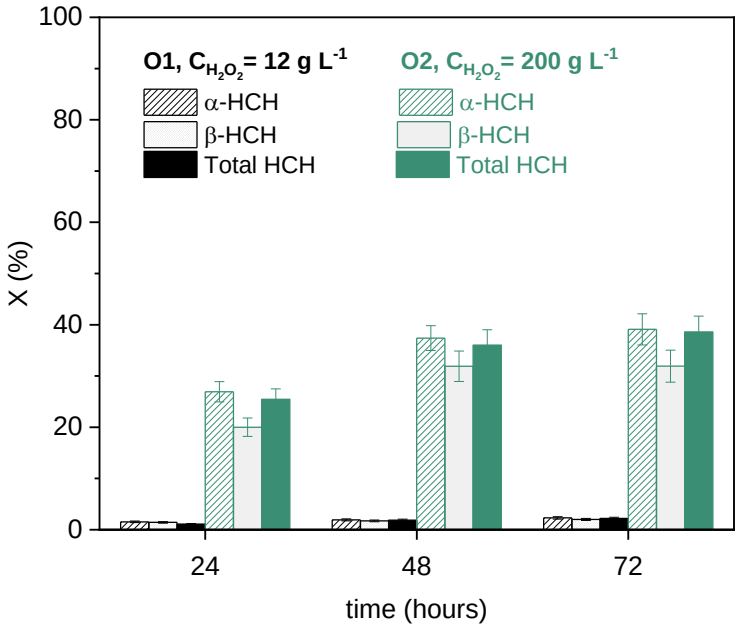

Figure 7.10. COCs conversion in the soil phase at different reaction times in Fenton experiments (O1 and O2, Table 7.6). Experimental conditions: V_L/W_S = 2, 20 ºC, $C_{HCHs,0}$ = 155 mg kg^{-1} (TS L2), pH ≈ 7, C_{Fe} = 0.5 g L^{-1} (Dominguez, Romero et al. 2021, **ART. 2**).

To confirm the high unproductive consumption of H_2O_2, the Natural Oxidant Demand (NOD) of the soil for this oxidant was evaluated. For that purpose, a 48h-experiment mixing unpolluted soil from the landfill (TS L0) with 200 g L^{-1} of the oxidant (same ratio V_L/W_S as that used in remediation experiments and ambient temperature) was carried out. The resulting NOD was > 400 g of H_2O_2 per kg of soil due to the high concentration of carbonates. This extremely high value corroborates the inadequacy of using hydrogen peroxide to remediate soils with these characteristics (high carbonate content, buffer capacity, pH = 7.4, Table 7.1).

On the other side, a dramatic decrease in the iron concentration in the solution was noticed from the beginning of the reaction (Figure 7.9). After 2 hours of reaction time, only 1% of the iron initially added remained in solution in both experiments (O1 and O2). The precipitation of this metal is associated with the neutral pH of the solution (Gayer and Woontner 1956). This parameter (pH) remained in values around 7 throughout the reaction because of the high concentration of carbonates in the soil (> 40%, Table 7.1), which act as a buffer. Thus, in the form of $Fe(OH)_3$, the catalyst is removed from the reaction medium at these conditions. Maintaining iron in solution is necessary for the generation of radical species from hydrogen peroxide and the sequential oxidation of the pollutants. It could be achieved: i) lowering the pH of the solution by the addition of acid species (discarded due to the high $CaCO_3$ content) or ii) using chelating agents (Checa-Fernández, Santos et al. 2021). In this way, iron could remain in the solution at near-neutral pH conditions. However, it should be noted that the chelating agents are usually organic compounds that compete with the pollutant for the oxidant (Pardo, Rosas et al. 2014). In this context, sodium citrate (10 mM) was used as a chelating agent, but a negligible amount of iron was available (< 2 mg L^{-1} after 24 h) due to the citrate oxidation, discarding its use. Considering the results obtained, applying the Fenton process for the remediation of these soils requires further research to find a feasible chelating agent to keep the iron in solution at neutral pH and a hydrogen peroxide stabilizer.

7.2.1.2. Persulfate (PS)

The use of persulfate (PS) as oxidant has been evaluated. Firstly, the NOD of the soil for PS (following the same procedure used in the case of H_2O_2) was measured. A low oxidant concentration (2 g L^{-1}) was used in this case to obtain more reliable results. In the first hours of the experiment, the concentration of PS slightly decreased (associated with organic matter in the soil) until reaching an asymptotic value (data not shown). The resulting NOD of the soil was 0.8 g of PS per kg of soil. This value is relatively low (especially considering the obtained for H_2O_2, 400 g kg^{-1}), and therefore, the unproductive contribution to the oxidant consumption has been neglected at the conditions applied. The evolution of total HCHs and PS conversion with reaction time is depicted in Figure 7.11. It has been reported that PS can be applied for the degradation of other pollutants in soil slurries at room conditions (Wang, Deng et al. 2014). However, the results indicate that, at circumneutral pH, PS is not active for the oxidation of HCH isomers in soils (Figure 7.11, O3, 20 °C). The consumption of PS in this experiment was significantly low (< 5% after 25 days of treatment). The pH of the aqueous phase remained at circumneutral values due to the presence of the soil, which acts as a buffer. This fact could explain the higher stability noticed for PS.

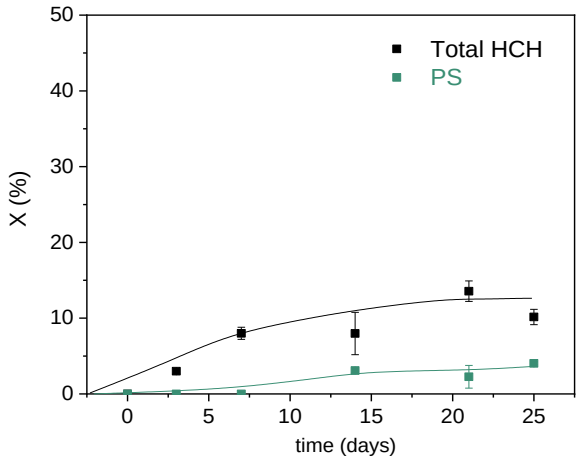

Figure 7.11. Conversion of HCHs in the soil phase and PS in the aqueous phase with reaction time in run O3 (Table 7.6). Experimental conditions: V_L/W_S = 2, $C_{HCHs,0}$ = 155 mg kg^{-1} (TS L2), C_{PS} = 40 g L^{-1}, 20 °C, circumneutral pH (Dominguez, Romero et al. 2021, **ART. 2**).

PS has been selected for remediating HCHs polluted soils due to its higher stability (*vs.* HP) at these conditions (soils with high carbonate content). Different PS activation methods have been evaluated to increase the efficiency of this oxidant in COCs degradation.

7.2.2. PS activation evaluation: NaOH and T

This section evaluates the activation of PS by **alkali** (PS/NaOH at 20 °C, A1) and **temperature** (PS/T at 40 °C, A2). The effect of temperature and PS concentration (without alkali addition) has been further evaluated for the PS/T treatment. The experimental conditions of these runs are listed in Table 7.7. This table contains the run number (A1-A9), the concentration of HCHs in the soil (TS L2), the objectives studied, the initial oxidant (C_{PS}) and activator (C_{NaOH}) concentrations, the temperature applied, and the ratio between the oxidant concentration employed to the stoichiometric concentration theoretically required for the HCHs mineralization (Ox/Ox_{stc}). The variable studied in each series of experiments has been highlighted in bold type. A soil contaminated with 155 mg kg^{-1} of HCHs was used to evaluate the PS activator (A1 and A2). A soil contaminated with 358 mg kg^{-1} of HCHs was used for the experiments to assess the effect of temperature and oxidant concentration in the PS/T treatment (runs A3-A9). The influence of temperature on HCH removal was studied from 35 to 55 °C (A3-A5), using an initial concentration of PS = 40 g L^{-1}. In contrast, initial concentrations of PS from 10 to 80 g L^{-1} were tested (A6-A9) at 55 °C. These temperatures are generally within the range typically used for thermally activated PS treatment of soil contaminants, varying from ambient temperature to 80 °C (Chen, Murugananthan et al. 2016, Liu, Wang et al. 2019).

Table 7.7. Operational conditions of the oxidation runs for the activator evaluation (TS L2, W_S = 10 g, V_L/W_S = 2, molar NaOH:PS = 2 where applicable).

Run	C_{HCHs} (mg kg^{-1})	Main objective	Treatment studied	C_{PS} (g L^{-1})	C_{NaOH} (g L^{-1})	T (°C)	Ox/Ox_{stc}
A1	155	**Activator evaluation**	**PS/NaOH**	40	**13.5**	20	6.6
A2			**PS/T**	40	-	**40**	26
A3	358	**Temperature effect**	**PS/T**	40	-	**35**	20
A4			**PS/T**	40	-	**45**	20
A5			**PS/T**	40	-	**55**	20
A6		**PS concentration effect**	**PS/T**	**10**	-	55	5
A7			**PS/T**	**20**	-	55	10
A5			**PS/T**	**40**	-	55	20
A8			**PS/T**	**60**	-	55	30
A9			**PS/T**	**80**	-	55	40

Additionally, control experiments without oxidant were performed at the three temperatures tested (35, 45, and 55 °C) to evaluate the possible loss of pollutants by volatilization (blanks B1-B3). The consumption of PS by thermal effect was assessed at

the three temperatures studied in the absence of soil (B4-B6) and in the presence of unpolluted soil (TS L0) (B7-B9). The experimental conditions of blank runs are summarized in Table 7.8. This table contains the variables studied, the type of soil used (polluted (TS L2)/unpolluted (TS L0)), the oxidant concentration, and the reaction temperature.

In the experiments using NaOH as PS activator (run A1, Table 7.7), the pH of the aqueous phase remained above 12 during the time studied (25 days). It has been reported that, at these pH values, HCHs, both in the aqueous (Santos, Fernandez et al. 2018) and soil phases (Lorenzo, García-Cervilla et al. 2020) were dehydrochlorinated to trichlorobenzenes (TCBs). As expected, the TCBs identified during the alkaline activation of PS experiments in this work were 1,2,4-TCB and 1,2,3-TCB, with a distribution of 85% and 15%, respectively, in accordance with that previously reported (Santos, Fernandez et al. 2018, Lorenzo, García-Cervilla et al. 2020). The hydrolysis reaction of α-HCH and β-HCH at pH > 12 and the TCBs distribution obtained, has been summarized in Figure 7.12.

Table 7.8. Operating conditions of the blank experiments. TS L2 = polluted soil ($C_{HCHs,0}$ = 358 mg kg^{-1}), TS L0 = unpolluted soil (Dominguez, Checa-Fernandez et al. 2021, **ART. 3**).

Objective	Experiment	Soil	C_{PS} (g L^{-1})	T (°C)
COCs volatilization	B1	**TS L2**	-	35
	B2	**TS L2**	-	45
	B3	**TS L2**	-	55
Unproductive PS consumption in the absence of soil	B4	**-**	40	35
	B5	**-**	40	45
	B6	**-**	40	55
Unproductive PS consumption with unpolluted soil	B7	**TS L0**	40	35
	B8	**TS L0**	40	45
	B9	**TS L0**	40	55

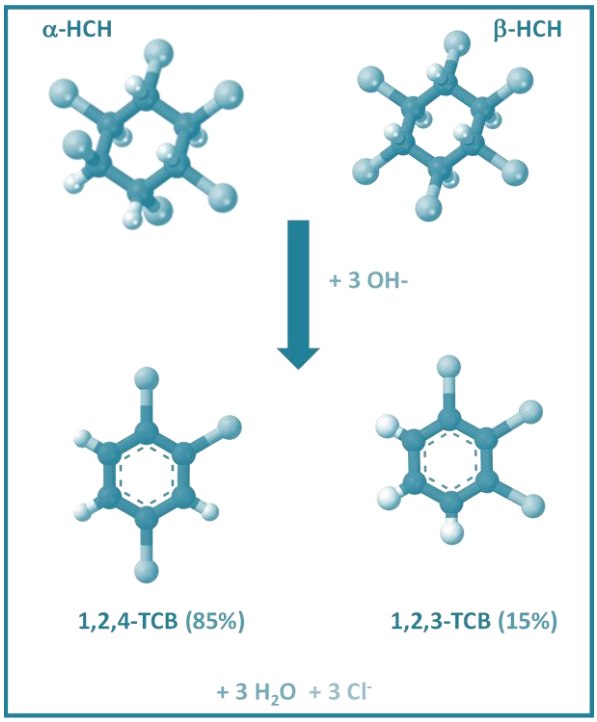

Figure 7.12. Distribution of TCB isomers in the hydrolysis of α-HCH and β-HCH at pH ≥ 12 (Dominguez, Romero et al. 2021, **ART. 2**).

Therefore, when evaluating the elimination of HCHs using the alkaline activation of PS it should be considered that TBCs are generated from HCHs hydrolysis and not from HCHs oxidation. The concentration of TCBs has been converted into the corresponding equivalent concentration of HCHs following Eq. (7.8) and named C'_{TCBs} .

$$C'_{TCBs}\left(\frac{\text{mg HCH}}{\text{kg soil}}\right) = C_{TCBs}\left(\frac{\text{mg TCBs}}{\text{kg soil}}\right) \cdot \frac{291}{181}\left(\frac{\text{mg HCH}}{\text{mg TCB}}\right) \quad (7.8)$$

Additionally, the sum of chlorinated organic compounds (COCs), expressed as mg HCH kg_{soil}^{-1}, has been calculated by Eq. (7.9).

$$C_{COCs}\left(\frac{\text{mg HCH}}{\text{kg}_{\text{soil}}}\right) = C_{\alpha-HCH} + C_{\beta-HCH} + C'_{TCBs} \quad (7.9)$$

The evolution of the sum of HCHs and TCBs (COCs in this case) with reaction time allows estimating the removal of COCs by oxidation and not because of alkaline hydrolysis transformations. Thus, the conversion of initial HCHs (X_{COCs}) can be defined as follows (Eq. (7.10)):

$$X_{COCs} = \frac{C_{\alpha\ HCH} + C_{\beta\ HCH} + C'_{TCBs}}{C_{HCH_o}} \quad (7.10)$$

The conversion of α-HCH, β-HCH, and COCs and the fraction C'_{TCBs}/C_{HCHo} (fraction of HCHs hydrolyzed to TCBs and not oxidized) with reaction time obtained when applying NaOH and temperature activation of PS are shown in Figure 7.13. The value of C'_{TCBs}/C_{HCHo} at zero reaction time at alkaline conditions has been theoretically calculated, assuming complete and null dehydrochlorination of α-HCH and β-HCH, respectively. As seen in Figure 7.13-a, an almost complete conversion of α-HCH was achieved from the beginning of the reaction at alkaline conditions (A1). However, in the case of thermal activation, only 52% of α-HCH conversion was found at 25 days. In the case of β-HCH, a 68% and 32% conversion was reached at the final reaction time when applying alkaline and thermal activation, respectively.

However, as stated above, the conversion of HCHs at alkaline conditions cannot be only attributable to oxidation reactions, and the HCHs hydrolysis to TCBs should be considered. The fast-initial drop in α-HCH concentration shown in Figure 7.13 corresponds to a quick increase in the concentration of TCBs', meaning that α-HCH is rapidly hydrolyzed at alkaline conditions. This finding was already reported when treating a subsoil highly polluted with residual DNAPL (> 9000 mg COCs kg_{soil}^{-1}) with PS activated by alkali (pH > 12) (García-Cervilla, Santos et al. 2020, Lorenzo, García-Cervilla et al. 2020). In that soil, α-HCH, γ-HCH, δ-HCH, and ε-HCH were initially present (among other COCs such as chlorobenzenes) and completely hydrolyzed to TCBs at 24-48 h of treatment time at alkaline conditions. The concentration of β-HCH was negligible in the DNAPL and, therefore, in the subsoil, so the hydrolysis rate of this compound was unknown. Therefore, this is the first work in which the alkaline hydrolysis of the β-HCH is studied. The significantly lower conversion of β-HCH (Figure 7.13) could be related to the lower alkaline hydrolysis rate of the β isomer.

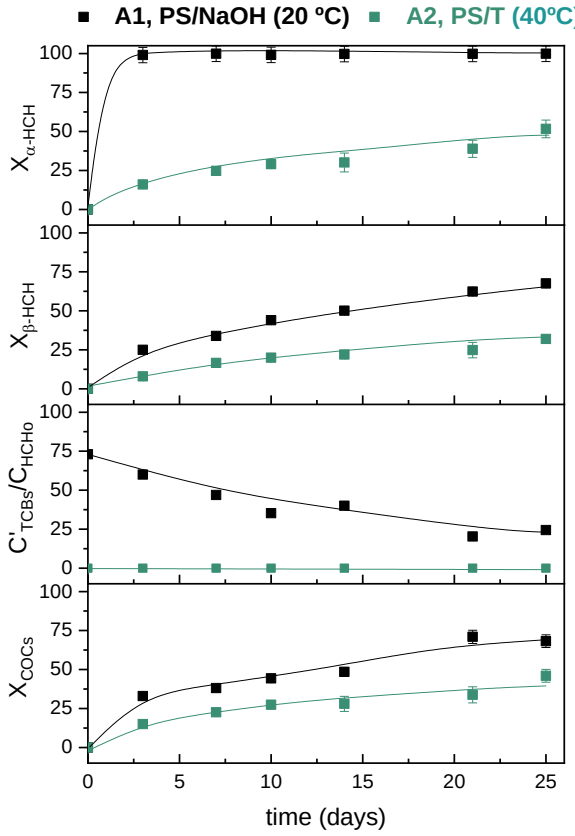

Figure 7.13. Conversion of α-HCH, β-HCH, and COCs and fraction of $C'_{TCBs}/C_{HCHs,0}$ in the soil phase with reaction time in runs A1 and A2 (Table 7.7). Experimental conditions: V_L/W_S = 2, C_{HCHs} = 155 mg kg^{-1} (TS L2), C_{PS} = 40 g L^{-1} (Dominguez, Romero et al. 2021, **ART. 2**).

TCBs generated from HCH hydrolysis are further oxidized by hydroxyl radicals (the predominant radical species when the pH is above 12 (Eqs. (4.4) and (4.5), Subsection 4.2). TCBs concentration progressively decreases with reaction time (Figure 7.13). No other chlorinated or aromatic compounds were detected in the reaction medium. Considering the evolution of α-HCH, β-HCH, and TCBs (Figure 7.13), the following reaction mechanism for the oxidation of HCHs at pH ≥ 12 has been proposed (Eqs. (7.11)-(7.13)):

$$r_1 \text{ (fast)} \quad \alpha - \text{HCH} \xrightarrow{3OH^-} \text{TCB} + 3\ Cl^- + 3\ H_2O \tag{7.11}$$

$$r_2 \text{ (slow)} \quad \beta - \text{HCH} \xrightarrow{3OH^-} \text{TCB} + 3\ Cl^- + 3\ H_2O \tag{7.12}$$

$$r_3 \quad \text{TCB} \xrightarrow{OH\cdot,\ O_2^{-}\cdot} \text{Oxidized Products} \tag{7.13}$$

The reaction rate of α-HCH alkaline hydrolysis (Eq. (7.11)) is notably higher than that of β-HCH (Eq. (7.12)). Thus, the lower alkaline hydrolysis of the β isomer is considered the

limiting step. The solubility of TCBs (generated from HCH hydrolysis, mainly 1,2,4-TCB) in water is significantly higher than HCH isomers solubility (Lorenzo, García-Cervilla et al. 2020, García-Cervilla, Santos et al. 2022). Moreover, TCBs are more susceptible to the attack by hydroxyl radicals (those predominant in the alkaline activation of PS) than HCHs. Hydroxyl radicals favour the attack of the aromatic ring by abstraction of one hydrogen from hexachlorocyclohexane isomers (Haag and Yao 1992, Dominguez, Romero et al. 2019). Taking into account the reaction constants of the pollutants with $OH^{\bullet}$ ($k_{HCH,\ OH\cdot}$ = 7.5 × 10^{8} $M^{-1}s^{-1}$ (Haag and Yao 1992) and $k_{TCB,\ OH\cdot}$ = 6.1 × 10^{9} $M^{-1}s^{-1}$ (Mandal 2018)), it can be stated that HCHs are 10 times less susceptible to be attacked by $OH^{\bullet}$ than TCBs. Therefore, the oxidation of TCBs by $OH^{\bullet}$ can be considered the main degradation route *vs.* the direct oxidation of the remaining β-HCH.

To evaluate the efficiency of the oxidation treatment when alkaline conditions are used, the conversion of total COCs (Eq. (7.10)) is more reliable than HCHs conversion. Attending to this parameter (Figure 7.13), the alkaline activation of PS (A1) leads to better results than the temperature activation of this oxidant (A2) at circumneutral pH. The conversion of COCs gradually increases with reaction time, achieving a degradation of COCs around 68% and 46% after 25 days of treatment when applying alkaline (20 ºC) and thermal (40 ºC) PS activations, respectively.

On the other side, the conversion of activated PS was slightly higher than without activation (Figure 7.14), but its consumption was still relatively low. At the conditions used, around 70% of the initial PS remained in solution at the end of the treatment (25 days). Therefore, the liquid phase could be reused to treat a new batch of contaminated soil.

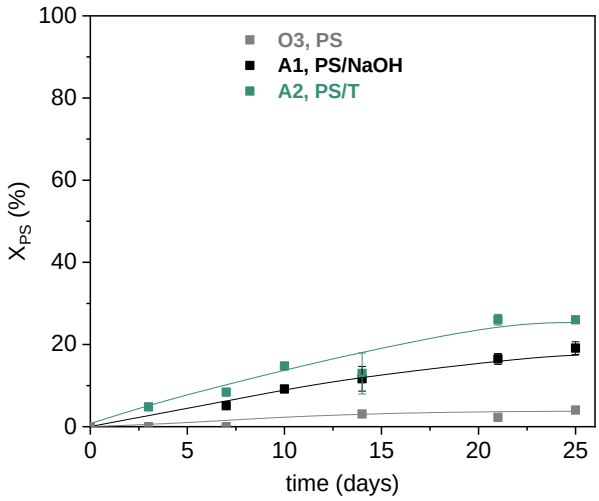

Figure 7.14. Conversion of PS in the aqueous phase with reaction time in runs O3 (PS without activator) A1 (PS/NaOH) and A2 (PS/T) (Table 7.6 and Table 7.7). Experimental conditions: V_L/W_S = 2, $C_{HCHs,0}$ = 155 mg kg^{-1} (TS L2), C_{PS} = 40 g L^{-1} (Dominguez, Romero et al. 2021, **ART. 2**).

The **temperature and PS concentration effect** has been further evaluated for the **PS/T treatment** (runs A3-A9, Table 7.7) without alkali addition. The reaction temperature is the main variable controlling the thermal activation of PS. This parameter was evaluated from 35 to 55 °C, maintaining the remaining operating conditions unaltered (PS = 40 g L^{-1}, V_L/W_s = 2/1, 100 rpm). Volatilization of HCHs at these temperatures was discarded after 25 days (B1-B3, Table 7.8). At the highest temperature tested (55 °C), the decrease in the concentration of HCHs was below 5% in all cases, which shows the low volatility of these pollutants.

The conversion of α-HCH and β-HCH with reaction time at the three temperatures tested is depicted in Figure 7.15, whereas the conversion of the other HCH isomers (γ-HCH, δ-HCH, and ε-HCH) is shown in Figure 7.16. As can be seen, the abatement of hexachlorocyclohexanes is highly favoured by temperature regardless of the isomer. This variable has a crucial role in the remediation process, which agrees with the results reported concerning other organic pollutants in soil systems, such as ibuprofen (Liu, Wang et al. 2019) or p-nitrophenol (Chen, Murugananthan et al. 2016).

It is worth noting a stagnation in the degradation of β-HCH from a conversion value of around 70% in the reaction at 55 °C (A5, Figure 7.15). This may be related to the dual nature of the topsoil contamination. The fraction of β-HCH corresponding to particulate matter degrades faster than that corresponding to β-HCH adsorbed on the soil. It should

be considered that β-HCH is the most recalcitrant isomer to oxidation due to the lack of axial chlorides (that are more susceptible to hydroxylation) (Wacławek, Silvestri et al. 2019).

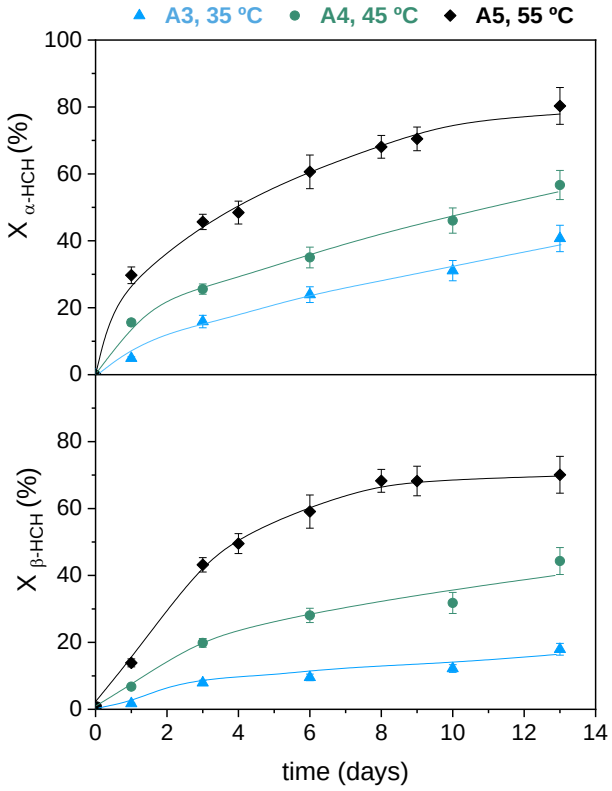

Figure 7.15. Conversion profiles of α-HCH and β-HCH with reaction time at the three temperatures tested. Operating conditions: $C_{HCHs,0}$ = 358 mg kg^{-1} (TS L2), C_{PS} = 40 g L^{-1}, V_L/W_S = 2, 100 rpm, pH_0 = 7 (A3-A5) (Dominguez, Checa-Fernandez et al. 2021, **ART. 3**).

An increase in the reaction temperature accelerates the decomposition of PS and, therefore, the production rate of sulfate radicals (Eq. (4.3), Subsection 4.2), increasing the oxidation of the pollutants. The pollutants desorption from the soil phase is also favoured when the temperature increases, especially in the case of hydrophobic organic contaminants (Peng, Deng et al. 2015). In this way, the degradation of HCHs was significantly favoured by raising the reaction temperature from 35 to 55 ºC. At 35 ºC, conversions below 40 and 20% were achieved for α-HCH and β-HCH at 12 days (Figure 7.15), respectively, and between 55 and 82% for the other isomers (Figure 7.16). On the other hand, conversions around 80 and 70% were obtained for α-HCH and β-HCH, respectively, and around 95% for the isomers present in low concentrations when using a reaction temperature of 55 ºC.

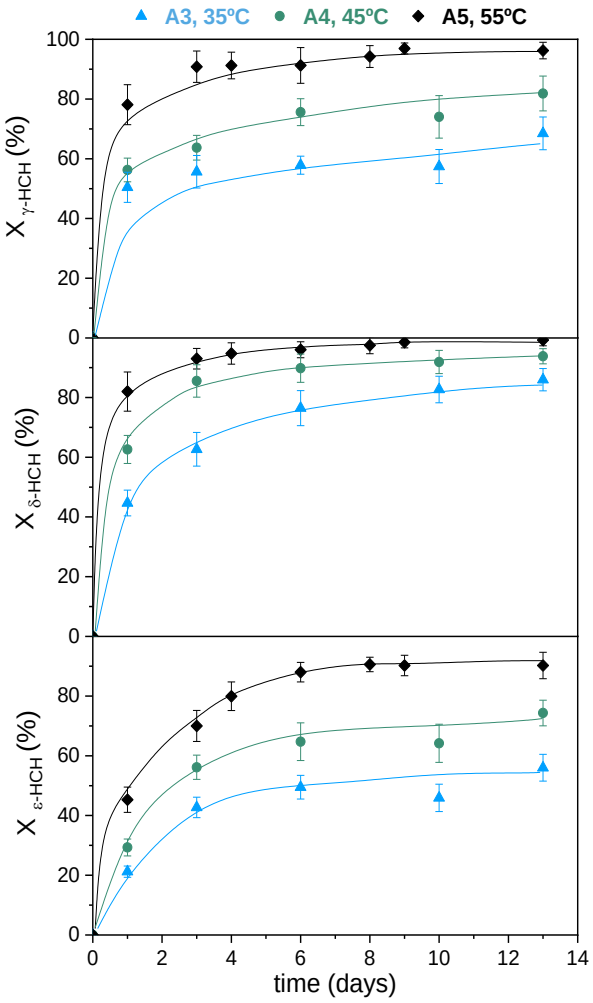

Figure 7.16. Conversion profiles of γ-HCH, δ-HCH, and ε-HCH with reaction time at the three temperatures tested. Operating conditions: $C_{HCHs,0}$ = 358 mg kg^{-1} (TS L2), C_{PS} = 40 g L^{-1}, V_L/W_S = 2, 100 rpm, pH_0 = 7 (A3-A5) (Dominguez, Checa-Fernandez et al. 2021, **ART. 3**).

Comparing the results obtained for the remediation of HCHs-polluted soil with those corresponding to the treatment of groundwater contaminated with chlorinated organic compounds (including HCHs) by oxidation with thermally activated PS (Dominguez, Romero et al. 2020), the following conclusions can be drawn: i) higher temperatures and reaction times are required for soil remediation since the abatement of soil pollutants is limited by their solubilization to the aqueous phase and the soil inhibitory effect, which hinders the diffusion of sulfate radicals (Chen, Murugananthan et al. 2016, Dominguez, Romero et al. 2021, **ART. 2**). ii) In the case of the groundwater, working at reaction temperatures above 40 °C was not recommended (it did not lead to higher pollutant removal rates and implied an excessive oxidant consumption). However, in the case of the

soil, the treatment efficiency highly increases with temperature in the temperature range studied (up to 55 °C).

Considering the conversion of the different isomers as a function of temperature, the following degradation trend has been found: β-HCH < α-HCH < ε-HCH < γ-HCH < δ-HCH, in agreement with that found in the literature (Dominguez, Parchao et al. 2016). The reactivity order of HCHs is related to the chlorine position on the cyclohexane ring, axial or equatorial chlorines (Wacławek, Silvestri et al. 2019). On the other hand, the pollutant mass removal is limited by its solubilization, being the solubility of β-HCH much lower than α-HCH (0.15-0.7 mg L^{-1} for β-HCH and 1.2-2 mg L^{-1} for α-HCH (Lorenzo, García-Cervilla et al. 2020)). Therefore, the higher the pollutant solubility, the higher the pollutant oxidation in the aqueous phase. Consequently, shorter reaction times are required to abate α-HCH than β-HCH, although the differences between them decrease as the temperature increases. Therefore, relatively high temperatures (55 ºC) are recommended for remediating soils contaminated with β -HCH when thermal activation of PS is selected.

The HCHs conversion and the dechlorination degree with reaction time at the three temperatures tested have been represented in Figure 7.17. The percentage of chlorides identified (chlorine balance, Eq. (7.6)) has also been included. If HCHs oxidation does not yield chlorinated byproducts, HCHs conversion, and dechlorination degree with reaction time will coincide. Differences between these values would indicate that chlorinated organic byproducts are formed. Therefore, the chlorine balance (Eq. (7.6)) provides valuable information to determine the process efficiency.

As stated above, the conversion of HCHs highly increases with temperature. The dechlorination of these compounds follows the same trend. Figure 7.17 shows significant differences between the HCHs conversion and the HCHs dechlorination achieved at 35 ºC, meaning that intermediate chlorinated compounds are generated. An important part of these intermediate compounds (potentially toxic compounds) could not be identified, leading to a considerable mismatch in the chlorine balance (< 70% at the end of the reaction time). As the temperature increases (and the reaction progresses), the difference between the evolution of pollutant conversion and dechlorination degree decreases (see Figure 7.17 at 45 and 55 ºC), obtaining quite similar profiles when working at 55 ºC, ensuring that chlorinated byproducts are not produced.

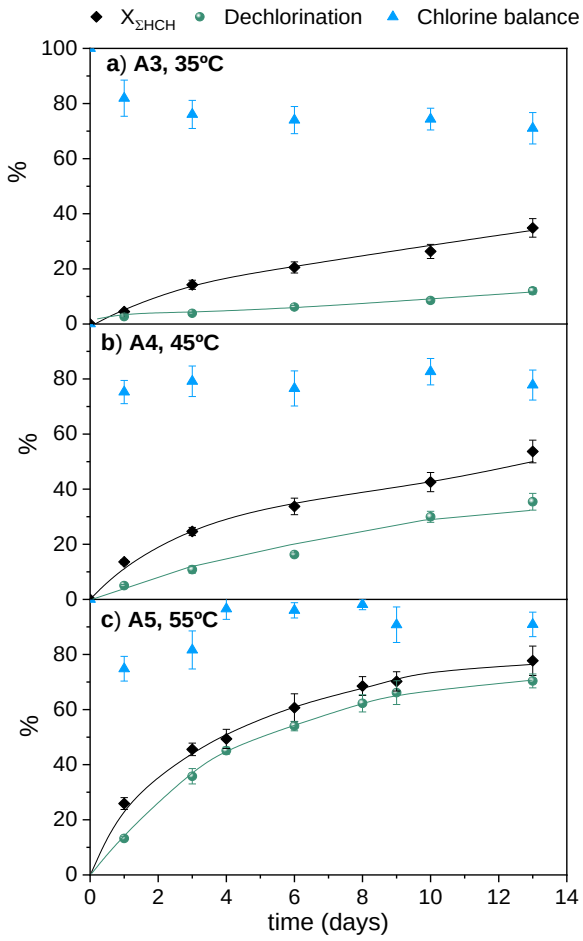

Figure 7.17. Conversion profiles of HCHs, dechlorination degree, and chlorine balance with reaction time at (a) 35 °C, (b) 45 °C, and (c) 55 °C. Operating conditions: $C_{HCHs,0}$ = 358 mg kg^{-1} (TS L2), C_{PS} = 40 g L^{-1}, V_L/W_S = 2, 100 rpm, pH_0 = 7 (A3-A5) (Dominguez, Checa-Fernandez et al. 2021, **ART. 3**).

Sulfate radicals can react with HCHs with HCl elimination to form, in a first step, pentachlorocyclohexene (PCX) (Khan, He et al. 2017, Wacławek, Silvestri et al. 2019, Conte, Legnettino et al. 2023). Traces of this compound (β-PCX) were detected in the reaction system, but it was also initially present in the soil (Figure 7.2). β-PCX rapidly disappeared from the reaction media without a maximum concentration with time. Therefore, the presence of PCX as a byproduct cannot be established. PCX oxidation could yield tetrachlorocyclohexadiene upon subsequent HCl removal (Wacławek, Silvestri et al. 2019, Conte, Legnettino et al. 2023) (no detected in the present work), which would be susceptible to further HCl elimination, resulting in trichlorobenzenes formation (1,2,4-TCB, 1,2,3-TCB and 1,3,5-TCB). These compounds were identified in trace amounts in our experimental system regardless of the temperature tested. On the contrary, in the present

study, 1,2-dichlorobenzene (1,2-DCB) and chlorobenzene (CB) were detected in significant concentrations in the reaction medium. The reaction of radical species with these aromatic compounds continues up to their complete dechlorination (Senthilnathan and Philip 2010, Wacławek, Silvestri et al. 2019), with the corresponding release of chlorides to the liquid phase.

The normalized concentration of the chlorinated byproducts (in mmol) measured (CB, 1,2-DCB) and HCH isomers (ΣHCHs) with reaction time have been depicted at the three temperatures tested (Figure 7.18). An increase in reaction temperature is associated with a faster HCH removal and subsequent faster generation of CB and 1,2-DCB. These compounds are slowly generated and oxidized at 35 ºC. At this temperature, their concentration increases continuously with reaction time (≈0.15 mmol/mmol HCH_0, 13 days), and, therefore, a maximum is not reached in the time interval studied. At 45 ºC, the maximum concentration of these intermediates is measured at 3-6 days of reaction time, and the concentration of these byproducts decreases slowly from this point. However, their oxidation is incomplete at the final time studied (0.17 and 0.05 mmol/mmol HCH_0 of CB and 1,2-DCB, respectively, 13 days). At 55 ºC, these intermediates show a maximum concentration between 4 and 8 days. After the maximum, the disappearing DCB and CB rate is higher than the generation rate. At 14 days, a concentration of these byproducts closed to zero is achieved. The higher oxidation rate of chlorobenzenes than HCHs whit the temperature increase was already reported in the remediation of groundwater contaminated with a mixture of COCs (Dominguez, Romero et al. 2020). It was concluded that the higher the chlorine content of the COC, the more recalcitrant the COC to PS oxidation, being this effect more marked when temperature increases.

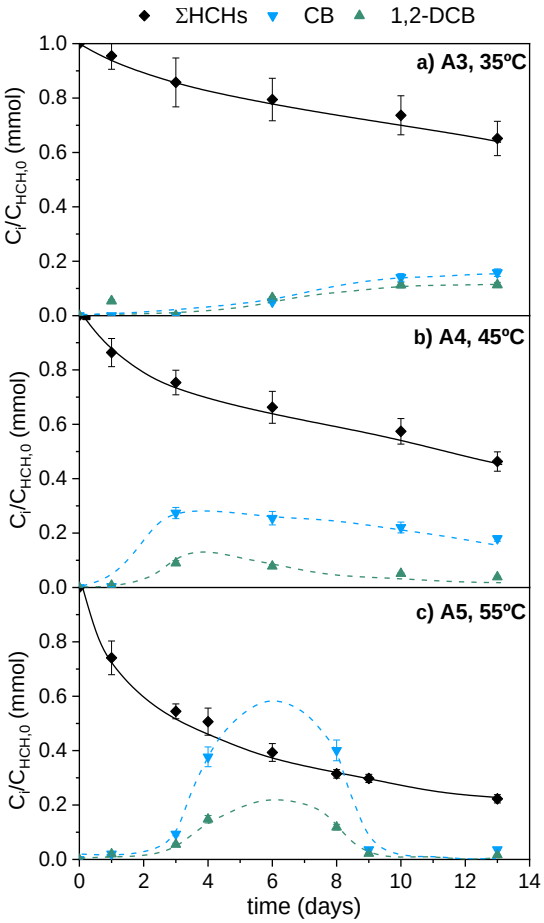

Figure 7.18. Normalized concentration profiles of HCHs and chlorinated intermediate compounds in the soil phase at (a) 35 ºC, (b) 45 ºC, (c) 55 ºC. Operating conditions: $C_{HCHs,0}$ = 358 mg kg^{-1} (TS L2), C_{PS} = 40 g L^{-1}, V_L/W_S = 2, 100 rpm, pH_0 = 7 (A3-A5) (Dominguez, Checa-Fernandez et al. 2021, **ART. 3**).

On the other hand, the lower the temperature, the lower the production and disappearing rates of CB and DCBs, lasting these compounds in the media longer times. Certain volatilization is expected when these byproducts remain in the reaction media due to their relatively high vapour pressure (12 and 1.36 mmHg for CB and DCBs, respectively) (Lorenzo, Santos et al. 2021). The longer the time required to oxidize the byproducts, the higher the loss of CB and DCBs by volatilization and, consequently, the higher the mismatch in the chlorine balance. This could explain the higher mismatch of chlorine found at the lowest temperature tested in Figure 7.17.

These results (Figure 7.17 and Figure 7.18) suggest that the oxidation of HCHs takes place through a series-parallel reaction mechanism, an aspect not previously reported in the bibliography. Two parallel routes could explain the attack of HCHs by sulfate radicals.

The first reaction path is the total dechlorination (or mineralization) of HCHs, without generating chlorinated byproducts (with the consequent release of chlorides to the aqueous phase). The second path is the generation of chlorinated byproducts: CB and DCBs were detected (with the resultant release of chlorides to the aqueous phase). If the reaction temperature is high enough (≥ 55 °C), these intermediates are rapidly generated and oxidized to non-chlorinated compounds, releasing chlorides. Based on these results, the oxidation route for treating HCHs-polluted soil by the thermal activation of PS has been proposed in Figure 7.19.

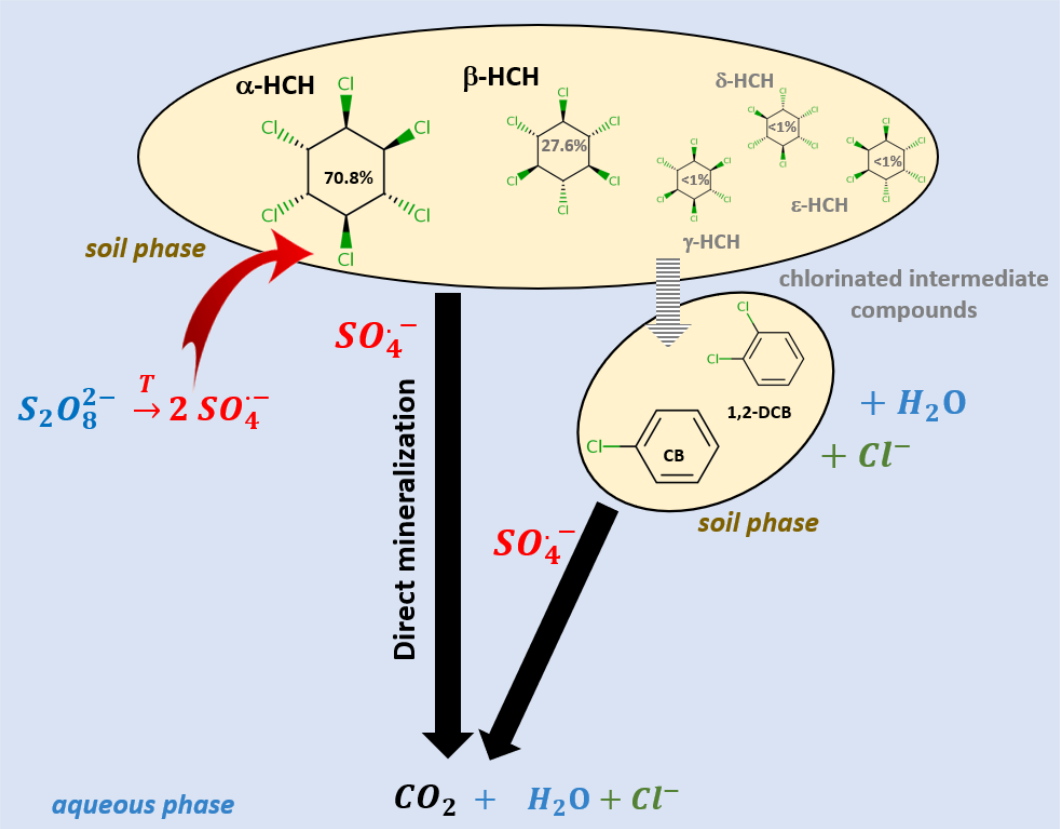

Figure 7.19. Reaction pathway for the oxidation of HCHs-polluted soil by thermal activation of PS (Dominguez, Checa-Fernandez et al. 2021, **ART. 3**).

The oxidation of COCs in the liquid phase should also be considered. However, the concentration of intermediate chlorinated compounds detected in this phase is too low (< 0.5 mg L^{-1}). The following reasons can explain this fact: i) once in solution, they are rapidly oxidized by the action of sulfate radicals and ii) the chlorinated byproducts generated from HCH oxidation are partially volatilized and disappear at the temperatures studied. Thus, based on the results obtained, it can be concluded that the oxidation of these pollutants occurs mainly in the soil phase.

The concentration of PS with reaction time was measured for the three temperatures tested in the absence of soil (runs B4-B6, Table 7.8) and the presence of unpolluted (TS-L0, runs B7-B9, Table 7.8) and polluted (TS L2, runs A3-A5, Table 7.7) soils. The results obtained have been depicted in Figure 7.20.

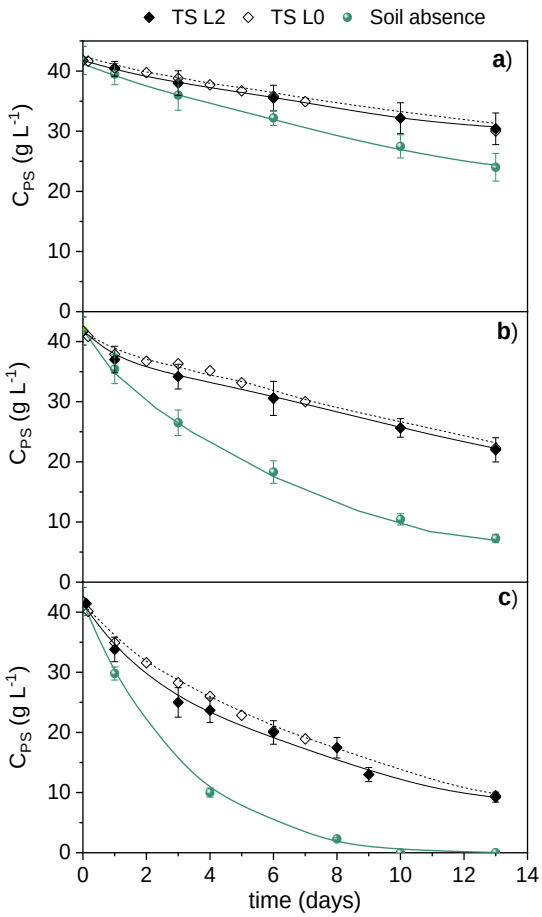

Figure 7.20. Concentration of PS with reaction time in the absence of soil (B4-B6) and in the presence of unpolluted (TS-L0, B7-B9) and polluted (TS-L2, A3-A5) soil at (a) 35 °C, (b) 45 °C, (c) 55 °C. Operating conditions: C_{PS} = 40 g L^{-1}, 100 rpm, pH_0 = 7 (all the experiments), $C_{HCHs,0}$ = 358 mg kg^{-1} (TS L2), V_L/W_S = 2 (when applicable) (Dominguez, Checa-Fernandez et al. 2021, **ART. 3**).

As expected, the higher the temperature, the higher the PS decomposition rate. Around 10, 18 and 30 g L^{-1} of PS were consumed at the end of the experiments with polluted soil at 35, 45, and 55 °C, respectively. The increase of the oxidant consumption with the reaction temperature can be attributable to i) the faster oxidation and dechlorination of HCHs by sulfate radicals (Eq. (7.2)) and ii) an increase in the unproductive decomposition of PS, generating sulfate anions, protons, and oxygen (Eq. (7.14)) (Kolthoff

and Miller 1951, Goulden and Anthony 1978). Once generated, $SO_4^{\cdot -}$may be scavenged persulfate anions, according to Eq. (7.15). Additionally, sulfate radicals can be consumed themselves (Eq. (7.16)) (Liang and Su 2009).

$$S_2O_8^{2-} + H_2O \rightarrow 2\,H^+ + 2\,SO_4^{2-} + \frac{1}{2}O_2 \quad (7.14)$$

$$SO_4^{\cdot -} + S_2O_8^{2-} \rightarrow SO_4^{2-} + S_2O_8^{\cdot -} \quad (7.15)$$

$$SO_4^{\cdot -} + SO_4^{\cdot -} \rightarrow S_2O_8^{2-} \quad (7.16)$$

The use of PS in the oxidation of COCs in soil can be evaluated from the difference between PS decomposition profiles in the presence or absence of contamination in soil. As expected, slight differences have been obtained regardless of the soil (polluted/unpolluted) due to the high excess of PS used in the oxidation experiments (20 times the stoichiometric amount, Table 7.7). However, the higher the temperature, the higher the differences in PS decomposition with unpolluted and polluted soils. This finding means that an increase in the reaction temperature leads to better use of the sulfate radicals produced. The results obtained in the aqueous phase (in the absence of polluted soil) are consistent with those published elsewhere (Dominguez, Romero et al. 2020). The PS decomposition rate is much higher when no soil is present at the three temperatures tested (Figure 7.20). As a result of proton release (Eq. (7.14)), the pH in the experiments carried out without soil highly decreased with reaction time (data not shown), being the pH drop faster when increasing the temperature. The acidic pH enhances the rate of PS decomposition (Vicente, Santos et al. 2011). On the contrary, in the presence of soil, the pH remains close to neutral (7- 8) at the three temperatures tested. The high carbonate content of the soil (> 40%, Table 7.1) allows to neutralize the protons generated from Eq. (7.14), acting the soil as a buffer. The neutral pH maintained in soil presence explains the lower unproductive consumption of the oxidant compared to the results obtained in the absence of soil with acidic pH (Figure 7.20). The efficiency in the oxidant consumption with reaction time at the different temperatures tested has been calculated Eq. (7.7). This parameter slightly decreases when reaction time or reaction temperature increase (Figure 7.21), although the differences are not significant. Thus, it can be concluded that the activation of PS at the maximum temperature tested (55 ºC) is efficient in the oxidation of COCs in TS and it is not associated with excessive oxidant consumption.

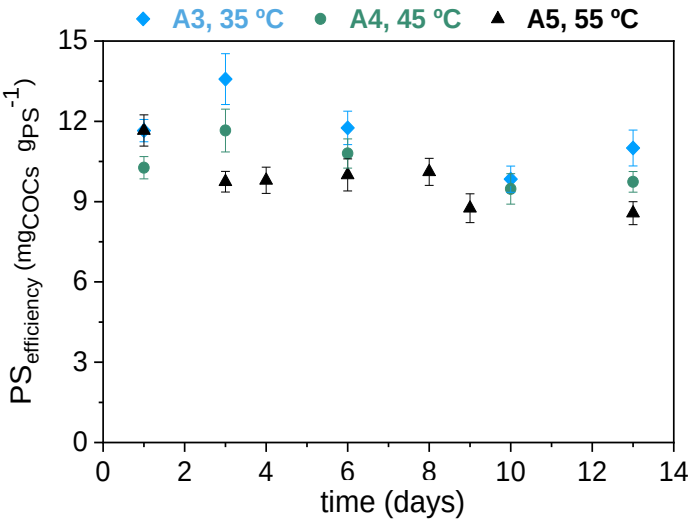

Figure 7.21. Evolution of the efficiency in the consumption of PS at the three temperatures tested. Operating conditions: $C_{HCHs,0}$ = 358 mg kg^{-1} (TS L2), C_{PS} = 40 g L^{-1}, V_L/W_S = 2, 100 rpm, pH_0 = 7 (A3-A5) (Dominguez, Checa-Fernandez et al. 2021, **ART. 3**).

Finally, a systematic study varying the **initial concentration of PS** (10, 20, 40, 60, and 80 g L^{-1}, A5-A9) was performed to remediate this soil at 55 ºC. The global conversion of HCHs, dechlorination degree, and chlorine balance at 3 and 9 days of treatment at the different initial PS concentrations tested is depicted in Figure 7.22.

As expected, as the oxidant concentration increases, the conversion of the pollutants increases due to the higher production of sulfate radicals. This finding agrees with the studies found in the literature (Chen, Murugananthan et al. 2016, Liu, Wang et al. 2019). The oxidant concentration affects more the degree of HCHs dechlorination achieved than the HCH degradation. When low oxidant concentrations (10 g L^{-1}) are used, significant differences between the HCHs conversion and dechlorination are obtained, indicating that non-negligible amounts of chlorinated intermediates are formed. Moreover, most of these compounds have not been identified based on the chlorine balance (C_{PS} = 10 g L^{-1}, 3 days, 67%). As the oxidant concentration increases (and the reaction progresses), the differences between the degradation of HCHs and their dechlorination are progressively reduced until they become non-existent when working with initial PS concentrations of ≥ 60 g L^{-1} (Figure 7.22-b). Under these conditions, the sulfate radicals have further oxidised the possible chlorinated intermediates generated during the oxidation of HCHs. Moreover, the chlorine balance is entirely accomplished, indicating no other unidentified chlorinated compounds in the reaction medium.

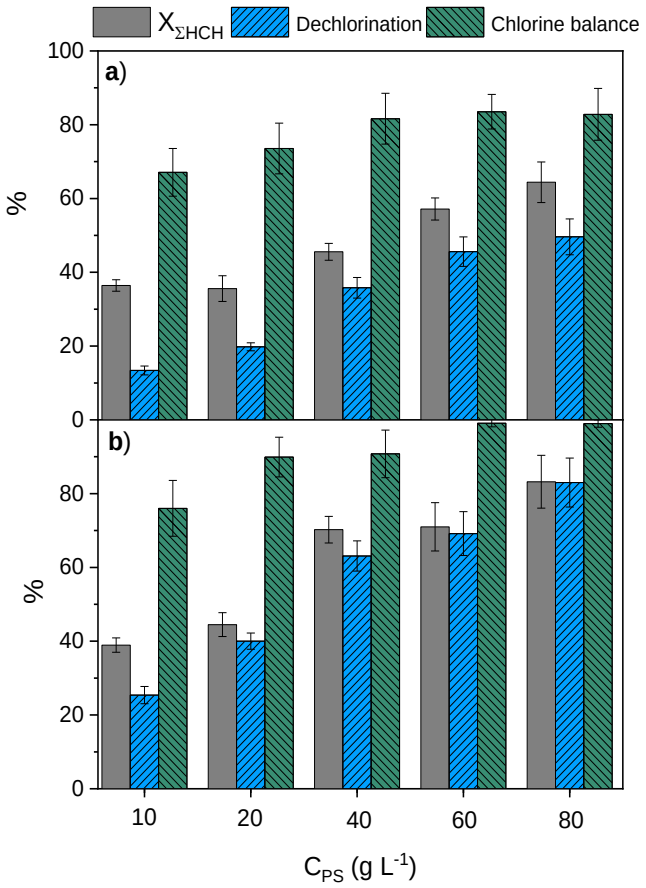

Figure 7.22. Conversion of HCHs, dechlorination degree, and chlorine balance at (a) 3 days and (b) 9 days when working with different initial concentrations of PS. Operating conditions: $C_{HCHs,0}$ = 358 mg kg^{-1} (TS L2), 55 ºC, V_L/W_S = 2, 100 rpm, pH_0 = 7 (A5-A9) (Dominguez, Checa-Fernandez et al. 2021, **ART. 3**).

The evolution of PS conversion with reaction time when working with different initial concentrations of this reagent has been measured, finding that PS consumption is independent of its initial concentration (Figure 7.23), which confirms that oxidant decomposition follows first-order-reaction, as described in the literature (Huang, Couttenye et al. 2002, Liang, Bruell et al. 2003, Waldemer, Tratnyek et al. 2007, Liang and Su 2009).

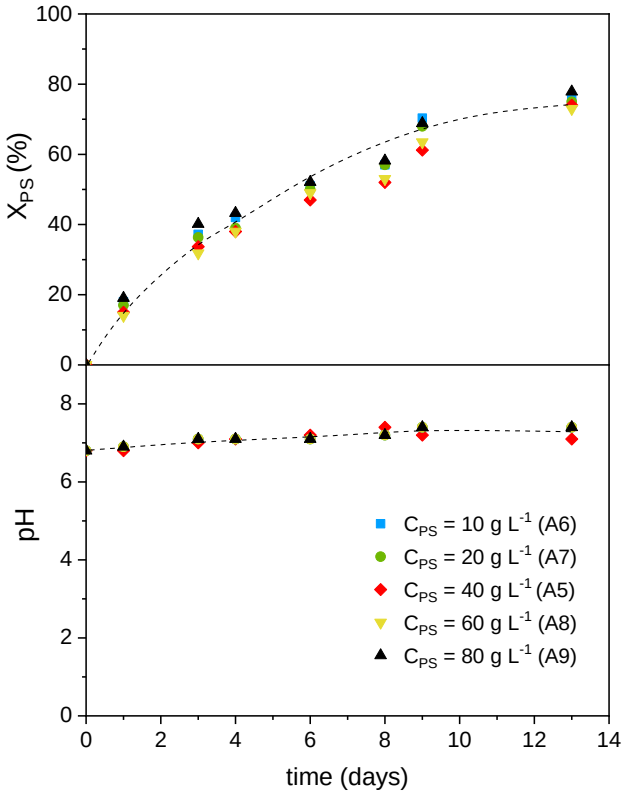

Figure 7.23. Conversion of PS and solution pH evolution with reaction time reaction when working with different initial concentrations of PS. Operating conditions: $C_{HCHs,0}$ = 358 mg kg^{-1} (TS L2), 55 °C, V_L/W_S = 2, 100 rpm, pH_0 =7 (A5-A9) (Dominguez, Checa-Fernandez et al. 2021, **ART. 3**).

The pH remained almost constant (close to neutrality) during the reaction time regardless of the PS concentration due to the buffer capacity of the soil. The soil physicochemical characteristics hardly change after the remediation process. Consequently, the application of a subsequent bioremediation treatment seems feasible.

Lastly, the efficiency of PS consumption (Eq. (7.7)) when increasing initial PS concentrations has been calculated at two reaction times (3 and 9 days, Figure 7.24). The efficiency of oxidant consumption decreases with the progress of the reaction. As HCHs break down, there is a lower concentration of pollutants to oxidize, while oxidant unproductive consumption does not change. There is also a significant decrease in the efficiency of PS when increasing the oxidant concentration. This decrease is more marked in the 10 to 20 g L^{-1} range. However, low PS concentrations are undesirable since they lead to insufficient soil dechlorination degrees (Figure 7.22). Similar oxidant efficiency values are obtained by increasing the initial oxidant concentration to values > 40 g L^{-1}, but pollutants removal and dechlorination significantly improve. Therefore, a PS concentration

of 80 g L^{-1} and a temperature of 55 ºC are recommended. At these conditions, it is possible to abate and dechlorinate 83% of the HCHs, with no intermediate chlorinated compounds, in the soil-aqueous system at 9 days.

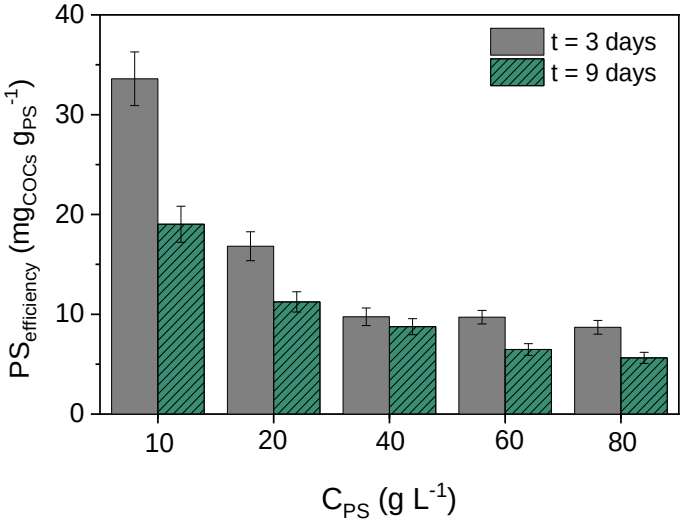

Figure 7.24. Efficiency in the PS consumption (Eq. (7.7)) at 3 and 9 days of reaction time when working with different initial concentrations of PS. Operating conditions: $C_{HCHs,0}$ = 358 mg kg^{-1} (TS L2), 55 ºC, V_L/W_S = 2, 100 rpm, pH_0 = 7 (A5-A9) (Dominguez, Checa-Fernandez et al. 2021, **ART. 3**).

7.2.3. Intensification of PS/NaOH

As previously shown (Subsection 7.2.2.), the alkaline activation of PS (PS/NaOH) led to interesting results in the remediation of HCHs-polluted soils. However, the reaction times necessary to reach acceptable conversions of contaminants at low temperatures are high. Thus, different intensification alternatives will be studied: i) **temperature** (PS/NaOH/**T**), ii) **ultrasound** (PS/NaOH/**US**), and iii) **surfactant** (**S/**PS/NaOH/T). The influence of the main operating conditions (reagent addition order, temperature or US power, aqueous/soil ratio, initial concentration of PS, and stirring rate) on HCHs degradation efficiency has been studied. Particular attention has been paid to evaluating the pollutants dechlorination degree and identifying oxidation intermediates at the different operating conditions tested, enabling practitioners to quickly screen the efficacy of base-activated persulfate under a wide range of operating conditions for future specific HCH remediation projects.

7.2.3.1. PS/NaOH/T

The experimental conditions of the alkaline activation of PS intensified by temperature, PS/NaOH/T system, are listed in Table 7.9. This table includes the objective studied, run (T) number, PS and NaOH concentration, temperature, stirring rate, the reagent addition order, the ratio between the soil and aqueous phase employed (V_L/W_S), and the stoichiometric concentration of PS theoretically required for the HCHs mineralization (PS/PS_{stc}). The variable studied in each series of experiments has been highlighted in bold type and blue color.

Table 7.9. Operating conditions of the PS/NaOH/T remediation experiments ($C_{HCHs,0}$ = 373 mg kg^{-1} (TS L2), W_S = 15 g, V_L/W_S = 2, molar NaOH:PS = 2) (Checa-Fernández, Santos et al. 2021, **ART. 4**).

	Objective	Run	C_{PS} (g L^{-1})	C_{NaOH} (g L^{-1})	T (°C)	Stirring rate (rpm)	Reagent addition order	Ratio V_L/W_S	PS/PS_{stc}
Preliminary exp.	**Blanks**	T1	-	-	60	100	-	2	-
		T2	-	13.5	40	100	-	2	-
		T3	40	-	40	100	-	2	5.4
	Reagent addition order	T4	40	13.5	40	100	**Sim.**	2	5.4
		T5	40	13.5	40	100	**Seq.**	2	5.4
Operation conditions study	**Temperature**	T4	40	13.5	**40**	100	Sim.	2	5.4
		T6	40	13.5	**50**	100	Sim.	2	5.4
		T7	40	13.5	**60**	100	Sim.	2	5.4
	V_L/W_S ratio	T8	40	13.5	50	100	Sim.	**1**	2.7
		T6	40	13.5	50	100	Sim.	**2**	5.4
	PS concentration	T9	**20**	**6.8**	40	100	Sim.	2	2.7
		T4	**40**	**13.5**	40	100	Sim.	2	5.4
		T10	**60**	**20.3**	40	100	Sim.	2	8.2
		T11	**20**	**6.8**	50	100	Sim.	2	2.7
		T6	**40**	**13.5**	50	100	Sim.	2	5.4
		T12	**60**	**20.3**	50	100	Sim.	2	8.2
	Stirring rate	T13	40	13.5	40	**10**	Sim.	2	5.4
		T14	40	13.5	40	**50**	Sim.	2	5.4
		T4	40	13.5	40	**100**	Sim.	2	5.4

"Sim." = simultaneous reagents addition. "Seq." = sequential reagents addition.

Preliminary experiments

Control experiments were carried out to evaluate the loss of COCs by volatilization at 60 ºC (T1) and the dehydrochlorination of HCHs to trichlorobenzenes (TCBs) with alkali, in the absence of the oxidant (T2). An experiment at 40 ºC in the absence of alkali was conducted (T3) and compared to the corresponding with NaOH addition (T4) to evaluate the synergetic effect of the alkaline and temperature activation of PS. The reagents (PS and NaOH) were added simultaneously ("sim", T4) or sequentially ("seq", T5). In the last case, NaOH was first added at 20 ºC, and the reactor stirred. After 48 h, the reactor was heated (40 ºC), and the required volume of PS was added (zero reaction time). The influence of temperature (40-60 ºC, T4, T6, and T7), liquid/soil ratio (1 and 2, T8 and T6), initial PS concentration (20-60 g L^{-1}, T4, T6, and T9-T12) and stirring rate (10-100 rpm, T4, T13 and T14) were studied. PS concentration and temperature values are in the typical range used in literature for soil remediation by PS activated by alkali or temperature (Peng, Deng et al. 2015, Liu, Liu et al. 2017, García-Cervilla, Santos et al. 2020).

The pollutants concentration in the run without PS and NaOH (T1) remained constant for 14 days (data not shown), confirming no loss of HCHs by volatilization at 60 ºC. At alkaline conditions (pH > 12, T2) without oxidant, α-HCH disappeared in less than 4 h, being converted in a mixture of 1,2,4-TCB, 1,2,3-TCB and 1,3,5-TCB. The dehydrochlorination rate of β-HCH was much slower, remaining an important fraction of this pollutant at the end of the experiment (52%, 55.3 mg kg^{-1}, 14 days) (Eq. (7.12)), as previously mentioned in Subsection 7.2.2. The TCBs generated persist in the reaction medium, highlighting the need for an oxidant for their degradation. The results obtained at 40 ºC, 40 g L^{-1} of PS, in the absence (T3), and the presence of alkali (T4) are shown in Figure 7.25-a. The initial pH of both experiments (pH > 12 and pH = 6.8, in T4 and T3, respectively) remains almost constant during reaction time. When applying the synergetic activation of PS (PS/NaOH/T, T4), the dehydrochlorination of α-HCH was complete, whereas, in the absence of alkali (PS/T, T3), only 16% was degraded after three days of treatment. Also, a higher conversion of β-HCH was achieved in the PS/NaOH/T system. Consequently, the COCs conversion (Eq. (7.10)) without NaOH (T3) was < 20%, while in the presence of this reagent (T4) reached 80%. PS conversion was higher in this run (T4), in agreement with the higher conversion of COCs achieved. Thus, the efficiency of the process was remarkably enhanced by the synergetic activation of PS by NaOH and temperature.

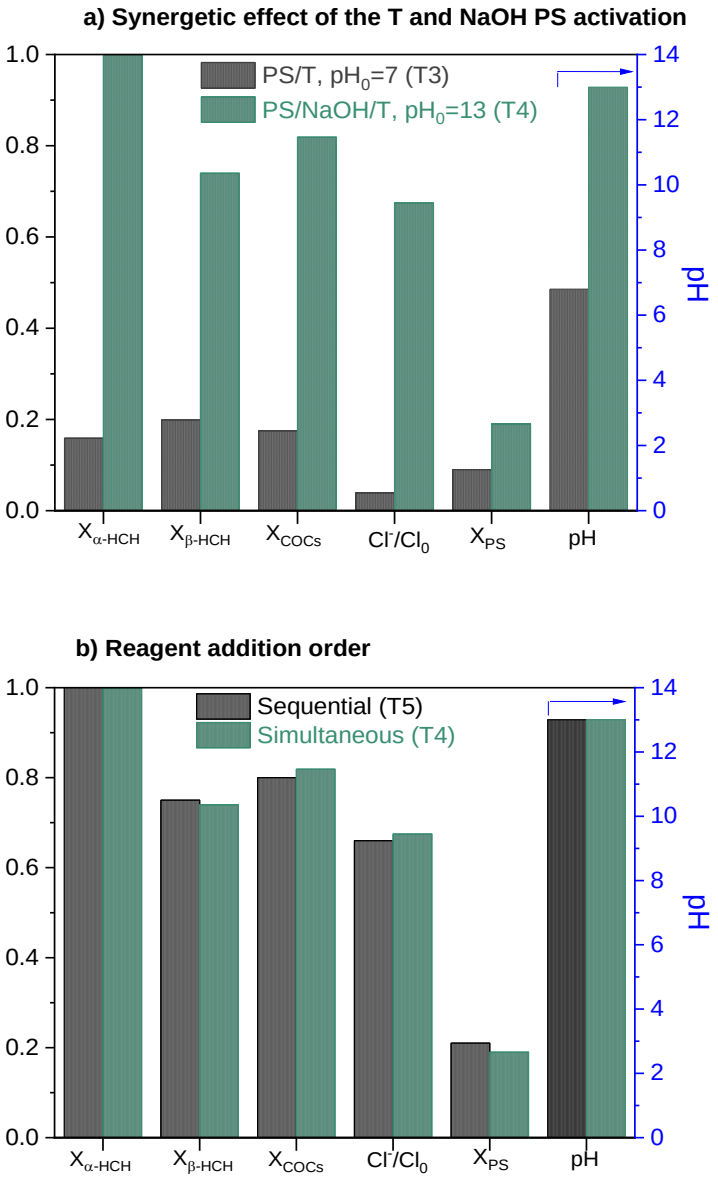

Figure 7.25. Conversion of α-HCH, β-HCH, COCs, and PS, dechlorination degree (Cl^-/Cl_0), and pH after 3 days of treatment. Experimental conditions: $C_{HCHs,0}$ = 373 mg kg^{-1} (TS L2), T = 40 °C, 100 rpm, V_L/W_S = 2, C_{PS} = 40 g L^{-1}, pH_0 = 7 (T3) and pH_0 = 13 (C_{NaOH} = 13.5 g L^{-1}) (T4 and T5) (Checa-Fernández, Santos et al. 2021, **ART. 4**).

A scheme for the degradation of HCHs with PS activated by alkali in serial steps has been proposed (Figure 7.26).

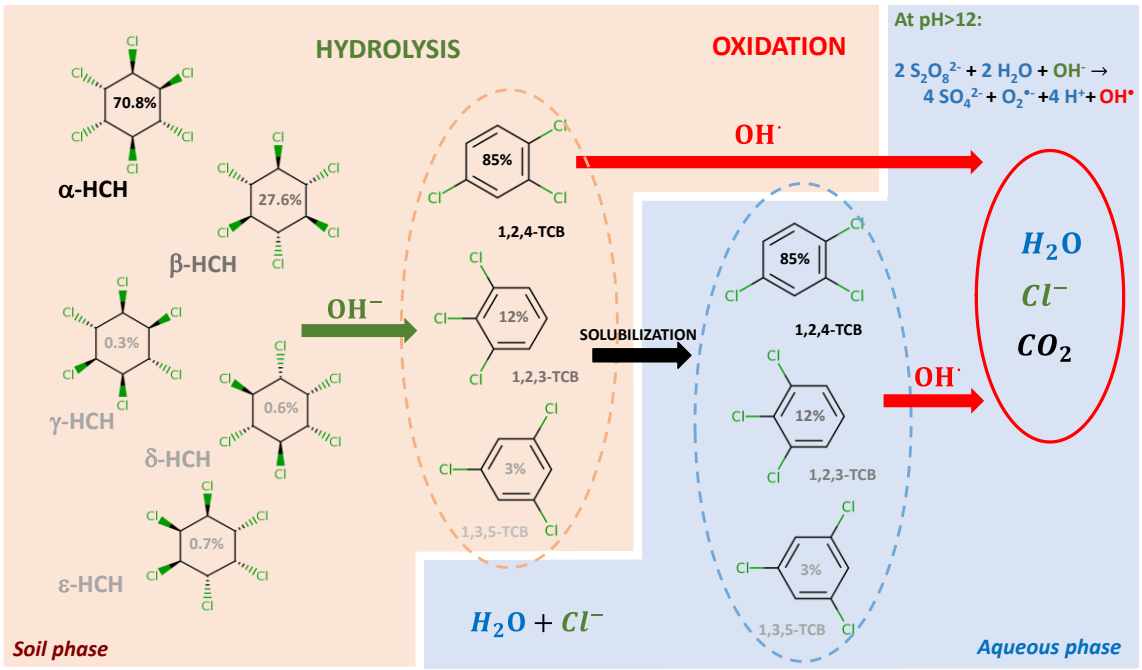

Figure 7.26. Scheme for the degradation of HCH isomers by alkali-activated PS (pH > 12). Soil and aqueous phases were represented in brown and blue, respectively (Checa-Fernández, Santos et al. 2021, **ART. 4**).

TCBs are first formed as an organic phase from HCHs hydrolysis at pH ≥12, releasing chlorides to the liquid phase (Eqs. (7.11) and (7.12)). The most favoured TCB isomer was 1,2,4-TCB (85%), followed by 1,2,3-TCB (12%) and 1,3,5-TCB (3%), according to previously published works (Lorenzo, García-Cervilla et al. 2020). The fact that 1,2,4-TCB is liquid at room temperature could favour the adsorption of this organic phase on the soil surface. Secondly, the TCBs adsorbed to the soil are progressively solubilized and oxidized in both soil and aqueous phases. The oxidation of TCBs in the aqueous phase and on the soil surface has been previously reported (García-Cervilla, Santos et al. 2020).

The effect of the reagent addition order (T4 *vs.* T5) on the process performance was studied, obtaining negligible differences in pollutant conversion after 3 days (Figure 7.25-b). Deviations below 5% in the conversion of α-HCH, β-HCH, and COCs or dechlorination degree were found (attributable to the experimental errors associated with the analytical methods). According to these results, the simultaneous addition of alkali and oxidant has been selected for further experiments, avoiding the implementation of two stages in the process, which would increase the time needed, and, therefore, the treatment cost.

Operation conditions study: Effect of temperature

Conversion of β-HCH and COCs in the soil phase and dechlorination degree, pH, and PS conversion in the aqueous phase were measured with reaction time as a temperature function (40, 50, and 60 °C, T4, T6, and T7, respectively). Results are shown in Figure 7.27 and Figure 7.28. Profiles of α-HCH conversion have not been included since the dehydrochlorination of this isomer at pH ≥ 12 is complete in less than 4 h, even at the minimum temperature studied.

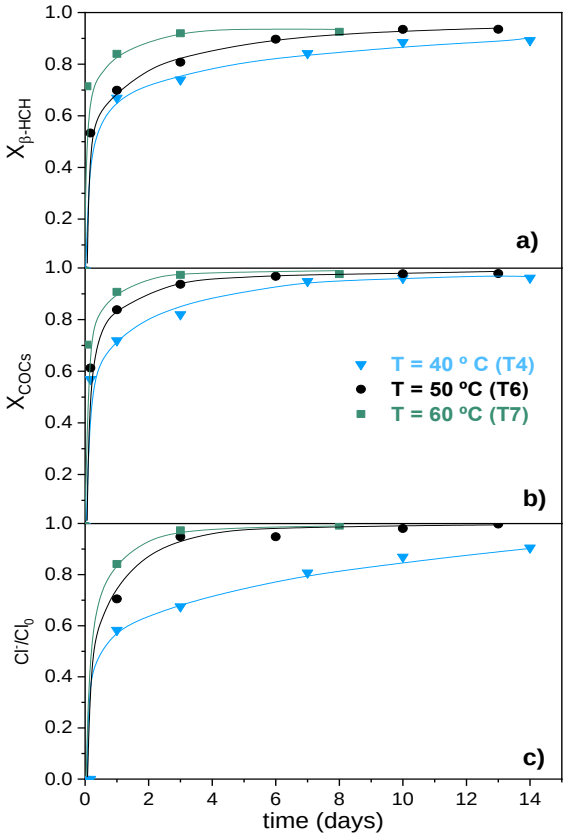

Figure 7.27. Conversion of β-HCH (a) and COCs (b) and dechlorination degree (c), with reaction time at different temperatures (40 °C (T4), 50 °C (T5) and 60 °C (T6)). Experimental conditions: $C_{HCHs,0}$ = 373 mg kg^{-1} (TS L2), 100 rpm, V_L/W_S = 2, C_{PS} = 40 g L^{-1}, C_{NaOH} = 13.5 g L^{-1} (Checa-Fernández, Santos et al. 2021, **ART. 4**).

As shown in Figure 7.27-a, the disappearance of β-HCH is notably enhanced by temperature. Two stages can be distinguished in the conversion profile of this pollutant. The first one (4-10 h, depending on the reaction temperature) has a high slope, whereas the second stage shows a slowdown. This behaviour can be explained considering that a percentage of β-HCH in the soil is strongly adsorbed (aged contamination) and not

present as HCH particulate matter. The fraction of β-HCH isomer corresponding to particulate matter is more easily solubilized and hydrolyzed than the β-HCH adsorbed (Ren, Zeng et al. 2018, Santos, Domínguez et al. 2020, Dominguez, Romero et al. 2021, **ART. 2**). Conversions of β-HCH around 65, 72, and 87% were obtained at 24 h at 40, 50, and 60 ºC, respectively, proving the positive effect of temperature on this isomer dehydrochlorination. When a temperature of 60 °C was applied (T7), an asymptotic value of β-HCH conversion (95%) was observed after 3 days of treatment. Similarly, the COCs conversion increases as the temperature rises (Figure 7.27-b), although asymptotic values were not achieved. This fact can be explained by considering that most of the initial COCs correspond to α-HCH, and this pollutant is rapidly dehydrochlorinated. Therefore, the contribution of β-HCH isomer not degraded to the asymptotic value of the final COCs conversion is small.

Moreover, a significant increase in the dechlorination degree is obtained by increasing the temperature (Figure 7.27-c), especially from 40 to 50 ºC. At these conditions, almost complete dechlorination of the pollutants was achieved (Cl^-/Cl_0 > 98%). The differences between the conversion profiles of COCs and dechlorination degree decrease with temperature increases, indicating that the production rate of chlorinated oxidation intermediates decreases with temperature. These results are consistent with those of Enell et al. (2005) and Peng et al. (2015), who found that temperature can accelerates the desorption rate of the pollutants (Enell, Reichenberg et al. 2005) and, therefore, makes the pollutants more accessible to the reactive species generated in the aqueous phase (Peng, Deng et al. 2015).

The evolution of the remaining concentration of HCHs as TCBs ($TCBs'/HCH_0$) with reaction time is shown in Figure 7.29. The value of $TCBs'/HCH_0$ at zero reaction time has been theoretically calculated, assuming complete and null dehydrochlorination of α-HCH and β-HCH, respectively.

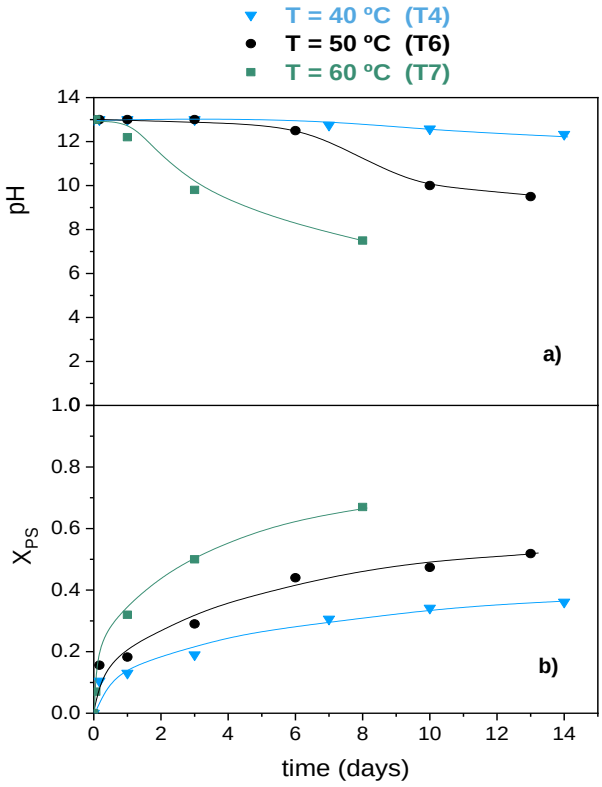

Figure 7.28. pH (a) and PS conversion (b) with reaction time at different temperatures (40 ºC (T4), 50 ºC (T5), and 60 ºC (T6)). Experimental conditions: $C_{HCHs,0}$ = 373 mg kg^{-1} (TS L2), 100 rpm, V_L/W_S = 2, C_{PS} = 40 g L^{-1}, C_{NaOH} = 13.5 g L^{-1} (Checa-Fernández, Santos et al. 2021, **ART. 4**).

As expected, the oxidation rate of the TCBs increases with reaction temperature (TCBs'/HCH_0 decrease), although slight differences were obtained from 50 to 60 ºC (Figure 7.29-a). The distribution of TCBs was almost constant during the reaction time, regardless of the reaction temperature (data not shown). This means that both TCB isomers generated are oxidized at the same reaction rate (Santos, Fernandez et al. 2018).

As shown in Figure 7.28-b, the PS decomposition rate increased with temperature, in agreement with that reported in the literature (Liang, Bruell et al. 2003, Zrinyi and Pham 2017, Dominguez, Romero et al. 2020). PS decomposition yields radicals that can either attack the pollutants or be unproductively consumed, both processes enhanced by the temperature rise (Dominguez, Romero et al. 2020). The PS conversion profiles show a higher slope in the first stage of the process (0-3 days), coincident with the high abatement of COCs produced in this period (Figure 7.27-b). Once the pollutants have been oxidized, the only contribution to PS decomposition is the non-productive radical reactions.

The oxidant efficiency, and therefore, the associated cost, decreases sharply in the high COCs conversion region. Lower temperatures lead to better oxidant utilization, but

longer reaction times are required (Figure 7.30-a). Hence, the temperature selection should consider reaction time, PS consumption, and the required COCs conversion value, considering economic and environmental aspects.

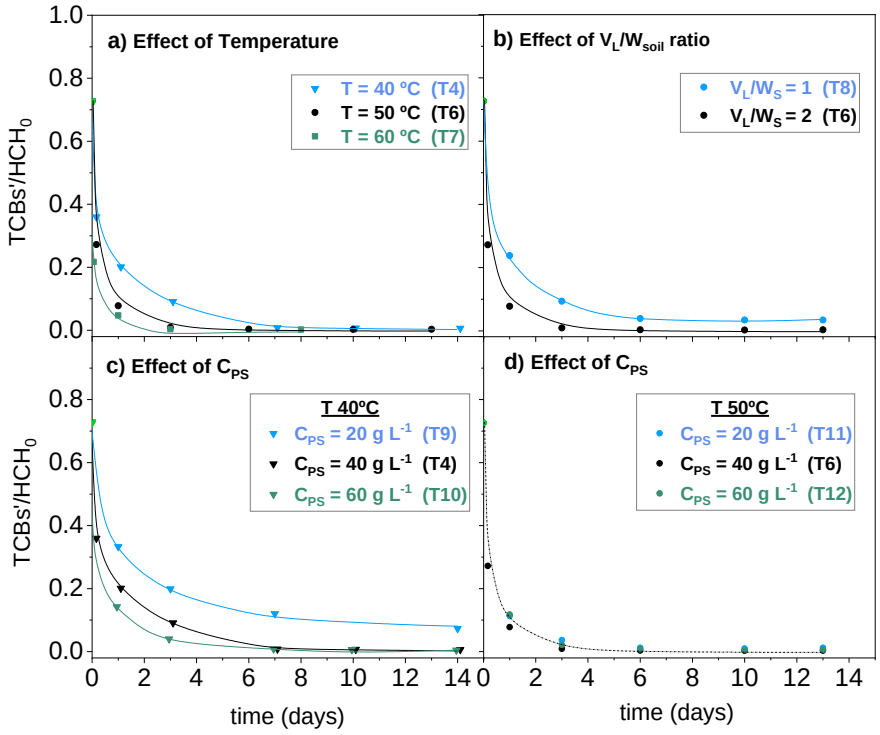

Figure 7.29. Remaining concentration of TCBs generated (TCBs'/HCH$_0$) with reaction time according to the different variables studied: Temperature (a), V_L/W_S ratio (b), PS concentration at 40 °C (c), and 50 °C (d). Operational conditions: Table 7.9 (Checa-Fernández, Santos et al. 2021, **ART. 4**).

The pH evolution depends significantly on the reaction temperature (Figure 7.28-a). At 40 °C (T4), the pH is maintained above 12 during the entire experimental time (14 days). However, a significant decrease was noticed at 50 °C (T5) after 6 days, reaching pH values around 10 at the final reaction time. This fact is more pronounced at 60 °C (T7), with neutral values at 8 days of treatment. The decrease in the pH of the solution is associated with NaOH consumption by the hydrogen cations generated during PS consumption. The hydrogen cations come from the generation of sulfate radicals (Eq. (4.4), Subsection 4.2) and the unproductive decomposition of PS (Eq. (7.14)) (Kolthoff and Miller 1951, Goulden and Anthony 1978)). Both reactions are favoured by temperature. The alkaline activation of PS no longer occurs once the pH drops below 12. At pH < 12, PS is activated mainly by temperature, which leads to the formation of sulfate radicals (Eq. (4.3), Subsection 4.2)

(Ike, Linden et al. 2018, Wang and Wang 2018). Furthermore, at pH < 12, the hydrolysis of HCHs (β-HCH is the only isomer present when the pH drop occurs) is quenched.

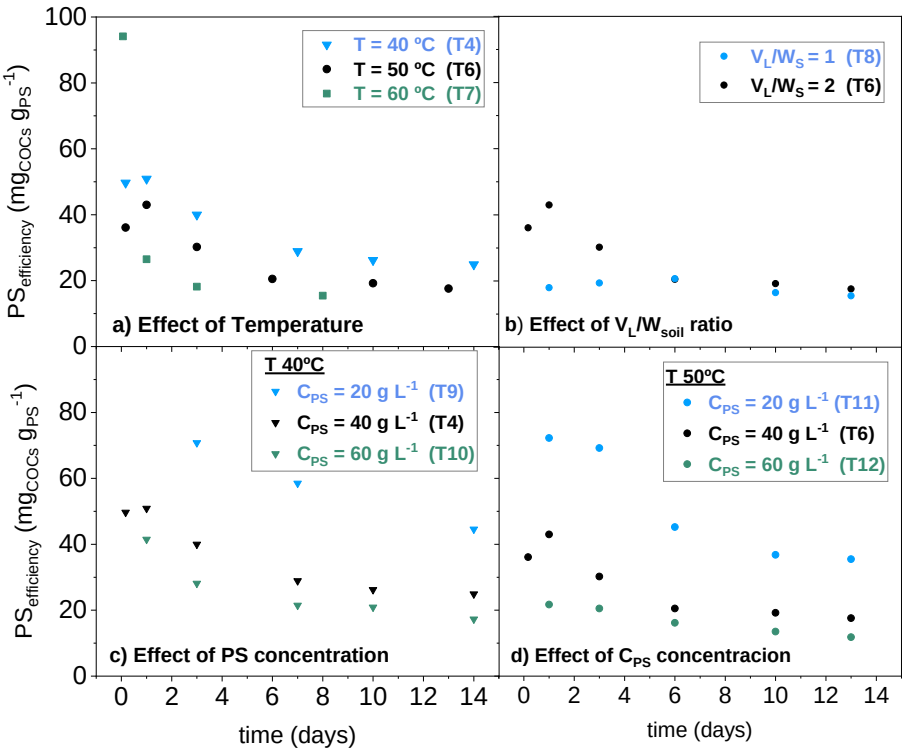

Figure 7.30. Evolution of $PS_{efficiency}$ with reaction time according to the different variables studied: Temperature (a), V_L/W_S ratio (b), PS concentration at 40 ºC (c) and 50 ºC (d). Operational conditions: Table 7.9 (Checa-Fernández, Santos et al. 2021, **ART. 4**).

A remarkable finding was that only TCBs were detected as chlorinated by-products when the solution pH was maintained > 12, suggesting that the oxidation of TCBs at alkaline conditions yields total dechlorinated oxidation byproducts. On the contrary, chlorobenzene (CB) appeared when the pH dropped under 12 (T6 (50 ºC) and T7 (60 ºC)). At 60 ºC, the CB concentration in the soil phase presented a maximum between 1 and 3 days (30 mg kg^{-1}) (Figure 7.31). This fact proved that CB was formed and further oxidized by the radical attack, disappearing entirely at 8 days of treatment. At 50 ºC, the appearance of CB was delayed until 10 days of treatment, coinciding with a pH solution drop. The same trend was observed for 1,2-dichlorobenzene (1,2-DCB), although this compound was detected in lower concentrations than CB. The appearance of CB and 1,2-DCB as intermediates in HCHs abatement has been also reported in the literature (Wang, Peng et al. 2009, Homolková, Hrabák et al. 2014). Therefore, the reaction mechanism seems to change when the pH decreases below 12.

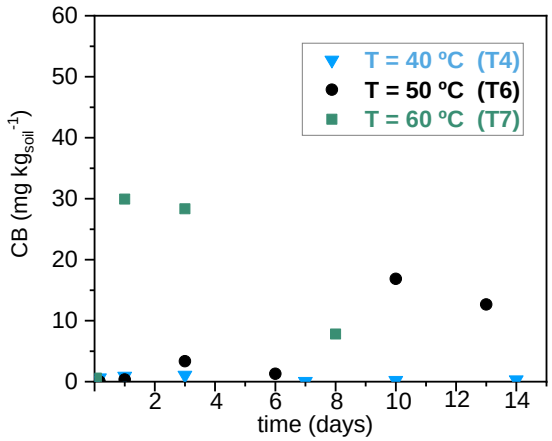

Figure 7.31. Concentration of CB generated in the soil phase as an intermediate oxidation compound with reaction time at 40, 50, and 60 ºC (T4, T6, and T7). Experimental conditions: $C_{HCHs,0}$ = 373 mg kg^{-1} (TS L2), 100 rpm, V_L/W_S = 2, C_{PS} = 40 g L^{-1}, C_{NaOH} = 13.5 g L^{-1} (Checa-Fernández, Santos et al. 2021, **ART. 4**).

Overall, the results obtained demonstrate a strong effect of temperature on the HCHs degradation. Equivalent conversions were achieved in 3 days at 50 ºC or 7 days at 40 ºC. However, the minor pollutant conversion improvement obtained by increasing the temperature from 50 to 60°C, added to the significant increase in PS consumption and the drop in the pH solution, suggests that temperatures > 50 ºC are undesirable.

Operation conditions study: Effect of liquid/soil ratio

Two liquid/soil ratios have been studied (V_L/W_S = 1 and 2, T8 and T6, respectively). As shown in Figure 7.32, the higher the V_L/W_S ratio, the higher the COCs reduction and the degree of dechlorination achieved.

Siddique, Okeke et al. (2002) found similar results when studied the biodegradation of HCHs in water and soil slurry by a *Pandoraea* species, concluding that a decrease in the V_L/W_S ratio produces a reduction in the pollutant conversion. The higher the V_L/W_S ratio, the greater the solubilized contaminants mass and, therefore, the higher the removal rate of COCs in the slurry. This finding can be justified if oxidation reaction in the aqueous phase contributes significantly to COCs removal. Similarly, the oxidation rate of the generated TCBs (TCBs'/HCH_0) decreased when a lower V_L/W_S ratio was used (Figure 7.29-b).

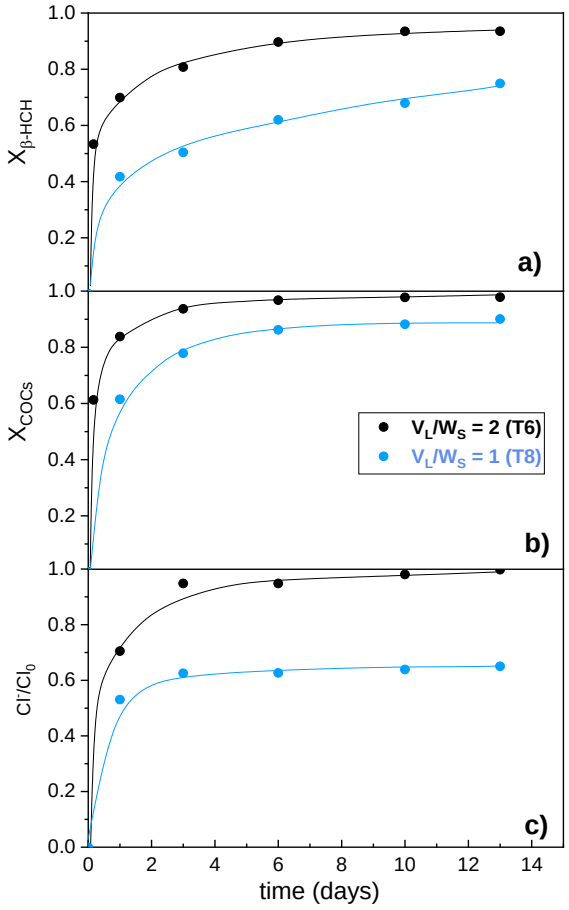

Figure 7.32. Conversion of β-HCH (a) and COCs (b), and dechlorination degree (c) with reaction time at V_L/W_S ratios of 1 (T6) and 2 (T8). Experimental conditions: $C_{HCHs,0}$ = 373 mg kg^{-1} (TS L2), T = 50 °C, 100 rpm, C_{PS} = 40 g L^{-1}, C_{NaOH} = 13.5 g L^{-1} (Checa-Fernández, Santos et al. 2021, **ART. 4**).

The solution pH decreased progressively with reaction time in both V_L/W_S ratios studied (Figure 7.33-a), but this decrease started earlier in the run performed with the lowest one (T8). This finding agrees with the higher PS conversion noticed in T8 at short reaction times (Figure 7.33-b), explained considering the lower excess of PS used (V_L/W_S = 1) compared to T6 (V_L/W_S = 2) (Table 7.9). As previously discussed, the higher the PS consumption, the lower the solution pH. Although slightly higher PS conversion values are obtained at reaction times up to 3 days when working with a V_L/W_S = 1, at longer times, PS consumption is equal in both experiments (Figure 7.33-b), and the solution pH trends to the same final value. This finding proves that the presence of soil has little influence on PS decomposition. In conclusion, an increase in the V_L/W_S ratio up to a value of 2 significantly reduces the reaction times required for the same COCs conversion. Therefore, a ratio V_L/W_S = 2 should be employed to favour the solubilization of contaminants and their

subsequent oxidation. If lower V_L/W_S ratios are used, and the initial concentration of PS keeps constant, a second addition of NaOH or molar ratios NaOH/PS > 2 will be required to maintain the pH above 12.

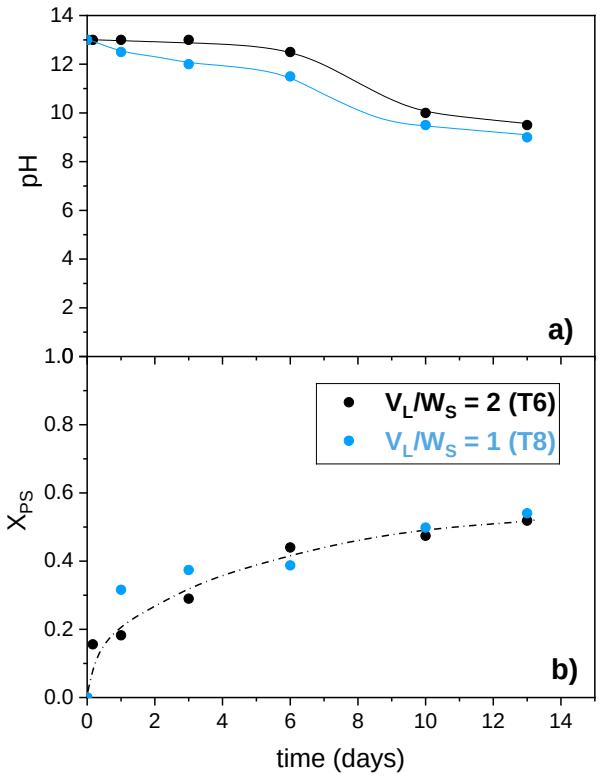

Figure 7.33. pH (a) and PS conversion (b) with reaction time at V_L/W_S ratios of 1 (T6) and 2 (T8). Experimental conditions: $C_{HCHs,0}$ = 373 mg kg^{-1} (TS L2), T = 50 °C, 100 rpm, C_{PS} = 40 g L^{-1}, C_{NaOH} = 13.5 g L^{-1} (Checa-Fernández, Santos et al. 2021, **ART. 4**).

Operation conditions study: Effect of oxidant concentration

The results of β-HCH, COCs conversion, and dechlorination degree varying the initial PS concentration (20, 40, and 60 g L^{-1}) at 40 °C (a, b, and c) and 50 °C (d, e, and f) are shown in Figure 7.34. The oxidation of the TCBs generated by HCHs alkaline hydrolysis ($TCBs'/HCH_0$) is shown in Figure 7.29-c and Figure 7.29-d, respectively.

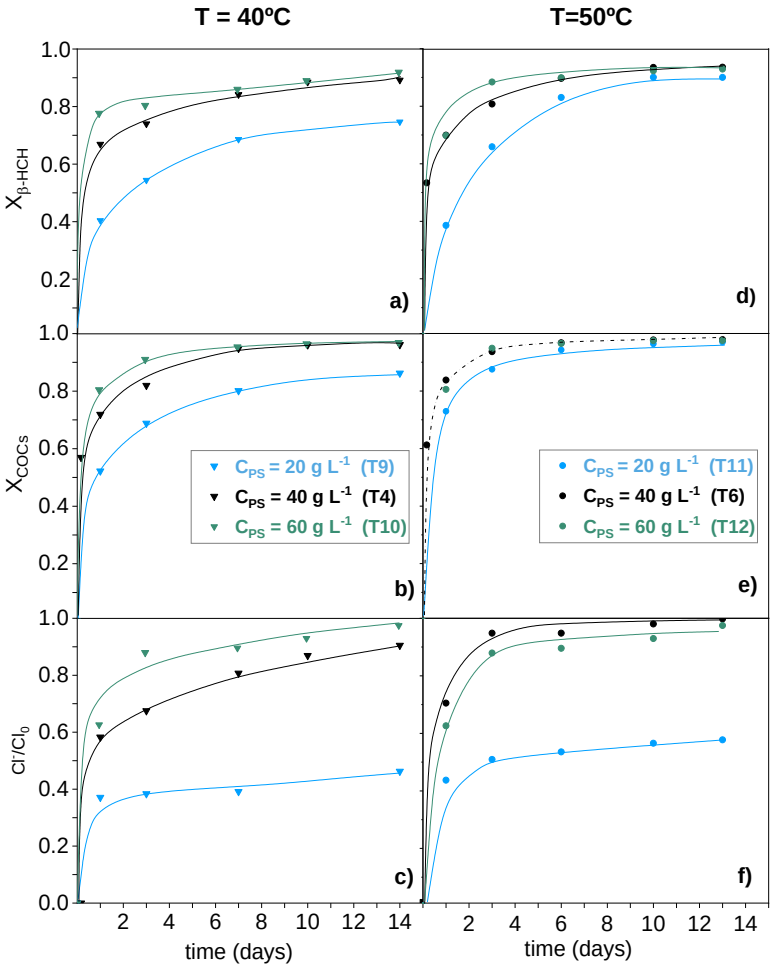

Figure 7.34. Conversion of β-HCH (a, d) and COCs (b, e) in the soil phase and dechlorination degree (c, f) with reaction time using different initial PS concentrations at 40 °C and 50 °C, respectively (Table 7.9). Experimental conditions: $C_{HCHs,0}$ = 373 mg kg^{-1} (TS L2), 100 rpm, V_L/W_S = 2, NaOH/PS = 2 (Checa-Fernández, Santos et al. 2021, **ART. 4**).

As can be seen, β-HCH and COCs conversion increased by increasing the initial concentration of PS, while the remaining concentration of TCBs decreased. The higher the initial PS concentration, the higher the production of hydroxyl radicals and the higher pollutant abatement. These results are in accordance with those reported in the literature for the alkaline activation of PS (Santos, Fernandez et al. 2018, Dominguez, Rodriguez et

al. 2020, García-Cervilla, Santos et al. 2020) and other types of PS activations (Zhao, Hou et al. 2014, Ji, Dong et al. 2015). The differences in β-HCH and COCs conversion and remaining TCBs' with the initial concentration of PS were more significant at 40 than 50 ºC (Figure 7.34 and Figure 7.29-c,d).

The influence of the initial oxidant concentration was more noticeable at short reaction times and low initial PS concentrations (Figure 7.34-b and Figure 7.34-e). At 40 ºC, the dechlorination degree increased by increasing the initial concentration of PS. This increase was more significant from 20 to 40 g L^{-1} than from 40 to 60 g L^{-1} (Figure 7.34-c and Figure 7.34-f). Therefore, oxidant concentrations significantly above the stoichiometric values ($PS/PS_{stc} \geq 5.4$) are required to achieve high pollutant dechlorination degrees. The same trend was noticed when PS dosage increased from 20 to 40 g L^{-1} at 50 ºC. However, a slight decrease in COCs dechlorination was observed at 50 ºC when increasing the PS concentration from 40 to 60 g L^{-1} (values close to the unity were achieved at both PS concentrations).

PS conversion was not appreciably modified when varying the initial oxidant concentration (Figure 7.35-b and Figure 7.35-d). Therefore, the decomposition rate of PS in the slurry system followed a pseudo-first-order reaction (Huang, Couttenye et al. 2002, Liang, Bruell et al. 2003, Waldemer, Tratnyek et al. 2007, Santos, Fernandez et al. 2018). The evolution of $PS_{efficiency}$ (Eq. (7.7)) has been considered to compare the effect of using different oxidant concentrations. The results showed a decrease in this parameter when increasing the initial oxidant concentration, regardless of the reaction temperature (Figure 7.30-c,d). Thus, for a given reaction time, the higher excess of PS concentration, the higher the unproductive PS consumption, and the lower the PS efficiency. As shown in Figure 7.35, the pH dropped slightly in the runs carried out at 40 ºC, with similar profiles at all the PS concentrations. However, at 50 ºC, the pH decreased more rapidly as the initial concentration of PS decreased. This finding can be explained because a lower initial concentration of PS implied a lower alkali concentration (NaOH/PS molar ratio was set to 2) and, therefore, a lower mass ratio of alkali to soil mass or alkali to contaminants.

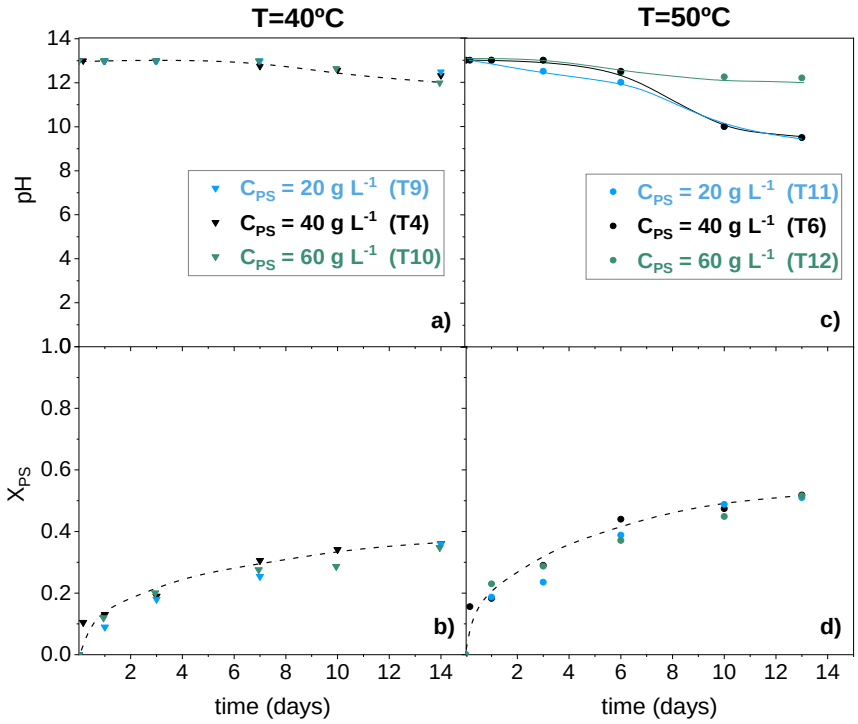

Figure 7.35. Evolution of pH (a, c) and PS conversion (b, d) with reaction time using different initial PS concentrations at 40 ºC and 50 ºC, respectively (Table 7.9). Experimental conditions: $C_{HCHs,0}$ = 373 mg kg^{-1} (TS L2), 100 rpm, V_L/W_S = 2, NaOH/PS = 2 (Checa-Fernández, Santos et al. 2021, **ART. 4**).

To summarize, the oxidant concentration must be selected considering the cost of the reagent, the $PS_{efficiency}$, and the time saved to reach the desired degradation of pollutants and dechlorination degree. Increasing the initial PS concentration from 20 to 60 g L^{-1} significantly decreased the $PS_{efficiency}$. However, low initial PS concentrations (20 g L^{-1}) resulted in insufficient pollutants dechlorination degrees, and a second NaOH addition or molar ratio of NaOH/PS > 2 is needed. Therefore, 40 g L^{-1} was selected as the most convenient initial PS concentration to remediate the HCHs-polluted soils.

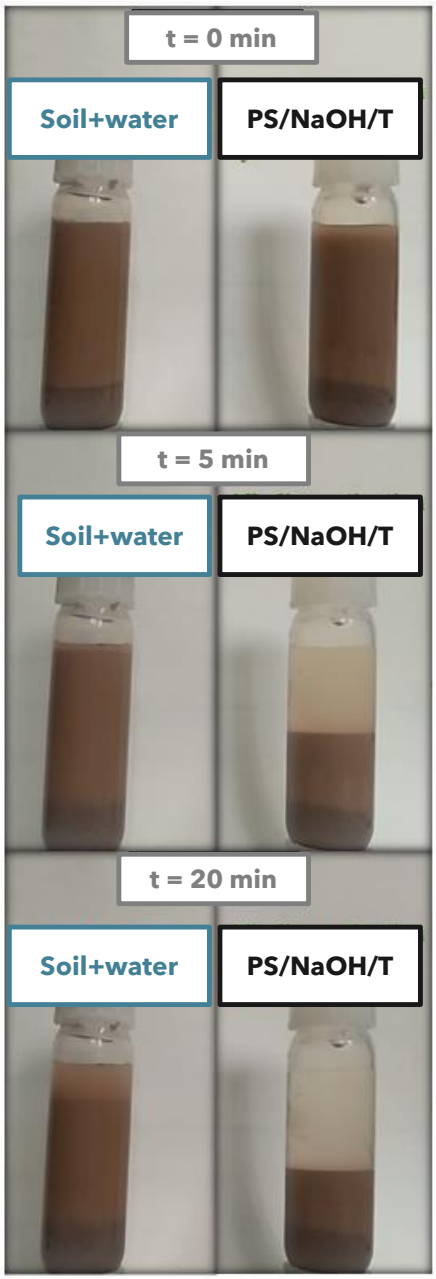

Figure 7.36. Separation of phases by gravitational sedimentation as a function of time in the presence of water (T1) and in the PS/NaOH/T system (T4) (Table 7.9) (Checa-Fernández, Santos et al. 2021, **ART. 4**).

At the selected operating conditions (T = 50 °C, PS = 40 g L^{-1}, V_L/W_S = 2 and 3 days of treatment), around 71% of the initial PS remained in solution. Therefore, the liquid phase could be reused to treat a new batch of contaminated soil, adjusting the corresponding initial concentration of NaOH (and PS). Moreover, fast separation of the aqueous and soil phases was observed in alkali and oxidant presence. The time required for soil sedimentation in the absence of these reagents was much longer. After only 20

minutes of gravitational sedimentation, a clear separation of phases was obtained when NaOH and PS were added, whereas a soil-water suspension remains at this time in the "soil-water" experiment under the same conditions (Figure 7.36). In this way, recovering the supernatant solution for a new remediation batch would be relatively simple.

Operation conditions study: Effect of stirring rate

The effect of stirring rate (10, 50, and 100 rpm) on the degradation of HCHs was investigated. To better appreciate the differences obtained (if any), the operating conditions in which lower reaction rates were previously obtained have been selected for this study (PS = 40 g L^{-1} and T = 40 ºC). The results after 7 days of treatment have been depicted in Figure 7.37. No significant differences in β-HCH and COCs conversion have been observed when increasing the stirring rate from 10 to 50 rpm, obtaining similar results for the rest of the variables studied. Nevertheless, a higher pollutants removal was achieved by increasing the stirring rate up to 100 rpm (T4), reaching a COCs conversion of 95% (10% higher than the values obtained at lower stirring rates). The fraction of remaining TCBs (TCBs'/HCH_0) decreased with the stirring rate (Figure 7.37). As the stirring rate increased, the resistance to external transport decreased, favouring the solubilization of TCBs from the soil to the aqueous phase. Consequently, the oxidation rate of the COCs is enhanced. Hence, based on the results obtained, a stirring rate of 100 rpm is recommended for the remediation experiments, although acceptable COCs conversions were also obtained at lower stirring rates. Nevertheless, additional tests on a larger scale and different reactor configurations are recommended to extrapolate the results obtained in the current study and obtain more representative results of field conditions.

The soil TOC concentration was practically unaffected (decreased only by 0.13% from the initial value) after the remediation process (T = 50 °C, PS = 40 g L^{-1}, V_L/W_S = 2, pH >12, 100 rpm, and 3 days). The soil organic matter, mainly attributable to humic acid-type compounds, was resistant to the oxidation treatment. Therefore, soil characteristics appear not to be significantly affected after treatment, and applying a subsequent bioremediation treatment seems feasible. However, before proceeding with bioremediation treatments, it is interesting to evaluate how the oxidation treatment affects the toxicity of the soils.

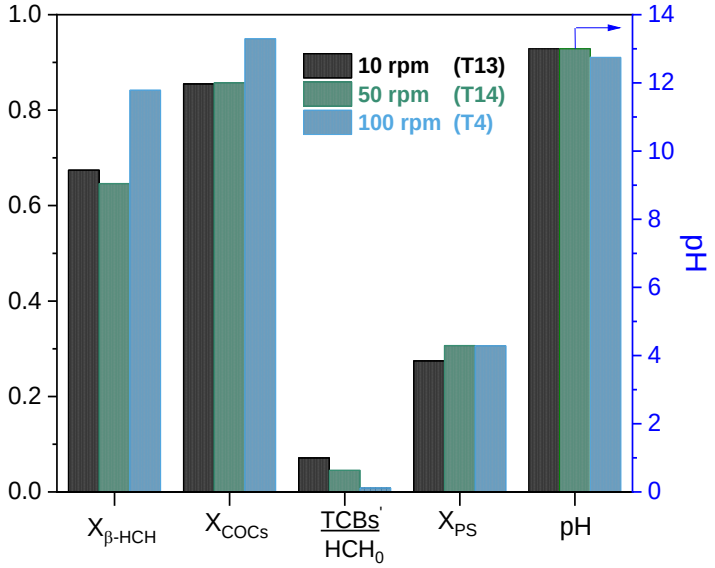

Figure 7.37. Conversion of β-HCH, COCs, and PS, TCBs'/HCH_0, and pH at different stirring rates (10, 50, and 100 rpm) after 7 days (T13, T14, and T4). Experimental conditions: $C_{HCHs,0}$ = 373 mg kg^{-1} (TS L2), T = 40 °C, V_L/W_S = 2, C_{PS} = 40 g L^{-1}, C_{NaOH} = 13.5 g L^{-1} (Checa-Fernández, Santos et al. 2021, **ART. 4**).

7.2.3.2. PS/NaOH/US

As stated, HCHs-polluted soil remediation is usually limited by the slow desorption of pollutants from the soil to the aqueous phase (Peng, Deng et al. 2015) and their low aqueous solubility. In this context, the global degradation rate is expected to increase by favoring the pollutants desorption, which can be achieved by intensifying the process through the application of US. The effect of US on COCs desorption from the soil to the aqueous phase has been first studied (desorption experiments, at alkaline conditions) to confirm this hypothesis. Subsequently, the efficiency of the **alkaline activation of PS intensified by US** (**PS/NaOH/US**) treatment has been evaluated (oxidation experiments).

Desorption experiments

The experimental conditions of the desorption experiments (runs "D") have been summarized in Table 7.10. The effect of US application on pollutant desorption has been determined in the absence of oxidant (D2) in a US bath (Figure 6.3-c, Subsection 6.2.1). The power density (energy input per unit volume) has been estimated considering the volume of the bath (2.5 L) and reactors (2 reactors of 30 mL each). The results were compared with those without US application (6 h, 22 ºC) (D1). Desorption experiments were conducted at alkaline conditions (C_{NaOH} =13.5g L^{-1}) considering that COCs distribution changes at pH ≥12 due to HCHs hydrolysis to TCBs (Santos, Fernandez et al. 2018, Checa-Fernández, Santos et al. 2021, **ART. 4**). A reference experiment (D_{eq}, equilibrium conditions, rotatory agitator (Figure 6.3-a) in the absence of US, 48 h, 22 ºC, 30 rpm) was also performed.

Table 7.10. Experimental conditions of desorption experiments ($C_{HCHs,0}$ = 404 mg kg^{-1} (TS L2), W_S = 15 g, V_L/W_S = 2) (Checa-Fernández, Santos et al. 2022, **ART. 5**).

Run	Soil	NaOH (g L^{-1})	US power (W)	US power density (W L^{-1})	Isothermal conditions	Reaction time (h)	Stirring
D1	TS L2	13.5	0	0	Yes (22 ºC)	6	No
D2	TS L2	13.5	350[b*]	137[*]	No (22-61 ºC)	6	No
D_{eq}	TS L2	13.5	0	0	Yes (22 ºC)	48	Yes (rotatory, 30 rpm)

D_{eq} = equilibrium experiment. [b]Experiment carried out in a US bath (*Figure 6.3-c*, 40 kHz, 2.56 L). [*]Calculated considering the volume of the bath (2.5 L) and reactors (2 reactors of 30 mL each).*

The concentration of COCs (mmol L^{-1}) solubilized to the aqueous phase with and without US application (D2 and D1, respectively) has been represented in Figure 7.38-a, together with the concentration of COCs solubilized in the aqueous phase at equilibrium conditions (D_{eq}) (blue line). The time required to achieve the equilibrium between both phases was previously evaluated by measuring the evolution of COCs concentration in the aqueous phase up to 48 h, and an asymptotic value was obtained from 24 h (data not shown). It should be noted that the temperature increase associated with US application can also favour the desorption process (Deng, Lin et al. 2015). Thus, to take advantage of this fact, D2 was carried out without temperature control, reaching 60 ºC after 6 h (D1 and D_{eq} were performed at room temperature, 22 ºC).

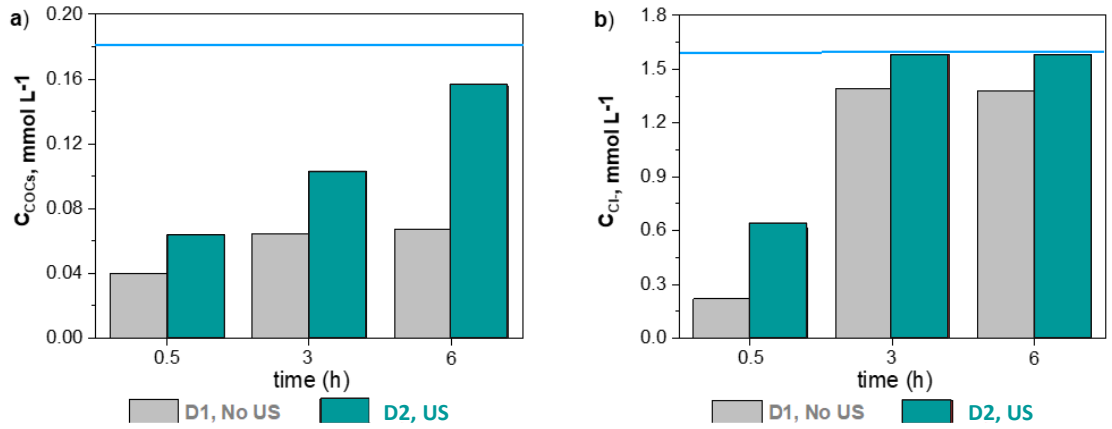

Figure 7.38. Effect of the US application on the desorption of COCs (a) and Cl^- (b) to the aqueous phase. The blue line represents the experimental value obtained at equilibrium conditions (D_{eq}, pH > 12, t ≥ 24h). Operational conditions summarized in Table **7.10** (Checa-Fernández, Santos et al. 2022, **ART. 5**).

COCs (mainly TCBs, pH > 12) desorption rate from the soil to the aqueous phase is notably increased when US irradiation was applied (and the induced temperature increased) (Figure 7.38-a). Hamdaoui, Naffrechoux et al. (2003) studied the effects of US on the desorption of *p*-chlorophenol from granular activated carbon, reporting that the desorption rate was favoured by increasing US intensity, temperature, and NaOH addition. Moreover, the chloride concentration released to the aqueous phase with and without US application has been compared (Figure 7.38-b). As can be seen, the concentration of chlorides generated from HCHs hydrolysis and subsequently released is minimal at short reaction times. The Cl^- concentration increased with US application and reaction time, reaching the value obtained in equilibrium conditions (24 h, blue line, 1.61 mmol L^{-1}) from only 3 h of US application. From these results, it can be concluded that i) US application enhances COCs desorption from the soil to the aqueous phase and ii) the solubilisation rate of COCs is more hindered than the release of chlorides.

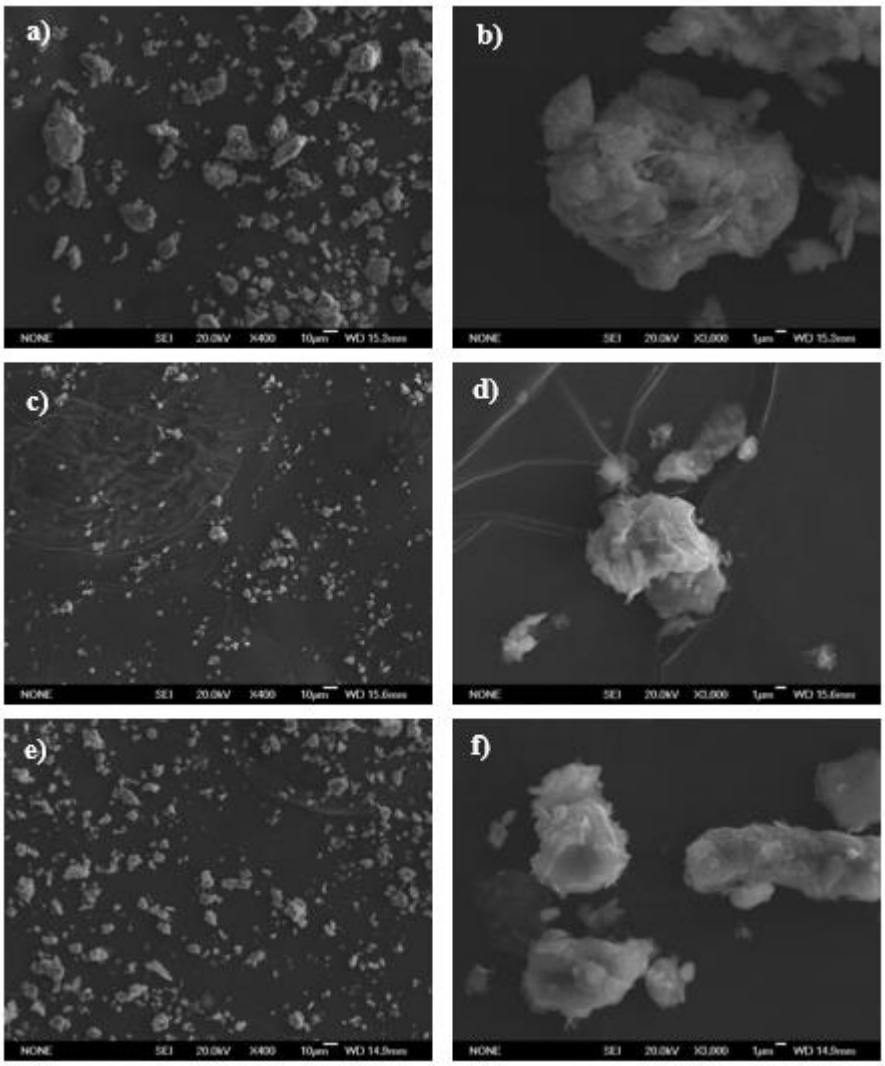

Figure 7.39. SEM images of the soil (TS L2) before treatment (a-b), after the US application at alkaline conditions (desorption experiment, D2) (c-d), and after the remediation treatment PS/NaOH/US (U10[b]) (e-f) (Checa-Fernández, Santos et al. 2022, **ART. 5**).

SEM analysis showed that US application facilitates the breakdown of soil aggregates, decreasing the soil particle size (Figure 7.39-a *vs*. Figure 7.39-c) without noticeable changes in particle morphology (Figure 7.39-b *vs.* Figure 7.39-d). These results are consistent with previous studies in which the effect of US on soil structure was evaluated (Goi and Viisimaa 2015, He, Tan et al. 2019, Lei, Zhang et al. 2020). Thus, the US application increases the surface area of the soil, allowing higher desorption of pollutants from the soil to the aqueous phase.

Oxidation experiments

The conditions used in the US oxidation experiments (runs "U": U1-U18) are listed in Table 7.11. The power density (energy input per unit volume) corresponding to each US power ([b]) has been estimated considering the total volume sonicated (2.68 L). First, to evaluate the effect of the US application, an experiment was carried out at isothermal conditions (U2), and the results obtained were compared with those obtained without US application (U1), and the results are shown in Figure 7.40.

Table 7.11. Operating conditions of PS/NaOH/US experiments ($C_{HCHs,0}$ = 404 mg kg^{-1} (TS L2), W_S = 15 g, V_L/W_S = 2, molar NaOH:PS = 2) (Checa-Fernández, Santos et al. 2022, **ART. 5**).

Objective	Run	Soil	C_{PS} (g L^{-1})	US Power (W)	US Power density (W L^{-1})	Isothermal conditions
Synergetic influence of US application and induced T	U1	TS L2	40	**0**	**0**	**Yes (22 °C)**
	U2	TS L2	40	**350[b*]**	**137**	**Yes (22 °C)**
Influence of US power	U3	TS L0	40	**0**	**0**	No
	U4	TS L2				
	U5	TS L0	40	**0[a]/20[b]**	**0/7**	No
	U6	TS L2				
	U7	TS L0	40	**0[a]/65[b]**	**0/24**	No
	U8	TS L2				
	U9	TS L0	40	**0[a]/165[b]**	**0/62**	No
	U10	TS L2				
	U11	TS L0	40	**0[a]/245[b]**	**0/91**	No
	U12	TS L2				
Influence of C_{PS}	U13	TS L0	**10**	0[a]/165[b]	0/62	No
	U14	TS L2				
	U15	TS L0	**20**	0[a]/165[b]	0/62	No
	U16	TS L2				
	U9	TS L0	**40**	0[a]/165[b]	0/62	No
	U10	TS L2				
	U17	TS L0	**60**	0[a]/165[b]	0/62	No
	U18	TS L2				

[a]Without US but reproducing the temperature ramp associated with each US power. [b]US bath (40 kHz, 2.56 L). [b]US probe (20 kHz, 2.68 L).*

After that, the effect of US power (0, 20, 65, 165, and 245 W) using a PS concentration of 40 g L^{-1} has been studied (U4, U6[b], U8[b], U10[b], U12[b], Table 7.11). The unproductive consumption of PS (conversion of oxidant not associated with pollutant abatement) was evaluated by carrying out equivalent runs but using unpolluted soil, TS L0 (U3, U5[b], U7[b], U9[b], U11[b]). The effect of the initial oxidant concentration (10, 20, 40, and 60 g L^{-1}) was

tested by applying a US power of 165 W (U14[b], U16[b], U10[b], U18[b]). Similarly, the unproductive consumption of PS (using the same initial C_{PS} values) has been evaluated in unpolluted soil (U13[b], U15[b], U9[b], U17[b]). It should be noted that the application of US increases the temperature of the reaction medium (Deng, Lin et al. 2015). The contribution of each effect (US and temperature) has been evaluated by carrying out additional experiments without the application of US but simulating the temperature ramp associated with each US power under study. The reactors were placed in a beaker (with the same volume as the US bath) on a temperature-controlled stir plate (IKA RCT Basic). These experiments have been assigned with the same number as the corresponding experiments carried out with US application ([b]) but with the superscript ([a]) (see Table 7.11).

Results obtained with US application at isothermal conditions (U2) have been compared with the equivalent without US application (U1) (Figure 7.40).

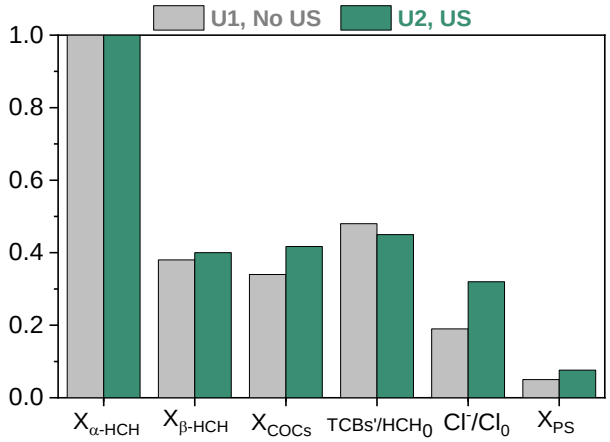

Figure 7.40. Effect of US application at isothermal conditions. Operational conditions: $C_{HCHs,0}$ = 404 mg kg^{-1} (TS L2), W_S = 15 g, V_L/W_S = 2, molar NaOH:PS = 2, C_{PS} = 40 g L^{-1}, US power = 350 W (when applicable, U2), T = 22°C (Table 7.11) (Checa-Fernández, Santos et al. 2022, **ART. 5**).

The conversion of α-HCH was complete in both experiments due to its almost instantaneous dehydrochlorination. The degradation of COCs at ambient temperature and the absence of US (U1) was low (X_{COCs} = 0.34). This value was slightly increased with US application (X_{COCs} = 0.42), according to the higher β-HCH conversion and lower concentration of remaining TCBs. Higher differences were obtained concerning the dechlorination degree, which could be partly associated with a greater concentration of COCs in the liquid phase with US application, and, therefore, a greater oxidant consumption. On the other side, it should be noted that the dechlorination degree achieved is even lower than the dechlorination degree expected considering the HCH

isomers instantaneously hydrolyzed (α-, γ-, δ-, ε-HCH), that β-HCH hydrolysis is negligible, and neglecting the degradation of the generated TCBs (Cl/Cl_0 = 0.36, Eqs. (7.11) and (7.5)). The low chlorinated concentration in the aqueous phase can be explained by attending to diffusional problems in the desorption of chlorides from the soil phase (where they are generated) to the aqueous one (where they are measured), as previously mentioned.

The improvements obtained in COCs degradation and dechlorination are considered insufficient to justify the use of US at room temperature, which is consistent with the results reported by other authors (Wang and Zhou 2016, Lei, Tian et al. 2020). The heat induced by US application is expected to significantly improve the process, playing a critical role in the i) desorption of pollutants from the soil phase (Peng, Deng et al. 2015), ii) thermal activation of PS, generating sulfate radicals (Eq. (4.3), Subsection 4.2), that, at these conditions (pH≥12), evolve to hydroxyl radicals (Eqs. (4.4) and (4.5), Subsection 4.2), and finally, iii) content of dissolved oxygen, that decreases at elevated temperature (Lei, Tian et al. 2019), also favouring the production of hydroxyl radicals (Eq. (7.19)) to the detriment of hydroperoxyl and superoxide radicals (Eqs. (7.17) and (7.18), respectively) (Monteagudo, El-taliawy et al. 2018). Consequently, there is a threshold temperature value in the PS/NaOH/US system required to generate radicals, and an elevated temperature could affect the efficiency of HCHs dechlorination.

$$H^{\bullet} + O_2 \rightarrow HO_2^{\bullet} \quad (7.17)$$

$$HO_2^{\bullet} \rightarrow H^+ + O_2^{\bullet -} \quad (7.18)$$

$$H^{\bullet} + H_2O \rightarrow OH^{\bullet} + H_2 \quad (7.19)$$

The temperature increase depends on different parameters such as the frequency, the US power, and the solution volume. As expected, the temperature of the aqueous medium increased because of the US application. The isolation of the experimental device also favoured temperature increase, which was proportional to the US power (Figure 7.41).

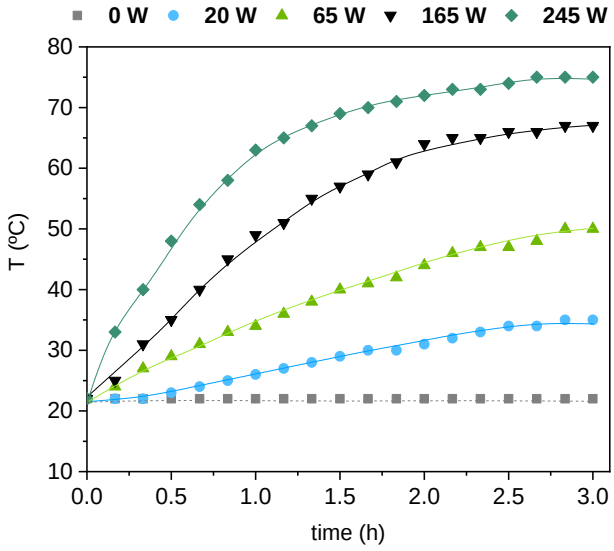

Figure 7.41. Temperature increase as a function of US power (0-245 W, corresponding to 0-91 W L^{-1}) (US probe, 20 kHz, 2.5 L) (Checa-Fernández, Santos et al. 2022, **ART. 5**).

Thus, once it has been demonstrated: i) the positive effect of US on pollutant desorption (which will also favour the subsequent oxidation of pollutants and overall kinetics) and ii) the slight positive effect of US on pollutants oxidation at room temperature, the combined effect of US with the associated temperature increase will be studied. For this purpose, the effect of the two most relevant variables will be evaluated: US power and initial PS concentration (carried out without temperature control).

US power was assessed from 0 to 245 W (corresponding to a power density of 0-91 W L^{-1}). The US power density range used in the current work is below the usually found for soil remediation using PS (Deng, Lin et al. 2015, Lei, Tian et al. 2019). The consumption of PS is the result of i) COCs oxidation (Eqs. (7.3) and (7.13)) and ii) its unproductive consumption (Eq. (7.14)) (Kolthoff and Miller 1951, Goulden and Anthony 1978). Therefore, to determine the cause of oxidant consumption, the results of PS conversion obtained at 3 h in the presence of polluted soil (TS L2, no-striped, green bars) at the different powers applied ($U6^b$, $U8^b$, $U10^b$, $U12^b$) have been compared with those obtained using unpolluted soil (TS L0, striped, green bars) ($U5^b$, $U7^b$, $U9^b$, $U11^b$). Moreover, to determine whether the consumption of PS is due to the US or the associated temperature increase, the results obtained with US (^{b}) application have been compared with those obtained without US (0 W) but reproducing the same temperature-ramp associated with each US power. This comparison has been carried out using both polluted (no-striped, grey bars) ($U6^a$, $U8^a$, $U10^a$, $U12^a$) and unpolluted (striped, grey bars) ($U5^a$, $U7^a$, $U9^a$, $U11^a$)

soils. The results obtained have been depicted in Figure 7.42-a (the temperature reached at the end of these runs, T_{3h}, has been included).

As expected, the higher the US power, the higher the PS conversion. However, this increase is more pronounced in the case of polluted soil. Around 0.03, 0.04, 0.10, and 0.20 of PS conversions were achieved with the reference soil at 20, 65, 165, and 245 W, respectively, which increased up to 0.07, 0.09, 0.24, and 0.38 in the presence of pollutants, suggesting that PS is consumed in the oxidation of COCs. On the other hand, the difference between PS conversion achieved in the experiments carried out with US application is higher than those obtained without US (green and grey bars, respectively, Figure 7.42-a). These differences increase with the US power, indicating that US favours an efficient use of PS.

The influence of US power input on the conversion of α-HCH and β-HCH and the molar fraction of TCBs generated and not oxidized (TCBs'/HCH_0) after 3 hours of reaction time is shown in Figure 7.43-a (the temperature reached has been included, the temperature ramp can be seen in Figure 7.41). Regardless of the US power applied, α-HCH conversion was complete in all runs at 1 h of reaction time (Eq. (7.11)), confirming the almost instantaneous hydrolysis of this compound (data not shown). The abatement of β-HCH (limiting step) is highly favored by the increase in US power and reaction time, reaching a maximum conversion of 0.74 at 3 h when using US power ≥ 165 W (62 W L^{-1}). In the same line, the molar fraction of generated and non-oxidized TCBs (TCBs'/HCH_0) decreased notably with US power. When comparing the results obtained with and without US under the same temperature conditions (Figure 7.42-b), a remarkable increase (approximately 20%) in the removal of β-HCH (the most refractory towards oxidation) was achieved under US application. Consequently, the conversion of COCs also increases (especially in the case of low power densities). However, this increase is less significant because α-HCH (majority isomer) conversion is 100% in all cases due to its fast hydrolysis. Likewise, the dechlorination degree and the chlorine balance increased moderately when US is applied (data not shown), indicating greater mineralization and lower concentration of chlorinated intermediate compounds at these conditions.

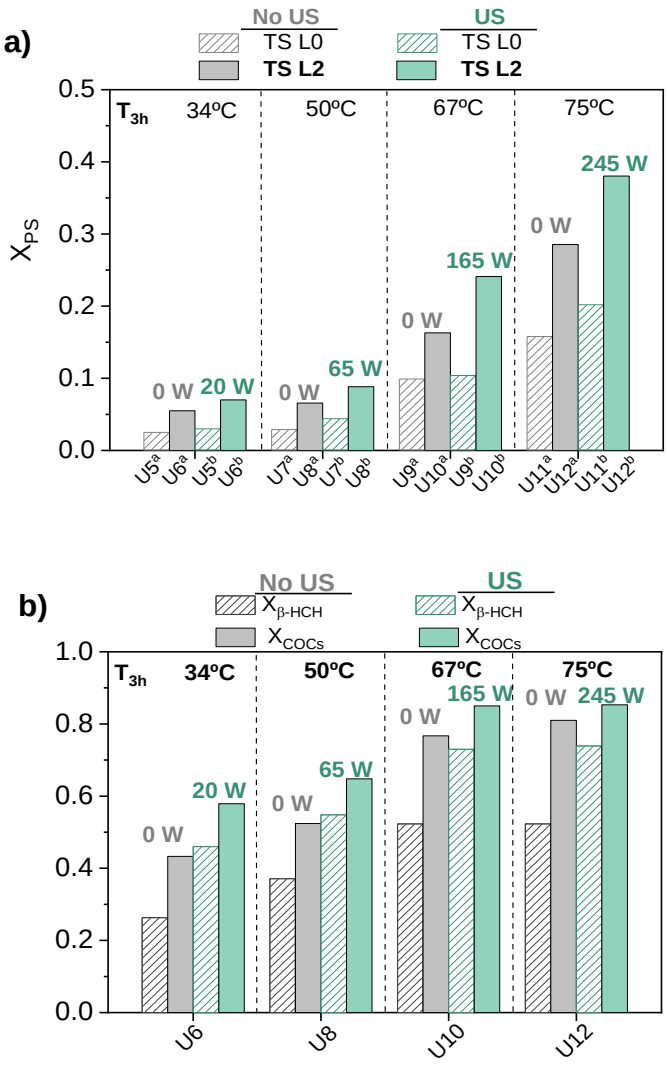

Figure 7.42. Effect of US application on (a) PS conversion (in the presence of polluted and unpolluted soil) and (b) β-HCH and total COCs conversion (in the presence of polluted soil) at different US power. T_{3h} = temperature reached at final reaction time. Operational conditions: $C_{HCHs,0}$ = 404 mg kg^{-1} (TS L2), W_S = 15 g, V_L/W_S = 2, molar NaOH:PS = 2, C_{PS} = 40 g L^{-1} (Table 7.11) (Checa-Fernández, Santos et al. 2022, **ART. 5**). *[a]Without US but reproducing the temperature ramp associated with each US power. [b]US probe (20 kHz, 2.68 L).*

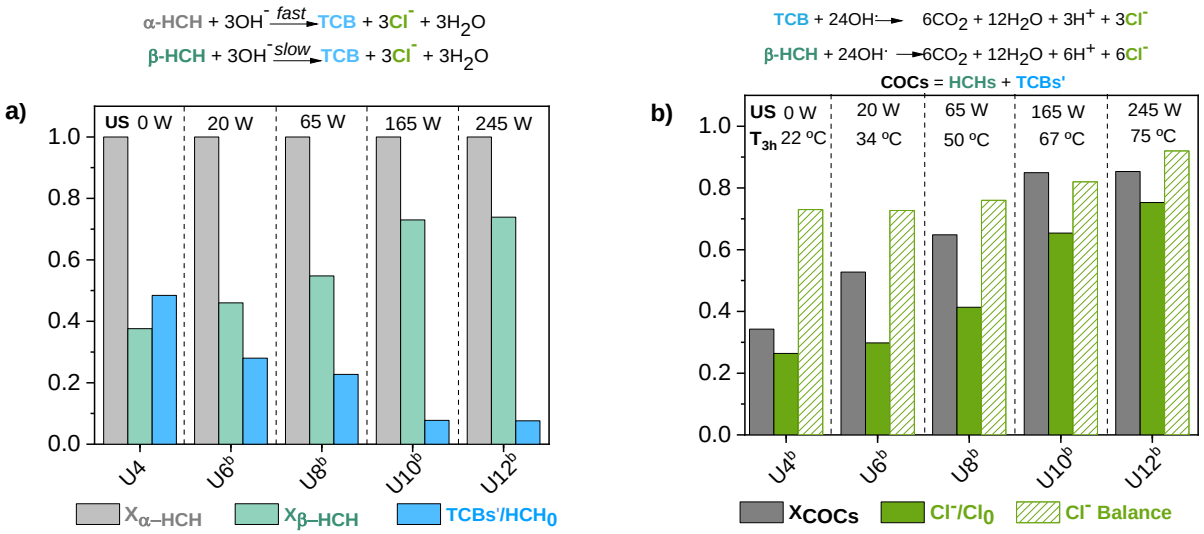

Figure 7.43. Influence of US power on (a) α-HCH and β-HCH conversion and TCBs'/HCH_0 ratio and (b) COCs conversion, dechlorination degree (Cl^-/Cl_0), and chlorine balance. T_{3h} = temperature reached at final reaction time. Operational conditions: $C_{HCHs,0}$ = 404 mg kg^{-1} (TS L2), W_S = 15 g, V_L/W_S = 2, molar NaOH:PS = 2, C_{PS} = 40 g L^{-1} (Table 7.11) (Checa-Fernández, Santos et al. 2022, **ART. 5**).

As expected, higher US power resulted in higher COCs conversion (Figure 7.43-b), demonstrating the crucial role of this variable in the remediation process. These results agree with those reported in the literature concerning the degradation of per- and poly-fluoroalkyl substances (PFAS) (Lei, Tian et al. 2020), total petroleum hydrocarbons (TPHs) (Lei, Zhang et al. 2020, Li, Zhang et al. 2022), and phenanthrene (Song, Li et al. 2012). Two reasons could explain this improvement i) increased US power generates more cavitation bubbles and heat, leading to a higher production of radical species (Eqs. (4.3), (4.7) and (4.8), Subsection 4.2) (Monteagudo, El-taliawy et al. 2018, Lei, Zhang et al. 2020); and ii) increased cavitation bubble collapse could produce more substantial turbulence and desorption of pollutants (Figure 7.38), facilitating the convection and mass transportation rate between the oxidant and the contaminants (Lei, Tian et al. 2019, Lei, Zhang et al. 2020). However, it is worth noting that no significant improvement in COCs conversion was observed when applying US power levels > 165 W, which corresponds to 62 W L^{-1}. Two facts can explain this: i) the tiny bubbles formed could coalesce to form larger ones reducing cavitation (Shrestha, Pham et al. 2009), and ii) the dual nature of the soil pollution: HCHs in the form of particulate matter and adsorbed to the soil. The fraction of β-HCH (the most resistant HCH isomer towards oxidation) in the form of particulate matter is more easily removed than that adsorbed onto the soil, as stated in previous chapters. The adsorbed one is probably strongly trapped in the soil, and consequently, its

solubilization (and further oxidation) is highly hindered. Thus, it seems that 165 W is sufficient to degrade the fraction of β-HCH corresponding to particulate matter (its degradation rate increases proportionally with the US power). In contrast, the adsorbed fraction (around 25% of the total) cannot be solubilized (and, therefore, degraded), even when using higher US powers (Figure 7.43-a). This fact results in a stagnation of COCs conversion from 165 W.

Additionally, the positive effect of US power is reflected in the dechlorination degree and chlorine balance (Figure 7.43-b). Dechlorination values below expected values from HCHs hydrolysis were obtained at low US power (Figure 7.43-b). This may be due to chloride diffusional problems from the soil to the aqueous phase (Figure 7.38). Chloride ions adsorbed into the soil cannot be quantified, leading to a mismatch in the chlorine balance at low US power. At the highest US power (245 W, 91 W L^{-1}), more than 90% of the total chlorine balance is accomplished. Moreover, the differences between the dechlorination degree and COCs conversion decrease as the US power increases. This suggests that lower concentrations of intermediate chlorinated compounds remain in the reaction medium when increasing this variable.

Finally, SEM images showed a decrease in particle size after the selected treatment (Figure 7.39-a (initial soil before treatment) *vs.* Figure 7.39-e (soil after treatment $U10^b$)) without noticeable changes in particle morphology (Figure 7.39-b *vs.* Figure 7.39-f). Thus, it is confirmed that the contact between COCs and oxidant (PS) is enhanced by US. On the other side, it should be noted that Na concentration increased in the treated soils. The Na percentage determined by EDS analyses was < 0.1, 0.8, and 1.2% for the untreated soil (TS L2), after the desorption experiment (D2, pH>12, Table 7.10), and after PS/NaOH/US treatment ($U10^b$, Table 7.11), probably in the form of sodium salts (NaOH and Na_2CO_3). This increase in Na concentration can be related to the Na introduced with the alkali (NaOH) and the oxidant (PS).

Once 165 W (62 W L^{-1}) has been selected as the most appropriate US power, the **effect of the initial PS concentration** (10, 20, 40, and 60 g L^{-1}) has been studied. The conversion of PS at 3 h of reaction time is shown in Figure 7.44. The results obtained in the presence of polluted soil (TS L2, no-striped, green bars) at the different PS concentrations ($U14^b$, $U16^b$, $U10^b$, $U18^b$) have been compared with those obtained using the unpolluted soil (TS L0, striped, green bars) ($U13^b$, $U15^b$, $U9^b$, $U17^b$). Moreover, to analyze the cause of PS consumption, the results obtained with US application (^{b}) have been compared with those obtained without US (0 W) but reproducing the same temperature ramp. This

comparison has been carried out using both polluted (TS L2, no-striped, grey bars) (U14[a], U16[a], U10[a], U18[a]) and unpolluted (TS L0, striped, grey bars) (U13[a], U15[a], U9[a], U17[a]) soils.

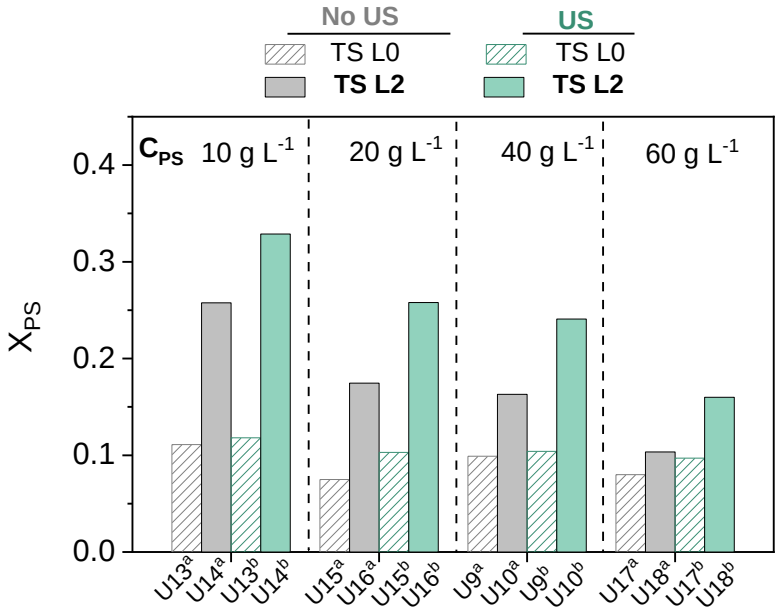

Figure 7.44. Influence of initial C_{PS} on PS conversion. Operational conditions: $C_{HCHs,0}$ = 404 mg kg^{-1} (TS L2), W_S = 15 g, V_L/W_S = 2, molar NaOH:PS = 2, US power = 165 W (Table 7.11). Temperature at final reaction time (3 h), 67 °C (Checa-Fernández, Santos et al. 2022, **ART. 5**).

In the case of TS L2 soil, PS conversion decreased when the initial concentration of this reagent increased, regardless of the application of US. On the other hand, the unproductive consumption of PS with the unpolluted soil (TS L0) remained constant at the different initial PS concentrations tested, following first order-kinetics (Liang, Bruell et al. 2003, Waldemer, Tratnyek et al. 2007, Liang and Su 2009). Considering that COCs degradation increased when increasing the oxidant concentration (Figure 7.45-a and -b), the consumption of PS is mainly attributable to the oxidation of these pollutants. Moreover, the low PS conversion reached at C_{PS} = 60 g L^{-1} and 165 W (X_{PS} < 0.2) would allow the reuse of the supernatant solution to treat a new batch of HCH-polluted soil, lowering the costs associated with the remediation treatment. Figure 7.45-a shows the influence of initial PS concentration (from 10 to 60 g L^{-1}) on the conversion of α-HCH and β-HCH and the molar fraction of TCBs generated and not oxidized (TCBs'/HCH_0). As can be seen, β-HCH and TCBs conversion was enhanced as the initial PS concentration increased. Similarly, the COCs conversion and the dechlorination degree increased when the oxidant concentration increased (Figure 7.45-b). In this line, the difference between the conversion of COCs and the dechlorination degree achieved also decreased with

increasing PS concentration, which indicates a lower concentration of chlorinated byproducts (at these conditions, 83% of the chlorine balance was accomplished). This is probably associated with the increase of active radicals yield ($OH^{\bullet}$ (mainly) and $SO_4^{\bullet-}$) (Lei, Tian et al. 2020, Lei, Zhang et al. 2020). Thus, it has been demonstrated that the treatment PS/NaOH/US may offer a promising on-site treatment option for zones with high levels of HCHs, considerably reducing the reaction time required for their degradation (3 h) in comparison with the results obtained without US: PS/T system (9 days) (Dominguez, Checa-Fernandez et al. 2021, **ART. 3**) and PS/NaOH/T system (3 days) (Checa-Fernández, Santos et al. 2021, **ART. 4**).

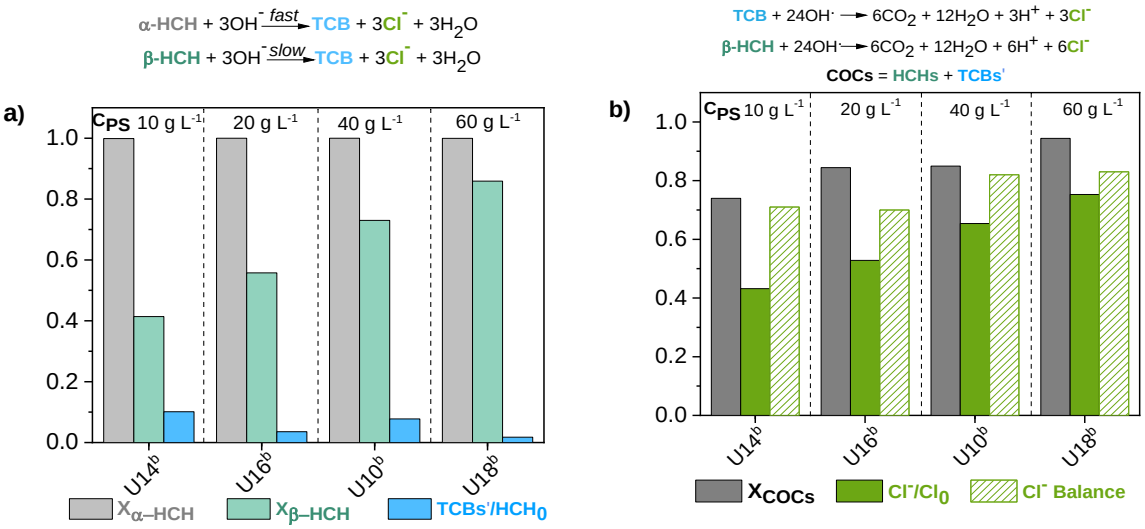

Figure 7.45. Influence of initial PS concentration on α-HCH and β-HCH conversion and TCBs'/HCH_0 degradation (a) and COCs conversion and dechlorination degree (Cl^-/Cl_0) (b). Operational conditions: $C_{HCHs,0}$ = 404 mg kg^{-1} (TS L2), W_S = 15 g, V_L/W_S = 2, molar NaOH:PS = 2, US power = 165 W (Table **7.11**). T_{3h} = temperature reached at final reaction time, 67 °C (Checa-Fernández, Santos et al. 2022, **ART. 5**).

7.2.3.3. S/PS/NaOH/T

The alkaline activation of PS intensified by temperature (PS/NaOH/T) has resulted in interesting results when remediating soils contaminated with HCHs, although relatively high reaction times were required (> 3 days). The degradation rate was increased by intensifying the process through the US application (PS/NaOH/US), significantly reducing the reaction time. However, the use of US is associated with a high cost for real-scale applications due to the high energy requirements. In this sense, a more economical and feasible alternative could be the use of surfactants, amphiphilic-nature substances able to reduce the surface tension of water (Wang and Mulligan 2004), enhancing HCHs solubilization (Cheng, Zeng et al. 2017). In this context, the use of different **surfactants** to solubilize the pollutants to an aqueous phase and the **treatment of the resulting emulsions** (**S/PS/NaOH/T**) has been evaluated. For that purpose, firstly, solubilization experiments were carried out to assess the surfactant-enhanced solubilization of COCs from soil ("solubilization experiments" (S)). Then, the treatment of the polluted emulsions ("Polluted Emulsion (PE) treatment") was accomplished.

The successful application of surfactants combined with oxidation treatments largely depends on the pollutant/surfactant/oxidant system. Thus, the global treatment efficiency will be determined by i) the surfactant ability to solubilize the HCHs from the polluted soil and ii) the oxidant ability to selectively degrade contaminants in the emulsions.

Solubilization experiments (S)

The main variables affecting the pollutants solubilization step (surfactant, pH, reagents addition order, reagents concentration, liquid/soil ratio, number of solubilization cycles, etc.) using surfactants have been studied. The operational conditions of these experiments (S1-S24) are listed in Table 7.12. This table includes the objective studied, the run number, the type and concentration of surfactant, the NaOH concentration, the ratio between the soil and aqueous phase employed (V_L/W_S), the number of solubilization cycles, and the reaction time used.

Firstly, two experiments in the absence of surfactant, at neutral (S1) and alkaline conditions (S2), were performed to evaluate the effect of pH on COCs solubilization. These results were compared to those carried out with 10 g L^{-1} of surfactant (Sodium dodecyl sulfate (SDS), E-Mulse®-3 (E3), and Tween®-80 (T80)) at neutral (SE3-SE5) and alkaline conditions (S6-S8, C_{NaOH} =13.5 g L^{-1}), respectively. Moreover, the reagents (NaOH and surfactant) addition order effect has been evaluated by adding them simultaneously ([a])

and sequentially ([b]). In the sequential reagents addition experiments, NaOH was firstly added (C_{NaOH} = 27 g L^{-1}, 15 mL), and the reactor stirred for 4 h, time enough to achieve the complete dehydrochlorination of α-HCH (the main soil pollutant, ≈85%) (Checa-Fernández, Santos et al. 2021, **ART. 4**). Afterwards, 15 mL of surfactant solution (C_{surf} = 20 g L^{-1}) was added and shaken for 20 h. The effect of alkali (C_{NaOH}, from 2.5 to 13.5 g L^{-1}, S6-S14) and surfactant concentration (C_{surf}, from 2 to 10 g L^{-1}, S10, S12, S15-S18) has also been evaluated. Finally, three successive solubilization cycles using SDS (S16, S19, and S20) and E3 (S18, S22, and S23) have been performed. The first cycle was carried out at alkaline conditions to favour the COCs dehydrochlorination in soil, enhancing their solubility (Checa-Fernández, Santos et al. 2022, **ART. 5**).

The second and third solubilization cycles were carried out at neutral pH. Lower surfactant concentrations were used in solubilization cycles 2 and 3, as the COCs content in the soil also decreased with solubilization cycles. The results after the third solubilization cycle were compared with those obtained in a single cycle using the highest surfactant concentration applied in the three consecutive washing cycles (5 g L^{-1}) and an aqueous volume and experimental time equal to the sum of that used in the three solubilization cycles (V_L/W_S = 6, t = 72 h). These experiments are named S21 and S24 for SDS and E3, respectively.

To evaluate the surfactant ability to solubilize the pollutants, the partition coefficient ($K_{d,COCs}$, L kg^{-1}), which represents the ratio between the COCs concentration in the soil ($q_{COCs,\ soil}$, mmol kg^{-1}) and aqueous ($C_{COCs,\ aq}$, mmol L^{-1}) phases at equilibrium conditions has been calculated by Eq. (7.20) (Garcia-Cervilla, Santos et al. 2021). The lower the partition coefficient, the greater the pollutants solubilization in the aqueous phase and, therefore, the greater the solubilization capacity of the evaluated surfactant.

$$K_{d,COCs} = \frac{q_{COCs,soil}}{C_{COCs,aq}} \qquad (7.20)$$

Table 7.12. Operational conditions of solubilization experiments ($C_{HCHs,0}$ = 373 mg kg^{-1} (TS L2), W_S = 15 g, V_L/W_S = 2) (Checa-Fernández, Santos et al. 2023, **ART. 6**).

Objective	Run number	Surfactant	$C_{surfactant}$ (g L^{-1})	C_{NaOH} (g L^{-1})	V_L/W_S	S cycle	S time (h)
Effect of surfactant and pH	S1	**No surfactant**	0	**0**	2	1	24
	S2	**No surfactant**	0	**13.5**	2	1	24
	S3	**SDS**	10	**0**	2	1	24
	S4	**E3**	10	**0**	2	1	24
	S5	**T80**	10	**0**	2	1	24
	S6[a,b]	**SDS**	10	**13.5**	2	1	24
	S7[a,b]	**E3**	10	**13.5**	2	1	24
	S8[a,b]	**T80**	10	**13.5**	2	1	24
Effect of alkali cc.	S9	SDS	10	**2.5**	2	1	24
	S10	SDS	10	**4**	2	1	24
	S6	SDS	10	**13.5**	2	1	24
	S11	E3	10	**2.5**	2	1	24
	S12	E3	10	**4**	2	1	24
	S7	E3	10	**13.5**	2	1	24
	S13	T80	10	**2.5**	2	1	24
	S14	T80	10	**4**	2	1	24
	S8	T80	10	**13.5**	2	1	24
Effect of surfactant cc.	S15	SDS	**2**	4	2	1	24
	S16	SDS	**5**	4	2	1	24
	S10	SDS	**10**	4	2	1	24
	S17	E3	**2**	4	2	1	24
	S18	E3	**5**	4	2	1	24
	S12	E3	**10**	4	2	1	24
Successive solubilization cycles and V_L/W_S ratio	S16	SDS	5	4	2	**1**	24
	S19	SDS	2.5	0	2	**2**	24
	S20	SDS	1.25	0	2	**3**	24
	S21	SDS	5	4	**6**	1	**72**
	S18	E3	5	4	2	**1**	24
	S22	E3	2.5	4	2	**2**	24
	S23	E3	1.25	0	2	**3**	24
	S24	E3	5	0	**6**	1	**72**

[a] *Simultaneous and* [b]*sequential reagents (NaOH and surfactant) addition order. When not specified, the addition of reagents has been carried out simultaneously. S =Solubilization.*

- *Effect of surfactant and pH*

To evaluate the surfactant capacity, the moles of COCs in the aqueous phase (blue bars) and the remaining COCs in the soil (grey bars) after solubilization experiments were determined in the presence of surfactants at neutral (Figure 7.46-a) and alkaline (Figure 7.46-b) conditions. The final pH of the aqueous phase has been depicted as points (right axis). The results obtained without surfactants have also been included to facilitate comparison. The partition coefficient ($K_{d,COCs}$, green bars, Eq. (7.20)) at neutral and alkaline pH have been represented in Figure 7.46-c and Figure 7.46-d, respectively.

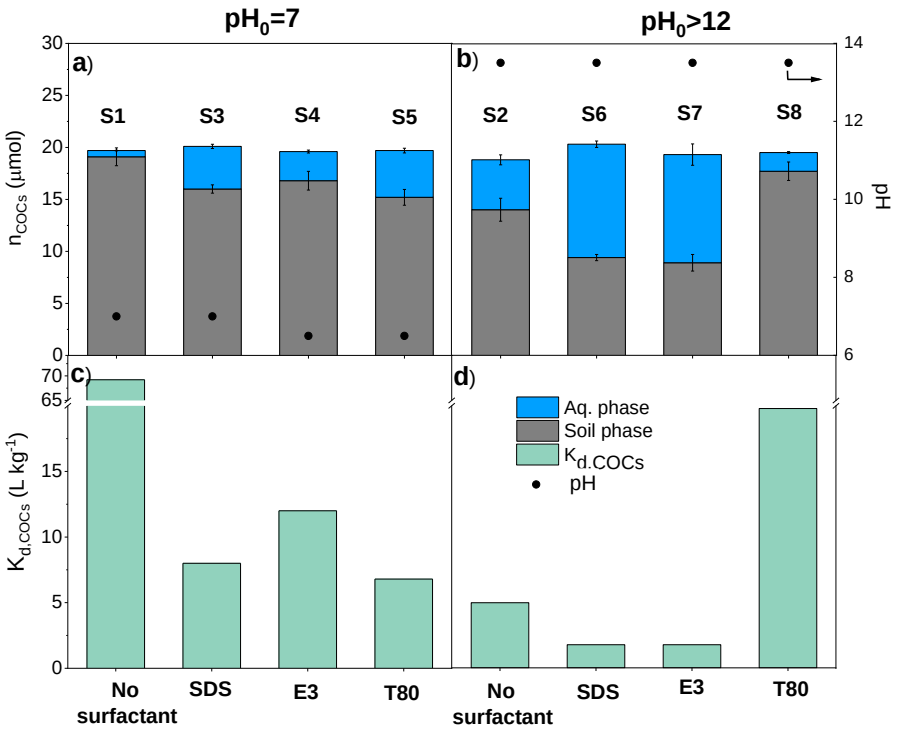

Figure 7.46. Effect of surfactants on COCs solubilization and $K_{d,COCs}$ (Eq. (7.20)) at pH = 7 (a and c) and pH > 12 (b and d, C_{NaOH} = 13.5 g L^{-1}). Final pH values (•). $C_{HCHs,0}$ = 373 mg kg^{-1} (TS L2). 15 g of soil and 30 g of aqueous phase. $C_{surfactant}$ = 10 g L^{-1} (Table 7.12) (Checa-Fernández, Santos et al. 2023, **ART. 6**).

As shown in Figure 7.46-a and -c, adding surfactants (SDS, E3, and T80) at neutral pH improved COCs solubilization from the soil, significantly decreasing $K_{d,COCs}$ values. The order obtained was T80 ≈ SDS > E3. Carboneras, Villaseñor et al. (2020) reported a lindane recovery of about 40% from spiked soil (1000 mg kg_{soil}^{-1}) when using 5 g L^{-1} of SDS and a V_L/W_S = 5. This value corresponds to $K_{d,COCs}$ = 7.5 L kg^{-1}, being similar to those obtained in this work at neutral pH but with higher surfactant concentration in the current

case (10 g L^{-1}). This fact could be explained by: i) pollutants of the soil treated in this research are mostly α- and β-HCH (isomers with lower water solubility than γ-HCH) and ii) it is a real polluted soil, with aged pollution (instead of a spiked soil). It is well known that the aging process leads to contaminant sequestration by soil (Wan, Yuan et al. 2009, Mousset, Huguenot et al. 2016), hindering pollutants solubilization. This point underlines the importance of studying aged-polluted soils (real contamination) instead of spiked soils.

A significantly higher COCs solubilization was obtained at alkaline conditions (pH > 12) with E3 and SDS ($K_{d,COCs}$ = 1.8 L kg^{-1}) than at neutral pH ($K_{d,COCs}$ = 8.0 and 12.0 L kg^{-1}, respectively) (Figure 7.46-c and d). On the contrary, a lower $K_{d,COCs}$ at neutral pH ($K_{d,COCs}$ = 6.8 L kg^{-1}) than at alkaline conditions ($K_{d,COCs}$ = 19.8 L kg^{-1}) was obtained with the nonionic surfactant T80 (Figure 7.46-c and d).

The different soil COCs composition with pH can explain differences in $K_{d,COCs}$ values at neutral and alkaline conditions. Dehydrochlorination of HCHs to TCBs at alkaline pH (Eqs. (7.11) and (7.12)) enhances the COCs solubilization. Moreover, the effect of pH on the surfactant properties must be considered. SDS critical micellar concentration (CMC) decreases when the pH increases (Pham, Kobayashi et al. 2015, García-Cervilla, Romero et al. 2020), contributing to the higher COCs solubilization. The pH effect on E3 CMC at room temperature was negligible in previous works (García-Cervilla, Romero et al. 2020). The results obtained suggest that T80 stability decreased with the pH increase due to surfactant precipitation at alkaline conditions, explaining the lower COCs solubilization and the higher $K_{d,COCs}$ (Figure 7.46-b and d, respectively). Iglesias, Sanromán et al. (2014) tested the stability of this surfactant over the pH range 2–10, finding that a pH increase had a positive effect on the surface tension of T80, which could be related to the better stability of fatty-acids-surfactant micelles in the presence of a base (Abouseoud, Yataghene et al. 2010). Thus, the poor results obtained for the T80 surfactant in the current work could be attributed to the strong alkaline conditions employed here (pH > 12, C_{NaOH} = 13.5 g L^{-1}). To increase T80 stability, the effect of NaOH concentration (maintaining pH > 12) and contacting time has been further analyzed.

The pollutants distribution (in mmol) in the soil and aqueous phases after the surfactant addition (runs S3-S8) at neutral and alkaline conditions are shown in Figure 7.47. As can be seen, the COCs distribution significantly changed as a function of pH, as previously mentioned (Subsection 7.2.2.). It should be highlighted that at pH ≥12, regardless of the surfactant, β-HCH was not completely dehydrochlorinated and remained

in the soil phase (Figure 7.47-d, -e, and -f). This emphasizes that β-HCH hydrolysis (to TCBs) is the limiting step in the solubilization process. This figure also shows the low T80 efficiency under alkaline conditions. At pH>12, the surfactant capacity of T80 was low, and it was no able to solubilize the TCBs generated.

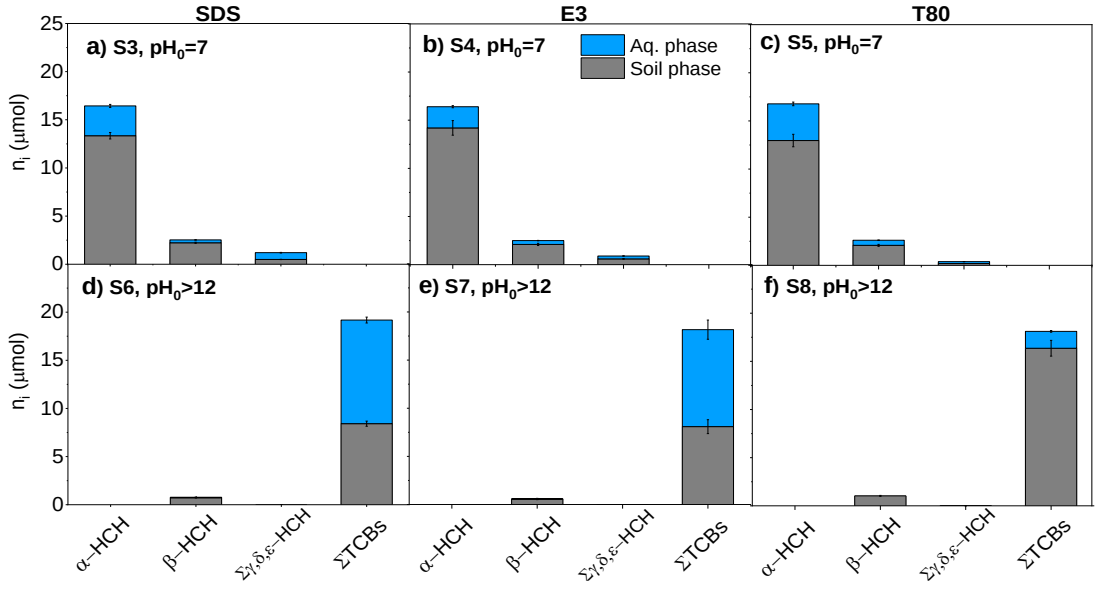

Figure 7.47. Effect of surfactants on COCs distribution (n_i in mmol) in soil and aqueous phases at a-c) pH_0 = 7 and d-f) pH_0 > 12. $C_{HCHs,0}$ = 373 mg kg $^{-1}$ (TS L2). $C_{surfactant}$ = 10 g L^{-1} (Table 7.12) (Checa-Fernández, Santos et al. 2023, **ART. 6**).

- *Effect of alkali concentration*

As previously observed, the COCs solubilization generally increased at alkaline conditions mainly due to the generation of TCBs. Regrettably, the stability of one of the tested surfactants (T80) is compromised in these conditions. Experiments at lower NaOH concentrations (4 and 2.5 g L^{-1}, $pH_0 \geq 12$ in all cases) have been performed with the three surfactants tested to analyze the alkali effect on surfactant stability. The distribution of COCs between the soil and the aqueous phase, the corresponding $K_{d,COCs,}$ and final pH values have been plotted in Figure 7.48. As NaOH concentration decreases, the pH of the emulsion (24 h) decreases regardless of the surfactant used. Nevertheless, it remains above 12 at all the NaOH concentrations, ensuring the HCHs conversion to TCBs in all the scenarios tested.

The decrease of NaOH increased the solubilized moles of COCs when T80 was used, with the consequent reduction in the partition coefficient ($K_{d,COCs}$ was 19.8, 7.0, and 2.4 L kg^{-1} for C_{NaOH} = 13.5, 4.0, and 2.5 g L^{-1}, respectively). However, this value was higher than

those obtained with the other two surfactants at the three NaOH concentrations tested and the use of T80 in subsequent tests was discarded.

Working with SDS and E3, the partition coefficient decreased when NaOH concentration decreased from 13.5 to 4 g L^{-1} but slightly increased at NaOH concentrations < 4 g L^{-1}. Therefore, a concentration of NaOH equal to 4 g L^{-1} has been selected for the pollutant solubilization step with these surfactants (SDS and E3). Lower alkali concentrations also resulted in lower costs and less impact on the treated soil.

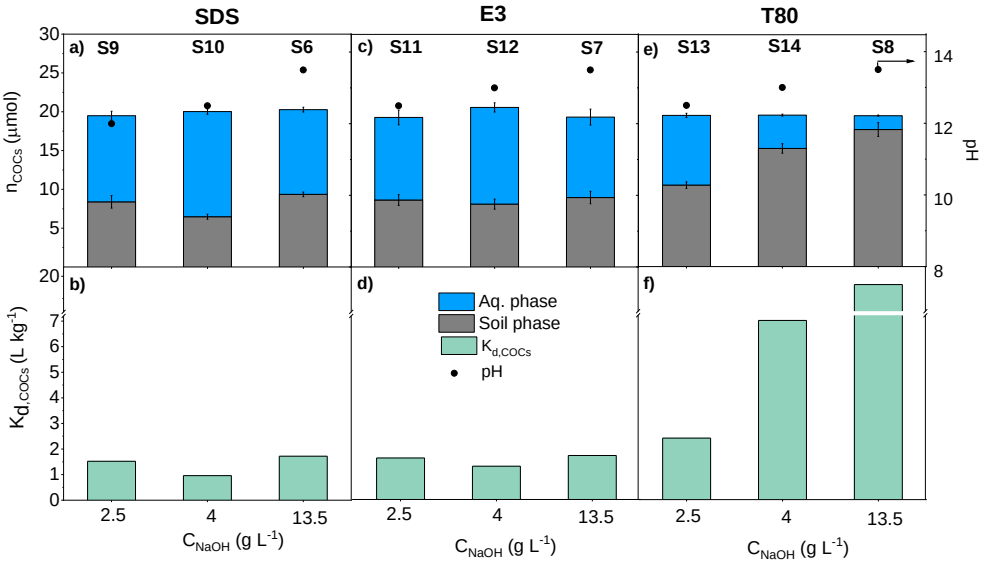

Figure 7.48. Effect of alkali concentration on COCs solubilization and $K_{d,COCs}$ (Eq. (7.20)) when using SDS (a-b), E3 (c-d), and T80 (e-f). Initial pH > 12 in all runs. Final pH values (•). $C_{HCHs,0}$ = 373 mg kg $^{-1}$ (TS L2). C_{surf} = 10 g L^{-1} (Table 7.12) (Checa-Fernández, Santos et al. 2023, **ART. 6**).

- *Effect of surfactant concentration*

The effect of surfactant concentration (2-10 g L^{-1}, SDS, and E3) was studied using 4 g L^{-1} of NaOH. The results obtained for COCs distribution, final pH, and $K_{d,COCs}$ have been depicted in Figure 7.49 a-d. The higher the surfactant concentration, the higher the COCs concentration in the emulsion, as reported in the literature (Zhou and Zhu 2005, Yang, Zhu et al. 2006, Congiu and Ortega-Calvo 2014, Iglesias, Sanromán et al. 2014, Lamichhane, Bal Krishna et al. 2017). Thus, $K_{d,COCs}$ decreased by increasing the surfactant concentration (Figure 7.49-b and Figure 7.49-d for SDS and E3, respectively), being more significant from 2 to 5 g L^{-1} than from 5 to 10 g L^{-1}. This fact may be due to the increase in the solubility

of contaminants with surfactant concentration but an asymptote was reached (Pan, Deng et al. 2016), highlighting the need to study each particular case.

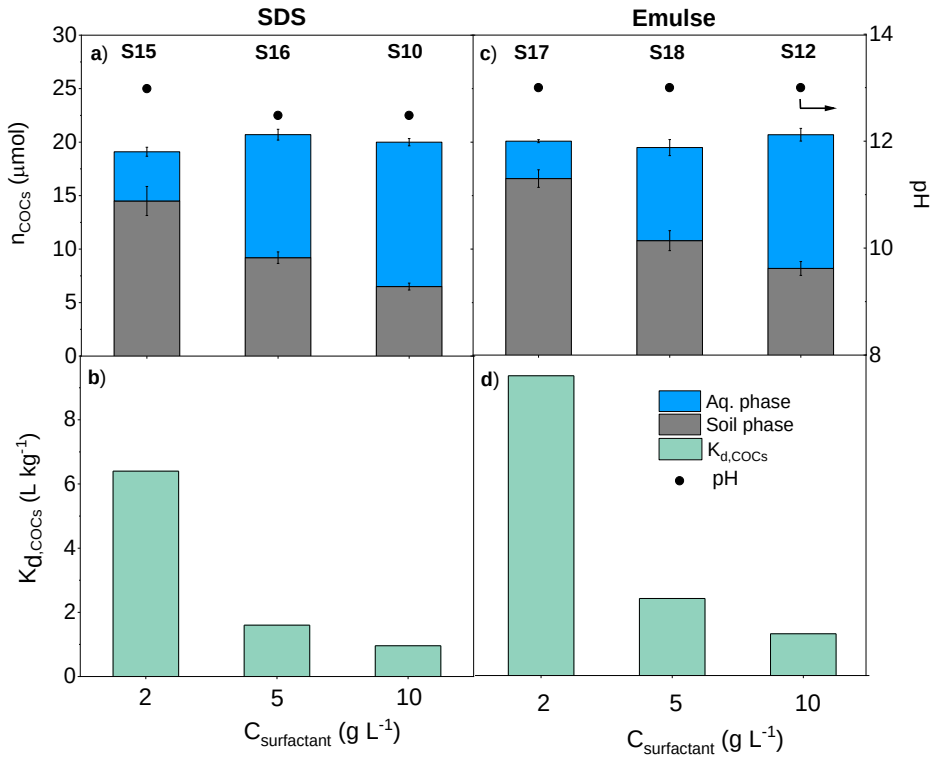

Figure 7.49. Effect of surfactant concentration on COCs solubilization and $K_{d,COCs}$ (Eq. (7.20)) when using SDS (a-b) and E3 (c-d). Final pH values (•). $C_{HCHs,0}$ = 373 mg kg $^{-1}$ (TS L2). C_{NaOH} = 4 g L^{-1} (Table 7.12) (Checa-Fernández, Santos et al. 2023, **ART. 6**).

On the other hand, an excess of surfactant concentration in the contaminated emulsions decreased the efficiency of the process due to: i) surfactant micelles can act as a protective medium, significantly reducing the COCs availability towards radicals oxidation (Trellu, Oturan et al. 2017, Dominguez, Romero et al. 2019), and ii) the surfactant can compete with the contaminants for the radicals formed (Bouzid, Maire et al. 2017, Trellu, Oturan et al. 2017). Thus, a concentration of surfactant of 5 g L^{-1} has been selected for the solubilization stage.

- *Effect of successive solubilization cycles*

Three successive solubilization cycles were performed with SDS and E3 at the conditions previously selected. COCs removal percentage from polluted soil in these cycles ("solubilization rate") has been calculated following Eq. (7.21), in which $C_{COCs,aq}$ is the COCs concentration in the aqueous phase, $q_{COCs,soil}$ is the initial COCs concentration in the polluted soil, and V_L/W_S is the liquid/soil ratio used. The results obtained are depicted in Figure 7.50. Additionally, the partition coefficient, $K_{d,COCs}$ (L Kg^{-1}) (Eq. (7.20)) for each solubilization cycle have been included.

$$\text{Solubilization rate } (\%) = \frac{C_{COCs,aq} \cdot \frac{V_L}{W_S}}{q_{COCs,soil}} \cdot 100 \qquad (7.21)$$

According to Figure 7.50, 58.4%, 21.1%, and 3.0% of the initial COCs in soil were solubilized to the aqueous phase after the first, second, and third solubilization cycle with SDS, with a total removal of pollutants from the soil of 82.5%. Total COCs removal was slightly higher with E3, with a solubilization rate of 88.8% (45.7%, 27.0%, and 16.1% after the first, second, and third solubilization cycles, respectively). $K_{d,COCs}$ values in the successive solubilization cycles increased in the case of SDS (Figure 7.50-a) and slightly decreased in E3 (Figure 7.50-b). In the first solubilization cycle with SDS, more COCs in the soil were solubilized (compared to E3). The remaining COCs in the soil after the first solubilization cycle seem less accessible to the surfactant due to stronger adsorption to the soil or a hindering effect of the adsorbed SDS. On the contrary, E3 allowed desorbing COCs with the same effectiveness in successive solubilization cycles (similar $K_{d,COCs}$ values). COCs solubilized in runs S21 (SDS) and S24 (E3) were lower (72%) despite the higher mass of surfactant used in these runs compared with the total surfactant added in the corresponding three successive solubilization runs.

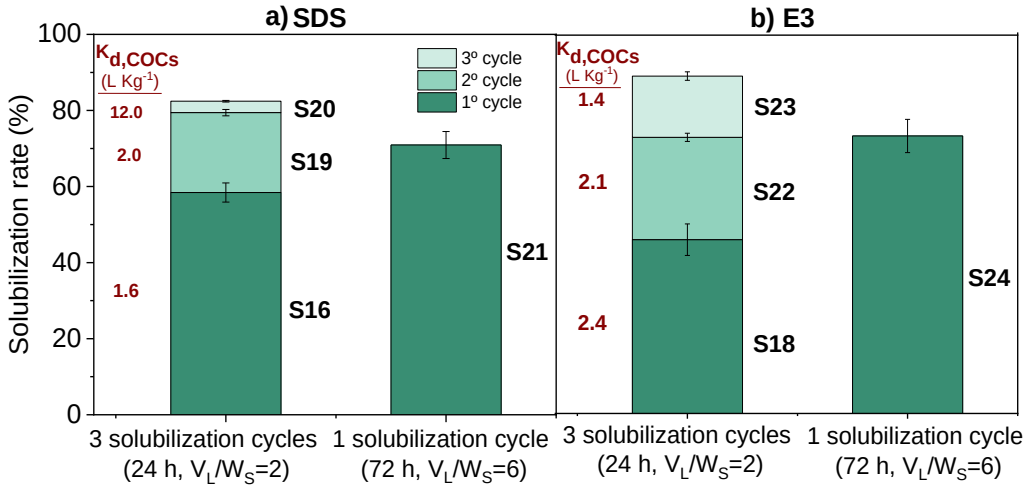

Figure 7.50. Effect of successive solubilization cycles and V_L/W_S in the percentage of COCs removed from the soil with SDS (a) and E3 (b). $K_{d,COCs}$ (Eq. (7.20)) are included. Operational conditions summarized in Table 7.12 (Checa-Fernández, Santos et al. 2023, **ART. 6**).

Polluted Emulsions (PEs) treatment

Subsequently, the resulting polluted emulsions (PEs) were treated by the alkaline activation of PS intensified by temperature. PEs were obtained from S16 (SDS) and S18 (E3) experiments, named PE-SDS-1 and PE-E3-1, respectively. Moreover, the emulsion resulting from the three successive solubilization cycles: PE-SDS-1,2,3 (sum of aqueous phases from S16, S19, and S20 runs) and PE-E3-1,2,3 (sum of aqueous phases form coming from S18, S22, and S23 experiments) have also been treated. The characteristics of these emulsions, the emulsion name, the solubilization experiments (S) they come from, the surfactant (C_{surf}), and pollutants (C_{COCS}) concentration (experimentally determined) have been included in Table 7.13. Blank runs were also carried out to determine the decrease in COCs concentration by adsorption or volatilization in the absence of PS. Unproductive oxidant consumption was also studied in the absence of solubilized COCs. The evolution of each reaction was followed by preparing several vials and sacrificing one at each selected reaction time. The vials were refrigerated for 1 hour using an ice bath, and the reaction media was immediately analyzed.

Table 7.13. Operational conditions of polluted emulsion (PE) oxidation experiments (molar NaOH:PS > 2 (when it applies), C_{PS} = 40 g L^{-1} (when it applies), T = 40 ºC) (Checa-Fernández, Santos et al. 2023, **ART. 6**).

Objective	Polluted emulsion	Solubilization experiment number	Surf.	C_{surf} (g L^{-1})	C_{COCs} (as TCBs, mg L^{-1})	C_{PS}/ $C_{PS,stc}$
Blank runs	PE-SDS-1	S16	SDS	4.1	70.1	-
	PE-SDS-1,2,3	S16+S19+S20	SDS	2.6	34.2	-
	PE-E3-1	S18	E3	3.1	52.7	-
	PE-E3-1,2,3	S18+S22+S23	E3	2.3	36.9	-
COCs oxidation	PE-SDS-1	S16	SDS	4.1	70.1	9.0
	PE-SDS-1,2,3	S16+S19+S20	SDS	2.6	34.2	18.4
	PE-E3-1	S18	E3	3.1	52.7	12.0
	PE-E3-1,2,3	S18+S22+S23	E3	2.3	36.9	17.1
Unproductive PS consumption	-	-	SDS	4.1	0	-
	-	-	SDS	2.6	0	-
	-	-	E3	3.1	0	-
	-	-	E3	2.3	0	-

Considering the alkaline pH of the polluted emulsions (pH ≥ 12), the oxidation system selected for the subsequent COCs abatement in the emulsion is PS activated by alkali (NaOH was added to ensure NaOH:PS ≥ 2). On the other hand, considering the promising results recently obtained when this process was intensified by temperature (Dominguez, Romero et al. 2020, Dominguez, Romero et al. 2021, **ART. 2,** Dominguez, Checa-Fernandez et al. 2021, **ART. 3,** Checa-Fernández, Santos et al. 2021, **ART. 4**) a temperature of 40 ºC was selected. The oxidizable organic matter in the reaction medium is comprised of solubilized COCs (mainly TCBs) and surfactant. A relatively high oxidant dose was used to avoid the oxidant depletion by an unproductive reaction with the surfactant (Chen, Luo et al. 2017, Dominguez, Romero et al. 2019, Qiu, Xu et al. 2019, Trellu, Pechaud et al. 2021, García-Cervilla, Santos et al. 2022). Therefore, a PS concentration of 40 g L^{-1} has been selected (Dominguez, Romero et al. 2020, Checa-Fernández, Santos et al. 2021, **ART. 4**). Finally, the molar NaOH/PS ratio was fixed at 2, a value commonly found in the literature which ensures a pH > 12 (necessary for alkaline activation of PS) during the reaction (García-Cervilla, Santos et al. 2020, Checa-Fernández, Santos et al. 2021, **ART. 4,** Checa-Fernández, Santos et al. 2022, **ART. 5**).

The time-evolution of COCs (X_{COCs}) and oxidant (X_{PS}) conversion under the selected operating conditions is shown in Figure 7.51-a and -b, respectively. The decrease of COCs concentration in blank runs (in the absence of PS) was below 20% in all cases (72 h, data not shown).

PS conversion was considerably higher when treating E3 (PE-E3-1, X_{PS} > 50%, 6 h) than SDS (PE-SDS-1, X_{PS} < 20%, 6 h) emulsions. Furthermore, the oxidant consumption was higher in the experiment with a higher initial concentration of E3 (PE-E3-1,2,3), which can be associated with the unproductive consumption of PS with this surfactant (Figure 7.51-b). In the case of SDS-emulsions, the differences in PS conversion in the tests with different surfactant concentrations (PE-SDS-1 and PE-SDS-1,2,3, respectively) were less significant (Figure 7.51-b). The rapid decomposition of PS in the experiments with E3 emulsions generated a high concentration of hydrogen cations (Checa-Fernández, Santos et al. 2021, **ART. 4**) which is associated with a considerable decrease in the pH of the reaction medium (Figure 7.51-c). In these experiments, the pH decreased below the required value for the alkaline activation of PS (pH ≥ 12), and thus, hydroxyl radicals were no longer produced (Checa-Fernández, Santos et al. 2021, **ART. 4**). All this led to low contaminant conversion (X_{COCs} < 30%, 72 h, Figure 7.51-a).

It should be noted that COCs conversion was slightly higher when treating PE-E3-1,2,3 (with lower surfactant concentration) than PE-E3-1 (Table 7.13), which can be attributed to a protecting effect of surfactant micelles against pollutants oxidation. This behaviour was previously observed in the oxidation of a complex liquid mixture of COCs by using PS activated by alkali as an oxidant and E3 as a surfactant (García-Cervilla, Santos et al. 2022). In that work, it was found that concentrations of E3 > 2.5 g L^{-1} caused only unproductive reactions without COCs removal. This hindering effect was also noticed in the presence of other surfactants and PS activation methods (Bouzid, Maire et al. 2017, Lamichhane, Bal Krishna et al. 2017, García-Cervilla, Santos et al. 2021). Thus, to improve the oxidation treatment, lower concentrations of E3 should have been used in the precedent solubilization process, which would limit the efficiency of this first stage.

When treating the SDS emulsions, higher COCs conversions were achieved, removing 96% of the contaminants in 72 h of treatment (Figure 7.51-a). At these conditions, no chlorinated intermediate compounds were detected, as previously observed in the treatment of this soil by PS-NaOH-T (Checa-Fernández, Santos et al. 2021, **ART. 4**). Compared with the results obtained in that work, it should be underlined the higher COCs conversion (96 *vs.* 80%) achieved in the presence of surfactant at the same operating conditions (C_{PS} = 40 g L^{-1}, 40 ºC, 72 h) (Checa-Fernández, Santos et al. 2021, **ART. 4**), highlighting the beneficial role of the surfactant. Additionally, due to the low solubility of β-HCH (the most recalcitrant HCH isomer) and low hydrolysis rate (to TCBs), the conversion of this compound when no surfactant was used was below 70% (Checa-

Fernández, Santos et al. 2021, **ART. 4**), whereas when the process was intensified by the use of surfactants the solubilization of β-HCH in the emulsion was almost 80% (Figure 7.47). This confirms the synergetic effect of NaOH and surfactant, enhancing the dehydrochlorination of this refractory compound and subsequent solubilization of TCBs (which were further removed in the oxidation treatment).

The unproductive oxidant consumption due to surfactant has been evaluated by performing experiments without COCs. The oxidant consumption was almost independent of the COCs presence (data not shown) for each surfactant. Therefore, PS was mainly consumed in an unproductive reaction with the surfactant at the temperature tested. The unproductive consumption of PS (40 g L^{-1}) at different temperatures in the absence of surfactant was studied in previous work, obtaining significantly lower oxidant consumption: 7.5% and 20% at 35 ºC and 45 ºC, respectively (72 h) (Dominguez, Checa-Fernandez et al. 2021, **ART. 3**). These results demonstrated that the presence of surfactants (both SDS and E3) significantly increased the unproductive oxidant consumption (X_{PS} > 70% in both cases). Additionally, as previously mentioned in the case PEs (Figure 7.51-b), the unproductive PS consumption in the presence of the nonionic surfactant (E3) was considerably higher than using SDS (data not shown), in accordance with that previously reported in the literature (Wang, Peng et al. 2017, Lominchar, Lorenzo et al. 2018, Wang, Wu et al. 2020, García-Cervilla, Santos et al. 2021). Wang et al. (2020) informed that the higher stability of SDS against PS was associated with the existence of repulsion forces between $SO_4^{\bullet-}$ radicals generated in the PS/T system and the sulfonate anions located at the exterior of the SDS micelle (Wang, Wu et al. 2020).

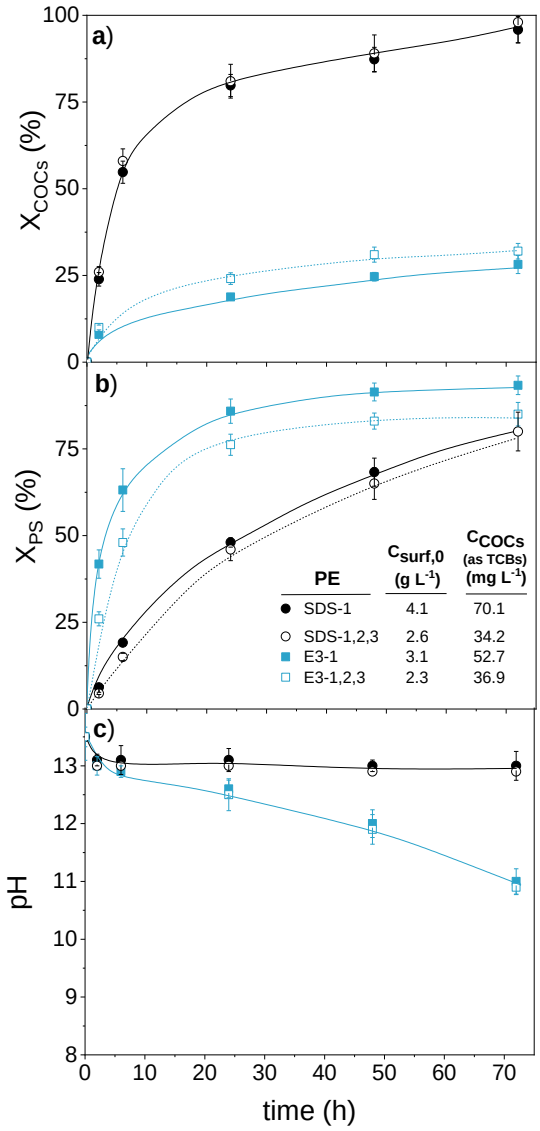

Figure 7.51. Evolution of COCs (mainly TCBs) (a), PS (b) conversion, and pH (c) with reaction time when treating PEs (Table 7.13). C_{PS} = 40 g L^{-1}, NaOH:PS = 2, T = 40 °C. (Checa-Fernández, Santos et al. 2023, **ART. 6**).

In conclusion, the lower unproductive consumption of PS with SDS and higher removal of COCs from the emulsion make SDS preferable for this treatment under the experimental conditions used. Thus, using SDS to solubilize a higher concentration of contaminants (at basic pH) and subsequent treatment of the polluted emulsion with alkaline PS and intensified with temperature represents an interesting alternative for the remediation of HCHs-polluted TS.

7.3. Acute toxicity of treated soils

The main objective of the Doctoral Thesis was the remediation of soils contaminated with lindane wastes. In previous sections, the efficiency of several on-site **topsoil** treatments (Dominguez, Romero et al. 2021, **ART. 2,** Dominguez, Checa-Fernandez et al. 2021, **ART. 3,** Checa-Fernández, Santos et al. 2021, **ART. 4,** Checa-Fernández, Santos et al. 2022, **ART. 5,** Checa-Fernández, Santos et al. 2023, **ART. 6**) has been demonstrated from the perspective of pollutant degradation. On the other hand, the efficiency of in situ treatments has been proven in the case of **subsoil** (García-Cervilla, Santos et al. 2020, Garcia-Cervilla, Santos et al. 2022). In addition to showing high degradation efficiency, a key aspect from the environmental point of view is that remediation treatments do not generate toxic chlorinated byproducts. An acute toxicity test can evaluate toxic byproducts remaining in soil. In some works dealing with soil remediation, acute toxicity has been studied. However, most of these studies have focused on characterizing the reaction supernatant obtained and not on the soil (Oh, Yoon et al. 2016). Nonetheless, it is necessary to study all phases involved in the treatment. In this context, in this Doctoral Thesis, the **acute toxicity of the treated soils** and the resulting **aqueous phases (reaction supernatants and elutriates)** has been determined using the **Microtox®** bioassay. The results related to topsoil (7.3.1) and subsoil (7.3.2) remediation is shown below.

7.3.1. Remediated Topsoil

The acute toxicity of TS after application of the previously selected on-site oxidation treatments: persulfate activated by temperature (**PS/T**) and persulfate activated by alkali and intensified by temperature (**PS/NaOH/T**) (Subsections 7.2.2. and 7.2.3.1., respectively) was evaluated. In addition, in future work, the acute toxicity of the soil after the S/PS/NaOH/T treatment will be considered. In field applications, soils are usually washed after chemical treatment to remove residual chemicals and subsequently returned to their origin (Peters 1999). Thus, the treated soils were water-washed before toxicity analyses. As discussed in Subsection 6.3.1.6, it is necessary to i) crush and sieve the soils to a size less than 0.25 mm, ii) remove the remaining PS concentration (using TiS), and iii) adjust the pH in the range of 6-8 (HCl).

As previously stated, the soil sample selected for oxidation experiments was TS L2 with a HCHs concentration of 409 mg kg^{-1} (Table 7.2). The experimental procedures followed for the remediation experiments are described in Subsection 6.2.1, and the

experimental conditions were selected based on the results obtained in Subsections 7.2.2 and 7.2.3.1 (Dominguez, Checa-Fernandez et al. 2021, **ART. 3,** Checa-Fernández, Santos et al. 2021, **ART. 4**):

- **PS/T:** C_{PS} = 60 g L^{-1}, 50 ºC, V_L/W_S = 2, 17 days
- **PS/NaOH/T:** C_{PS} = 60 g L^{-1}, molar NaOH:PS = 2, 50 ºC, V_L/W_S = 2, 11 days

At the final reaction time, soil and aqueous phases were separated by centrifugation (as described in Subsection 6.2.1), and both were characterized. In the case of the soil phase, the remanent COCs and TOC concentrations were analysed. In the case of the reaction supernatant, pH, COCs, PS, chloride concentration, and acute toxicity were determined. Once the soil phase and the reaction supernatant were separated, the soil was dry for 24 h. Subsequently, 30 ml of water (V_L/W_S = 2) was added to the reactor and stirred for 24 h (time required to reach equilibrium conditions). Finally, both phases (soil and elutriates) were separated.

The remanent contaminants concentration in the treated soils and aqueous phases (reaction supernatants and elutriates) has been included in Table 7.14. Additionally, the COCs concentration of the polluted soil (TS L2) and its corresponding elutriate has been added for comparative purposes.

As shown in Table 7.14, the initial COCs concentration (mainly HCHs) in the soil phase was 409 mg kg^{-1}. After the remediation treatments, the remanent COCs concentration in the treated soils was higher in the PS/T system (44 mg kg^{-1}) than in the PS/NaOH/T (6.3 mg kg^{-1}). In the case of the reaction supernatants, a total COCs concentration ($C_{COC,\ aq.\ supernatant}$) of 1.8 and 3.1 mg L^{-1} was detected for the PS/T and PS/NaOH/T treatments, respectively. The PS/T supernatant was mainly composed of α-HCH, whereas the majority compound in the PS/NaOH/T was 1,2,4-TCB. The COCs composition in the reaction supernatants agreed with that of the compounds in the soil phase at the final reaction time. The higher COCs concentration of PS/NaOH/T than PS/T supernatant was related to the higher solubility of TCBs than HCHs (Lorenzo, García-Cervilla et al. 2020, García-Cervilla, Santos et al. 2022). The concentration of COCs solubilized in the elutriate of the polluted soil (TS L2, $C_{COC,\ aq.\ elutriate}$) was 4.5 mg L^{-1} with a significant contribution of α-HCH. As expected, the concentration of COCs in the elutriates ($C_{COC,\ aq.\ elutriate}$) of the treated soils decreased to 1.5 mg L^{-1} and 0.6 mg L^{-1} for the PS/T and PS/NaOH/T systems, respectively. The low concentration of COCs in the case of the PS/NaOH/T elutriate can be associated with the possible loss of TCBs by volatilization (Lide 2004, Lorenzo, Santos et al. 2021,

Conte, Dominguez et al. 2022). In the case of the thermal activation of PS, residual α-HCH remained in the soil phase and was solubilized at a slower rate.

Table 7.14. COCs concentration in the soil phases ($C_{COC,soil}$), the reaction supernatants ($C_{COC, aq, supernantant}$), and the elutriates ($C_{COC, aq}$ elutriate) of PS/T and PS/NaOH/T treatments.

	Polluted (TS L2)		**PS/T**			**PS/NaOH/T**		
	$C_{COC, soil}$ (mg kg^{-1})	$C_{COC, aq}$ elutriate (mg L^{-1})	$C_{COC, soil}$ (mg kg^{-1})	$C_{COC, aq}$ supernatant (mg L^{-1})	$C_{COC, aq}$ elutriate (mg L^{-1})	$C_{COC, soil}$ (mg kg^{-1})	$C_{COC, aq}$ supernatant (mg L^{-1})	$C_{COC, aq}$ elutriate (mg L^{-1})
β-PCX	7.0	0.0	1.2	0.0	0.0	0.0	0.0	0.0
α-HCH	335.0	2.2	33.0	1.7	1.5	0.0	0.0	0.0
β-HCH	45.2	0.6	10.0	0.1	0.0	0.9	0.0	0.0
γ-HCH	5.7	0.8	0.1	0.0	0.0	0.0	0.0	0.0
δ-HCH	7.8	0.9	0.1	0.0	0.0	0.0	0.0	0.0
ε-HCH	7.8	0.3	0.0	0.0	0.0	0.0	0.0	0.0
1,2,3-TCB	0.0	0.0	0.0	0.0	0.0	0.5	0.1	0.0
1,2,4-TCB	0.0	0.0	0.0	0.0	0.0	6.6	3.0	0.6
1,3,5-TCB	0.0	0.0	0.0	0.0	0.0	0.7	0.0	0.0
ΣCOCs	**409.0**	**4.7**	**44.4**	**1.8**	**1.5**	**8.7**	**3.1**	**0.6**

Figure 7.52 shows the conversions of α-HCH, β-HCH isomers, and total COCs, the dechlorination degree (Cl^-/Cl_0), and oxidant conversion (PS) for the PS/T and PS/NaOH/T treatments at final reaction time.

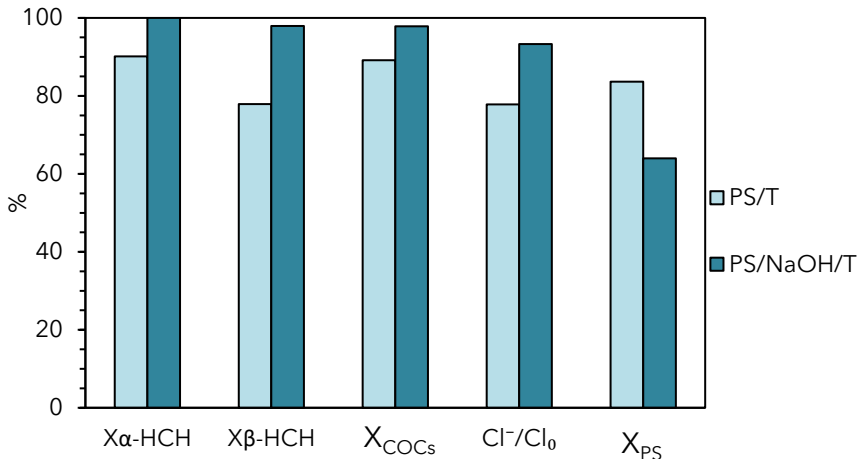

Figure 7.52. Conversion of α-HCH, β-HCH and COCs, dechlorination degree (Cl^-/Cl_0), and PS consumption for remediation treatments (PS/T) and (PS/NaOH/T) applied on sample TS L2

(C_{HCHs} = 409 mg kg^{-1}). Operational conditions: C_{PS} = 60 g L^{-1}, T = 50 ºC, V_L/W_S = 2. PS/T = 17 days. PS/NaOH/T = 11 days (molar NaOH:PS = 2).

As previously mentioned, COCs degradation was very high in both cases, demonstrating the efficiency of the two treatments under the conditions previously selected (Subsection 7.2). A slightly higher COCs degradation was achieved with the alkaline activation of PS intensified by temperature (PS/NaOH/T) than the exclusive thermal activation (PS/T): 97.8% *vs.* 89.1% (Figure 7.52). Moreover, it is worth noting that the treatment time of PS/NaOH/T was six days less than the corresponding to PS/T. The higher COCs conversion in the case of PS/NaOH/T system was mainly due to the dehydrochlorination reaction of HCHs to TCBs occurring at alkaline conditions (pH ≥ 12) (Santos, Fernandez et al. 2018, Dominguez, Romero et al. 2021, **ART. 2,** Checa-Fernández, Santos et al. 2021, **ART. 4**). The dechlorination degree was very high in both treatments (Figure 7.52), especially that obtained under alkaline conditions (98%). A dechlorination degree of 100% would indicate the absence of chlorinated organic compounds, including HCHs, TCBs, or chlorinated intermediates generated from the oxidation treatments. Therefore, it can be assumed that the concentration of chlorinated oxidation intermediates at the end time was very low. It should be noted that the chlorine balance (data not shown) was almost accomplished at the end of the treatments, guaranteeing an adequate quantification of the different chlorinated species.

Finally, greater consumption of PS was observed in the PS/T (83.7%) treatment than in PS/NaOH/T (64%) (Figure 7.52), mainly because of the longer treatment time (17 *vs.* 11 days, respectively). The remaining PS in the aqueous phase could be reused for the treatment of a new batch of contaminated soil (21.6 g L^{-1} and 10.2 g L^{-1} of PS in the case of PS/NaOH/T and PS/T treatments, respectively), provided that the contaminants present in the aqueous medium were oxidised entirely, and the oxidant concentration was again adjusted to the required value.

Due to the buffer effect of the soil, the pH was neutral during the whole reaction time in the case of the thermal activation of PS. pH changed from > 12 to 11.5 at the end of the alkaline activation of PS (Figure 7.53).

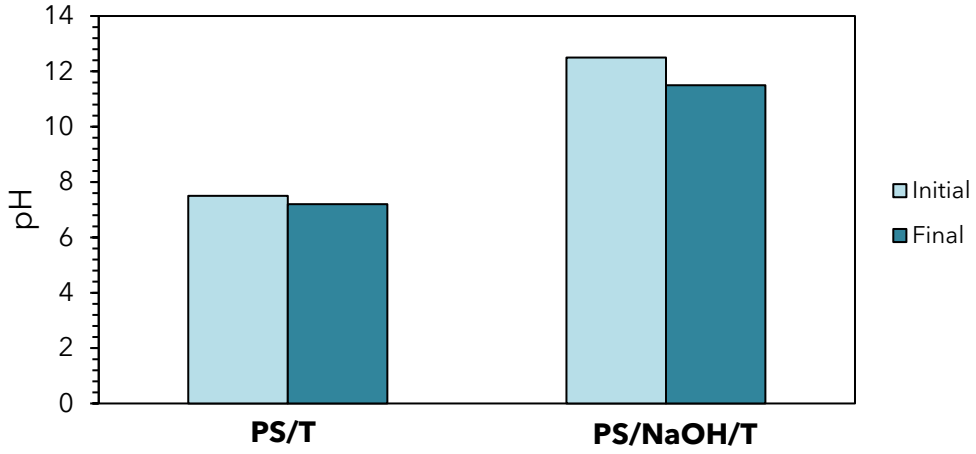

Figure 7.53. pH values at initial and final reaction time in PS/T and PS/NaOH/T treatments. Operational conditions: C_{PS} = 60 g L^{-1}, T = 50 ºC, V_L/W_S = 2. PS/T = 17 days. PS/NaOH/T = 11 days (molar NaOH:PS = 2).

The toxicity of the different phases obtained in the remediation reactions has been evaluated: i) treated **soils**, ii) **reaction supernatants**, and iii) **elutriates** (of great importance as it simulates water in contact with topsoils (leachate)). Figure 7.54-a shows the soil phase toxicity (expressed as $1/EC_{50,\ soil}$, in L g_{soil}^{-1}, Eq. (6.5), Subsection 6.3.1.6, Microtox® modified Basic Solid-Phase Test) obtained before (polluted sample, TS L2) and after the application of the remediation treatments (PS/T and PS/NaOH/T). Likewise, the acute toxicity value corresponding to a reference soil (TS L0, C_{COCs} < 1 mg kg^{-1}) was included.

As stated in the soil characterization Subsection (7.1.2), these soils show some acute toxicity (EC_{50} of polluted soil of 1.3 g_{soil} L^{-1}), even in the absence of contaminants (with a reference value of 2.2 g_{soil} L^{-1}). According to the classification proposed by Kwan and Dutka (1995): EC_{50} > 10 g L^{-1} is considered a nontoxic sample, 5 g L^{-1} < EC_{50} ≤ 10 g L^{-1} is a moderately toxic sample, and EC_{50} ≤ 5 g L^{-1} is a toxic sample. Thus, the polluted and unpolluted soils (TS L2 and TS L0) are classified as toxic (EC_{50} ≤ 5 g L^{-1}). The fact that the reference samples (TS L0), with low COCs concentration, exhibit intrinsic acute toxicity would indicate that there are toxic compounds for the Microtox bacteria (*Vibrio fischeri*) in the soil matrix.

Figure 7.54-a shows that after **PS/T treatment** the acute toxicity of the soil is reduced to the baseline, that is, to the intrinsic toxicity of the soil with a negligible concentration of contaminants (reference soil, TS L0). After the remediation process, the pH was unaltered (Figure 7.53) whereas the soil TOC concentration was practically unaffected (decreased <

0.2% from the initial value, 1.5%). Thus, the soil organic matter, mainly attributable to humic acid-type compounds, was resistant to the oxidation treatment. Both the toxicity reduction and the maintenance of the physico-chemical characteristics of the soil are decisive factors to ensure that no toxic byproducts are generated, and a subsequent bioremediation treatment could be applied. As mentioned above, both factors are fulfilled in the case of the PS/T treatment.

In the case of the **PS/NaOH/T system,** no increase in toxicity associated with the treatment has been detected. Nevertheless, although a low contaminants concentration remained in the soil phase ($C_{COCs,soil}$ = 8.7 mg kg_{soil}^{-1}, Table 7.14), the soil toxicity was similar to that of polluted soil ($C_{COCs,soil}$ = 409 mg kg_{soil}^{-}) (Figure 7.54-a). Since the soils resulting from both treatments present an equivalent concentration of COCs, the higher toxicity obtained for the soil treated by PS/NaOH/T than PS/T could be attributed to the high concentration of NaOH used (and the V_L/W_S ratio). Thus, the role of using such high NaOH concentrations in soil toxicity has been evaluated. For that purpose, the toxicity of the reference soil (TS L0 (Ref)) placed in contact with NaOH (20.2 g L^{-1}, 50 °C, 100 rpm, 11 days, Ref+NaOH) was analyzed. The results of Ref, Ref+NaOH, and TS L2 treated by PS/T/NaOH are shown in Figure 7.54-b. The increase of toxicity from Ref to Ref+NaOH can be attributed to the effect of the high NaOH concentration to which the soil is subjected during the treatment. On the other side, the acute toxicity of Ref+NaOH is equivalent to that of the soil treated by PS/NaOH/T and thus, it could be concluded that the higher toxicity exhibited when applying the PS/NaOH/T than PS/T is associated with the effect of the remaining NaOH on the Microtox bacteria. The increase in Na concentration (coming mainly from NaOH) in soil was previously pointed out in the EDS results of soils treated with PS/NaOH/US (Subsection 7.2.3.2). Thus, from the point of view of acute toxicity, this result points out the need for a more thorough washing of the soils after PS/NaOH/T treatment.

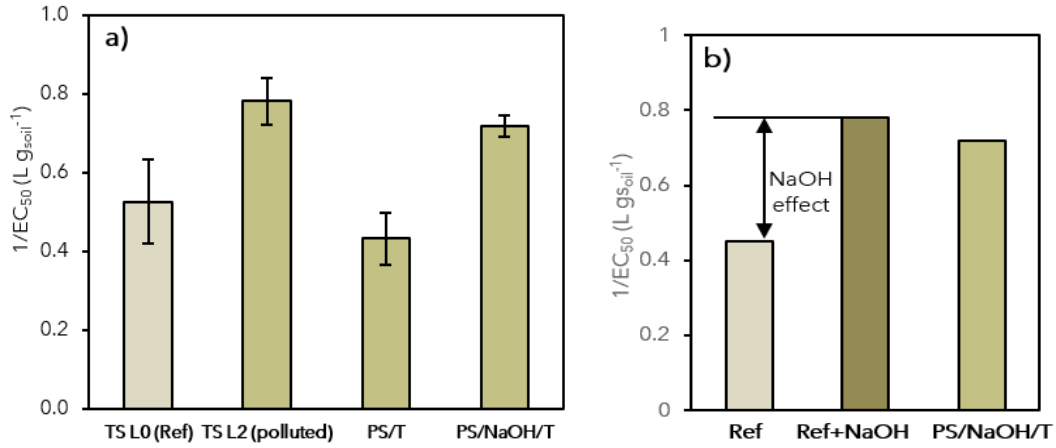

Figure 7.54. Toxicity ($1/EC_{50}$, Microtox® mBSPT) of the soil phase of the (a) reference (TS L0, Ref), polluted (TS L2) and soils treated by PS/T and PS/NaOH/T, and (b) the reference (Ref) soil before and after contact with NaOH (Ref+NaOH) (NaOH effect), and after the PS/NaOH/T treatment.

The toxicity results related to the **aqueous phase** (expressed as TUs, Eq. (6.2), Microtox® BT), including the elutriates and reaction supernatant, are shown in Figure 7.55. As previously mentioned in Subsection (7.1.2), the elutriates toxicity evaluation has been carried out according to the classification proposed by Libralato, Annamaria et al. (2010): $EC_{50} > 100$ g L^{-1} is considered a low toxicity sample, 10 g $L^{-1} \leq EC_{50} \leq 100$ g L^{-1} a moderately toxic sample, and $EC_{50} < 10$ g L^{-1} a very toxic sample. As seen in Figure 7.55, reference (ND) and polluted (EC_{50} = 307 g L^{-1}, TUs = 1.6) TS elutriates presented low toxicity, indicating that the possible leachates from the surface soil of the landfills are not an environmental issue in terms of acute toxicity. This fact highlights that besides removing HCHs present in TS samples, reducing toxicity elutriates after treatment should be evaluated to select a practical option that does not increase their toxicity, and toxic byproducts are not produced.

As shown in Figure 7.55, the reaction supernatant obtained in the PS/T treatment (after removal of the remaining PS by adding thiosulfate, without pH adjustment) did not exhibit toxicity. However, the aqueous supernatant obtained from the PS/NaOH/T treatment (after PS removal and pH adjustment) showed acute toxicity (TUs = 8.7) even five times higher than the polluted soil (TUs = 1.7). The justification for this toxicological response lies in the presence of TCBs (generated from the hydrolysis of HCHs) in the aqueous reaction phase (C_{TBCs} = 3 mg L^{-1}, Table 7.14), which have non-negligible toxicity

for the *Vibrio fischeri* bacteria, as was detailed discussed in the soil characterization Subsection (Table 7.7).

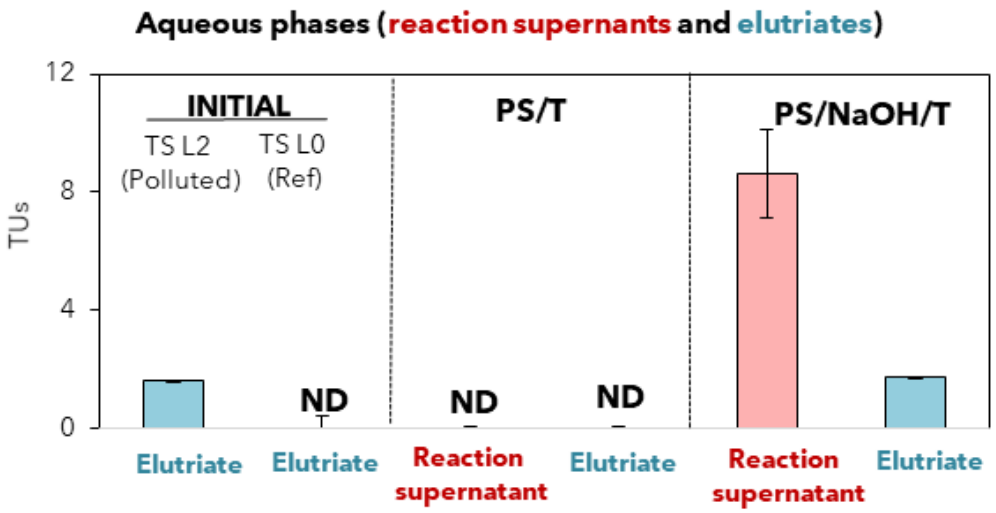

Figure 7.55. Toxicity of aqueous phases (reaction supernatants and elutriates, BT) before (reference (TS L0) and polluted (TS L2) soils) and after applying the remediation processes (PS/T and PS/NaOH/T). ND: toxicity not detected.

Due to the pre-adjustment of pH to 7 before the Microtox® bioassay, possible toxicity from alkaline pH was discarded. Oh, Yoon et al. (2016) reported similar results when evaluating the toxicity (Microtox® bioassay, BT) of effluent resulting from the application of ex-situ alkaline hydrolysis for the remediation of explosive-polluted soils. Their results showed that for all explosives, even after complete hydrolytic degradation in the soil system, the alkaline hydrolysis did not decrease the acute toxicity effluent, indicating that products from alkaline hydrolysis of the three explosives were toxic (Oh, Yoon et al. 2016). The clarification of acute toxicity increases after alkali treatment must be accomplished. The ratio 2/1 of aqueous to soil used in the TS treatments and the NaOH excess could explain the acute toxicity increase after the treatment.

To have a complete overview of the acute toxicity evaluation the **organic extract phases** (Domínguez, Ventura et al. 2023, **ART. 1**) were analyzed. The results obtained (expressed as $1/EC_{50,soil}$, in $mL_{MeOH}\ g_{soil}^{-1}$, Eq. (6.6), Microtox® aOSSST) before and after the different treatments under study are shown in Figure 7.56. Results show that the reference soil (TS L0), with a COCs concentration < 1 mg kg^{-1}, does not exhibit toxicity, and the polluted soil presents a considerably higher value. The differences between polluted and reference soil toxicity are more significant in this case. This finding can be explained as most of the COCs in soil are extracted to the organic phase, highlighting the aOSSST

ensures the total availability of the pollutants (Čvančarová, Křesinová et al. 2013). Moreover, the absence of acute toxicity in the organic extract of TS L0 confirm that the residual toxicity of the soil (Figure 7.54) is not attributed to organic compounds.

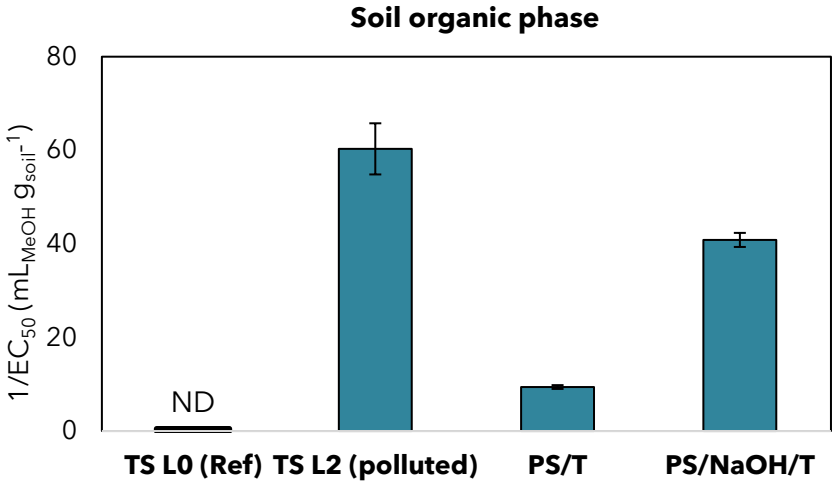

Figure 7.56. Toxicity of organic phases (aOSSST) of the reference topsoil (TS L0), polluted soil (TS L2), and treated soils after applying the remediation processes (PS/T and PS/NaOH/T). ND: toxicity not detected.

As can be seen, the trend obtained for soil toxicity reduction after the remediation treatment application is similar to that above shown for the soil phase results (Figure 7.54). As previously mentioned for the soil phase toxicity, the more significant toxicity detected in the organic phase of PS/NaOH/T than in the PS/T treatment (Figure 7.56) can be justified by the TCBs present in the alkaline treated soil (C_{TCBs}=8.7 mg kg_{soil}^{-1}, Table 7.14) which were transferred to the organic extract. In the case of PS/T, in the treated soil, there are only HCHs (C_{HCHs} = 44 mg kg_{soil}^{-1}), with lower acute toxicity (Table 7.4).

The selection of the most suitable and practical treatment should not be based entirely on the efficacy of contaminant removal but also the reduction of toxicity of all the phases involved in the treatment. Based on the results obtained, **PS/T treatment** is preferable to alkaline activation (PS/NaOH/T) when remediating TS in terms of acute toxicity. This treatment reduced the soil toxicity to the levels obtained in the reference sample. In addition, the aqueous reaction phase obtained did not exhibit toxicity, facilitating its management. Soil characteristics such as pH and TOC were not affected; therefore, a subsequent bioremediation treatment could be applied. In this context, further tests are required to prove its effectiveness.

7.3.2. Remediated Subsoil

The acute toxicity of SS after application of the in situ oxidation treatments: **ISCO** (PS/NaOH) and **S-ISCO** (E-Mulse®-3 (E3)/PS/NaOH), was evaluated. As previously stated, the soil sample selected for in situ oxidation experiments was SS-C L2, Table 6.2, Subsection 6.1.2). The experimental procedures followed for these experiments are described in Subsection 6.2.2. Remediation experiments were performed in glass columns (diameter = 3 cm) with two side ports (4.7 cm between them). Three columns were prepared: one for ISCO treatment and two for S-ISCO treatments. A scheme of the column assembly is shown in Figure 6.6 (Subsection 6.2.2). Firstly, one pore volume (Pv) of Milli-Q water was injected into the columns to achieve pore water saturation (0.3 mL min^{-1}, 35 min approx.). Subsequently, an alkaline pretreatment was applied (2 Pvs, NaOH solution (210 mM)). After that, 8 Pvs (containing the desired concentration of surfactant/oxidant/activator (E3/PS/NaOH) were injected into each column (0.3 mL min^{-1}) with a time elapsed between each Pv injection of 96 h. After the chemical treatment, 8 Pvs of tap water were injected simulating the groundwater flow in the subsoil. The operational conditions employed were selected from previous work (Garcia-Cervilla, Santos et al. 2022):

- **ISCO:** C_{PS} = 210 mM, NaOH:PS = 1, **C_{E3} = 0 g L^{-1}**, T = 22 ºC, 32 days.
- **S-ISCO-5:** C_{PS} = 210 mM, NaOH:PS = 1, **C_{E3} = 5 g L^{-1}**, T = 22 ºC, 32 days.
- **S-ISCO-10:** C_{PS} = 210 mM, NaOH:PS = 1, **C_{E3} = 10 g L^{-1}**, T = 22 ºC, 32 days.

All the resulting effluents were collected, and the COCs, oxidant (PS) and surfactant (E3) concentration, pH, and acute toxicity (Microtox®, Basic Test) were analyzed. Additionally, COCs concentration and toxicity (Microtox®; modified Basic Solid-Phase Test and adapted Organic Solvent Sample Solubilization Test) of the soil phase were analyzed before and after ISCO and S-ISCO treatments. To evaluate the effect of the remediation treatments, the characterization of the unpolluted soil, used as reference (SS-CL0), the polluted soil (SS-C L2), and its corresponding elutriate, which simulates groundwater in contact with contaminated subsoil, has been considered (previously described in Subsection 7.1).

Table 7.15. PS concentration (Mm) measured at each Pv in ISCO and S-ISCO experiments of SS-C L2 (Santos, García-Cervilla et al. 2022, **ART. 7**).

Pv	ISCO	S-ISCO 5	S-ISCO 10
1	31.7	19.2	17.2
2	53.5	25.9	18.1
3	60.7	36.2	26.0
4	85.1	71.7	42.6
5	110.0	110.0	76.0
6	130.2	125.0	82.0
7	170.0	130.1	90.2
8	200.0	145.2	98.1

The pH value (not shown) was always higher than 12. PS concentration at each Pv flushed is shown in Table 7.15. As can be seen, a significant oxidant concentration remains unreacted at each Pv, increasing as the number of Pvs increases. In addition, as expected, the lower the surfactant concentration, the higher the remaining PS, which is explained by the unproductive consumption of PS due to surfactant oxidation (García-Cervilla, Santos et al. 2021).

The Pvs flushed from the different columns were gathered, allowing the oxidation reaction to continues in the aqueous phase, which simulates the progress of the aqueous phase in the subsoil. The remanent concentration of each contaminant, PS, and surfactant concentration in the 8 gathered Pvs aqueous phases after applying ISCO and S-ISCO treatments has been included in Table 7.16. Additionally, the COCs concentration of the unpolluted (SS-C L0) and polluted (SS-C L2) initial soil elutriates at neutral pH (simulating groundwater) and the composition of the aqueous Pv flushed from the polluted soil column (SS-C L2) after the alkali pretreatment (pH > 12) has also been included for comparative purposes.

As shown in Table 7.16, the elutriate of the polluted soil at neutral conditions presents a high COCs concentration (56.9 mg L^{-1}), highlighting the problem associated with groundwater contamination and the need to develop effective remediation techniques. In the alkaline effluent, HCHs, PCXs, HCXs, and HeptaCHs were not present, in agreement with the dehydrochlorination of these compounds to TCBs and TetraCBs, respectively (García-Cervilla, Santos et al. 2020, Lorenzo, García-Cervilla et al. 2020). In the case of the 8 gathered Pvs flushed from columns ISCO and S-ISCO, the surfactant injection enhanced the COCs solubilization in the aqueous phase. Moreover, as can be seen, a higher surfactant concentration injection resulted in higher COCs solubilization and higher

surfactant concentration in the effluent. Finally, PS conversion increased as the surfactant concentration increased.

Table 7.16. COCs concentration and toxicity units (TUs) of the initial elutriates at neutral pH of unpolluted (SS-C L0) and polluted (SS-C L2) soils (V_L/W_S = 2 L kg^{-1}), and Pv after alkaline conditions of SS-C L2 soil (V_L/W_S = 0.4 L kg^{-1}). COCs, PS, and surfactant concentration in the 8 gathered Pvs flushed from columns ISCO and S-ISCO experiments 96 h after the last Pv was eluted is included, as well as the effective nominal concentration (EC_{50}) of commercial COCs (Santos, García-Cervilla et al. 2022, **ART. 7**).

		Elutriate unpolluted soil (SS-C L0, pH=7)	**Elutriate polluted soil (SS-C L2, pH=7)**	**Pv alkaline pretreatment (SS-C L2, pH>12)**	**ISCO**	**S-ISCO-5**	**S-ISCO-10**
Acronym	EC_{50j} (mg L^{-1})	C_j (mg L^{-1})			C_j (mg L^{-1}) Σ8 Pvs flushed		
CB	11.30	0.00	0.00	0.00	0.00	0.00	0.00
1,3-DCB	5.10	0.00	0.06	0.05	0.00	0.00	0.03
1,4-DCB	4.50	0.00	0.43	0.04	0.04	0.00	0.01
1,2-DCB	4.05	0.00	0.41	0.23	0.03	0.00	0.07
1,3,5-TCB	3.44	0.00	0.03	0.14	0.02	0.07	0.71
1,2,4-TCB	3.44	0.00	1.97	6.96	0.84	1.85	18.00
1,2,3-TCB	0.82	0.00	0.12	1.27	0.12	0.43	3.20
TetraCB-a	0.61	0.00	0.24	0.28	0.08	0.69	2.10
TetraCB-b	0.61	0.01	0.35	0.49	0.10	1.21	3.20
γ-PCX	-	0.00	0.85	0.00	0.00	0.03	0.50
PCB	-	0.00	0.00	0.01	0.00	0.01	0.64
δ-PCX	-	0.01	7.10	0.00	0.03	0.00	0.00
θ-PCX	-	0.00	0.79	0.00	0.00	0.00	0.00
HCX-a	-	0.00	0.20	0.00	0.00	0.00	0.00
β-PCX	-	0.00	2.48	0.00	0.00	0.00	0.00
η-PCX	-	0.00	0.29	0.00	0.00	0.00	0.00
HCX-b	-	0.00	0.01	0.00	0.00	0.00	0.00
HCX-c	-	0.00	1.32	0.00	0.00	0.00	0.00
α-HCH	-	0.00	3.14	0.00	0.00	0.00	0.00
HCX-d	-	0.00	0.00	0.00	0.00	0.00	0.00
β-HCH	-	0.00	0.65	0.00	0.00	0.00	0.00
γ-HCH	2.03	0.03	7.79	0.00	0.00	0.00	0.00
HeptaCH-1	-	0.01	2.24	0.00	0.00	0.00	0.00
δ-HCH	3.50	0.02	15.15	0.00	0.00	0.00	0.00
ε-HCH	-	0.00	7.29	0.00	0.00	0.00	0.00
HeptaCH-2	-	0.00	2.03	0.00	0.00	0.00	0.00
HeptaCH-3	-	0.00	1.94	0.00	0.00	0.00	0.00
Total COCs (mg L^{-1})	-	**0.06**	**56.89**	**9.47**	**1.26**	**4.30**	**28.46**
PS (mM)	-	-	-	-	95	86	71
C_{surf} average (g L^{-1})	-	-	-	-	0	0.13	0.22
TUs exp. Eq. (6.2)	-	ND	17.24	5.72	ND	5.60	22.10
TUs estim. Eq. (6.4)	-	0.03	10.07	4.95	ND	4.20	18.30

"-": not applicable, ND: not detected.

Additionally, the remaining COCs concentration measured in the soil after ISCO, S-ISCO-5, and S-ISCO-10 treatments are included in Table 7.17.

Table 7.17. COCs concentration in soil (mg kg^{-1}) after ISCO, S-ISCO-5, and S-ISCO-10 treatments.

	C_i (mg kg^{-1}) Soil		
Acronym	**ISCO**	**S-ISCO-5**	**S-ISCO-10**
1,3-DCB	0.00	0.14	0.03
1,4-DCB	0.00	0.00	0.05
1,2-DCB	0.00	1.27	1.30
1,3,5-TCB	3.52	0.55	0.56
1,2,4-TCB	98.06	6.92	6.65
1,2,3-TCB	17.39	1.39	1.21
TetraCB-a	36.41	10.15	9.06
TetraCB-b	66.06	12.19	17.25
γ-PCX	0.00	12.91	20.63
PCB	3.00	2.1	2.03
δ-PCX	0.00	0.00	0.00
θ-PCX	0.00	0.00	0.00
HCX-a	0.00	0.00	0.00
β-PCX	0.00	0.00	0.00
η-PCX	0.00	0.00	0.00
HCX-c	0.00	0.00	0.00
α-HCH	0.00	0.00	0.00
β-HCH	0.00	0.00	0.00
γ-HCH	0.00	0.00	0.00
HeptaCH-1	0.00	0.00	0.00
δ-HCH	0.00	0.00	0.00
ε-HCH	0.00	0.00	0.20
HeptaCH-2	0.00	0.00	0.00
HeptaCH-3	0.00	0.00	0.00
Total COCs	**224.43**	**47.62**	**62.08**

A mass balance of COCs has been accomplished considering the initial mass of COCs in the polluted subsoil SS-C L2 ($w_{COC_s\ initial\ SS}$), the mass of COCs recovered in the treated soil ($w_{COC_s\ treated\ SS}$), the mass of COCs in flushed Pvs from the columns ISCO, S-ISCO-5, and S-ISCO-10 ($w_{COCs_{P_v}}$) and the mass of COCs in the flushed Pvs of tap water ($w_{COCs_{P_{v_{TW}}}}$). The conversion of COCs in the ISCO and S-ISCO experiments has been calculated by Eq. (7.22), obtaining values of 90%, 97%, and 94% for the ISCO, S-ISCO-5, and S-ISCO-10 treatments, respectively.

$$X_{COCs}(\%) = \left(1 - \frac{w_{COC_s\ treated\ SS} + w_{COCs_{P_v}} + w_{COCs_{P_{v_{TW}}}}}{w_{COC_s\ initial\ SS}}\right) \cdot 100 \qquad (7.22)$$

Under these experimental conditions, the surfactant addition increased the COCs conversion. The COCs removal obtained from the same landfill and soil was studied in previous works by ISCO and S-ISCO in batch and column operation (Garcia-Cervilla, Santos et al. 2022). Column study was conducted with fewer Pvs (4) and a lower reaction

time (15 days). Therefore, lower COCs conversion (from 0.5 to 0.7) was found in that work than in the current study (from 0.9 to 0.97). Garcia-Cervilla, Santos et al. (2022) found COCs conversion in ISCO treatment was lower than in S-ISCO, as corroborated in this work.

The **acute toxicity** of the unpolluted (SS- L0), polluted (SS-C L2), and treated (ISCO, S-ISCO-5, and S-ISCO-10) **soils** have been determined by the modified Basic Solid-Phase Test (mBSPT, described in Subsection 6.3.1.6). The results (expressed as $1/EC_{50}$, L g_{soil}^{-1}, Eq. (6.5)) have been represented in Figure 7.57. As previously stated, the polluted soil (EC_{50} = 0.55 g L^{-1}) is considered highly toxic. The unpolluted soil (reference), with low COCs concentration (20.4 mg kg_{soil}^{-1}), exhibits intrinsic toxicity (EC_{50} = 1.64 g L^{-1}), indicating that there are toxic compounds for the bacteria in the soil matrix (Domínguez, Ventura et al. 2023, **ART. 1**).

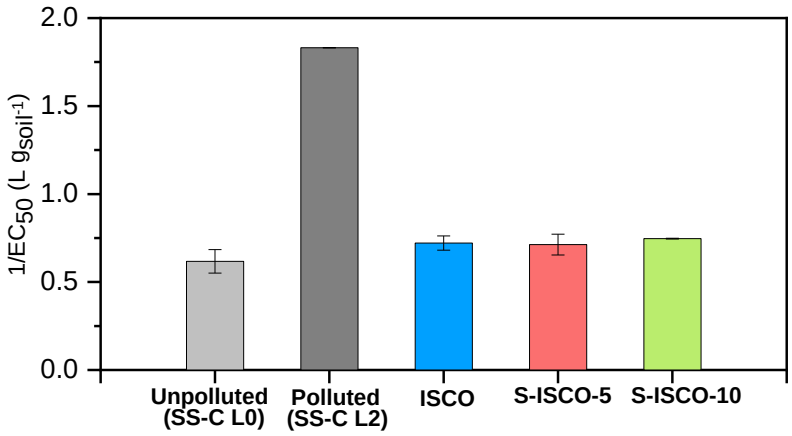

Figure 7.57. Soil toxicity ($1/EC_{50}$, Microtox® mBSPT) of the unpolluted, polluted, and treated soils (Santos, García-Cervilla et al. 2022, **ART. 7**).

The toxicity of soils treated by ISCO and S-ISCO (followed by washing post-treatments) decreased significantly, reaching toxicity values equivalent to that of the unpolluted soil (Figure 7.57). No differences were found between the toxicity values obtained for ISCO and S-ISCO experiments with the surfactant concentration range studied. As previously mentioned, high COCs conversion (≥ 90%) was obtained in all these runs due to the high number of Pvs injected. From the results obtained, it can be concluded that neither the surfactant application (at the conditions tested) nor its concentration generates acute toxicity in the treated soil.

The toxicity of SS-C L0 (unpolluted) and SS-C L2 (polluted) **elutriates**, as well as Pv after alkaline pretreatment, was experimentally determined using the Microtox Basic Test (BT). The results obtained are expressed as toxicity units (TUs), calculated using Eq. (6.2), Subsection 6.3.1.6, and named TUs exp. (Table 7.16). The obtained values were compared with those estimated using Eq. (6.6), TUs estim. For the estimate TUs, the EC_{50} (mg L^{-1}) of each COC obtained experimentally or from literature (Kaiser and Palabrica 1991, Domínguez, Ventura et al. 2023, **ART. 1**) were considered (Table 7.16). About half of the COCs are non-commercial or to the best of our knowledge, have unknown EC_{50i} values in the literature (these compounds have been designated as "-" in the table). As can be seen, the experimental TUs values obtained for the polluted soil (17.2) were higher than the estimated values (10.1) because of the unknown EC_{50i} values of some compounds. The toxicity of the **8 gathered Pvs flushed from columns ISCO and S-ISCO** is also included in Table 7.16. In this case, the experimental TUs values obtained are in good agreement with those estimated, which is justified by the fact that the EC_{50i} values of all COCs present in the aqueous phases obtained after ISCO and S-ISCO treatments (under alkaline conditions) are known, and therefore, the estimation is quite accurate. This indicates that no toxic compounds other than COCs were in the aqueous phase extracted from the soil (Pvs flushed from the columns). Therefore, intrinsic soil toxicity corresponds to compounds in the soil that do not pass to the aqueous phase.

Moreover, the results obtained showed that the toxicity (TUs) of the Pvs flushed from the different treatments slightly increased as the concentration of surfactant increased (ISCO (ND) < S-ISCO-5 (5.6) < S-ISCO-10 (22.1)), which is associated with a higher COCs solubilization in the aqueous phase.

The EC_{50} values of the **soil organic extract** (3.2% of methanol) have been obtained by applying the *adapted Organic Solvent Sample Solubilization Test* (aSSSOT, Subsection 6.3.1.6) for the five soils under study: SS-C L0 (unpolluted), SS-C L2 (polluted) and soils recovered from the column after ISCO, S-ISCO-5 and S-ISCO-10 treatments and the values obtained (expressed as 1/EC50 (L_{MeOH} g_{soil}^{-1}) are shown in Figure 7.58-a. COCs concentrations in the soil organic extract (as mg kg_{MeOH}^{-1}) were similar to COCs concentration in soil (as mg kg_{soil}^{-1}) since about 98% of COCs in soil were extracted (as stated in the experimental section, 6.3.1.1). The mass ratio MeOH/soil used for preparing the organic extract was 1:1. As can be seen, the trend obtained for soil toxicity reduction is similar to that shown for the mBSPT results. In this case, the differences between polluted and unpolluted soil toxicity are more significant in the organic phase. This finding can be explained as most of the COCs in soil are in the organic extract.

On the contrary, due to its hydrophobic character, most COCs remain in the soil phase when the soil is in contact with the aqueous phase (mBSPT method). As the aOSSST measures the toxicity of the compounds extracted in the organic phase (methanol), the concentration of COCs in the different soils organic extracts has been represented (Figure 7.58-b) to confirm the proportionality between both measures. (It is demonstrated that the toxicity of the organic extracts correlates well with the COCs concentration in the soil as shown in Figure 7.58-a and b (Domínguez, Ventura et al. 2023, **ART. 1**).

The toxicity of the organic extracts of the treated soils decreases significantly (including the percentage of the initial one), reaching values equivalent to those of the reference soil (SS-C L0).

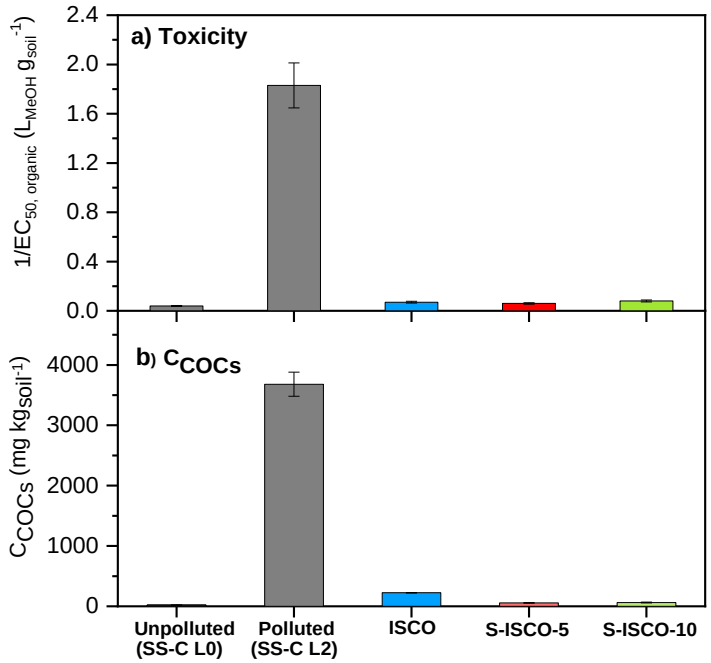

Figure 7.58. Soil organic extract toxicity ($1/EC_{50}$, Microtox® aOSSST) (a) and COCs concentration (mg kg_{soil}^{-1}) (b) of the unpolluted, polluted, and treated soils (Santos, García-Cervilla et al. 2022, **ART. 7**).

Finally, as previously mentioned for the case of soil toxicity, the aOSSST confirms that the addition of surfactant in the range studied (5-10 g L^{-1}) does not cause an increase in soil toxicity (S-ISCO *vs.* ISCO experiments). Thus, the proposed in situ treatments (ISCO or S-ISCO, with alkaline activation of PS) can be proposed for a full-scale application, as they lead to a high COCs reduction and restore the soil to its original toxicity value.

Chapter 8.

CONCLUSIONS

This section summarizes the main **conclusions** obtained concerning each partial objective of the Doctoral Thesis.

Characterization of polluted samples

The main conclusions obtained after the characterization of soil samples (topsoil (TS) and subsoil (SS)), the elutriates, and the sources of pollution causing this contamination (HCH particulate matter and DNAPL) are shown below.

Topsoil

- The solid waste generated in lindane (γ-HCH) manufacturing (**HCH particulate matter**) presented the following distribution: α-HCH (83%) > β-HCH (9%) > Σγ,δ,ε-HCH (8%) (Figure 7.5). The production process of lindane (described in Subsection 4.3, Figure 4.10) justified the composition of this solid waste. The low concentration found for γ-HCH (1.8%) can be explained by attending to the proportion of each isomer in the technical-HCH obtained during lindane production (α: 55–80%, β: 5–14%, γ: 10-15%, δ: 2-16% and ε: 3-5%). After the technical HCH purification process to obtain lindane (for its subsequent use as a pesticide), the solid HCH waste was enriched in the other isomers.
- The concentration of HCHs measured in polluted TS samples ranged from 40 to 1150 mg kg_{soil}^{-1} (from L1 to L4), with **α-HCH** (75 ± 5%) and **β-HCH** (22 ± 8%) as primary pollutants.
- The percentage of α-HCH found in HCHs particulate matter (83%) was only slightly higher than that noticed in TS samples (75%). Thus, the contamination of TS can be associated with the presence of **particulate HCHs**, with a small contribution of these pollutants **adsorbed** into the soil.

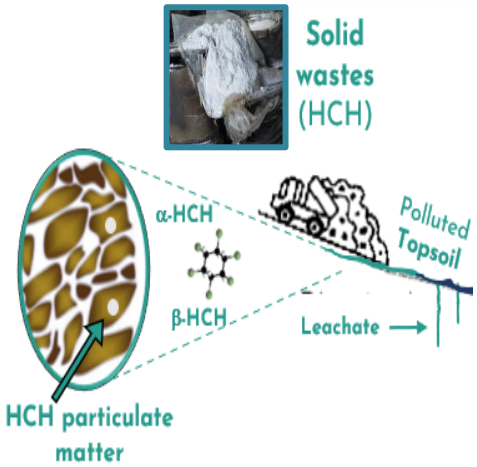

- TS elutriates, which simulate leachates of contaminated superficial soil, presented a total HCHs concentration between 0.1 and 10.9 mg L^{-1}. The concentration of

HCHs in the elutriates increased with increasing soil pollutants concentration but was limited by the low solubility of these compounds.

- TS presented moderately alkaline pH with buffer capacity due to the significant carbonate content (≈ 40% as calcium carbonate), which can limit the application of the Fenton process (requiring acidic pHs, optimal pH = 3), and relatively low organic matter content (TOC = 1.5%). Only a small percentage of this TOC corresponded to pollutants; the rest was attributable to natural organic matter as humic acid-like compounds.
- The contamination level of TS in the most polluted areas was too high for bioremediation, and other technologies must be first applied.

Subsoil

- The liquid waste (**DNAPL**) from the chlorination failed reaction (lindane production) and distillation tails (lindane purification) are the source of pollution of subsoil and, therefore, groundwater. DNAPL from Sardas Landfill was composed of a mixture of 28 chlorinated organic compounds (**COCs**): HCHs (29%)> HeptaCHs (17%) > TCBs (16%) > TetraCBs (13%) > DCBs (9%) > CB ≈ PCXs (7%) > HCXs (3%) (Figure 7.5).

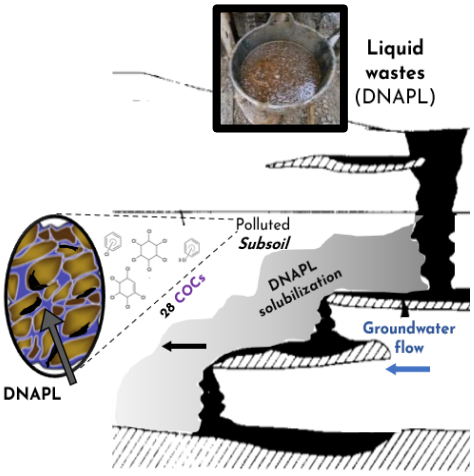

- COCs found in DNAPL were identified in SS samples with a total COCs concentration (500-9500 mg kg^{-1}) significantly higher than in TS (40 -1150 mg kg^{-1}). This fact was attributed to the different sources of soil pollution (HCH particulate matter for TS and DNAPL for SS).
- COCs composition was very variable in the coarse (C) fraction of SS obtained at several depths in the alluvial. The contribution of γ-HCH was exceptionally high in L1. In contrast, in the fine (F) fraction, pollutants distribution was similar regardless of the contamination level, and γ-HCH percentage increased with COCs concentration.
- SS elutriates, which simulate the groundwater in contact with polluted SS and the residual DNAPL concentration, presented a maximum value of COCs solubilized of around 40-50 mg L^{-1} (asymptotic trend, Figure 7.4), which can be attributed to

the saturation of COCs in the aqueous phase. These high COCs concentrations constitute a high risk due to the proximity of the Gállego River.

- SS elutriates presented a significantly higher COCs concentration than TS elutriates. The origin of this result lies in the contamination source. DNAPL (SS) contains a mixture of chlorinated organic compounds (among them, chlorobenzenes) with high water solubility, while HCH isomers (TS) are poorly soluble in water.

Initial acute toxicity

The three different Microtox® tests were applied in this study: soil (mBST), soil elutriates (BT), and soil organic extracts (aOSSST) revealed interesting and complementary information, providing a complete and comprehensive evaluation of the acute toxicity of these polluted sites.

- **Soil samples** (TS and SS) presented high acute toxicity in the Microtox® mBSPT ($EC_{50,\ soil} \leq 5$ g L^{-1}, Table 7.3). The reference samples (L0), with low COCs concentration, exhibit intrinsic acute toxicity in this test, indicating that there are toxic compounds for the Microtox bacteria in the soil matrix. The higher the COCs concentration in the soil, the higher the acute toxicity (Figure 7.6-a), highlighting the need for remediation of these sites. However, an asymptote in EC_{50} values was obtained as the COCs concentration in the soil increased due to the limited solubility of COCs in the aqueous phase, being more pronounced in SS samples.
- EC_{50} of **soil elutriates** (Microtox® BT) was higher than EC_{50} of soils (Microtox® mBSPT), indicating that the toxicity of soils is higher than that of the COCs solubilized to the aqueous phase. The toxicity of soil elutriates (for TS and SS) was well correlated with dissolved COCs (Figure 7.6-b).
- TS elutriates showed low acute toxicity ($EC_{50} > 100$ g L^{-1}), indicating that the possible leachates from the landfill surface soil did not pose an acute toxicity risk. In contrast, SS elutriates presented moderate acute toxicity (10 g $L^{-1} \leq EC_{50} \leq 100$ g L^{-1}), meaning a higher risk of groundwater in contact with contaminated subsoil, mainly due to the higher COCs solubilized in this case.
- **Soil organic extracts** of both types of soils (TS and SS) represented more plainly the acute toxicity of these soils without this asymptotic trend since this method is not limited by COCs solubility in water. Moreover, the EC_{50} of hydrophobic organic

compounds (HOCs) with low acute toxicity (high EC_{50} values) could be determined by this method.

- Contamination from **DNAPL** produced a more significant inhibition in bacteria light emission than contamination by **HCHs**, which explained the higher toxicity of SS than TS.
- Regarding their bioavailability, contaminants in the finest SS fraction were more strongly adsorbed and less accessible to *Vibrio fischeri*.

Topsoil (TS) oxidation treatments

Oxidant evaluation

Among the oxidants tested (hydrogen peroxide, HP, and persulfate, PS) **persulfate** was selected for the on-site remediation of topsoil (TS) based on the following reasons:

- The application of the **Fenton process** (HP+Fe) at the conditions tested (neutral pH, ambient temperature) was not efficient due to the excessive unproductive consumption of hydrogen peroxide (NOD > 400 g_{H2O2} kg_{soil}^{-1}) and iron precipitation explained by soil characteristics (high carbonates content, ≈ 40 %). Thus, further research is required to apply the Fenton process, including using biodegradable and refractory chelating agents capable of maintaining iron in solution at circumneutral pH and stabilizing agents that increase the stability of hydrogen peroxide.
- **Persulfate** (PS) was much more stable than HP (NOD = 0.8 g_{PS} kg_{soil}^{-1}). However, low pollutants conversions were obtained when this oxidant was not activated (ambient temperature, 14 days of treatment).

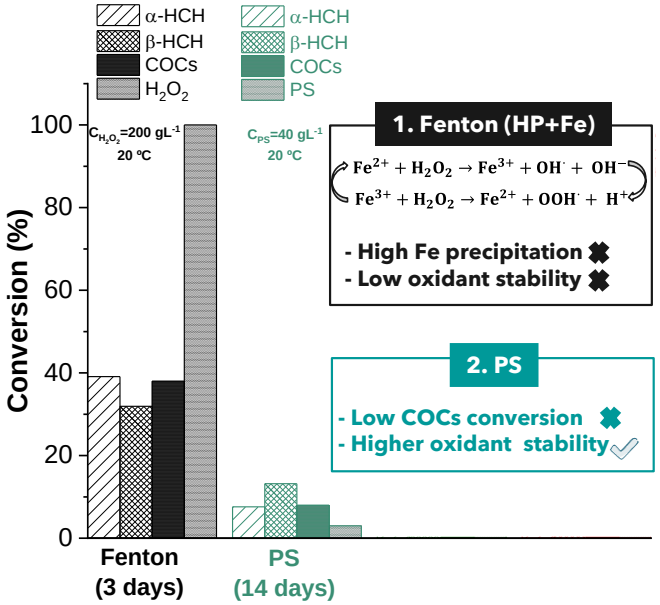

PS activation evaluation

To enhance the COCs oxidation, the application of different PS activations methods, such as **alkali** (NaOH at 20 °C) and **temperature** (40 °C), which increase the generation of radicals (species able to degrade the organic compounds), was evaluated:

- In the **alkaline activation** of PS (**PS/NaOH**, pH > 12), HCHs were dehydrochlorinated to a mixture of trichlorobenzenes (TCBs): 1,2,4-TCB (85%), 1,2,3-TCB (12%), and 1,3,5-TCB (3%). TCBs have a higher solubility in water than HCHs and are more easily oxidable. β-HCH was more recalcitrant to dehydrochlorination than α-HCH due to its lower solubility in the aqueous phase and lower hydrolysis rate (to TCBs), increasing the reaction times required to remediate HCHs-polluted TS.
- The alkaline activation of PS (**PS/NaOH**, 20°C) led to higher COCs conversion than the thermal activation of this oxidant (**PS/T**, 40°C) at circumneutral pH. This can be explained by the lower HCHs solubility than TCBs and the higher refractoriness of these compounds towards oxidation by $SO_4^{\bullet-}$ radicals (generated in PS/T system) than $OH^{\bullet}$ (generated in PS/NaOH system).

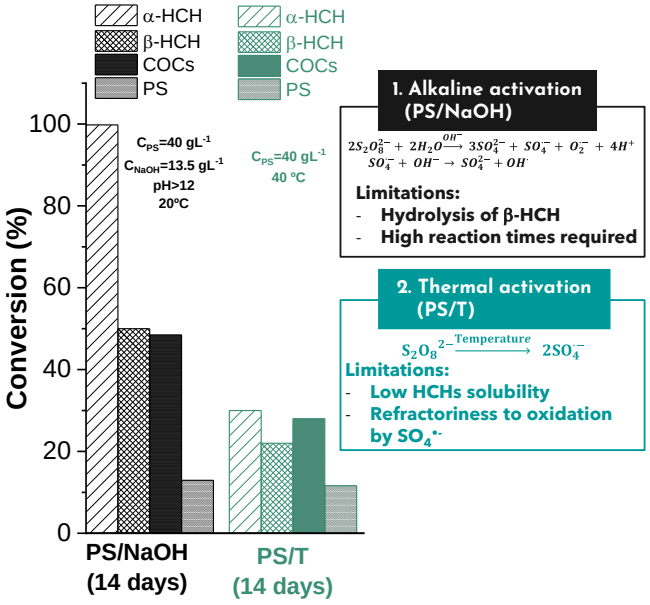

- The reaction temperature (from 20 to 80 °C) played a fundamental role in the **PS/T system**, increasing the production of sulfate radicals and, consequently, the dechlorination degree and HCHs degradation and decreasing the concentration of the chlorinated byproducts generated. The initial concentration of PS (from 10 to 80 g L^{-1}) also had a determinant role, significantly increasing the degradation of HCHs and reducing the chlorinated byproducts concentration in the reaction media.
- Based on the identified species, a series-parallel reaction pathway for the degradation of HCHs in soil by thermally activated PS was proposed.

- The decomposition of the oxidant follows first-order kinetics. Oxidant stability increased in the presence of soil, and the efficiency of its consumption ($mg_{COCs,removed}/g_{PS,consumed}$) was not significantly affected by temperature.
- The best results were obtained at **55 °C, C_{PS} = 80 g L^{-1}, V_L/W_S = 2/1, 100 rpm (9 days)**, achieving a degradation of HCHs around 83% with no chlorinated byproducts at the end of the reaction (chlorine balance ≈ 100%). It should be noted that higher temperatures and reaction times were required for soil remediation than treating polluted aqueous phases (Dominguez, Romero et al. 2020) since the low solubilization of these compounds to the aqueous phase limits their degradation. On the other hand, the soil inhibitory effect hindered the diffusion of sulfate radicals.

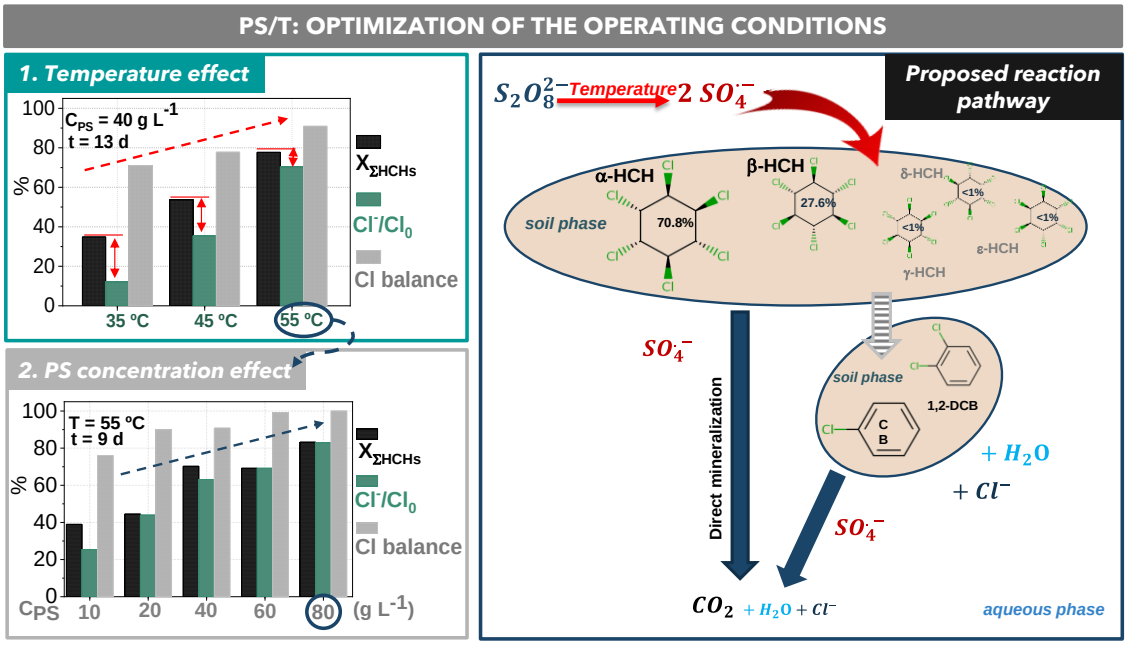

Intensification of PS/NaOH

The intensification of the PS/NaOH system has been explored using different alternatives to reduce treatment times and/or increase process efficiency. The efficacy of base-activated persulfate under a wide range of operating conditions has been evaluated providing practitioners for future specific HCH remediation projects.

1. *PS/NaOH/T*

- The intensification of the PS/NaOH by temperature has been demonstrated to be an effective method for the remediation of HCHs in the soil at relatively short reaction times.
- The disappearance rate of β-HCH (limiting step of the process) increased with the reaction temperature, the initial concentration of PS, and the ratio V_L/W_S. A balance between reaction temperature, PS consumption, reaction time, and final decontamination requirements should be accomplished to select suitable operating conditions. The selected conditions (after a systematic study) imply the **simultaneous addition of reagents (PS and NaOH), T = 50 °C, C_{PS} = 40 g L^{-1}, V_L/W_S = 2, pH > 12**, achieving 100% and 81% of α-HCH and β-HCH conversion (3 days), 94% of COCs depletion and 29% of PS consumption. A dechlorination degree of 94% was achieved, with no chlorinated byproducts.
- The solution pH should remain above 12 to guarantee the alkaline activation of PS and the consequent generation of hydroxyl radicals. Thus, if high temperatures (50, 60 °C) and PS concentrations (40, 60 g L^{-1}) were used (conditions involving increased NaOH consumption), the concentration of NaOH should be adjusted.
- After the on-site remediation process (without losing natural organic matter from the soil), sedimentation can easily separate both phases. This step facilitates the supernatant reuse (still containing 28 g L^{-1} of PS) for a new batch of contaminated soil.

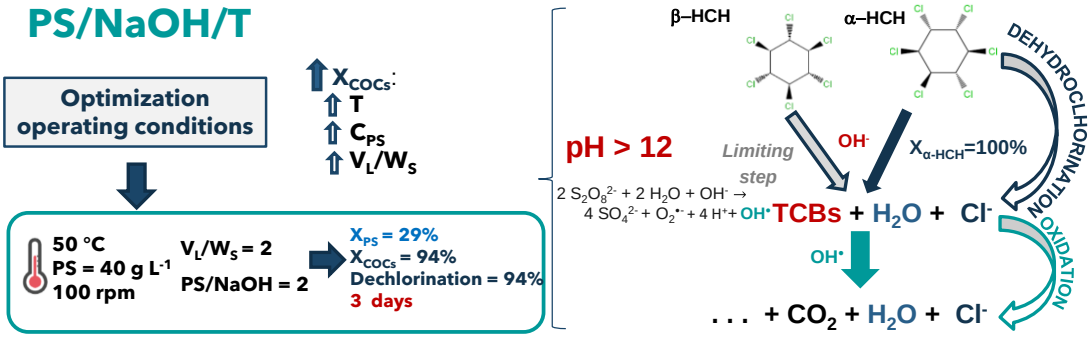

2. *PS/NaOH/US*

- The intensification of the PS/NaOH by US increased the efficiency of the remediation of HCH-polluted TS due to i) the enhanced desorption of the pollutants from the soil to the aqueous phase (according to SEM images, US application breaks the soil aggregates), ii) the increase in the radical production, and iii) the improved COCs oxidation kinetics. The application of US led to an increase in the reaction temperature

(inducing thermal PS activation), which was also beneficial for the remediation process.

- Increasing the US power (from 0 to165 W), corresponding to 0-62 W L^{-1} of US power density) and the initial concentration of PS (from 10 to 60 g L^{-1}), the degradation of HCHs and TCBs (the hydrolysis products of HCHs) increased. Moreover, the dechlorination of HCHs was also favoured, decreasing the concentration of chlorinated byproducts. No aromatic or non-oxygenated chlorinated compounds were detected in any case.
- At selected operating conditions (**V_L/W_S = 2, C_{PS} = 60 g L^{-1}, NaOH/PS = 2, 165 W**), a conversion and dechlorination degree of HCHs of 94% and 74% were achieved in only **3 h** of reaction time, respectively. At these conditions, a chlorine balance of 83% was reached.
- The PS/NaOH/US system may offer a promising on-site treatment option for the remediation of source zones with high levels of HCHs (or other similar HOCs), considerably reducing the reaction times required.
- When selecting this technology, the cost associated with the application of US and the volume of soil to be treated must be considered. It should be highlighted that the power density range used in the current work (0-91 W L^{-1}) was relatively low compared to those usually reported in the literature (Deng, Lin et al. 2015, Lei, Tian et al. 2019), indicating moderate energy consumption. Pilot studies using large-scale US reactors must also be performed to scale up this treatment.

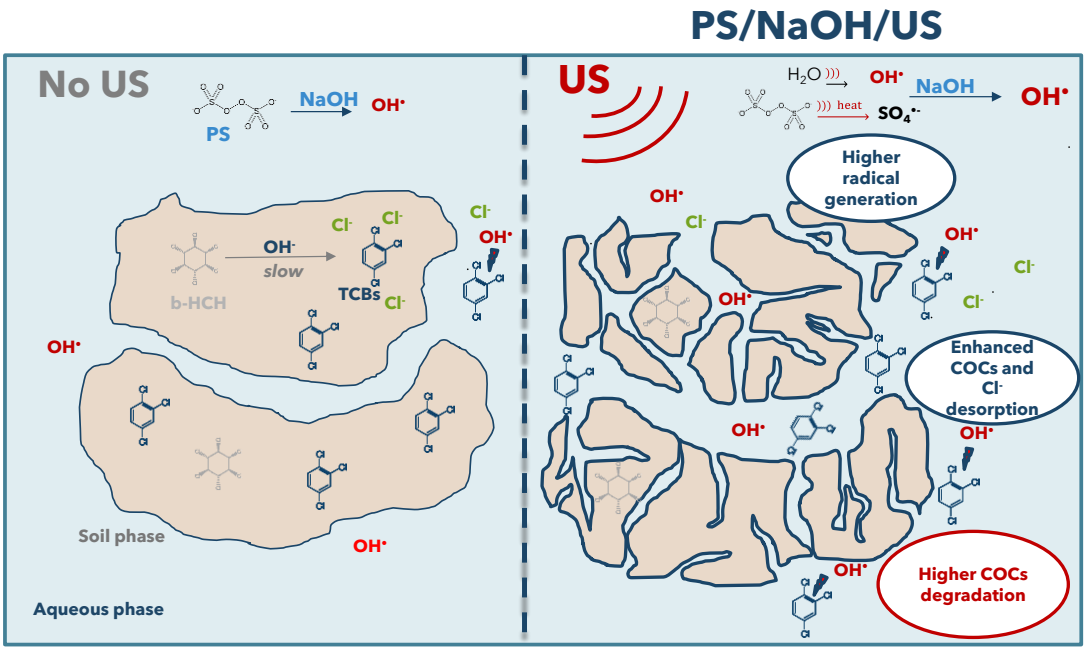

3. *Surfactant/PS/NaOH/T*

- The pH was fundamental in the solubilization of COCs enhanced by surfactants (T80, E3, and SDS). At neutral pH, surfactant addition slightly increased the solubilized mass of COCs, decreasing the partition coefficients ($K_{d,COCs}$). At pH > 12, higher COCs solubility was achieved since HCHs hydrolyze to trichlorobenzenes, with significantly higher water solubility than the parent compounds.
- T80 was unstable at pH > 12; therefore, the concentration of COCs solubilized decreased at these conditions.
- NaOH and surfactant concentration remarkably affected the pollutants solubilization efficiency. The highest COCs solubilization was obtained at moderate NaOH concentration (4 g L^{-1}), finding the surfactant solubilization order: SDS ($K_{d,COCs}$ = 1.0 L kg^{-1}) > E3 ($K_{d,COCs}$ = 1.3 L kg^{-1}) > T80 ($K_{d,COCs}$ = 7.0 L kg^{-1}). The higher the surfactant concentration, the lower the $K_{d,COCs}$ value, being this improvement lower as the surfactant concentration increases.
- More than 80% of COCs were extracted from the soil using the following solubilization conditions: **SDS or E3 (5 g L^{-1}), pH > 12, simultaneous addition of reagents, V_L/W_S = 2 and 3 successive solubilization cycles of 24 h**.
- The resulting emulsions (ΣCOCs = 34-70 mg L^{-1} (mainly as TCBs)) were subsequently treated by PS/NaOH/T (**C_{PS} = 40 g L^{-1}, NaOH: PS = 2, and T = 40 °C**). COCs conversions of 30% and 96% were achieved in 72 h when treating E3 and SDS-emulsions, respectively, highlighting the suitability of SDS for the integrated surfactant-enhanced solubilization and emulsion treatment process.

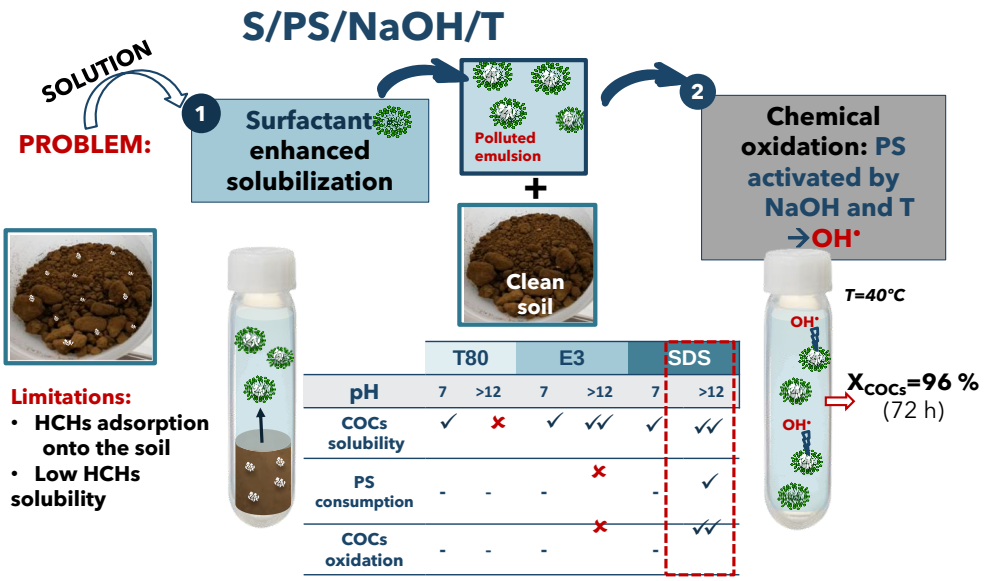

Acute toxicity of treated soils

Remediated Topsoil

- Before a full-scale application, it is essential to verify that chemical treatments (with high concentrations of oxidant and activator (NaOH)) will not cause an increase in the acute toxicity of the soils.
- At the remediation conditions used (C_{PS} = 60 g L^{-1}, 50 °C, V_L/W_S = 2, 17 days), the **PS/T treatment** reduces the acute toxicity of the TS (Microtox® mBST) to the minimum level, that is, to the intrinsic toxicity of the soil with a negligible concentration of contaminants (L0, reference soil). In the case of the aqueous phases analyzed, neither the reaction supernatant nor its aqueous leachate (Microtox® BT) exhibited toxicity. Similar to the soil phase results, a significant soil organic extract (Microtox® aOSSST) toxicity reduction was obtained after the remediation treatment.
- On the other hand, the soil organic matter, mainly attributable to humic acid-type compounds, was resistant to the oxidation treatment (PS/T). The toxicity reduction and the maintenance of the physico-chemical characteristics of the soil suggest that a bioremediation post-treatment could be applied.
- Although TS toxicity was not significantly reduced after the application of **PS/NaOH/T** treatment (C_{PS} = 60 g L^{-1}, molar NaOH:PS = 2, 50 °C, V_L/W_S = 2, 11 days), it was demonstrated that the reagent addition (PS and NaOH) and/or by-products generation did not increase the acute TS toxicity. Despite the COCs concentration was significantly reduced (X_{COCs} = 98%) by the remediation process, the fact that this was not reflected in an acute toxicity reduction can be attributable to the high NaOH concentration and the V_L/W_S ratio used. Thus, a more thorough washing of the soils after alkaline treatment would be necessary.
- The PS/NaOH/T aqueous reaction supernatant exhibits considerably acute toxicity, justified by TCBs presence. These compounds are soluble in the aqueous phase and present considerable acute toxicity to *Vibrio fischeri*. However, the elutriate of this treated soil showed significantly lower acute toxicity (low concentration of TCBs).
- It should be highlighted that the acute toxicity of treated soils has been only performed by applying the Microtox® analysis, and therefore, for more comprehensive and practical information (before the implementation of the process), further research should be conducted to assess the toxicity in the presence of other organisms and trophic levels (*Artemia salina*, *Daphnia magna*, etc.,) and to evaluate

the biodegradability of treated soils. These aspects will be further assessed (see Chapter 9, "Ongoing and future work").

Acute toxicity of treated TS

		PS/T	PS/NaOH/T
	Treatment efficiency	✓	✓✓
Acute toxicity	Soil	✓✓	✓
	Aqueous phases - Reaction supernatant	✓✓	✗
	- Elutriate	✓✓	✓
	Organic extract	✓✓	✓

Remediated Subsoil

- The initial polluted soil showed high acute toxicity, and the toxicity of the soils treated by ISCO and S-ISCO at column scale decreased significantly.
- EC_{50} values of treated soils were equivalent to that obtained for the non-contaminated soil (mBSPT), and the toxicity of Soil Organic Extract (aOSSST) of treated soils were orders of magnitude lower than that of the initial polluted soil.
- Neither the application of E3 nor its concentration (within the concentration range studied) generated toxicity in the treated soil. Thus, either of the proposed in situ treatments (ISCO or S-ISCO, with alkaline activation of PS) is suitable for a full-scale application, as they lead to a high COCs abatement (> 90%) and restore the soil to its original toxicity value.

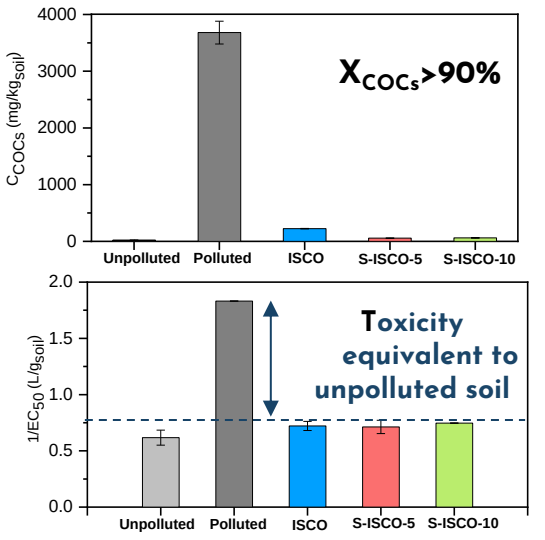

ISCO and S-ISCO
✓ full-scale application

Chapter 9.

ONGOING AND FUTURE WORK

9.1. Biorremediation

9.2. Additional evaluation of toxicity and biodegradability

9.2.1. Rapid biodegradability test

9.2.2. *Artemia salina*

9.2.3. *Daphnia magna*

9.3. Field scale application

9.4. Remediation of aqueous phases contaminated with other organics pollutants

9.4.1. Remediation experiments

9.4.1.1. Synthesized materials

9.4.1.2. Washing of synthesized materials

9.4.1.3. Variables studied

9.4.2. Results

9.1. Bioremediation

The contamination level of TS in the most polluted areas is too high to apply bioremediation treatments directly, and other technologies should be used as the first step. In this context, the evaluation of **bioremediation** by applying **organic amendments** as the final part of a treatment train after chemical oxidation has been carried out. This study is being performed in collaboration with the research group "Soil and its environmental impact" of the Chemical in Pharmaceutical Sciences Department at the University Complutense of Madrid.

Three different soil samples free of contamination were collected from the Bailín landfill (P1, P2, and P3) to evaluate the effects of soil physicochemical characteristics. Subsequently, these soils were spiked by adding HCH particles (Figure 9.1) to reach a constant concentration of 500 mg kg^{-1} in each soil sample.

Figure 9.1. Contaminant (HCH particles) addition to soil samples.

First, soils (P1, P2, and P3) were subjected to **PS/T treatment**. For this purpose, 1.2 kg of soil was in contact with 3.6 L of aqueous phase (V_L/W_S = 2) containing a PS concentration of 60 g L^{-1}. The reactors were placed in a thermostatic bath at 50 °C (30 rpm). The experimental conditions were selected according to previous results (Dominguez, Checa-Fernandez et al. 2021, **ART. 3**).

Figure 9.2. Experimental device for treatment of soils P1, P2 and P3.

The aqueous and soil phases were separated and characterised at the final reaction time (12 d). The conversion of the oxidant (PS) and contaminant (HCH isomers) conversion is shown in Figure 9.3. These results were equivalent to those previously reported (Dominguez, Checa-Fernandez et al. 2021, **ART. 3**). There were no significant differences in oxidant and HCHs conversion depending on the type of treated soil.

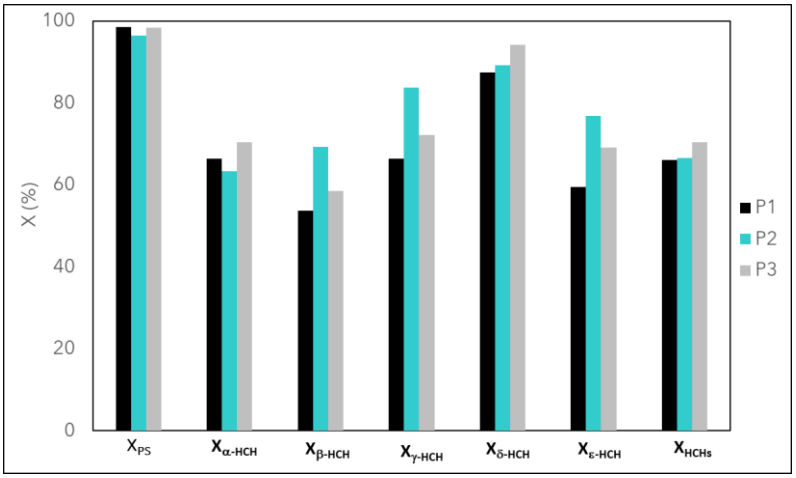

Figure 9.3. Conversion of oxidant and HCH isomers when treating P1, P2, and P3 soils.

Subsequently, the ability of a bioremediation treatment to remove the remanent HCH isomer from soils under controlled conditions was assessed. The bioremediation of organic contaminants can be achieved using three different strategies: bioattenuation, biostimulation, and bioaugmentation. Among them, biostimulation is a promising option that focuses on the adjustment of environmental conditions (e.g., moisture, aeration, pH, and temperature), the application of indispensable nutrients (e.g., nitrogen, and phosphorus), and the required electron acceptors, stimulating the activity of degrading microbes and, therefore, decreasing the concentration of soil pollutants (Garbisu,

Garaiyurrebaso et al. 2017). Using organic wastes as soil amendments is a sustainable and cost-effective approach to biostimulation (Kanissery and Sims 2011). **Organic amendments** act as a food source for microorganisms, promoting their growth and activity, increasing biological activity and remediation efficiency (Hoang, Sarkar et al. 2021). In this study, an **organic horse amendment** was used. This organic amendment (at 5% dry weight) was added to the treated soils, and the samples were analyzed at different incubation times (1, 3, 7, 15, 30, 60, and 90 days). For this purpose, the temporal evolution of **enzymatic activity** and concentration of residual HCHs will be analyzed. Six enzyme activities will be systematically analyzed: enzymes related to C cycling: β-glucosidase (β-GLU) and phenoloxidase (PHE), N cycling: arylamidase (ARYLN), and urease (URE), and P cycling: phosphatase (PHOS). Dehydrogenase (DH) activity will be further evaluated. Currently, the results of these experiments are still under development and interpretation.

9.2. Additional evaluation of toxicity and biodegradability

Soil toxicity and biodegradability testing are essential for assessing the potential ecological risks of polluted soils and verifying the development of effective remediation strategies. Thus, three additional assays will be applied to evaluate further the soils treated by the selected remediation techniques:

- **Rapid biodegradability test**
- ***Artemia salina* test**
- ***Daphnia magna* test**

It should be noted that these assays are commonly used to characterize aqueous samples. Thus, a previous study will be carried out to adapt them (as in the case of the Microtox® bioassay). For example, analysis of the corresponding elutriates will also be evaluated.

9.2.1. Rapid biodegradability test

The **biodegradability** of the initial and treated samples will be evaluated using a rapid biodegradability assay (Herraiz-Carboné, Cotillas et al. 2020). For this purpose, **real sludge** from a wastewater treatment plant will be used. Rapid biodegradability assays will be carried out by placing the target sample in contact with the endogenous activated sludge. Dissolved oxygen concentration will be monitored using an oximeter (HI9142, Hanna Instruments) as a function of experimental time. The rapid biodegradability of the

samples will be calculated as a relation between rapid biochemical oxygen demand (BOD) and chemical oxygen demand (COD) using Eq. (9.1).

$$\text{Rapid biodegradability (\%)} = \frac{\text{BOD}_{\text{rapid}} \cdot \text{V}_{\text{biological reactor}}}{\text{COD}_{\text{sample}} \cdot \text{V}_{\text{sample}}} \quad (9.1)$$

The rapid BOD will be calculated as the difference in dissolved oxygen decay (mg O_2 dm^{-3}) between the slope of endogenous activated sludge and the slope when the studied sample is added to endogenous activated sludge.

9.2.2. *Artemia salina*

The ***Artemia salina*** test, commonly known as **brine shrimp**, is widely used in various scientific fields because of its many advantages, such as simplicity, low cost, and short-term reliability (Vanhaecke and Persoone 1981). The toxicity of the initial polluted and treated samples will be analyzed using the *Artemia salina* test, which involves exposing brine shrimp to the tested substance and observing their mortality rate. The small size, high reproduction rate, and sensitivity to toxins of brine shrimp make it a suitable organism for this type of sample. Additionally, this organism has a high-water filtration rate. Therefore, it is more susceptible to pollution exposure than other aquatic species, being recognized as an outstanding model organism for toxicity testing (Zhu, Xue et al. 2017). The procedure followed will be based on previous studies (Ozkan, Altinok et al. 2016, Munoz, Nieto-Sandoval et al. 2019). Firstly, *Artemia salina* larvae were obtained. The egg-hatching process consisted of adding 0.5 g of eggs (Figure 9.4) in a beaker containing 230 mL of saline water (35 g L^{-1} of Marinium® salt), previously oxygenated for 24 h.

Figure 9.4. Eggs (Artemio Pur®, left) and live (right) *Artemia salina*.

It was placed on an IKC RCT Basic hot plate for temperature control. For hatching, the following conditions were maintained: temperature of 30°C, pH value of 7, uninterrupted oxygenation using a compressed air pump, and light exposure. After the eggs hatched at

24 h and with the *Artemia salina* in the larval stage (Figure 9.4), size of approximately 1 to 2 mm, the preparation of the samples was accomplished.

Different serial solutions are prepared with the sample under analysis in vials in which 20 artemia salina larvae are previously added. Vials were placed in a Julabo SW22 water bath at 30°C and under dark conditions for 72 h. The mortality of the microcrustacean was monitored after 24 h, 48 h, and 72 h of exposure to the samples, and the number of dead individuals was checked by visual inspection. The LC_{50} value (at 24, 48, and 72 h) can be determined with the mortality values. The results obtained are currently being interpreted.

9.2.3. *Daphnia magna*

The ***Daphnia magna*** is one of the most commonly used model organisms to assess the toxicity of a wide range of contaminants (Tkaczyk, Bownik et al. 2021). This test employs a **freshwater crustacean** to determine the sample toxicity. These organisms (young daphnids aged less than 24 hours at the start of the test) will be exposed to polluted and treated samples at a range of concentrations for 48 hours. 20 (actively swimming) neonates are transferred into each test well of a multiwell plate (Figure 9.5). Previously, each well of the test plates had to be filled with 10 ml of increasing concentration of toxicant solution (or Standard Freshwater in the control column). The test plate is incubated in darkness at 20 °C. Their survival rates will be monitored to assess the toxicity of the treated soils and elutriates. The daphnids immobilisation is recorded at 24 and 48 hours and compared with control values by placing the test plate under a light table (Figure 9.5). The results are analysed to calculate the EC_{50} (preferably at 48h). This method is currently being adapted to analyze the samples under study.

Figure 9.5. Multiwell plate on a light table employed for *Daphnia magna* test.

9.3. Field-scale application

Part of the experimentation of this Doctoral Tesis has been carried out within the framework of a project in collaboration with the company SARGA (Contract Art. 83. Sediment and drag-out remediation service for the Ballín and Sardas facilities, 2020, N/Ref.: 5507001-182).

The most relevant results obtained were the optimal operational conditions of different PS-based treatments (previously selected in the SARGA project (540-2019)) for the remediation of sediments from the Bailín landfill heavily contaminated by residues from the manufacture of lindane. The effect of oxidant concentration, activator, and temperature on the temporal evolution of contaminants (α- and β-HCH isomers) in soil was investigated. The best conditions for cost-effective soil remediation were selected in less than two days of treatment.

The results of this contract were used to select the optimal conditions, to build the prototype by the company, and to estimate the treatment costs. The company successfully evaluated at pilot scale the treatment application at the site, which successfully replicated the laboratory conditions, and a larger-scale implementation is under consideration. The results obtained in the laboratory (and presented in this Doctoral Thesis) have served as the basis for a pilot-scale prototype treatment for the remediation of soils contaminated with HCH particulate matter in the most HCH-polluted areas of the old Bailín landfill.

9.4. Remediation of aqueous phases contaminated with other organic pollutants

During this Thesis, a 3-month stay (from 1st September to 1st December 2022) at the **Università degli Studi di Roma Tor Vergata** was conducted. The application of different types of oxidants and activations for removing chlorinated organic pollutants from water was studied during this period. The following secondary objectives were carried out to achieve this overall objective:

- Analysis of the current situation of contaminated sites in European countries to identify the potential organic pollutants present and the need for environmental remediation.
- Selection of the model pollutant to be investigated (4-chlorophenol), as well as the treatments to be applied, considering previous results obtained in the literature.

- Set-up of experimental devices (reactor selection, operating conditions, agitation system, etc.) and analysis equipment (gas chromatography, ion chromatography, spectrophotometer, etc.).
- Evaluation of the feasibility of different oxidants (persulfate (PS) and peroxymonosulfate (PMS)) and the application of different activators (Fe (II), zero-valent iron microparticles (ZVI), and bimetallic particles (Fe-Cu)). The efficiency of each treatment was determined based on pollutant elimination, oxidant conversion, and reaction time necessary to reach the desired degree of decontamination.
- Evaluation of the stability of different oxidants in the presence of different activators.
- Selection of the main optimal operating variables for each of the treatments under study: i) concentration of reagents (oxidant and activator), ii) Fe/Cu mass ratio in the bimetals, iii) contact time (ZVI particles and/or bimetals), iv) milling of the activator, etc.
- Evaluation of kinetic equations, reaction mechanisms, etc.

9.4.1. Remediation experiments

9.4.1.1. Synthesis of materials

Milling of the ZVI microparticles and synthesis of the bimetals (Fe-Cu) were carried out by the physical method of disk milling (Figure 9.6).

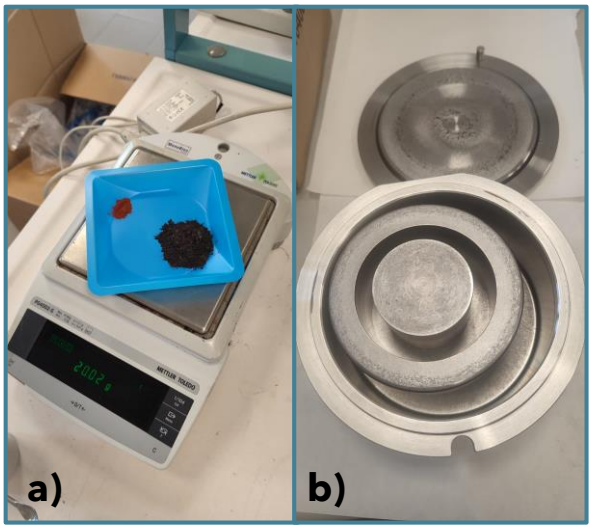

Figure 9.6. Synthesis of the bimetals Fe-Cu by mixing Fe and Cu microparticles (a) and subsequent disk milled (b).

Fe-Cu bimetals were synthesized by mixing ZVI and Cu microparticles using three different weight percentages of Cu (1%, 5%, and 50%). For their synthesis, the disk mill was loaded with ZVI and Cu and milled for 60 min, which allowed the production of a bimetallic phase by the continuous fracture of the particles induced by the impact of the disks.

9.4.1.2. Washing of synthesized materials

Both iron microparticles (ZVI) and bimetals (Fe-Cu) were pretreated with 0.1 M HCl for 30 min, rinsed with N_2-purged water for 10 min, and dried in N_2 atmosphere. As other authors have shown, acid pretreatment can lead to surface cleaning by metal dissolution and oxide layer breakdown, with a consequent increase in the reactive site density and specific surface area (Settimi, Zingaretti et al. 2022).

9.4.1.3. Variables studied

Tests were performed in 40 mL PTFE vials. A constant contaminant concentration of 20 mg L^{-1} and agitation speed of 80 rpm (LBX RR80 rotary shaker) was used. The tests were performed in triplicate. The following variables were studied:

- Effect of oxidant (PS, PMS)
- Effect of activator type (without, Fe (II), ZVI, Fe-Cu5%)
- Effect of the activator concentration (Fe-Cu 5%, 0.05-0.2 g L^{-1})
- Effect of the Fe/Cu ratio present in bimetals (1-50%)
- Effect of milling

Additionally, tests were conducted in the absence of contaminant to study the unproductive consumption of the oxidant (PS/PMS) in the presence of the different activators studied. Furthermore, tests were carried out in the presence of TBA ($OH^{\bullet}$ scavenger) and methanol ($OH^{\bullet}$ and $SO4^{\bullet-}$ scavenger) to identify the main radical species in the different systems studied.

9.4.2. Results

The efficiency of each treatment was studied based on the following criteria:

- Removal of the model pollutant (4-chlorophenol)
- Oxidant conversion
- Degree of dechlorination
- Mineralization

As a result of the stay, the evaluation of the effect of the type of activator, its concentration, the effect of the Fe/Cu ratio in the manufactured bimetals, as well as the milling of the bimetals should be highlighted. The results of these experiments are still under development and interpretation.

Chapter 10.

REFERENCES

REFERENCES

Strategic Diagnostics Inc. Microtox Rapid Toxicity Testing System, DIANE Publishing.

Abouseoud, M., A. Yataghene, A. Amrane and R. Maachi (2010). "Effect of pH and salinity on the emulsifying capacity and naphthalene solubility of a biosurfactant produced by Pseudomonas fluorescens." Journal of Hazardous Materials **180**(1-3): 131-136.

Adithya, S., R. S. Jayaraman, A. Krishnan, R. Malolan, K. P. Gopinath, J. Arun, W. Kim and M. Govarthanan (2021). "A critical review on the formation, fate and degradation of the persistent organic pollutant hexachlorocyclohexane in water systems and waste streams." Chemosphere **271**: 129866.

Ahile, U. J., R. A. Wuana, A. U. Itodo, R. Sha'Ato and R. F. Dantas (2020). "A review on the use of chelating agents as an alternative to promote photo-Fenton at neutral pH: Current trends, knowledge gap and future studies." Science of The Total Environment **710**: 134872.

Amanat, N., B. Barbati, M. M. Rossi, M. Bellagamba, M. Buccolini, L. Galantini and M. Petrangeli Papini (2022). "Synthetic and Natural Surfactants for Potential Application in Mobilization of Organic Contaminants: Characterization and Batch Study." Water **14**(8): 1182.

Baciocchi, R., M. R. Boni and L. D'Aprile (2003). "Hydrogen peroxide lifetime as an indicator of the efficiency of 3-chlorophenol Fenton's and Fenton-like oxidation in soils." Journal of Hazardous materials **96**(2-3): 305-329.

Baciocchi, R., M. R. Boni and L. D'Aprile (2004). "Application of H2O2 lifetime as an indicator of TCE Fenton-like oxidation in soils." Journal of hazardous materials **107**(3): 97-102.

Baran, A., M. Tarnawski, T. Koniarz and M. Szara (2019). "Content of nutrients, trace elements, and ecotoxicity of sediment cores from Rożnów reservoir (Southern Poland)." Environmental Geochemistry and Health **41**(6): 2929-2948.

Barbati, B., L. Lorini, N. Amanat, M. Bellagamba, L. Galantini and M. P. Papini (2023). "Enhanced Solubilization of Strongly Adsorbed Organic Pollutants using Synthetic and Natural Surfactants in Soil Flushing: Column Experiment Simulation." Journal of Environmental Chemical Engineering: 110758.

Benschoten, J. E. V., M. R. Matsumoto and W. H. Young (1997). "Evaluation and analysis of soil washing for seven lead-contaminated soils." Journal of Environmental Engineering **123**(3): 217-224.

Besha, A. T., D. N. Bekele, R. Naidu and S. Chadalavada (2018). "Recent advances in surfactant-enhanced In-Situ Chemical Oxidation for the remediation of non-aqueous phase liquid contaminated soils and aquifers." Environmental Technology & Innovation **9**: 303-322.

Bhatt, P., M. S. Kumar and T. Chakrabarti (2009). "Fate and degradation of POP-hexachlorocyclohexane." Critical Reviews in Environmental Science and Technology **39**(8): 655-695.

Bond, G. P. and J. Martin (2005). Microtox. Encyclopedia of Toxicology (Second Edition). P. Wexler. New York, Elsevier**:** 110-111.

Bouzid, I., J. Maire, E. Brunol, S. Caradec and N. Fatin-Rouge (2017). "Compatibility of surfactants with activated-persulfate for the selective oxidation of PAH in groundwater remediation." Journal of Environmental Chemical Engineering **5**(6): 6098-6106.

Brebbia, C. A., Ed. (2013). Sustainable Development and Planning VI, Wit Press, Southampton, UK.

Camarsa, G., J. Sliva, J. Toland, T. Hudson, S. Nottingham, N. Rosskopf and C. Thévignot (2014). Life and soil protection, The EU LIFE Programme-European Commission.

Campisi, T., F. Abbondanzi, C. Casado-Martinez, T. DelValls, R. Guerra and A. Iacondini (2005). "Effect of sediment turbidity and color on light output measurement for Microtox® Basic Solid-Phase Test." Chemosphere **60**(1): 9-15.

Carboneras, M. B., J. Villaseñor, F. J. Fernández, M. A. Rodrigo and P. Cañizares (2020). "Selection of anodic material for the combined electrochemical-biological treatment of lindane polluted soil washing effluents." Journal of Hazardous Materials **384**: 121237.

Checa-Fernández, A., A. Santos, L. O. Conte, A. Romero and C. M. Domínguez (2022, **ART. 5**). "Enhanced remediation of a real HCH-polluted soil by the synergetic alkaline and ultrasonic activation of persulfate." Chemical Engineering Journal **440**: 135901.

Checa-Fernández, A., A. Santos, A. Romero and C. M. Domínguez (2021). "Application of Chelating Agents to Enhance Fenton Process in Soil Remediation: A Review." Catalysts.

Checa-Fernández, A., A. Santos, A. Romero and C. M. Domínguez (2021, **ART. 4**). "Remediation of real soil polluted with hexachlorocyclohexanes (α-HCH and β-HCH) using

combined thermal and alkaline activation of persulfate: Optimization of the operating conditions." Separation and Purification Technology **270**: 118795.

Checa-Fernández, A., A. Santos, A. Romero and C. M. Domínguez (2023, **ART. 6**). "Remediation of real soils polluted with pesticides by activated persulfate and surfactant addition." Journal of Water Process Engineering **53**: 103829.

Chen, C.-Y. and C.-L. Lu (2002). "An analysis of the combined effects of organic toxicants." Science of The Total Environment **289**(1): 123-132.

Chen, F., Z. Luo, G. Liu, Y. Yang, S. Zhang and J. Ma (2017). "Remediation of electronic waste polluted soil using a combination of persulfate oxidation and chemical washing." Journal of Environmental Management **204**: 170-178.

Chen, X., M. Murugananthan and Y. Zhang (2016). "Degradation of p-Nitrophenol by thermally activated persulfate in soil system." Chemical Engineering Journal **283**: 1357-1365.

Cheng, M., G. Zeng, D. Huang, C. Lai, P. Xu, C. Zhang and Y. Liu (2016). "Hydroxyl radicals based advanced oxidation processes (AOPs) for remediation of soils contaminated with organic compounds: A review." Chemical Engineering Journal **284**: 582-598.

Cheng, M., G. Zeng, D. Huang, C. Yang, C. Lai, C. Zhang and Y. Liu (2017). "Advantages and challenges of Tween 80 surfactant-enhanced technologies for the remediation of soils contaminated with hydrophobic organic compounds." Chemical Engineering Journal **314**: 98-113.

Ciampi, P., C. Esposito, E. Bartsch, E. J. Alesi and M. Petrangeli Papini (2021). "3D dynamic model empowering the knowledge of the decontamination mechanisms and controlling the complex remediation strategy of a contaminated industrial site." Sci Total Environ **793**: 148649.

Ciampi, P., C. Esposito, G. Cassiani, G. P. Deidda, P. Rizzetto and M. P. Papini (2021). "A field-scale remediation of residual light non-aqueous phase liquid (LNAPL): chemical enhancers for pump and treat." Environ Sci Pollut Res Int **28**(26): 35286-35296.

Congiu, E. and J.-J. Ortega-Calvo (2014). "Role of desorption kinetics in the rhamnolipid-enhanced biodegradation of polycyclic aromatic hydrocarbons." Environmental science & technology **48**(18): 10869-10877.

Conte, L. O., C. M. Dominguez, A. Checa-Fernandez and A. Santos (2022). "Vis LED Photo-Fenton Degradation of 124-Trichlorobenzene at a Neutral pH Using Ferrioxalate as Catalyst." International Journal of Environmental Research and Public Health **19**(15): 9733.

Conte, L. O., G. Legnettino, D. Lorenzo, S. Cotillas, M. Prisciandaro and A. Santos (2023). "Degradation of Lindane by persulfate/ferrioxalate/solar light process: Influential operating parameters, kinetic model and by-products." Applied Catalysis B: Environmental **324**: 122288.

Corporation, M. (1995). Microtox® Acute Toxicity Basic Test Procedures. Carlsbad, CA.

Cruz-González, G., C. Julcour, H. Chaumat, V. Bourdon, F. Ramon-Portugal, S. Gaspard, U. J. Jáuregui-Haza and H. Delmas (2018). "Degradation of chlordecone and beta-hexachlorocyclohexane by photolysis,(photo-) fenton oxidation and ozonation." Journal of Environmental Science and Health, Part B **53**(2): 121-125.

Čvančarová, M., Z. Křesinová and T. Cajthaml (2013). "Influence of the bioaccessible fraction of polycyclic aromatic hydrocarbons on the ecotoxicity of historically contaminated soils." Journal of Hazardous Materials **254-255**: 116-124.

De Albergaria J.T.V.S. , N. H. P. A. (2016). "Soil Remediation: Applications and New Technologies (1st ed.)." CRC Press.

Deng, D., X. Lin, J. Ou, Z. Wang, S. Li, M. Deng and Y. Shu (2015). "Efficient chemical oxidation of high levels of soil-sorbed phenanthrene by ultrasound induced, thermally activated persulfate." Chemical Engineering Journal **265**: 176-183.

Devi, P., U. Das and A. K. Dalai (2016). "In-situ chemical oxidation: Principle and applications of peroxide and persulfate treatments in wastewater systems." Science of The Total Environment **571**: 643-657.

Doherty, F. G. (2001). "A review of the Microtox® toxicity test system for assessing the toxicity of sediments and soils." Water Quality Research Journal **36**(3): 475-518.

Domínguez, C. M., A. Checa-Fernández, R. García-Cervilla, D. Lorenzo, S. Cotillas, S. Rodríguez, J. Fernández and A. Santos (2023). "Clean water: next generation technologies. Chapter 28 Removal of organochlorine pesticides from soil and water. Springer.".

Dominguez, C. M., A. Checa-Fernandez, A. Romero and A. Santos (2021, **ART. 3**). "Degradation of HCHs by thermally activated persulfate in soil system: Effect of

temperature and oxidant concentration." Journal of Environmental Chemical Engineering **9**(4): 105668.

Dominguez, C. M., N. Oturan, A. Romero, A. Santos and M. A. Oturan (2018). "Lindane degradation by electrooxidation process: Effect of electrode materials on oxidation and mineralization kinetics." Water Research **135**: 220-230.

Dominguez, C. M., J. Parchao, S. Rodriguez, D. Lorenzo, A. Romero and A. Santos (2016). "Kinetics of lindane dechlorination by zerovalent iron microparticles: effect of different salts and stability study." Industrial & Engineering Chemistry Research **55**(50): 12776-12785.

Dominguez, C. M., S. Rodriguez, D. Lorenzo, A. Romero and A. Santos (2016). "Degradation of hexachlorocyclohexanes (HCHs) by stable zero valent iron (ZVI) microparticles." Water, Air, & Soil Pollution **227**(12): 1-12.

Dominguez, C. M., V. Rodriguez, E. Montero, A. Romero and A. Santos (2020). "Abatement of dichloromethane using persulfate activated by alkali: A kinetic study." Separation and Purification Technology **241**: 116679.

Dominguez, C. M., A. Romero, A. Checa-Fernandez and A. Santos (2021, **ART. 2**). "Remediation of HCHs-contaminated sediments by chemical oxidation treatments." Science of The Total Environment **751**: 141754.

Dominguez, C. M., A. Romero, J. Fernandez and A. Santos (2018). "In situ chemical reduction of chlorinated organic compounds from lindane production wastes by zero valent iron microparticles." Journal of Water Process Engineering **26**: 146-155.

Dominguez, C. M., A. Romero, D. Lorenzo and A. Santos (2020). "Thermally activated persulfate for the chemical oxidation of chlorinated organic compounds in groundwater." Journal of Environmental Management **261**: 110240.

Dominguez, C. M., A. Romero and A. Santos (2019). "Selective removal of chlorinated organic compounds from lindane wastes by combination of nonionic surfactant soil flushing and Fenton oxidation." Chemical Engineering Journal **376**: 120009.

Domínguez, C. M., P. Ventura, A. Checa-Fernández and A. Santos (2023, **ART. 1**). "Comprehensive study of acute toxicity using Microtox® bioassay in soils contaminated by lindane wastes." Science of The Total Environment **856**: 159146.

EEA (2007). "Progress in management of contaminated sites." CSI 015, DK-1050 Copenhagen K.

Effendi, A. J., M. Wulandari and T. Setiadi (2019). "Ultrasonic application in contaminated soil remediation." Current Opinion in Environmental Science & Health **12**: 66-71.

Eisenberg, G. (1943). "Colorimetric Determination of Hydrogen Peroxide." Industrial & Engineering Chemistry Analytical Edition **15**(5): 327-328.

Enell, A., F. Reichenberg, G. Ewald and P. Warfvinge (2005). "Desorption kinetics studies on PAH-contaminated soil under varying temperatures." Chemosphere **61**(10): 1529-1538.

EPA, U. (2003). "Integrated Risk Information System 2003."

FAO, I. (2015). "Status of the World's Soil Resources (SWSR) - Main Report. Rome, Italy, ood and Agriculture Organization of the United Nations and Intergovernmental Technical Panel on Soils." (also available at https://www.fao.org/3/i5199e/i5199e.pdf).

Fernández, J., M. Arjol and C. Cacho (2013). "POP-contaminated sites from HCH production in Sabiñánigo, Spain." Environmental Science and Pollution Research **20**(4): 1937-1950.

Garbisu, C., O. Garaiyurrebaso, L. Epelde, E. Grohmann and I. Alkorta (2017). "Plasmid-mediated bioaugmentation for the bioremediation of contaminated soils." Frontiers in microbiology **8**: 1966.

García-Cervilla, R., A. Romero, A. Santos and D. Lorenzo (2020). "Surfactant-Enhanced Solubilization of Chlorinated Organic Compounds Contained in DNAPL from Lindane Waste: Effect of Surfactant Type and pH." International Journal of Environmental Research and Public Health **17**(12).

Garcia-Cervilla, R., A. Santos, A. Romero and D. Lorenzo (2021). "Partition of a mixture of chlorinated organic compounds in real contaminated soils between soil and aqueous phase using surfactants: Influence of pH and surfactant type." Journal of Environmental Chemical Engineering **9**(5): 105908.

Garcia-Cervilla, R., A. Santos, A. Romero and D. Lorenzo (2022). "Simultaneous addition of surfactant and oxidant to remediate a polluted soil with chlorinated organic compounds: Slurry and column experiments." Journal of Environmental Chemical Engineering **10**(3): 107625.

García-Cervilla, R., A. Santos, A. Romero and D. Lorenzo (2020). "Remediation of soil contaminated by lindane wastes using alkaline activated persulfate: Kinetic model." Chemical Engineering Journal **393**: 124646.

García-Cervilla, R., A. Santos, A. Romero and D. Lorenzo (2021). "Compatibility of nonionic and anionic surfactants with persulfate activated by alkali in the abatement of chlorinated organic compounds in aqueous phase." Science of The Total Environment **751**: 141782.

García-Cervilla, R., A. Santos, A. Romero and D. Lorenzo (2022). "Abatement of chlorobenzenes in aqueous phase by persulfate activated by alkali enhanced by surfactant addition." Journal of Environmental Management **306**: 114475.

Garg, N., P. Lata, S. Jit, N. Sangwan, A. K. Singh, V. Dwivedi, N. Niharika, J. Kaur, A. Saxena, A. Dua, N. Nayyar, P. Kohli, B. Geueke, P. Kunz, D. Rentsch, C. Holliger, H.-P. E. Kohler and R. Lal (2016). "Laboratory and field scale bioremediation of hexachlorocyclohexane (HCH) contaminated soils by means of bioaugmentation and biostimulation." Biodegradation **27**(2): 179-193.

Gayer, K. and L. Woontner (1956). "The solubility of ferrous hydroxide and ferric hydroxide in acidic and basic media at 25." The Journal of Physical Chemistry **60**(11): 1569-1571.

Geissen, V., H. Mol, E. Klumpp, G. Umlauf, M. Nadal, M. van der Ploeg, S. E. A. T. M. van de Zee and C. J. Ritsema (2015). "Emerging pollutants in the environment: A challenge for water resource management." International Soil and Water Conservation Research **3**(1): 57-65.

Goi, A. and M. Viisimaa (2015). "Integration of ozonation and sonication with hydrogen peroxide and persulfate oxidation for polychlorinated biphenyls-contaminated soil treatment." Journal of Environmental Chemical Engineering **3**(4, Part A): 2839-2847.

Goulden, P. D. and D. H. J. Anthony (1978). "Kinetics of uncatalyzed peroxydisulfate oxidation of organic material in fresh water." Analytical Chemistry **50**(7): 953-958.

Haag, W. R. and C. D. Yao (1992). "Rate constants for reaction of hydroxyl radicals with several drinking water contaminants." Environmental science & technology **26**(5): 1005-1013.

Hamdaoui, O., E. Naffrechoux, L. Tifouti and C. Pétrier (2003). "Effects of ultrasound on adsorption–desorption of p-chlorophenol on granular activated carbon." Ultrasonics Sonochemistry **10**(2): 109-114.

He, S., X. Tan, X. Hu and Y. Gao (2019). "Effect of ultrasound on oil recovery from crude oil containing sludge." Environmental Technology **40**(11): 1401-1407.

Herraiz-Carboné, M., S. Cotillas, E. Lacasa, Á. Moratalla, P. Cañizares, M. A. Rodrigo and C. Sáez (2020). "Improving the biodegradability of hospital urines polluted with

chloramphenicol by the application of electrochemical oxidation." Science of The Total Environment **725**: 138430.

Hoag, G. E. and J. Collins (2011). Soil remediation method and composition. United State patent US7976241.

Hoang, S. A., B. Sarkar, B. Seshadri, D. Lamb, H. Wijesekara, M. Vithanage, C. Liyanage, P. A. Kolivabandara, J. Rinklebe, S. S. Lam, A. Vinu, H. Wang, M. B. Kirkham and N. S. Bolan (2021). "Mitigation of petroleum-hydrocarbon-contaminated hazardous soils using organic amendments: A review." Journal of Hazardous Materials **416**: 125702.

Homolková, M., P. Hrabák, M. Kolář and M. Černík (2014). "Degradability of hexachlorocyclohexanes in water using ferrate (VI)." Water Science and Technology **71**(3): 405-411.

Huang, K.-C., R. A. Couttenye and G. E. Hoag (2002). "Kinetics of heat-assisted persulfate oxidation of methyl tert-butyl ether (MTBE)." Chemosphere **49**(4): 413-420.

Huo, L., G. Liu, X. Yang, Z. Ahmad and H. Zhong (2020). "Surfactant-enhanced aquifer remediation: Mechanisms, influences, limitations and the countermeasures." Chemosphere **252**: 126620.

Iglesias, O., M. A. Sanromán and M. Pazos (2014). "Surfactant-enhanced solubilization and simultaneous degradation of phenanthrene in marine sediment by electro-fenton treatment." Industrial & Engineering Chemistry Research **53**(8): 2917-2923.

Ike, I. A., K. G. Linden, J. D. Orbell and M. Duke (2018). "Critical review of the science and sustainability of persulphate advanced oxidation processes." Chemical Engineering Journal **338**: 651-669.

Jackson, R. E. (2004). "Recognizing emerging environmental problems: the case of chlorinated solvents in groundwater." Technology and culture **45**(1): 55-79.

James, R., A. Dindal, Z. Willenberg and K. Riggs (2003). "Strategic Diagnostics Inc. Microtox® Rapid Toxicity Testing System." Environmental technology verification report. ETV Advanced Monitoring Systems Center, US Environmental Protection Agency, Columbus, Ohio.

Javanbakht, G., M. Arshadi, T. Qin and L. Goual (2017). "Micro-scale displacement of NAPL by surfactant and microemulsion in heterogeneous porous media." Advances in Water Resources **105**: 173-187.

Ji, Y., C. Dong, D. Kong, J. Lu and Q. Zhou (2015). "Heat-activated persulfate oxidation of atrazine: Implications for remediation of groundwater contaminated by herbicides." Chemical Engineering Journal **263**: 45-54.

Joly, P., F. Bonnemoy, J.-C. Charvy, J. Bohatier and C. Mallet (2013). "Toxicity assessment of the maize herbicides S-metolachlor, benoxacor, mesotrione and nicosulfuron, and their corresponding commercial formulations, alone and in mixtures, using the Microtox® test." Chemosphere **93**(10): 2444-2450.

Kaiser, K. L. E. and V. S. Palabrica (1991). "Photobacterium phosphoreum toxicity data index." Water pollution research journal of Canada **26**(3): 361-431.

Kanissery, R. G. and G. K. Sims (2011). "Biostimulation for the Enhanced Degradation of Herbicides in Soil." Applied and Environmental Soil Science **2011**: 843450.

Karaoglu, A. G., N. K. Copty, N. H. Akyol, S. A. Kilavuz and M. Babaei (2019). "Experiments and sensitivity coefficients analysis for multiphase flow model calibration of enhanced DNAPL dissolution." Journal of Contaminant Hydrology **225**: 103515.

Kavanaugh, M. C., P. Suresh and C. Rao (2003). The DNAPL remediation challenge: Is there a case for source depletion?, ENVIRONMENTAL PROTECTION AGENCY WASHINGTON DC.

Khan, S., X. He, J. A. Khan, H. M. Khan, D. L. Boccelli and D. D. Dionysiou (2017). "Kinetics and mechanism of sulfate radical-and hydroxyl radical-induced degradation of highly chlorinated pesticide lindane in UV/peroxymonosulfate system." Chemical engineering journal **318**: 135-142.

Kida, M., S. Ziembowicz and P. Koszelnik (2018). "Removal of organochlorine pesticides (OCPs) from aqueous solutions using hydrogen peroxide, ultrasonic waves, and a hybrid process." Separation and Purification Technology **192**: 457-464.

Kolthoff, I. M. and I. K. Miller (1951). "The Chemistry of Persulfate. I. The Kinetics and Mechanism of the Decomposition of the Persulfate Ion in Aqueous Medium1." Journal of the American Chemical Society **73**(7): 3055-3059.

Kwan, K. and u. B. Dutka (1990). "Simple two-step sediment extraction procedure for use in genotoxicity and toxicity bioassays." Toxicity Assessment **5**(4): 395-404.

Kwan, K. K. and B. J. Dutka (1995). "Comparative assessment of two solid-phase toxicity bioassays: The direct sediment toxicity testing procedure (DSTTP) and the microtox®

solid-phase test (SPT)." Bulletin of Environmental Contamination and Toxicology **55**(3): 338-346.

Lamichhane, S., K. C. Bal Krishna and R. Sarukkalige (2017). "Surfactant-enhanced remediation of polycyclic aromatic hydrocarbons: A review." Journal of Environmental Management **199**: 46-61.

Lei, Y.-J., Y. Tian, C. Fang, W. Zhan, L.-C. Duan, J. Zhang, W. Zuo and X.-W. Kong (2019). "Insights into the oxidation kinetics and mechanism of diesel hydrocarbons by ultrasound activated persulfate in a soil system." Chemical Engineering Journal **378**: 122253.

Lei, Y.-J., Y. Tian, Z. Sobhani, R. Naidu and C. Fang (2020). "Synergistic degradation of PFAS in water and soil by dual-frequency ultrasonic activated persulfate." Chemical Engineering Journal **388**: 124215.

Lei, Y.-J., J. Zhang, Y. Tian, J. Yao, Q.-S. Duan and W. Zuo (2020). "Enhanced degradation of total petroleum hydrocarbons in real soil by dual-frequency ultrasound-activated persulfate." Science of The Total Environment **748**: 141414.

Li, Y.-T., J.-J. Zhang, Y.-H. Li, J.-L. Chen and W.-Y. Du (2022). "Treatment of soil contaminated with petroleum hydrocarbons using activated persulfate oxidation, ultrasound, and heat: A kinetic and thermodynamic study." Chemical Engineering Journal **428**: 131336.

Liang, C., C.-F. Huang, N. Mohanty and R. M. Kurakalva (2008). "A rapid spectrophotometric determination of persulfate anion in ISCO." Chemosphere **73**(9): 1540-1543.

Liang, C. and H.-W. Su (2009). "Identification of Sulfate and Hydroxyl Radicals in Thermally Activated Persulfate." Industrial & Engineering Chemistry Research **48**(11): 5558-5562.

Liang, C. J., C. J. Bruell, M. C. Marley and K. L. Sperry (2003). "Thermally Activated Persulfate Oxidation of Trichloroethylene (TCE) and 1,1,1-Trichloroethane (TCA) in Aqueous Systems and Soil Slurries." Soil and Sediment Contamination: An International Journal **12**(2): 207-228.

Libralato, G., V. G. Annamaria and A. Francesco (2010). "How toxic is toxic? A proposal for wastewater toxicity hazard assessment." Ecotoxicology and environmental safety **73**(7): 1602-1611.

Lide, D. R. (2004). CRC handbook of chemistry and physics, CRC press.

Liu, J., Z. Liu, F. Zhang, X. Su and C. Lyu (2017). "Thermally activated persulfate oxidation of NAPL chlorinated organic compounds: effect of soil composition on oxidant demand in different soil-persulfate systems." Water Science and Technology **75**(8): 1794-1803.

Liu, Y., S. Wang, Y. Wu, H. Chen, Y. Shi, M. Liu and W. Dong (2019). "Degradation of ibuprofen by thermally activated persulfate in soil systems." Chemical Engineering Journal **356**: 799-810.

Lombi, E. and R. Hamon (2005). "Remediation of polluted soils." Encyclopedia of Soils in the Environment **4**: 379-385.

Lominchar, M. A., D. Lorenzo, A. Romero and A. Santos (2018). "Remediation of soil contaminated by PAHs and TPH using alkaline activated persulfate enhanced by surfactant addition at flow conditions." Journal of Chemical Technology & Biotechnology **93**(5): 1270-1278.

Lorenzo, D., R. García-Cervilla, A. Romero and A. Santos (2020). "Partitioning of chlorinated organic compounds from dense non-aqueous phase liquids and contaminated soils from lindane production wastes to the aqueous phase." Chemosphere **239**: 124798.

Lorenzo, D., A. Santos, A. Sánchez-Yepes, L. O. Conte and C. M. Domínguez (2021). "Abatement of 1, 2, 4-trichlorobencene by wet peroxide oxidation catalysed by goethite and enhanced by visible led light at neutral ph." Catalysts **11**(1): 139.

Luo, X., H. Gong, Z. He, P. Zhang and L. He (2021). "Recent advances in applications of power ultrasound for petroleum industry." Ultrasonics Sonochemistry **70**: 105337.

Mandal, S. (2018). "Reaction rate constants of hydroxyl radicals with micropollutants and their significance in advanced oxidation processes." J. Adv. Oxid. Technol **21**(178): e195.

Mao, X., R. Jiang, W. Xiao and J. Yu (2015). "Use of surfactants for the remediation of contaminated soils: A review." Journal of Hazardous Materials **285**: 419-435.

Matzek, L. W. and K. E. Carter (2016). "Activated persulfate for organic chemical degradation: A review." Chemosphere **151**: 178-188.

McGuire, T. M., J. M. McDade, C. J. J. G. M. Newell and Remediation (2006). "Performance of DNAPL source depletion technologies at 59 chlorinated solvent-impacted sites." **26**(1): 73-84.

Michael-Igolima, U., S. J. Abbey and A. O. Ifelebuegu (2022). "A systematic review on the effectiveness of remediation methods for oil contaminated soils." Environmental Advances: 100319.

Montanarella, L. and P. Panagos (2021). "The relevance of sustainable soil management within the European Green Deal." Land use policy **100**: 104950.

Monteagudo, J. M., H. El-taliawy, A. Durán, G. Caro and K. Bester (2018). "Sono-activated persulfate oxidation of diclofenac: Degradation, kinetics, pathway and contribution of the different radicals involved." Journal of Hazardous Materials **357**: 457-465.

Mousset, E., D. Huguenot, E. D. van Hullebusch, N. Oturan, G. Guibaud, G. Esposito and M. A. Oturan (2016). "Impact of electrochemical treatment of soil washing solution on PAH degradation efficiency and soil respirometry." Environmental Pollution **211**: 354-362.

Mowat, F. S. and K. J. Bundy (2002). "Experimental and mathematical/computational assessment of the acute toxicity of chemical mixtures from the Microtox® assay." Advances in Environmental Research **6**(4): 547-558.

Mueller, N. C., J. Braun, J. Bruns, M. Černík, P. Rissing, D. Rickerby and B. Nowack (2012). "Application of nanoscale zero valent iron (NZVI) for groundwater remediation in Europe." Environmental Science and Pollution Research **19**(2): 550-558.

Munoz, M., J. Nieto-Sandoval, S. Cirés, Z. M. de Pedro, A. Quesada and J. A. Casas (2019). "Degradation of widespread cyanotoxins with high impact in drinking water (microcystins, cylindrospermopsin, anatoxin-a and saxitoxin) by CWPO." Water Research **163**: 114853.

Oh, S. Y., H. S. Yoon, T. Y. Jeong and S. D. Kim (2016). "Evaluation of remediation processes for explosive-contaminated soils: kinetics and Microtox® bioassay." Journal of Chemical Technology & Biotechnology **91**(4): 928-937.

Ossai, I. C., A. Ahmed, A. Hassan and F. S. Hamid (2020). "Remediation of soil and water contaminated with petroleum hydrocarbon: A review." Environmental Technology & Innovation **17**: 100526.

Ozkan, Y., I. Altinok, H. Ilhan and M. Sokmen (2016). "Determination of TiO 2 and AgTiO 2 nanoparticles in Artemia salina: toxicity, morphological changes, uptake and depuration." Bulletin of environmental contamination and toxicology **96**: 36-42.

Pan, T., T. Deng, X. Zeng, W. Dong and S. Yu (2016). "Extractive biodegradation and bioavailability assessment of phenanthrene in the cloud point system by Sphingomonas polyaromaticivorans." Applied microbiology and biotechnology **100**: 431-437.

Panagos, P. and L. Montanarella (2018). "Soil Thematic Strategy: An important contribution to policy support, research, data development and raising the awareness." Current Opinion in Environmental Science & Health **5**: 38-41.

Panagos, P., M. Van Liedekerke, Y. Yigini and L. Montanarella (2013). "Contaminated sites in Europe: review of the current situation based on data collected through a European network." Journal of environmental and public health **2013**.

Pardo, F., J. M. Rosas, A. Santos and A. Romero (2014). "Remediation of a biodiesel blend-contaminated soil by using a modified Fenton process." Environmental Science and Pollution Research **21**(21): 12198-12207.

Peng, L., D. Deng, M. Guan, X. Fang and Q. Zhu (2015). "Remediation HCHs POPs-contaminated soil by activated persulfate technologies: Feasibility, impact of activation methods and mechanistic implications." Separation and Purification Technology **150**: 215-222.

Peters, R. W. (1999). "Chelant extraction of heavy metals from contaminated soils." Journal of Hazardous Materials **66**(1): 151-210.

Pham, T. D., M. Kobayashi and Y. Adachi (2015). "Adsorption of anionic surfactant sodium dodecyl sulfate onto alpha alumina with small surface area." Colloid and Polymer Science **293**(1): 217-227.

Qiu, Y., M. Xu, Z. Sun and H. Li (2019). "Remediation of PAH-Contaminated Soil by Combining Surfactant Enhanced Soil Washing and Iron-Activated Persulfate Oxidation Process." International Journal of Environmental Research and Public Health **16**(3): 441.

Rajendran, S., T. A. K. Priya, K. S. Khoo, T. K. A. Hoang, H.-S. Ng, H. S. H. Munawaroh, C. Karaman, Y. Orooji and P. L. Show (2022). "A critical review on various remediation approaches for heavy metal contaminants removal from contaminated soils." Chemosphere **287**: 132369.

Ren, X., G. Zeng, L. Tang, J. Wang, J. Wan, Y. Liu, J. Yu, H. Yi, S. Ye and R. Deng (2018). "Sorption, transport and biodegradation – An insight into bioavailability of persistent organic pollutants in soil." Science of The Total Environment **610-611**: 1154-1163.

Ren, X., G. Zeng, L. Tang, J. Wang, J. Wan, J. Wang, Y. Deng, Y. Liu and B. Peng (2018). "The potential impact on the biodegradation of organic pollutants from composting technology for soil remediation." Waste Management **72**: 138-149.

Rodríguez-Eugenio, N. M., M.; Pennock, D. (2018). "Soil Pollution: a hidden reality. Rome, FAO. 142 pp.".

Rodríguez, N. and A. Payá Pérez (2017). Status of local soil contamination in Europe.

Roig, N., M. Nadal, J. Sierra, A. Ginebreda, M. Schuhmacher and J. L. Domingo (2011). "Novel approach for assessing heavy metal pollution and ecotoxicological status of rivers by means of passive sampling methods." Environment International **37**(4): 671-677.

Romero, A., A. Santos, F. Vicente, S. Rodriguez and A. L. Lafuente (2009). "In situ oxidation remediation technologies: Kinetic of hydrogen peroxide decomposition on soil organic matter." Journal of Hazardous Materials **170**(2-3): 627-632.

Ruiz, M. J., L. López-Jaramillo, M. J. Redondo and G. Font (1997). "Toxicity Assessment of Pesticides Using the Microtox Test: Application to Environmental Samples." Bulletin of Environmental Contamination and Toxicology **59**(4): 619-625.

Sandell, E. B. (1945). Colorimetric determination of traces of metals, LWW.

Santos, A., C. Domínguez and D. Lorenzo (2020). HCH-Contaminated Soils and Remediation Technologies.

Santos, A., J. Fernandez, J. Guadano, D. Lorenzo and A. Romero (2018). "Chlorinated organic compounds in liquid wastes (DNAPL) from lindane production dumped in landfills in Sabinanigo (Spain)." Environmental Pollution **242**: 1616-1624.

Santos, A., J. Fernandez, S. Rodriguez, C. M. Dominguez, M. A. Lominchar, D. Lorenzo and A. Romero (2018). "Abatement of chlorinated compounds in groundwater contaminated by HCH wastes using ISCO with alkali activated persulfate." Science of The Total Environment **615**: 1070-1077.

Santos, A., R. García-Cervilla, A. Checa-Fernández, C. M. Domínguez and D. Lorenzo (2022, **ART. 7**). "Acute Toxicity Evaluation of Lindane-Waste Contaminated Soils Treated by Surfactant-Enhanced ISCO." Molecules **27**(24): 8965.

Santos, A., D. Lorenzo and C. M. Dominguez (2021). Persulfate in remediation of soil and groundwater contaminated by organic compounds. Electrochemically Assisted Remediation of Contaminated Soils, Springer**:** 221-262.

Santos, A. and J. M. Rosas (2016). "In situ chemical oxidation (ISCO)." Soil Remediation: Applications and New Technologies **75**.

Santos, A., P. Yustos, A. Quintanilla, F. García-Ochoa, J. A. Casas and J. J. Rodríguez (2004). "Evolution of Toxicity upon Wet Catalytic Oxidation of Phenol." Environmental Science & Technology **38**(1): 133-138.

Semple, K. T., A. W. J. Morriss and G. I. Paton (2003). "Bioavailability of hydrophobic organic contaminants in soils: fundamental concepts and techniques for analysis." European Journal of Soil Science **54**(4): 809-818.

Senthilnathan, J. and L. Philip (2010). "Photocatalytic degradation of lindane under UV and visible light using N-doped TiO2." Chemical Engineering Journal **161**(1): 83-92.

Settimi, C., D. Zingaretti, S. Sanna, I. Verginelli, I. Luisetto, A. Tebano and R. Baciocchi (2022). "Synthesis and Characterization of Zero-Valent Fe-Cu and Fe-Ni Bimetals for the Dehalogenation of Trichloroethylene Vapors." Sustainability **14**(13): 7760.

Shrestha, R. A., T. D. Pham and M. Sillanpää (2009). "Effect of ultrasound on removal of persistent organic pollutants (POPs) from different types of soils." Journal of Hazardous Materials **170**(2): 871-875.

Siddique, T., B. C. Okeke, M. Arshad and W. T. Frankenberger (2002). "Temperature and pH Effects on Biodegradation of Hexachlorocyclohexane Isomers in Water and a Soil Slurry." Journal of Agricultural and Food Chemistry **50**(18): 5070-5076.

Siegrist, R. L., M. Crimi and T. J. Simpkin (2011). In situ chemical oxidation for groundwater remediation, Springer Science & Business Media.

Song, W., J. Li, W. Zhang, X. Hu and L. Wang (2012). "An experimental study on the remediation of phenanthrene in soil using ultrasound and soil washing." Environmental Earth Sciences **66**(5): 1487-1496.

Svenson, A., E. Edsholt, M. Ricking, M. Remberger and J. Röttorp (1996). "Sediment contaminants and Microtox toxicity tested in a direct contact exposure test." Environmental Toxicology and Water Quality: An International Journal **11**(4): 293-300.

Swartjes, F. A. (2011). Dealing with contaminated sites: from theory towards practical application, Springer Science & Business Media.

Teel, A. L., D. D. Finn, J. T. Schmidt, L. M. Cutler and R. J. Watts (2007). "Rates of trace mineral-catalyzed decomposition of hydrogen peroxide." Journal of Environmental Engineering **133**(8): 853-858.

Teramoto, E. H., M. A. Z. Pede and H. K. Chang (2020). "Impact of water table fluctuations on the seasonal effectiveness of the pump-and-treat remediation in wet–dry tropical regions." Environmental Earth Sciences **79**: 1-15.

Thomé, A., C. Reginatto, G. Vanzetto and A. B. Braun (2019). Remediation technologies applied in polluted soils: new perspectives in this field. Proceedings of the 8th International Congress on Environmental Geotechnics Volume 1: Towards a Sustainable Geoenvironment 8th, Springer.

Tkaczyk, A., A. Bownik, J. Dudka, K. Kowal and B. Ślaska (2021). "Daphnia magna model in the toxicity assessment of pharmaceuticals: A review." Sci Total Environ **763**: 143038.

Trellu, C., E. Mousset, Y. Pechaud, D. Huguenot, E. D. van Hullebusch, G. Esposito and M. A. Oturan (2016). "Removal of hydrophobic organic pollutants from soil washing/flushing solutions: A critical review." Journal of Hazardous Materials **306**: 149-174.

Trellu, C., N. Oturan, Y. Pechaud, E. D. van Hullebusch, G. Esposito and M. A. Oturan (2017). "Anodic oxidation of surfactants and organic compounds entrapped in micelles – Selective degradation mechanisms and soil washing solution reuse." Water Research **118**: 1-11.

Trellu, C., Y. Pechaud, N. Oturan, E. Mousset, E. D. van Hullebusch, D. Huguenot and M. A. Oturan (2021). "Remediation of soils contaminated by hydrophobic organic compounds: How to recover extracting agents from soil washing solutions?" Journal of Hazardous Materials **404**: 124137.

UNEP, F. a. (2021). "Global assessment of soil pollution: Report."

Usman, M., O. Tascone, P. Faure and K. Hanna (2014). "Chemical oxidation of hexachlorocyclohexanes (HCHs) in contaminated soils." Sci Total Environ **476-477**: 434-439.

Vanhaecke, P. and G. Persoone (1981). "Report on an intercalibration exercise on a short-term standard toxicity test with Artemia nauplii (ARC-test)." Inserm **106**: 359-376.

Vega, M., D. Romano and E. Uotila (2016). Lindane (persistent organic pollutant) in the EU E. P. s. P. D. f. C. R. a. C. Affairs.

Verginelli, I., O. Capobianco, N. Hartog and R. Baciocchi (2017). "Analytical model for the design of in situ horizontal permeable reactive barriers (HPRBs) for the mitigation of chlorinated solvent vapors in the unsaturated zone." J Contam Hydrol **197**: 50-61.

Vicente, F., J. M. Rosas, A. Santos and A. Romero (2011). "Improvement soil remediation by using stabilizers and chelating agents in a Fenton-like process." Chemical Engineering Journal **172**(2): 689-697.

Vicente, F., A. Santos, A. Romero and S. Rodriguez (2011). "Kinetic study of diuron oxidation and mineralization by persulphate: Effects of temperature, oxidant concentration and iron dosage method." Chemical Engineering Journal **170**(1): 127-135.

Vijgen, J., P. C. Abhilash, Y. F. Li, R. Lal, M. Forter, J. Torres, N. Singh, M. Yunus, C. Tian, A. Schäffer and R. Weber (2011). "Hexachlorocyclohexane (HCH) as new Stockholm Convention POPs—a global perspective on the management of Lindane and its waste isomers." Environmental Science and Pollution Research **18**(2): 152-162.

Wacławek, S., V. Antoš, P. Hrabák, M. Černík and D. Elliott (2016). "Remediation of hexachlorocyclohexanes by electrochemically activated persulfates." Environmental Science and Pollution Research **23**(1): 765-773.

Wacławek, S., D. Silvestri, P. Hrabák, V. V. T. Padil, R. Torres-Mendieta, M. Wacławek, M. Černík and D. D. Dionysiou (2019). "Chemical oxidation and reduction of hexachlorocyclohexanes: A review." Water Research **162**: 302-319.

Waldemer, R. H., P. G. Tratnyek, R. L. Johnson and J. T. Nurmi (2007). "Oxidation of Chlorinated Ethenes by Heat-Activated Persulfate: Kinetics and Products." Environmental Science & Technology **41**(3): 1010-1015.

Wan, J., S. Yuan, K. Mak, J. Chen, T. Li, L. Lin and X. Lu (2009). "Enhanced washing of HCB contaminated soils by methyl-β-cyclodextrin combined with ethanol." Chemosphere **75**(6): 759-764.

Wang, J. and S. Wang (2018). "Activation of persulfate (PS) and peroxymonosulfate (PMS) and application for the degradation of emerging contaminants." Chemical Engineering Journal **334**: 1502-1517.

Wang, L., L. Peng, L. Xie, P. Deng and D. Deng (2017). "Compatibility of Surfactants and Thermally Activated Persulfate for Enhanced Subsurface Remediation." Environmental Science & Technology **51**(12): 7055-7064.

Wang, L., H. Wu and D. Deng (2020). "Role of surfactants in accelerating or retarding persulfate decomposition." Chemical Engineering Journal **384**: 123303.

Wang, S. and C. N. Mulligan (2004). "An evaluation of surfactant foam technology in remediation of contaminated soil." Chemosphere **57**(9): 1079-1089.

Wang, S. and N. Zhou (2016). "Removal of carbamazepine from aqueous solution using sono-activated persulfate process." Ultrasonics Sonochemistry **29**: 156-162.

Wang, W. H., G. E. Hoag, J. B. Collins and R. Naidu (2013). "Evaluation of Surfactant-Enhanced In Situ Chemical Oxidation (S-ISCO) in Contaminated Soil." Water Air and Soil Pollution **224**(12).

Wang, X., M. Brigante, W. Dong, Z. Wu and G. Mailhot (2020). "Degradation of Acetaminophen via UVA-induced advanced oxidation processes (AOPs). Involvement of different radical species: HO, SO4− and HO2/O2−." Chemosphere **258**: 127268.

Wang, Z., D. Deng and L. Yang (2014). "Degradation of dimethyl phthalate in solutions and soil slurries by persulfate at ambient temperature." Journal of hazardous materials **271**: 202-209.

Wang, Z., P. a. Peng and W. Huang (2009). "Dechlorination of γ-hexachlorocyclohexane by zero-valent metallic iron." Journal of Hazardous Materials **166**(2): 992-997.

Wei, Z., F. A. Villamena and L. K. Weavers (2017). "Kinetics and Mechanism of Ultrasonic Activation of Persulfate: An in Situ EPR Spin Trapping Study." Environmental Science & Technology **51**(6): 3410-3417.

Wentworth, C. K. (1922). "A scale of grade and class terms for clastic sediments." The journal of geology **30**(5): 377-392.

Yang, K., L. Zhu and B. Xing (2006). "Enhanced Soil Washing of Phenanthrene by Mixed Solutions of TX100 and SDBS." Environmental Science & Technology **40**(13): 4274-4280.

Zhang, T., Y. Liu, S. Zhong and L. Zhang (2020). "AOPs-based remediation of petroleum hydrocarbons-contaminated soils: Efficiency, influencing factors and environmental impacts." Chemosphere **246**: 125726.

Zhang, W., Z. Lin, S. Pang, P. Bhatt and S. Chen (2020). "Insights into the biodegradation of lindane (γ-hexachlorocyclohexane) using a microbial system." Frontiers in microbiology **11**: 522.

Zhang, Y. and M. Zhou (2019). "A critical review of the application of chelating agents to enable Fenton and Fenton-like reactions at high pH values." Journal of Hazardous Materials **362**: 436-450.

Zhao, L., H. Hou, A. Fujii, M. Hosomi and F. Li (2014). "Degradation of 1,4-dioxane in water with heat- and Fe2+-activated persulfate oxidation." Environmental Science and Pollution Research **21**(12): 7457-7465.

Zhou, W. and L. Zhu (2005). "Distribution of polycyclic aromatic hydrocarbons in soil–water system containing a nonionic surfactant." Chemosphere **60**(9): 1237-1245.

Zhou, Z., X. Liu, K. Sun, C. Lin, J. Ma, M. He and W. Ouyang (2019). "Persulfate-based advanced oxidation processes (AOPs) for organic-contaminated soil remediation: A review." Chemical Engineering Journal **372**: 836-851.

Zhu, S., M.-Y. Xue, F. Luo, W.-C. Chen, B. Zhu and G.-X. Wang (2017). "Developmental toxicity of Fe3O4 nanoparticles on cysts and three larval stages of Artemia salina." Environmental Pollution **230**: 683-691.

Zrinyi, N. and A. L.-T. Pham (2017). "Oxidation of benzoic acid by heat-activated persulfate: Effect of temperature on transformation pathway and product distribution." Water Research **120**: 43-51.

Chapter 11.

APPENDICES

APPENDIX I

-Other publications-

Type: Review
Title: Application of Chelating Agents to Enhance Fenton Process in Soil Remediation: A Review
Authors: **A. Checa-Fernández,** A. Santos, A. Romero, C. M. Domínguez
Journal: Catalyst
Publication year: 2021
Volume, Page: 11, 722
DOI: 10.3390/catal11060722
Quartile (Area): Q2 (Catalysis)
Cited by (SCOPUS): 21

catalysts

MDPI

Review

Application of Chelating Agents to Enhance Fenton Process in Soil Remediation: A Review

Alicia Checa-Fernandez, Aurora Santos, Arturo Romero and Carmen M. Dominguez *

Chemical Engineering and Materials Department, Facultad de Ciencias Químicas, Universidad Complutense de Madrid, Ciudad Universitaria S/N, 28040 Madrid, Spain; crcheca@ucm.es (A.C.-F.); aursan@quim.ucm.es (A.S.); aromeros@quim.ucm.es (A.R.)
* Correspondence: carmdomi@ucm.es; Tel.: +91-394-4170

Abstract: Persistent organic contaminants affecting soil and groundwater pose a significant threat to ecosystems and human health. Fenton oxidation is an efficient treatment for removing these pollutants in the aqueous phase at acidic pH. However, the in-situ application of this technology for soil remediation (where pHs around neutrality are required) presents important limitations, such as catalyst (iron) availability and oxidant (H_2O_2) stability. The addition of chelating agents (CAs), forming complexes with Fe and enabling Fenton reactions under these conditions, so-called chelate-modified Fenton process (MF), tries to overcome the challenges identified in conventional Fenton. Despite the growing interest in this technology, there is not yet a critical review compiling the information needed for its real application. The advantages and drawbacks of MF must be clarified, and the recent achievements should be shared with the scientific community. This review provides a general overview of the application of CAs to enhance the Fenton process for the remediation of soils polluted with the most common organic contaminants, especially for a deep understanding of the activation mechanisms and influential factors. The existing shortcomings and research needs have been highlighted. Finally, future research perspectives on the use of CAs in MF and recommendations have been provided.

Keywords: chelating agents (CAs); modified Fenton (MF); soil remediation; organic pollutants; H_2O_2 stability; reactive oxygen species (ROS); ligand

Citation: Checa-Fernandez, A.; Santos, A.; Romero, A.; Dominguez, C.M. Application of Chelating Agents to Enhance Fenton Process in Soil Remediation: A Review. *Catalysts* **2021**, *11*, 722. https://doi.org/10.3390/catal11060722

Academic Editor: Stanisław Wacławek

Received: 30 April 2021
Accepted: 7 June 2021
Published: 10 June 2021

1. Introduction

In recent years, many persistent and toxic contaminants found in soils have attracted the attention of the scientific community. Soil and sediment contamination by organic compounds, resulting from industrial and municipal waste discharge and improper use of chemical fertilizer and pesticides, is a widespread problem worldwide due to its great harm to the ecological environment and public health [1–3]. Nowadays, the principal substances contributing to soil pollution are petroleum oil hydrocarbons (e.g., aliphatic, aromatic, polycyclic aromatic hydrocarbons (PAHs), BTEX (benzene, toluene, ethylbenzene, and xylenes), chlorinated hydrocarbons like polychlorinated biphenyls (PCBs), trichloroethylene (TCE), and perchloroethylene, nitroaromatic compounds, organophosphorus compounds), solvents, and pesticides [4]. In China, 2.5% of total farmland is too contaminated to be used [5], whereas more than 80,000 sites suffer from soil pollution in the European Union [6]. In this context, the remediation of organic-contaminated soils is crucial, becoming a priority objective for both government institutions and society [3,7].

Extensive work has been devoted to developing soil remediation techniques [8], which mainly involves physical, chemical, and biological processes or/and their combinations. Advanced oxidation processes (AOPs) are powerful chemical methods with growing popularity for organic-contaminated soil remediation, being considered more effective than physical and biological approaches [9]. AOPs are considered capable of oxidizing different classes of organic pollutants by reactive radical species, achieving high levels

161. Popescu, M.; Rosales, E.; Sandu, C.; Meijide, J.; Pazos, M.; Lazar, G.; Sanromán, M.A. Soil flushing and simultaneous degradation of organic pollutants in soils by electrokinetic-Fenton treatment. *Process. Saf. Environ. Prot.* **2017**, *108*, 99–107. [CrossRef]
162. Polli, F.; Zingaretti, D.; Crognale, S.; Pesciaroli, L.; D'Annibale, A.; Petruccioli, M.; Baciocchi, R. Impact of the Fenton-like treatment on the microbial community of a diesel-contaminated soil. *Chemosphere* **2018**, *191*, 580–588. [CrossRef]
163. Kakosová, E.; Hrabák, P.; Černík, M.; Novotný, V.; Czinnerová, M.; Trögl, J.; Popelka, J.; Kuráň, P.; Zoubková, L.; Vrtoch, Ľ. Effect of various chemical oxidation agents on soil microbial communities. *Chem. Eng. J.* **2017**, *314*, 257–265. [CrossRef]
164. Watts, R.J.; Dilly, S.E. Evaluation of iron catalysts for the Fenton-like remediation of diesel-contaminated soils. *J. Hazard. Mater.* **1996**, *51*, 209–224. [CrossRef]
165. Gong, X.-B. Remediation of weathered petroleum oil-contaminated soil using a combination of biostimulation and modified Fenton oxidation. *Int. Biodeterior. Biodegrad.* **2012**, *70*, 89–95. [CrossRef]
166. Guzmán-López, O.; Cuevas-Díaz, M.D.C.; Toledo, A.M.; Contreras-Morales, M.E.; Ruiz-Reyes, C.I.; Martínez, A. del C.O. Fenton-biostimulation sequential treatment of a petroleum-contaminated soil amended with oil palm bagasse (*Elaeis guineensis*). *Chem. Ecol.* **2021**, 1–16. [CrossRef]
167. Ko, S.; Crimi, M.; Marvin, B.K.; Holmes, V.; Huling, S.G. Comparative study on oxidative treatments of NAPL containing chlorinated ethanes and ethenes using hydrogen peroxide and persulfate in soils. *J. Environ. Manag.* **2012**, *108*, 42–48. [CrossRef] [PubMed]
168. Tan, C.; Gao, N.; Chu, W.; Li, C.; Templeton, M.R. Degradation of diuron by persulfate activated with ferrous ion. *Sep. Purif. Technol.* **2012**, *95*, 44–48. [CrossRef]
169. Deng, J.; Shao, Y.; Gao, N.; Deng, Y.; Tan, C.; Zhou, S. Zero-valent iron/persulfate(Fe0/PS) oxidation acetaminophen in water. *Int. J. Environ. Sci. Technol.* **2013**, *11*, 881–890. [CrossRef]
170. Lee, C.; Sedlak, D.L. A novel homogeneous Fenton-like system with Fe(III)–phosphotungstate for oxidation of organic compounds at neutral pH values. *J. Mol. Catal. A Chem.* **2009**, *311*, 1–6. [CrossRef]
171. Zhang, L.; Zeng, H.; Zeng, Y.; Zhang, Z.; Zhao, X. Heterogeneous Fenton-like degradation of 4-chlorophenol using a novel FeIII-containing polyoxometalate as the catalyst. *J. Mol. Catal. A Chem.* **2014**, *392*, 202–207. [CrossRef]
172. Lee, C.; Keenan, C.R.; Sedlak, D.L. Polyoxometalate-Enhanced Oxidation of Organic Compounds by Nanoparticulate Zero-Valent Iron and Ferrous Ion in the Presence of Oxygen. *Environ. Sci. Technol.* **2008**, *42*, 4921–4926. [CrossRef]
173. Chen, H.; Zhang, L.; Zeng, H.; Yin, D.; Zhai, Q.; Zhao, X.; Li, J. Highly active iron-containing silicotungstate catalyst for heterogeneous Fenton oxidation of 4-chlorophenol. *J. Mol. Catal. A Chem.* **2015**, *406*, 72–77. [CrossRef]
174. Lee, J.; Kim, J.; Choi, W. Oxidation on Zerovalent Iron Promoted by Polyoxometalate as an Electron Shuttle. *Environ. Sci. Technol.* **2007**, *41*, 3335–3340. [CrossRef] [PubMed]
175. Zhang, C.; Li, T.; Zhang, J.; Yan, S.; Qin, C. Degradation of p-nitrophenol using a ferrous-tripolyphosphate complex in the presence of oxygen: The key role of superoxide radicals. *Appl. Catal. B Environ.* **2019**, *259*, 118030. [CrossRef]
176. Deng, F.; Qiu, S.; Zhu, Y.; Zhang, X.; Yang, J.; Ma, F. Tripolyphosphate-assisted electro-Fenton process for coking wastewater treatment at neutral pH. *Environ. Sci. Pollut. Res.* **2019**, *26*, 11928–11939. [CrossRef] [PubMed]
177. Yehia, F.; Eshaq, G.; ElMetwally, A. Enhancement of the working pH range for degradation of p-nitrophenol using Fe^{2+}–aspartate and Fe^{2+}–glutamate complexes as modified Fenton reagents. *Egypt. J. Pet.* **2016**, *25*, 239–245. [CrossRef]
178. Li, Y.C.; Bachas, L.; Bhattacharyya, D. Kinetics Studies of Trichlorophenol Destruction by Chelate-Based Fenton Reaction. *Environ. Eng. Sci.* **2005**, *22*, 756–771. [CrossRef]

Type: Research paper
Title: Vis LED Photo-Fenton Degradation of 124-Trichlorobenzene at a Neutral pH Using Ferrioxalate as Catalyst
Authors: L. O. Conte, C. M. Domínguez, **A. Checa-Fernández**, A. Santos
Journal: International Journal of Enivronmental Research and Public Health
Publication year: 2022
Volume, Page: 19, 9733
DOI: 10.3390/ijerph19159733
Quartile (Area): Q2 (Pollution)
Cited by (SCOPUS): 1

International Journal of
Environmental Research and Public Health

MDPI

Article

Vis LED Photo-Fenton Degradation of 124-Trichlorobenzene at a Neutral pH Using Ferrioxalate as Catalyst

Leandro O. Conte [1,2], Carmen M. Dominguez [1], Alicia Checa-Fernandez [1] and Aurora Santos [1,*]

[1] Chemical Engineering and Materials Department, Chemical Sciences Faculty, Complutense University of Madrid, 28040 Madrid, Spain
[2] Instituto de Desarrollo Tecnológico para la Industria Química (INTEC), Consejo Nacional de Investigaciones Científicas y Técnicas (CONICET) and Universidad Nacional del Litoral (UNL), Santa Fe 3100, Argentina
* Correspondence: aursan@ucm.es

Abstract: Chlorinated organic compounds (COCs) are among the more toxic organic compounds frequently found in soil and groundwater. Among these, toxic and low-degradable chlorobenzenes are commonly found in the environment. In this work, an innovative process using hydrogen peroxide as the oxidant, ferrioxalate as the catalyst and a visible light-emitting diode lamp (Vis LED) were applied to successfully oxidize 124-trichlorobenzene (124-TCB) in a saturated aqueous solution of 124-TCB (28 mg L^{-1}) at a neutral pH. The influence of a hydrogen peroxide (HP) concentration (61.5–612 mg L^{-1}), Fe^{3+} (Fe) dosage (3–10 mg L^{-1}), and irradiation level (Rad) (I = 0.12 W cm^{-2} and I = 0.18 W cm^{-2}) on 124-TCB conversion and dechlorination was studied. A D–Optimal experimental design combined with response surface methodology (RSM) was implemented to maximize the quality of the information obtained. The ANOVA test was used to assess the significance of the model and its coefficients. The maximum pollutant conversion at 180 min (98.50%) was obtained with Fe = 7 mg L^{-1}, HP = 305 mg L^{-1}, and I = 0.12 W cm^{-2}. The effect of two inorganic anions usually presents in real groundwater (bicarbonate and chloride, 600 mg L^{-1} each) was investigated under those optimized operating conditions. A slight reduction in the 124-TCB conversion after 180 min of reaction was noticed in the presence of bicarbonate (8.31%) and chloride (7.85%). Toxicity was studied with Microtox®(Azur Environmental, Carlsbad, CA, USA) bioassay, and a remarkable toxicity decrease was found in the treated samples, with the inhibition proportional to the remaining 124-TCB concentration. That means that nontoxic byproducts are produced in agreement with the high dechlorination degrees noticed.

Keywords: Photo-Fenton; chlorinated organic compounds; 124-Trichlorobenzene; visible LED; neutral pH; ferrioxalate

Citation: Conte, L.O.; Dominguez, C.M.; Checa-Fernandez, A.; Santos, A. Vis LED Photo-Fenton Degradation of 124-Trichlorobenzene at a Neutral pH Using Ferrioxalate as Catalyst. *Int. J. Environ. Res. Public Health* **2022**, *19*, 9733. https://doi.org/10.3390/ijerph19159733

Academic Editor: Paul B. Tchounwou

Received: 11 July 2022
Accepted: 5 August 2022
Published: 7 August 2022

1. Introduction

The occurrence of chlorinated organic compounds (COCs) in wastewater, surface water, and groundwater environments has become an emerging public and scientific concern due to their potential adverse impacts on biota and human health. Because of their high persistence in the environment and their toxic, carcinogenic, and hydrophobic characteristics, several COCs (chloroethanes, chlorophenols, chlorobenzenes, etc.) are listed as priority substances by the EU Water Framework Directive [1]. Trichlorobenzenes (TCBs) are synthetic chemicals extensively used in synthesizing pesticides, repellents, dyes, solvents, etc. [2–4]. Furthermore, TCBs are byproducts of highly chlorinated pesticide degradation, such as hexachlorocyclohexanes [5–7]. Consequently, they have become ubiquitous pollutants [8,9], being detected (concentration from ng L^{-1} to mg L^{-1}) in water, soil, and sediments [10].

Due to their high chemical stability and low biodegradability, TCBs are refractory to degradation using conventional physicochemical or biological processes, and the development of more effective treatments is required. Adsorption was an effective method

42. Giménez, B.N.; Conte, L.O.; Alfano, O.M.; Schenone, A.V. Paracetamol removal by photo-Fenton processes at near-neutral pH using a solar simulator: Optimization by D-optimal experimental design and toxicity evaluation. *J. Photochem. Photobiol. A Chem.* **2020**, *397*, 112584. [CrossRef]
43. Malato, S.; Fernandez-Ibañez, P.; Maldonado, M.I.; Blanco, J.; Gernjak, W. Decontamination and disinfection of water by solar photocatalysis: Recent overview and trends. *Catal. Today* **2009**, *147*, 1–59. [CrossRef]
44. Montgomery, D.C. *Design and Analysis of Experiments*; John Wiley & Sons: Hoboken, NJ, USA, 2017.
45. Boutra, B.; Sebti, A.; Trari, M. Response surface methodology and artificial neural network for optimization and modeling the photodegradation of organic pollutants in water. *Int. J. Environ. Sci. Technol.* **2022**. [CrossRef]
46. Lojo-López, M.; Andrades, J.; Egea-Corbacho, A.; Coello, M.; Quiroga, J. Degradation of simazine by photolysis of hydrogen peroxide Fenton and photo-Fenton under darkness, sunlight and UV light. *J. Water Process Eng.* **2021**, *42*, 102115. [CrossRef]
47. Schenone, A.; Conte, L.; Botta, M.A.; Alfano, O.M. Modeling and optimization of photo-Fenton degradation of 2,4-D using ferrioxalate complex and response surface methodology (RSM). *J. Environ. Manag.* **2015**, *155*, 177–183. [CrossRef] [PubMed]
48. Lide, D.R. *CRC Handbook of Chemistry and Physics*; CRC Press: Boca Raton, FL, USA, 2005.
49. Jewett, J.W.; Serway, R. Physics for scientists and engineers with modern physics. *Vectors* **2008**, *1*.
50. Lorenzo, D.; Santos, A.; Sánchez-Yepes, A.; Conte, L.; Domínguez, C.M. Abatement of 1,2,4-Trichlorobencene by Wet Peroxide Oxidation Catalysed by Goethite and Enhanced by Visible LED Light at Neutral pH. *Catalysts* **2021**, *11*, 139. [CrossRef]
51. Murov, S.L.; Carmichael, I.; Hug, G.L. *Handbook of Photochemistry*; CRC Press: Boca Raton, FL, USA, 1993.
52. Santos, A.; Fernandez, J.; Rodriguez, S.; Dominguez, C.; Lominchar, M.; Lorenzo, D.; Romero, A. Abatement of chlorinated compounds in groundwater contaminated by HCH wastes using ISCO with alkali activated persulfate. *Sci. Total Environ.* **2017**, *615*, 1070–1077. [CrossRef]
53. *ISO, D. 11348-3*; Water Quality—Determination of the Inhibitory Effect of Water Samples on the Light Emission of Vibrio Fischeri (Luminescent Bacteria Test)—part 3: Method using Freeze-Dried Bacteria. International Organization for Standardization: Geneve, Switzerland, 2007.
54. Conte, L.O.; Schenone, A.V.; Alfano, O.M. Ferrioxalate-assisted solar photo-Fenton degradation of a herbicide at pH conditions close to neutrality. *Environ. Sci. Pollut. Res.* **2017**, *24*, 6205–6212. [CrossRef]
55. Grčić, I.; Vujevic, D.; Koprivanac, N. The use of D-optimal design to model the effects of process parameters on mineralization and discoloration kinetics of Fenton-type oxidation. *Chem. Eng. J.* **2010**, *157*, 408–419. [CrossRef]
56. Dean, A.; Voss, D.; Draguljić, D. Response Surface Methodology. In *Design and Analysis of Experiments*; Dean, A., Voss, D., Draguljić, D., Eds.; Springer International Publishing: Cham, Switzerland, 2017; pp. 565–614.
57. Myers, R.H.; Montgomery, D.C.; Vining, G.G.; Borror, C.M.; Kowalski, S.M. Response Surface Methodology: A Retrospective and Literature Survey. *J. Qual. Technol.* **2004**, *36*, 53–77. [CrossRef]
58. Kusic, H.; Peternel, I.; Ukic, S.; Koprivanac, N.; Bolanca, T.; Papic, S.; Bozic, A.L. Modeling of iron activated persulfate oxidation treating reactive azo dye in water matrix. *Chem. Eng. J.* **2011**, *172*, 109–121. [CrossRef]
59. De Laat, J.; Truong Le, G.; Legube, B. A comparative study of the effects of chloride, sulfate and nitrate ions on the rates of decomposition of H_2O_2 and organic compounds by Fe(II)/H_2O_2 and Fe(III)/H_2O_2. *Chemosphere* **2004**, *55*, 715–723. [CrossRef]
60. Wang, J.; Wang, S. Effect of inorganic anions on the performance of advanced oxidation processes for degradation of organic contaminants. *Chem. Eng. J.* **2021**, *411*, 128392. [CrossRef]
61. Conte, L.O.; Schenone, A.V.; Giménez, B.N.; Alfano, O.M. Photo-Fenton degradation of a herbicide (2,4-D) in groundwater for conditions of neutral pH and presence of inorganic anions. *J. Hazard. Mater.* **2019**, *372*, 113–120. [CrossRef] [PubMed]
62. Kaiser, K.L.; Palabrica, V.S. Photobacterium phosphoreum Toxicity Data Index. *Water Qual. Res. J.* **1991**, *26*, 361–431. [CrossRef]
63. Blaschke, U.; Paschke, A.; Rensch, I.; Schüürmann, G. Acute and Chronic Toxicity toward the Bacteria *Vibrio fischeri* of Organic Narcotics and Epoxides: Structural Alerts for Epoxide Excess Toxicity. *Chem. Res. Toxicol.* **2010**, *23*, 1936–1946. [CrossRef]

Type: Book chapter
Title: Removal of organochlorine pesticides from soil and water
Authors: Carmen M. Domínguez, **Alicia Checa-Fernández,** Raúl García-Cervilla, David Lorenzo, Salvador Cotillas, Sergio Rodríguez, Jesús Fernández, Aurora Santos
Book: Clean water: next generation technologies, book series: Advances in Science, Technology & Innovation
Chapter: 28
Editorial: Springer
Publication year: *Accepted*

APPENDIX II

-Contributions to congresses-

International conference contributions

1. **Alicia Checa-Fernández**, Marta Subiran, Carmen M. Dominguez, Arturo Romero, Aurora Santos. *Treatment of soil contaminated by HCH using alkaline activation of PS intensified by US*. MECCE 2020. 14th Mediterranean Congress of Chemical Engineering. Barcelona, November 2020. ***Oral communication.***
2. Carmen M. Dominguez, **Alicia Checa-Fernández**, Arturo Romero, Aurora Santos. *Exploring the application of chemical oxidation treatments for the remediation of HCHs-contaminated soil*. MECCE 2020. 14th Mediterranean Congress of Chemical Engineering. Barcelona, November 2020. ***Oral communication.***
3. **Alicia Checa-Fernández**, Carmen M. Domínguez, Leandro O. Conte, Aurora Santos. Synergetic remediation of HCH-polluted sediments by the alkaline and ultrasonic activation of persulfate: performance and residual toxicity. CRETE 2021. 7th International Conference on Industrial and Hazardous Waste Management. Crete (Greece), July 2021. ***Oral communication.***
4. Leandro O. Conte, **Alicia Checa-Fernández**, Carmen M. Domínguez, Aurora Santos. *Modelling and optimization of photo-Fenton degradation of 124- TCB at neutral pH conditions using a visible led source*. CRETE 2021. 7th International Conference on Industrial and Hazardous Waste Management. Crete (Greece), July 2021. ***Oral communication.***
5. **Alicia Checa-Fernández**, Carmen M. Domínguez, Arturo Romero, Aurora Santos. *Thermally activated persulfate for the remediation of real HCHs* contaminated soils. ECCE & ECAB 2021. 13th European Congress of Chemical Engineering and 6th European Congress of Applied Biotechnology. Frankfurt, September 2021. ***Oral communication.***
6. Andrés Sánchez-Yepes, **Alicia Checa-Fernández**, Raúl García-Cervilla, Patricia Sáez, Salvador Cotillas, David Lorenzo, Leandro O. Conte, Carmen M. Domínguez, Sergio Rodríguez, Arturo Romero, Aurora Santos. *Application of Advanced Oxidation Processes to the remediation of groundwater polluted with HCHs*. RSEQ

Symposium 2021. XXXVII Reunión Bienal de la Real Sociedad Española de Química. Madrid, September 2021. ***Poster communication.***

7. Aurora Santos, **Alicia Checa-Fernández**, Carmen M. Dominguez, David Lorenzo, Raúl García-Cervilla. *Enhancement in the remediation of soil and groundwater polluted with lindane wastes by alkali addition.* SARDINIA Symposium 2021. 18th International Symposium on Waste Management and Sustainable Landfilling. Sardinia (Italy). October 2021. ***Oral communication.***
8. **Alicia Checa-Fernández**, Aurora Santos, Marta Subirán, Arturo Romero, Carmen M. Dominguez. *Exploring the use of surfactants for soil washing and subsequent persulfate-based oxidation treatments.* SARDINIA Symposium 2021. 18th International Symposium on Waste Management and Sustainable Landfilling. Sardinia (Italy). October 2021. ***Oral communication.***
9. **Alicia Checa-Fernández,** Paula Ventura, Raúl García-Cervilla, David Lorenzo, Aurora Santos, Carmen M. Domínguez. *Toxicity evaluation of lindane-wastes contaminated soils treated by surfactant-enhanced ISCO.* RSEQ Symposium 2022. XXXVIII Reunión Bienal de la Real Sociedad Española de Química. Granada, June 2022. ***Poster communication.***
10. **Alicia Checa-Fernández**, Aurora Santos, Arturo Romero, Carmen M. Domínguez. Remediation of HCHs-polluted soils by surfactant-enhanced washing and activated persulfate Oxidation. 14th International HCH and pesticides fórum. Zaragoza, February 2023. ***Oral communication.***
11. Aurora Santos, **Alicia Checa-Fernández**, Carmen M. Domínguez, Juan P. Martin-Sanz, Inmaculada Valverde-Asenjo, Jose R. Quintana, Javier Fernández. Preliminary study of the bioremediation capacity of horse amendment in soils contaminated with HCHs. 14th International HCH and pesticides fórum. Zaragoza, February 2023. ***Oral communication.***
12. David Lorenzo, Carmen M. Domínguez, Raul Garcia-Cervilla, Aurora Santos, **Alicia Checa-Fernández**, Jesús Fernández, Joaquín Guadaño, Jorge Gómez. ISCO and S-ISCO evaluation in the remediation of Sardas alluvium. 14th International HCH and pesticides fórum. Zaragoza, February 2023. ***Oral communication.***

National conference contributions

1. **Alicia Checa-Fernández**, Aurora Santos, Arturo Romero, Carmen M. Domínguez. Remediación de suelos contaminados con HCHs mediante activación alcalina de

PS intensificada con ultrasonidos. META: XIV Congreso de la mesa española de tratamiento de aguas. Sevilla, June 2022. ***Poster communication.***

2. Carmen M. Domínguez, **Alicia Checa-Fernández**, Paula Ventura, Aurora Santos. Evaluación de la toxicidad aguda de los suelos contaminados por HCHs tras la aplicación de tratamientos de remediación con persulfato. META: XIV Congreso de la mesa española de tratamiento de aguas. Sevilla, June 2022. ***Oral communication.***